Groundwater Contaminant Transport Modeling and Aquifer Vulnerability Assessment of Gazipur District, Bangladesh

PhD Thesis

Md. Jowaher Raza
Registration no. 24; Session: 2017-2018

Department of Geology
Faculty of Earth and Environmental Sciences
University of Dhaka

February 2023

Groundwater Contaminant Transport Modeling and Aquifer Vulnerability Assessment of Gazipur District, Bangladesh

A thesis submitted to the Department of Geology under the Faculty of Earth and Environmental Sciences, University of Dhaka, Bangladesh, as a requirement for the degree of Doctor of Philosophy in Geology.

by

Md. Jowaher Raza

M.Sc. (KFUPM, Saudi Arabia), M.Sc. (DU, Bangladesh), B.Sc. (DU, Bangladesh)

Registration no. 24, Session: 2017-2018

February 2023

Certificate

This is to certify that this thesis, entitled "Groundwater Contaminant Transport Modeling and Aquifer Vulnerability Assessment of Gazipur District, Bangladesh," has been prepared and submitted for the degree of Doctor of Philosophy of the Department of Geology, Faculty of Earth and Environmental Sciences, the University of Dhaka by Jowaher Raza under our supervision.

It is further to certify that the research work embodied in the thesis is original and suitable for awarding a Ph.D. degree in Geology.

Supervisor

Prof. Dr. rer.nat. Muhammad Qumrul Hassan
Professor, Department of Geology
Faculty of Earth and Environmental Sciences
University of Dhaka

Co-Supervisor

Prof. Dr. Kazi Matin Uddin Ahmed
Professor, Department of Geology
Faculty of Earth and Environmental Sciences
University of Dhaka

Title

Groundwater Contaminant Transport Modeling and Aquifer Vulnerability Assessment of Gazipur District, Bangladesh.

Document type

A thesis requirement for the fulfillment of the degree of Doctor of Philosophy in Geology.

Submitted to

The Department of Geology under the Faculty of Earth and Environmental Sciences, University of Dhaka, Bangladesh

Prepared By

Md. Jowaher Raza
Registration no. 24; Session: 2017-2018

Supervisors:

Prof. Dr. Muhammad Qumrul Hassan
Professor, Department of Geology
Faculty of Earth and Environmental Sciences
University of Dhaka

Prof. Dr. Kazi Matin Uddin Ahmed
Professor, Department of Geology
Faculty of Earth and Environmental Sciences
University of Dhaka

Keywords

Groundwater, Contaminant Transport Modeling, Vulnerability Assessment, DRASTIC, Water Quality Index, Urbanization, Industrialization, Land Cover, Land Use

Disciplines to be considered

Geology, Hydrogeology, Geochemistry, GIS, Vulnerability Assessment, Modeling.

DEDICATION

My Parents

DR MD RAKIBUR RAZA and **MRS. RASHEDA RAZA**

ABSTRACT

Gazipur District is located in the Dhaka Division of central Bangladesh, covering an area of approximately 1,741 square kilometers, of which 17.53 km^2 is river and water bodies, and 273.42 km^2 is forest area, while the rest includes rural and urban settlements, agricultural lands, and industrial areas. As per the 2021 census the total population of the district is approximately 3.4 million, one of the most populous districts in the country. Gazipur is situated north of the capital city, Dhaka, and shares its borders with Mymensingh, Tangail, Kishoreganj, Narsingdi, and Narayanganj. It has a tropical monsoon climate characterized by high temperatures and heavy annual rainfall. The average annual temperature in Gazipur ranges from 25 to 30°C, with the highest temperatures occurring between April and June. The average annual rainfall in the district is around 2,200 millimeters, with the highest precipitation occurring during the monsoon season from June to September, while the dry season from December to February typically experiences little to no rainfall.

Gazipur District is divided into five administrative Upazila or sub-districts, *viz.*, Gazipur Sadar, Kaliganj, Kapasia, Sreepur, and Kaliakair. Due to a wide range of economic and industrial activities, and fast-growing job market, movement of people form the neighbouring rural areas resulted into a continuous rising trend of population, that doubled during the last two decades. It is a major industrial city, a hub for the country's textile industry with almost 1500 industries. About one-third of the export-oriented ready-made garment factories of the country is located in the district, resulting in significant urbanization over recent years, with drastic changes to infrastructures.

The district has been facing a significant increase in groundwater extraction over the years, due to population growth, urbanization, and industrialization. Almost all the drinking water supply in the area comes from groundwater sources. Rapid urbanization and industrialization caused sharp rise in abstraction of groundwater alongside the preexisting usage for irrigation. The highest groundwater consumption is in the urban (85%) and industrial settings (15%). Groundwater reserves are dwindling due to the continuous increase of uncontrolled abstraction alongside gradual decrease in recharge rate due to change in land use an land cover types. Higher abstractions and lower recharge result in an average annual drop of >2 meters in the groundwater levels of the underlying aquifers.

This research aimed to determine the impact of rapid urbanization and increasing industrialization on groundwater in the Gazipur District; and relate contamination levels of groundwater with growing land cover and land use changes. To meet the increased demand for water, there has been a surge in abstraction, which raised challenges in managing water resources and caused sustainability challenges.

Electrical conductivity (EC) and Total Dissolved Solids (TDS) were measured throughout the district between 2018 to 2021. Over the years, the average high EC value increased from 1071 µS/cm to 1781 µS/cm, higher values in urban and industrial areas of the District. A similar comparative increasing trend can be observed with historical measurements. Contaminants introduce additional ions into the water causing an increase in EC values, indicating contamination. This increase can be attributed to the heavy metal from industrial waste and domestic effluents into groundwater, observed within the main urban and industrial settings of the district.

A detailed sampling plan was prepared with a target to cover the district's main urban settlements, industrial hubs, growing areas, forests, and agricultural areas. A Total of 143 groundwater samples were collected from the district and analyzed; thirteen parameters were considered for WQI calculation: pH, TDS, sodium, potassium, calcium, magnesium, iron, manganese, bicarbonate, chloride, sulfate, nitrate, and fluoride. The computed WQI shows that 48% of the water sample falls in excellent and 48% in good water categories. Spatially, WQI values exceed the limit in areas with high urbanization and industrialization setups. Significantly high values were found in the eastern part of Kaliakair, the central part of Gazipur Sadar, the northern part of Sreepur, the eastern part of Kapasia, and the northern part of Kaliganj within the growing urban and industrial areas of the district. Urbanization and industrialization lead to an increased demand for water, affecting quality and sustainability of groundwater.

The DRASTIC method has been modified to assess groundwater vulnerability by incorporating population density, an outcome of urbanization and industrialization. The new assessment methodology of groundwater vulnerability is termed as DRASTIC-P. According to the new produced DRASTIC-P Map, urbanization and industrialization have been found to be hazardous activities impacting the district's groundwater resources. According to the vulnerability map most part of the district is impacted, with minimum impacts in the southeastern part. Industrial processes often use large amounts of water, and the growing population in urban areas also requires more water for domestic use. This increased demand lead to the over-extraction of groundwater, causing depletion of aquifers and lowering of the water table.

The solute transport model predicts spreading contaminants will spread to the neighboring regions in less than ten years. Flow is more rapid in the regions with high abstraction rates. This study indicated the limitations of modeling using hypothetical data and generalized information. Though MODFLOW will give a generalized flow pattern and contamination transport, yet lack of data can make the observations flawed. Fundamentally, this study indicates that the cone of depression may expand outside the district area; hence, further work should concentrate on a more precise measurement of in-situ hydrogeological parameters.

ACKNOWLEDGEMENTS

All praise to the Almighty Allah for giving me the courage and patience to carry out this work. May I remain sincere and committed through this small accomplishment and ask for forgiveness for my shortcomings. May Allah guide me along the right path (Aameen).

I like to mention that this research work leading to the achievement of my Ph.D. is the result of the sacrifice, support, patience, and prayers of my mother, Mrs. Rasheda Raza. She always wanted me to follow my siblings in academic excellence. This degree is her property. I believe, and I know, my father, Dr. Md. Rakibur Raza, would have been proud knowing this accomplishment. His absence was felt. May Allah grant him Jannatul Firdaus, Ameen!

I want to express my respect and gratitude to my thesis and research advisors, Prof. Dr. Muhammad Qumrul Hassan and Prof. Dr. Kazi Matin Uddin Ahmed. Dr. Hassan has always been with me since my undergrad years. His contribution extends beyond my academic career. I received his unconditional support, help, and guidance at the most unending level. Perhaps what I enjoyed the most was his tolerance of my discretions. Dr. Ahmed is highly regarded for his technical specialty and research contributions. His advice and opinions were the major force in completing this research work. His technical input has always put me on the right track.

I want to thank Dr. Anwar Zahid, Director, BWDB. He has been the information and research backbone of this work. He always made time to help and advise. Discussions with him made the research very understandable.

I am grateful for the support and guidance from Professor Dr. Subrota Kumar Saha, Department Chairman. I would also like to thank the former Department Chairman, Professor Dr. Aziz Hasan, for his help, support, and assistance.

I like to share this degree with my daughter, Sidra Raza, knowing she will join me one day to enjoy the outcome of this success. My Eldest brother Dr. Md. Ishfaqur Raza; my second eldest brother Md. Touhidur Raza; my third eldest brother Dr. Md. Tanveer Raza; and my little Sister, Farah Shahrookh Raza, stood by me and behind me as an umbrella to ensure I got through this challenge. All my Bhabhi's, Nieces, and Nephews' dua gave me the moral high ground. Allah has blessed me.

I thank the Department of Geology, Faculty of Earth and Environmental Sciences, University of Dhaka. Mr. Masruk went beyond and above to help me with fieldwork and activities. Mr. Shah Alam's support with the water sample analysis work. Mr. Najib and his colleague's support with departmental issues were outstanding.

This thesis must acknowledge the kind support and assistance of many individuals. I want to take this opportunity to thank all who supported and encouraged me in doing this research work.

TABLE OF CONTENTS

LIST OF FIGURES

LIST OF TABLES

LIST OF ABBREVIATIONS (ACRONYMS)

µs/cm	Micro-siemens per centimeter
A	Aquifer Media
AAS	Atomic Absorption Spectrometry
AD	Advance in Time
Ar	Rating assigned to aquifer media
ASTER	Advanced Spaceborne Thermal Emission and Reflection Radiometer
AVI	Advanced Vegetation Index
Aw	The weight assigned to aquifer media
BARI	Bangladesh Agrarian Investigate Organized
BBS	Bangladesh Bureau of Statistics
BGS	Bangladesh Geological Survey
BIT	Bangladesh Organized Innovation
BRAC	Bangladesh Rehabilitation Assistance Committee
BRRI	Bangladesh Rice Investigate Organized
BSCIC	Bangladesh Small and Cottage Industries Corporation
BWDB	Bangladesh Water Development Board
C	Hydraulic conductivity
C	Hydraulic Conductivity
Ca	Calcium (Ca2+)
$CaSO_4$	Calcium Sulfate
CCMEWQI	Canadian Council of Ministers of the Environment Water Quality Index
Cl	Chloride (Cl-)
cm	Centimeter
CMB	Chloride Mass Balance
CO3	Carbonate
COP	Chemical Component
Cu	COPPER
D	Depth to water
D	Depth to Groundwater
DEM	Digital Elevation Map
DI	DRASTIC Index
DPHE	Department of Public Health Engineering
Dr	Rating to 'the depth to the water table'
DRASTIC	D: aquifer depth, R: recharge rate, A: aquifer lithology, S: soil type, T: topography, I: impact of the vadose zone, C: aquifer hydraulic conductivity
DRASTIC-P	DRASTIC-Population Density
Dw	The weight assigned to the depth to the water table
EC	Electrical Conductivity
EO	Earth observation
EPA	Environmental Protection Agency
meq/l	Millieuivalent per Liter
Mg	Magnesium (Mg2+)
mg/l	milligram per liter
mm	millimeters
Mn	Manganese
MODFLOW	Modular Three-Dimensional Finite-Difference Ground-Water Flow Model
MODPATH	Modernization Path
MPO	Master Plan Organization
MT3D	Modular Three-Dimensional Solute Transport Model
MT3DMS	Modular Three-Dimensional Multispecies Transport Model for Simulation
MW	Monitoring Wells
Na	Sodium (Na+)
NO_3	Nitrate (N03-)
NSF	National Sanitation Foundation
NSFWQI	Foundation Water Quality Index
NWMP	National Water Management Plan
^oC	Degree Centigrade
OC	Output Control
ORP	Oxidation-Reduction Potential
Ot	Output
OWQI	Oregon Water Quality Index
P	Population Density
pH	hydrogen-ion concentration
PWD	Public Works Datum
R	Net Recharge
RIVA	Risk and Vulnerability Assessment
Rr	Rating for ranges of aquifer recharge
RS	Remote Sensing
Rw	Weight for the aquifer recharge
S	Soil media
S	Soil Media
SD	standard deviation
SI	Sensitivity Index
SINTACS	Water table depth (S), Effective infiltration (I), Unsaturated zone (N), Soil media (T), Aquifer media (A), Hydraulic conductivity zone (C), Topographic slope (S)
SO_4	Sulfate (So42-)
Sr	Rating for the soil media
ST	Stress
STW	Shallow Tube Wells
Sw	The weight assigned for soil media
SWIR	Short-wave Infrared
T	Transmissivity (m2/d)

EPIK	Epikarst, Protective cover, Infiltration conditions, and Karst network development
EPSG	European Petroleum Survey Group
ERDAS	Earth Resources Data Analysis System
et al.	et al. ia / and others
ETM	Enhanced Thematic Mapper Plus
Fe	Iron (Ferrum)
F-Test	Snedecor's F Distribution Test
GFM	Groundwater Flow Model
GHG	Greenhouse Gas
GIS	Geographic Information System
GOD	Groundwater occurrence, Overall lithology of the aquifer, and Depth to groundwater level
GWF	Groundwater Flow
GWL	Groundwater Level
HCO_3	Bicarbonate (HCO3-)
HCS	Hydrogeological Complex and Settings methods
HTW	Hand Tube Wells
I	Impact of Vadose Zone
IAEA	International Atomic Energy Agency
ICDDRB	International Centre for Diarrhoeal Disease Research
IDW	Distance Weighting method
Ir	Rating assigned to vadose zone
K	Potassium (K+)
km^2	Square Kilometer
LANDSAT	Land Remote-Sensing Satellite (System
LULC	Land Use and Land Cover
m	meters
m^3/d	cubic meter per day
T	Temperature
T	Topography
TCS	Total Correctly Classified Sample
TDS	Total Dissolved Solids
TIRS	Thermal Infrared Sensor
TM	Thematic Mapper
Tr	Rating for topography (slope)
TS	Total Sample
t-test	Student's t-Test
Tw	The weight assigned to topography
UNDP	United Nations Development Program
US	United States
USGS	United States Geological Survey
USSL	United States Salinity Laboratory
WAWQI	Weight Arithmetic Water Quality Index
WGS	World Geodetic System
WHO	World Health Organization
WQ	Water Quality
WQI	Water Quality Indices
WTF	Water Table Fluctuation
Zn	Zinc

1 INTRODUCTION

INTRODUCTION

Groundwater is known as the world's largest distributed store of freshwater, especially for drinking water. Irrigation is the primary user of groundwater globally, and aquifer depletions have been recorded for different years. Unfortunately, the rapid increase in population related to Urban development is causing groundwater abstraction at an unprecedented level to meet the growing demands (Kolokotroni and Giridharan, 2008; Foster & Chilton, 2003).

Groundwater is a major water source for irrigation, residential use (potable water), and industrial reasons in Bangladesh. Approximately 80% of irrigation comes from groundwater, primarily for agriculture. Intensive groundwater use impacts the groundwater table, which has gradually declined in different parts of Bangladesh. Specifically, in the greater Dhaka region, where groundwater is reported to account for 87% of all drinking water, groundwater levels have declined to 75m in some specific locations. Studies indicate that the recharge rate is below the abstraction rates in these areas (Aghazadeb & Mogaddam, 2010; BWP, 2019).

There has been an increase in unrestricted abstraction, which has generated sustainability issues in the management of water resources. To fulfill the rising demand for fresh water, there has been an increase in unrestricted abstraction, which has generated sustainability issues in the management of water resources. The recharging areas are increasingly diminishing owing to uncontrolled urbanization. An increasing drop in the water table has occurred throughout the last thirty decades (Deng et al., 2009; Dewan & Yamaguchi, 2009). Unsustainable groundwater usage is a possible risk factor that gradually affects diverse water uses, including urban water resource management and socioeconomic impact. Increasing population pressure and unrestricted groundwater extraction diminish groundwater levels (Mitchell et al., 2007). Increasing the degree of a temporal sequence of urban growth effects requires land use variability analysis. Remote sensing provides precise spatial resolution and temporal frequencies; measuring the complete continuum of urban expansion using satellite images is essential. (Foster et al., 1998; Harris & Ventura, 1995).

1.1. Background

Groundwater is a crucial natural resource that varies in quality and quantity across Bangladesh. Increased population and urbanization place enormous demands on groundwater supplies, reducing both their quality and quantity. Groundwater is one of the essential natural resources comprising about 34% of the total freshwater in the world. It is the main water and considered less contaminated than other water sources. It provides approximately half of the accessible freshwater used for daily cooking, drinking, and cleaning. In Bangladesh, 97% of rural and 82% of urban people depend on groundwater supply. Around 79% of agricultural land depends on groundwater for crop production. (Qureshi et al., 2014; Haq, 2006; Zahid et al., 2006)

Gazipur District was selected as the study area because of its geographic location and fast urbanization. The area relies heavily on groundwater for drinking water, irrigation, and industrial use. Increased demand for water due to population growth, urbanization, and agricultural and industrial activities can lead to the over-extraction of groundwater, causing the depletion of aquifers and the intrusion of contaminants. The extensive use of agrochemicals such as fertilizers and pesticides in Gazipur's agricultural areas can contaminate the groundwater. These contaminants can percolate through the soil and enter the aquifer, posing a risk to human health and the environment. Gazipur has several industrial areas and a rapidly growing urban population. The discharge of untreated or inadequately treated industrial effluents and domestic wastewater can lead to the contamination of aquifers. (Yesmin et al., 2014; BWP, 2019; Rahman et al., 2022).

Groundwater transport modeling is an essential tool to understand and predict the movement of water and contaminants in the subsurface environment. It is particularly useful for managing water resources and identifying potential risks to public health or the environment. Assessing the vulnerability of aquifers will ensure the sustainable use of groundwater resources and to prevent contamination that could pose risks to public health and the environment. Aquifer vulnerability refers to the susceptibility of an aquifer to contamination from human activities or natural processes.

1.2. Research Objectives

The main objective of this research is to assess the impacts on groundwater of increased urbanization and industrialization in Gazipur District. This research work intends to conduct quantitative modeling of groundwater and understand the influencing factors of contamination. A comparative overview of historical data perhaps will assist in delineating a contamination pattern, with which a predictive simulation can be conducted.

This research work attempts to understand the groundwater management issues in Gazipur District, where the water resource demand is increasing due to growing urban, industrial, and agricultural activities (Arifeen et al., 2021). The approach plan of this work included monitoring, sampling, mapping, analysis, and interpretation. A detailed baseline was established to understand the aquifers' hydrogeological condition, flow pathways, and water movement rate.

The primary objectives of this research work can be stated as follows;

- Understanding the factors influencing aquifer and groundwater flow conditions.
- Identify and delineate groundwater contamination zones, groundwater pumping effects, and water availability issues, and
- Conducting a comprehensive groundwater vulnerability assessment for preparing a groundwater management plan for easing sustainability.

1.3. Technical Significance

This research is focused on understanding the analysis and investigation of the groundwater condition and antecedents. The technical significance of this research work can be stated in the following

- Decipher the urbanization and industrialization impacts on groundwater.
- Understand the factors influencing contaminant migration, and
- Identifying the research limitations.

1.4. Limitations

This research work started swiftly and smoothly and progressed aggressively in the early stages, covering two years. Unfortunately, the pandemic spread hindered the routine sampling and analysis approach to preparing a geochemical trend, followed by financial limitations and movement restrictions. As such, requesting a six-month extension to complete the necessary work was necessary. A major technical limitation was acquiring high-resolution images to ensure appropriate classification and the accuracy of the flow and contaminant model.

2 STUDY AREA

DESCRIPTION OF THE STUDY AREA

The study area, Gazipur District, belongs to the 'Madhupur Tract,' which is situated in the northern part of Dhaka, the central upland area of Bangladesh. Gazipur district is situated between 23˚53' to 24˚20' North latitudes and between 90˚09' to 90˚42' east longitude (BBS, 2013; Parvin, 2018; Figure 2.1).

Gazipur District is located in the Dhaka Division, which is part of the floodplain region of Bangladesh. Specifically, the district lies within the Ganges-Brahmaputra-Meghna delta. The floodplains are characterized by the deposition of sediments from the Ganges, Brahmaputra, and Meghna rivers, resulting in fertile soil and flat terrain. The floodplain region can be further subdivided into the active floodplains, where sediment deposition is ongoing, and the older floodplains, where sediment deposition has reduced or ceased.

1.1. Geographical

The district's total area is 1,806.36 $km^{2,}$ of which 17.53 km^2 is riverine, and 273.42 km^2 is forest area. The Zila is bounded on the north by Mymensingh Zila and Kishoreganj Zila, on the east by Narsingdi Zila, on the south by Narayanganj and Dhaka zilas, and on the west by Tangail Zila (Figure 1). The district consists of 5 Upazilas, 43 unios, and 725 mauzas. The Upazilas are Gazipur Sadar, Kaliakair, Kaliganj, Kapasia and Sreepur (BBS, 2013; BBS, 2015; Parvin, 2018; Table 2.1; Figure 2.2).

The terrain of the research region resembles terraces, with surface elevations ranging from 16 to 19 meters. The soil is a light to medium grey, fine sand to clay silt composition. The soils are poorly stratified and composed of Pleistocene alluvium soil. The majority of soils are rich in manganese and iron. Gazipur's principal rivers include the Old Brahmaputra, Shitalakshya, Turag, Bangshi, Balu, and Banar (BBS, 2013; BBS, 2015).

1.2. Geological Setting

Bengal Basin is among the deepest sedimentary basins, with its landward portion at the head of the Bay of Bengal, bounded on the west by the outcropping Precambrian rocks of the Indian shield, on the north by the Precambrian Shillong massif, and on the east by the Folded belt of the Indo-Burman mountains. The three great rivers, Ganges, Brahmaputra, and Meghna, have created a massive deltaic sedimentary complex extending into the Bay of Bengal Deep-Sea Fan, the world's largest undersea fan. Bangladesh and portions of several nearby Indian states make up the Basin. (Morgan and McIntire, 1959; Khandoker, 1989; Zahid, 2008). The Bengal Basin has two primary tectonic features: the western and northwestern stable shelf (the Platform) and the Bengal Foredeep. The platform flank runs from the Shillong plateau to the Bay of Bengal.

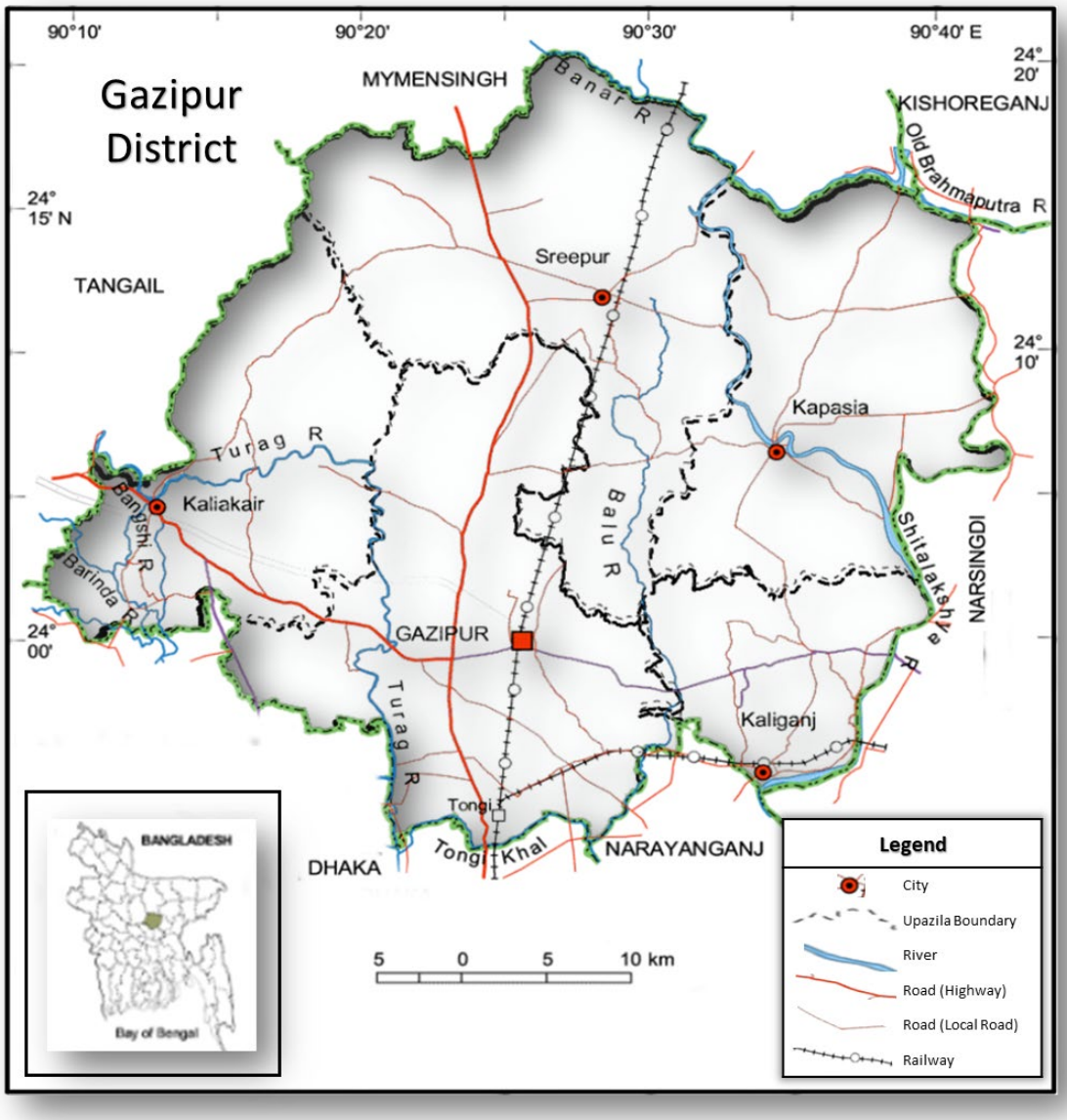

Figure 2.1: Map showing the study Area, Gazipur District.

Table 2.1: Census results of the Gazipur District. (Source: BBS, 2015)

	Population	**Density** (/km^2)	**Urban Population** (%)
Gazipur District			
2001	20,31,891	1,231	30.48
2011	34,03,912	1,884	45.8
Gazipur Sadar Upazila			
2001	8,66,540	1,941	
2011	18,20,374	3,977	37.87
Kaliakair Upazila			
2001	2,67,003	850	7.28
2011	4,83,308	1,539	33.83
Sreepur Upazila			
2001	3,37,367	75	5.15
2011	4,92,792	1,064	25.62
Kapasia Upazila			
2001	3,21,454	900	3.53
2011	3,42,162	958	3.8
Kaliganj Upazila			
2001	2,39,527	1,508	6.45
2011	2,65,276	1,236	17.13

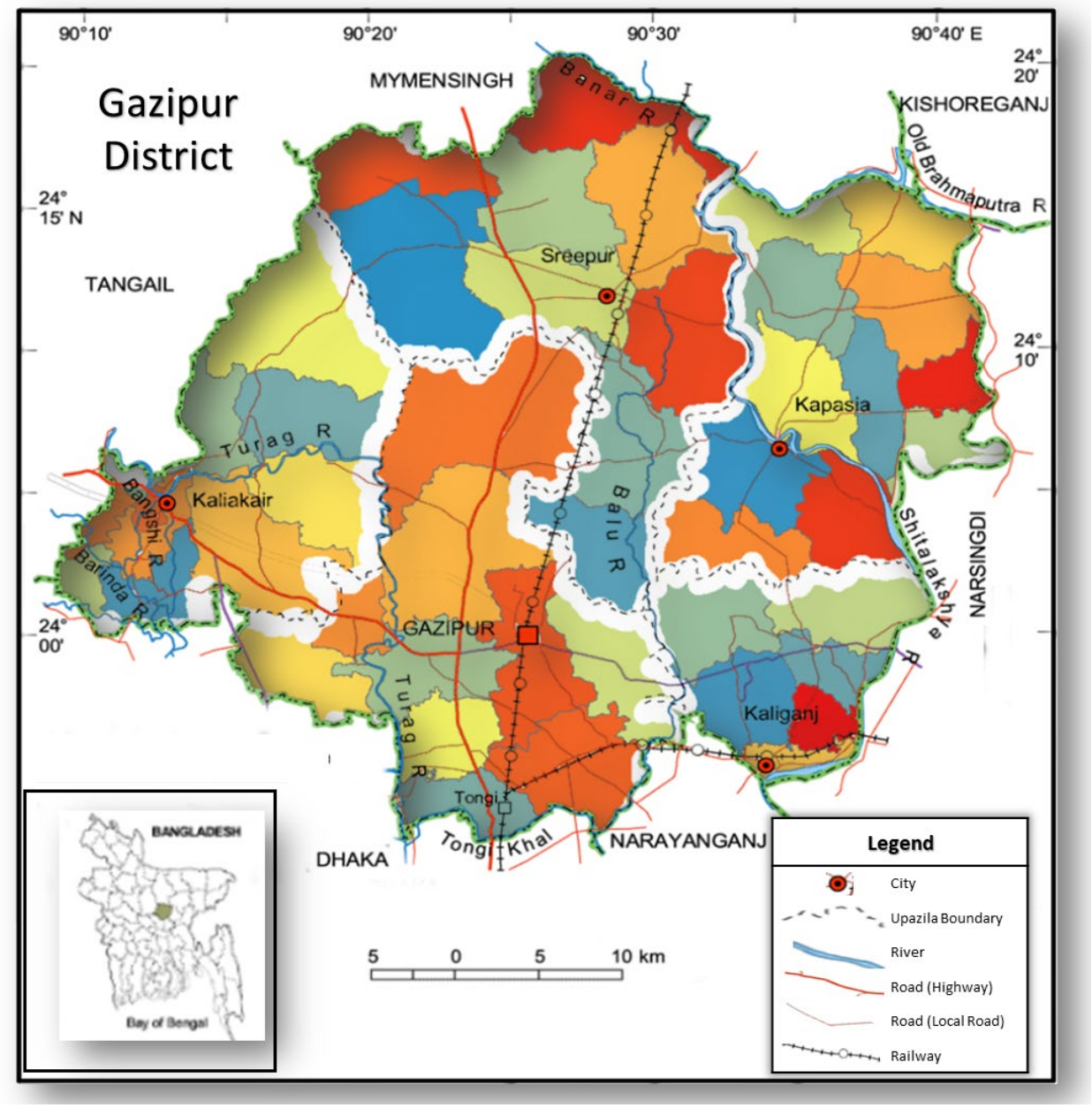

Figure 2.2: Map showing different administrative parts of Gazipur District. The district consists of 5 Upazilas (demarcated by white border), 43 Unions (color differentiated), and 725 Mauzas.

It contains the Sylhet trough, the Faridpur trough, the Hatia trough, and the Madhupur High, delimited by faults separating blocks of uplift and subsidence (Figure 2.3; Figure 2.4; Reiman, 1993; Curray, 1994; Islam & Alam, 2009).

The Madhupur Tract consists of high Pleistocene deposits that are surrounded by faults. The Madhupur Clay is a succession of complicated, over-consolidated, reddish-brown to grey silty clays found at the surface of the Madhupur Tract. Its base is built of fine sandstone and reaches a maximum thickness of 45 meters (on average, I5 meters in Gazipur). The Bashabo Formation of the Holocene comprises organic-rich grey and yellow sands and clays that cover drainage channels and tiny depressions in the Madhupur Tract. Recent flood plain deposits from the Rivers Turag, Buriganga, Balu, and Tongi can be found along the boundaries of the Madhupur Tract (Hasan, 1999; Jamil & Ahmed, 2015; Table 2.2).

Gazipur is situated in the Platform region of the Bengal Basin, close to the country's geographic center. It is located at the southernmost border of the Madhupur Tract, where the Madhupur Clay overlies the Dupi Tila Formation. The Dupi Tila Formation consists of fine to coarse-grained, Plio-Pleistocene fluvial-deltaic sands. The Dupi Tila sands form an aquifer system consisting of two aquifers separated by a discontinuous clay layer. The thickness of the Dupi Tila aquifer ranges from 100 to 200 meters, whereas the thickness of the Madhupur Clay is approximately 10 meters (Hasan, 1999).

1.3. Hydrogeological Setting

Sedimentary fluxes from the Himalayan and Indo-Burman Mountain Ranges are drained by the Ganges-Brahmaputra-Meghna (GBM) river system and deposited over the Bengal Basin, forming the GBM Delta and covering most of Bangladesh (Shamsudduha and Uddin, 2007).

Along the central part of Bangladesh slightly elevated (10-20m amsl) Pleistocene terrace deposits or Madhupur Tract can be identified. Gazipur is situated along the southern limit of the fault-bounded Madhupur Tract. Stratigraphically, the region is characterized by a sequence of unconsolidated Flavio-deltaic deposits hundreds of meters thick that are often made of Plio-Pleistocene gravels, sands, silts, and clays, known as Madhupur Clay. The Madhupur Clay formation (aquitard) is of a red clay to silty clay, unconformably overlain by alluvial deposits and underlain by micaceous, quartzo-feldspathic sands. (Hasan, 1999; Davies, 1994; Ravenscroft, 2003). The semi-pervious Madhupur Clay efficiently confines the local aquifers and significantly reduces the amount of direct recharge to the aquifer.

Throughout Gazipur the Madhupur Clay overlies the Dupi Tila Formation, which is composed of fine to coarse-grained, fluvio-deltaic sands of Plio-Pleistocene age.

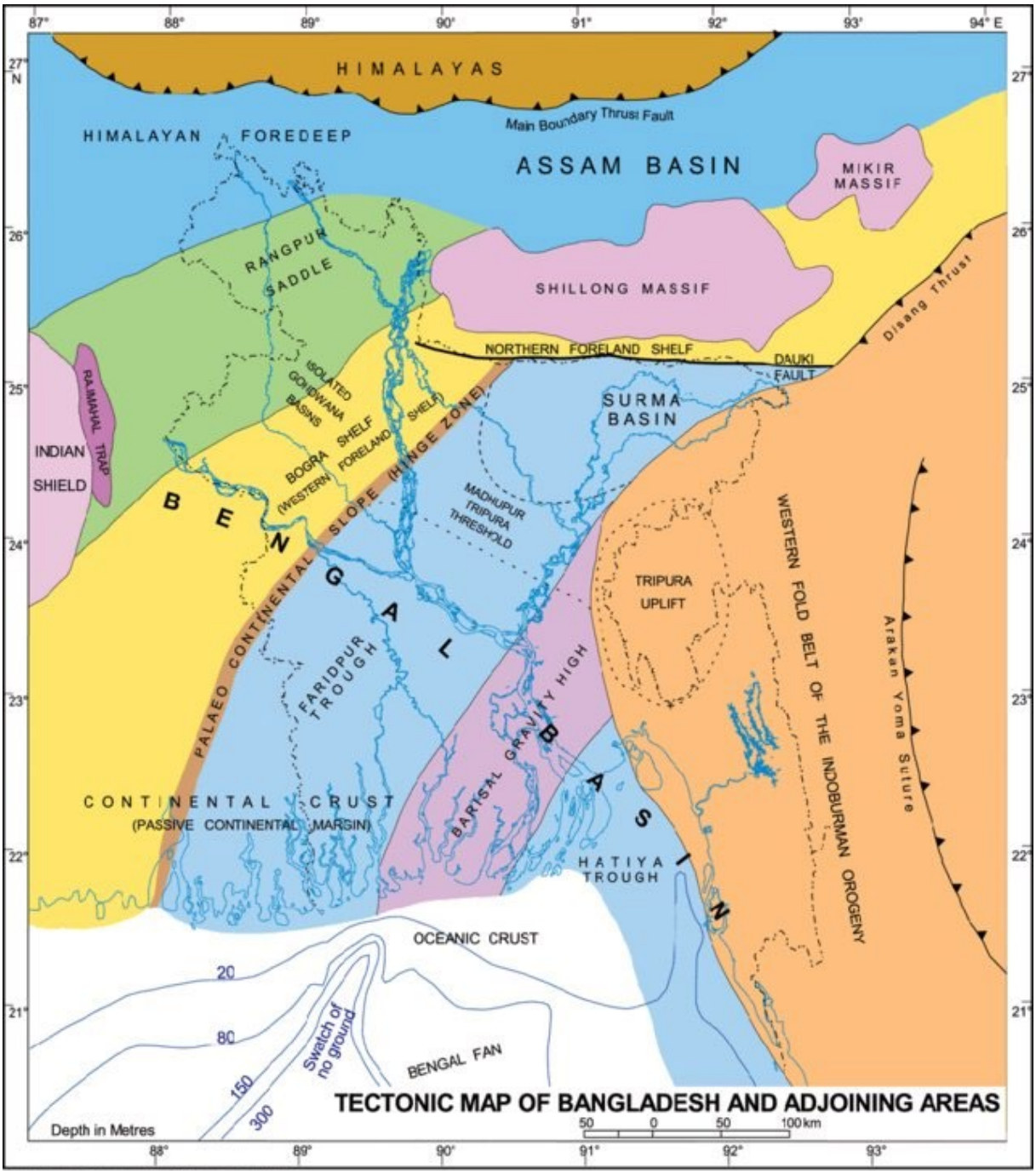

Figure 2.3: Tectonic Map of Bangladesh and adjoining Areas. Gazipur is situated in the Platform region of Bangladesh, close to the country's geographic center. It is located at the southernmost border of the Madhupur Tract. (Modified from Reiman, 1993; Islam and Alam, 2009; Choudhury and Khan, 2011)

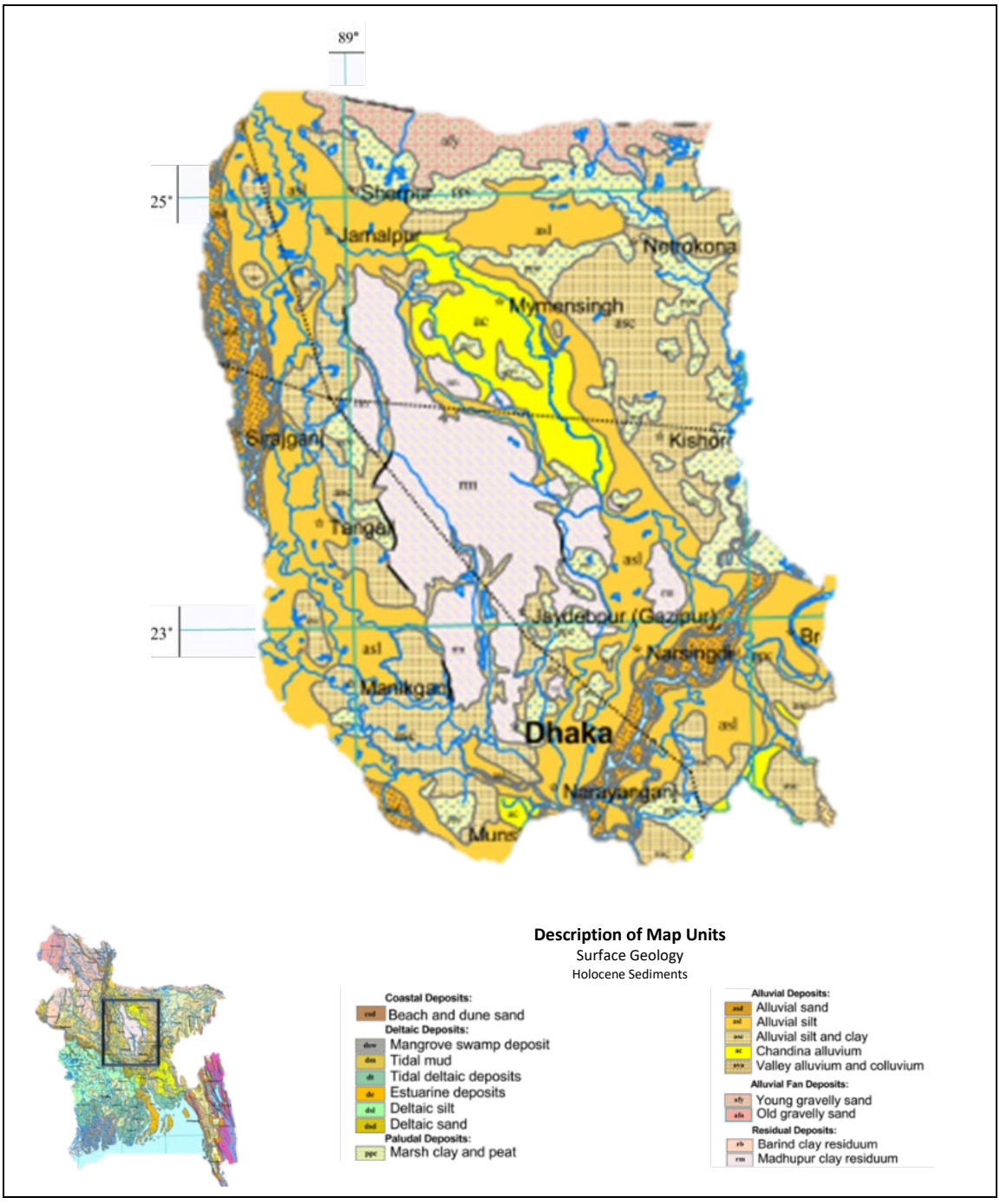

Figure 2.4: Map showing the geological features of Gazipur District and surrounding area. At Gazipur the Madhupur Clay overlies the Dupi Tila Formation. Stratigraphically, the region is characterized by a sequence of unconsolidated Flavio-deltaic deposits hundreds of meters thick that are often made of Plio-Pleistocene gravels, sands, silts, and clays. (Modified from Reiman, 1993; Islam and Alam, 2009)

Table 2.2: Stratigraphy of the Madhupur Tract. (Modified from Mansour, 1990; Burgess et al. 2011; Jamil & Ahmed, 2015; Islam et al., 2017)

Age	Formation	Lithology	Average Thickness (m)
Holocene	Alluvium	**Low Land Alluvium:** River Bed Deposits grey sand and silty sand, medium to fine grained, and unconsolidated	variable
		Local Unconformity	
		Natural Levee and Interstream deposits: Fine sand, sandy silt, and clayey silt grey, massive and friable.	0-25
		Back Swamp and Depression: Deposits Clay and silty clay, grey bluish grey to dark grey to black, peaty and sticky.	
		High Land Alluvium: Mainly silt and clay, occasionally sand, occurs as incised channels infilling the Madhupur Tract's high land.	
		Local Unconformity	
Pleistocene	Madhupur Clay	**Red Clay:** Highly weathered, brownish red to brick red, massive, sticky, interbedded with fine sand and silt, and contains ferruginous concretions and ferruginous and calcareous nodules, plant roots, and manganese spots.	6-25
		Mottled Clay Earthy grey with mottlings of red, brown, yellow, and orange colors; massive, contains micas and calcareous nodules. It is oolitic and sticky and shows the increasing amount of sand to the base.	
		Regional Unconformity	
Pliocene	Dupi TIla	Yellow to yellowish-grey, massive, cross-bedded, moderately consolidated, fine to medium-grained as well as coarse-grained sands with intraformational clay beds and contains large silicified wood fragments and occasional gravels at depth	120

The Dupi Tila sands constitute an aquifer system, which is made up of two aquifers separated by a discontinuous clay layer varying in thickness from 100 to 200 m, whereas the thickness of the Madhupur Clay is about 10 m. Direct recharge to the aquifer is largely reduced by the presence of the clay (Hasan, 1999). The aquifer and aquitard set up of the study area can be explained accordingly with accordance to accepted studies.

- **UPPER AQUITARD:** The cover over the aquifers is Madhupur Clay. Its thickness from ground surface varies from 8m to 20 m according to the thickness of the overlying clays. (Hasan, 1999)
- **UPPER AQUIFER:** It is mainly composed of fine to medium-fine sands and is found all over the model area at a thickness of 25 to 40m. It represents the upper part of the Dupi Tila Formation (Hasan, 1999).
- **LOWER AQUITARD:** It represents the clay lenses that separates the lower aquifer from the upper aquifer within the Dupi Tila Formation. Its thickness varies and is even absent at some points (Hasan, 1999).
- **LOWER AQUIFER:** The deeper part of the Dupi Tila aquifer consists mainly of medium to coarse sands. Its thickness ranges between 80 to 120 m. It's the main deep aquifer, targeted by deep tube wells (Hasan, 1999).

MPO (1987) stated that as per the conventional aquifer nomenclature of Bangladesh the Dupi Tila aquifer is termed as a composite aquifer. Slahuddin (1990) subdivided the Dupi Tila aquifer into 3 sub-units: the Upper Aquifer Sub-unit, the Middle Aquifer Sub-unit and the Lower or Main Aquifer Sub-unit (Hasan, 1999; Davies, 1994; MPO (1987); Ravenscroft, 2003; Figure: 2.5).

1.4. Water Level

Groundwater plays a vital role in providing water for agriculture, industry, and domestic use in Gazipur. It is under pressure mainly due to factors as increasing population, urbanization, and industrial growth. Rapid industrialization and urbanization have increased the demand for groundwater, leading to excessive extraction in some areas. The extensive extraction of groundwater, combined with other factors such as climate change and land-use changes, has contributed to declining groundwater levels in Gazipur. In some areas, this has resulted in the deepening of wells and reduced well yields. (Islam et al., 2017; Parvin, 2019)

Groundwater level conditions of Gazipur district were reviewed following a systematic approach by using secondary data collected from Bangladesh Water Development Board (BWDB), Department of Public Health Engineering (DPHE). Weekly groundwater level (GwL) data collected for time period covering more than three decades between 1989 to 2020. The water level measurements were calibrated using records from 18 observation wells (Figure 2.6). Annual mean groundwater level for the district were plotted against time to assess variability of GwL, indicating water level depth increases with urbanization and industrialization concentrations.

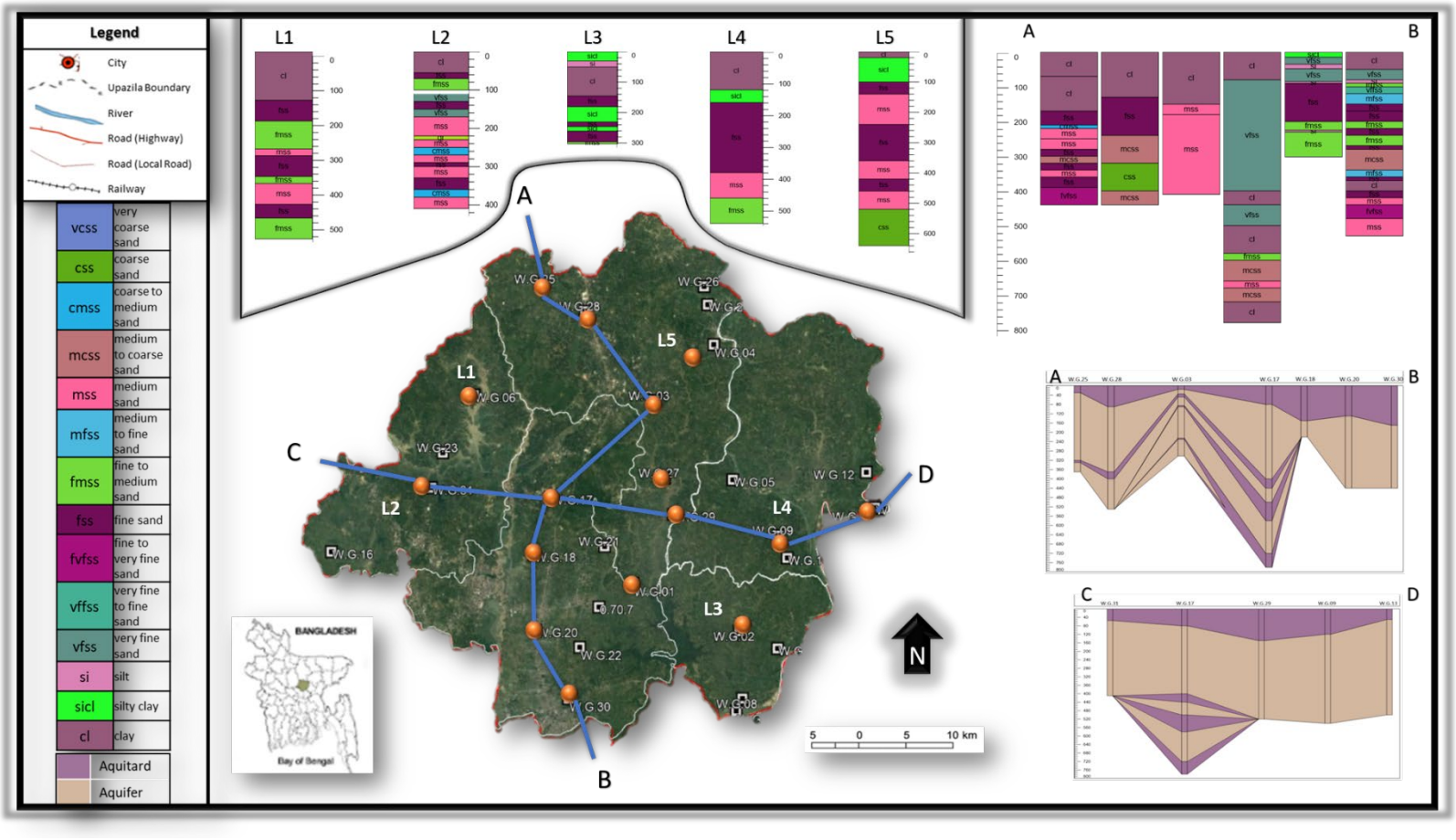

Figure 2.5: Stratigraphic and hydrostratigraphic profile across Gazipur District.

Figure 2.6: Map shows the location of BWDB water level observation wells in Gazipur District. Well numbers on the map signifies the BWDB wells as mentioned below.

A dramatic shift of groundwater level can be observed during 2016 - 2017 period, as no evidence of weather affects it can be attributed to a sudden increase of urbanization and industrial activities (Figure 2.7). Almost 1.13 million m^3/d of water was abstracted from Gazipur district area for domestic and industrial purpose and 0.7 million m^3/d for irrigation. Spatial distribution map of the district indicate that greater drop of water table must be due to regional settlements and industrial localities. (Figure 2.8; Figure 2.9; Figure 2.10)

1.5. Climatological Condition

The average temperature in Gazipur is 25.8 °C, with the most noteworthy normal in May, at around 28.9 °C, and the most reduced normal in January, around 18.8 °C. Gazipur locale features a subtropical rainstorm climate. It receives 2036 millimeters of precipitation annually, with 5 millimeters of typical rainfall in December. With an average of 388 millimeters, June is the month with the most precipitation. The distribution of rain throughout the region is irregular. (Parvin, 2019; Figure 2.1.

1.6. Land Cover and Land Use

The total land area in Gazipur City Corporation (Gazipur area) is 41300 hectares; cultivable land is 30645 hectares, fallow land is 1140 hectares, and forests are 5052 hectares; the single crop is 49.3 percent, double-crop is 26.2 percent, and the treble crop is 24.5 percent; 42 percent of the land is irrigated (BBS 2014a; BBS 2014b; BBS, 2015).

1.7. Urbanization and Industrialization

Rapid industrialization in Bangladesh ensures the opportunity to become a middle-incomecountry by 2021. Urbanization and Industrialization are growing simultaneously, both are interconnected and dependent on each other (Islam et al., 2016; Simu et al., 2016; Figure 2.12).

The district covers an area of 1,741.53 square kilometers and has a population of over 4.2 million people, making it one of the most populous districts in the country. In recent years, Gazipur has experienced rapid urbanization, as people from rural areas have migrated to the district in search of employment opportunities. The growth of the ready-made garment industry and other manufacturing sectors has also contributed to the urbanization of the district., and as such, it has many settlements of different sizes and types.

The largest settlement in Gazipur is the city of Gazipur itself, which serves as the administrative headquarters of the district. It is home to a population of over 1.5 million people and is known for its vibrant markets, shopping malls, and industrial zones. Gazipur City zone covers almost 48.50 km^2, subdivided into a center range, which encompasses 16 km^2 surrounding the city's core, and a periphery region, which includes the remaining 32.5 km^2 (BBS, 2020; BWP, 2019).

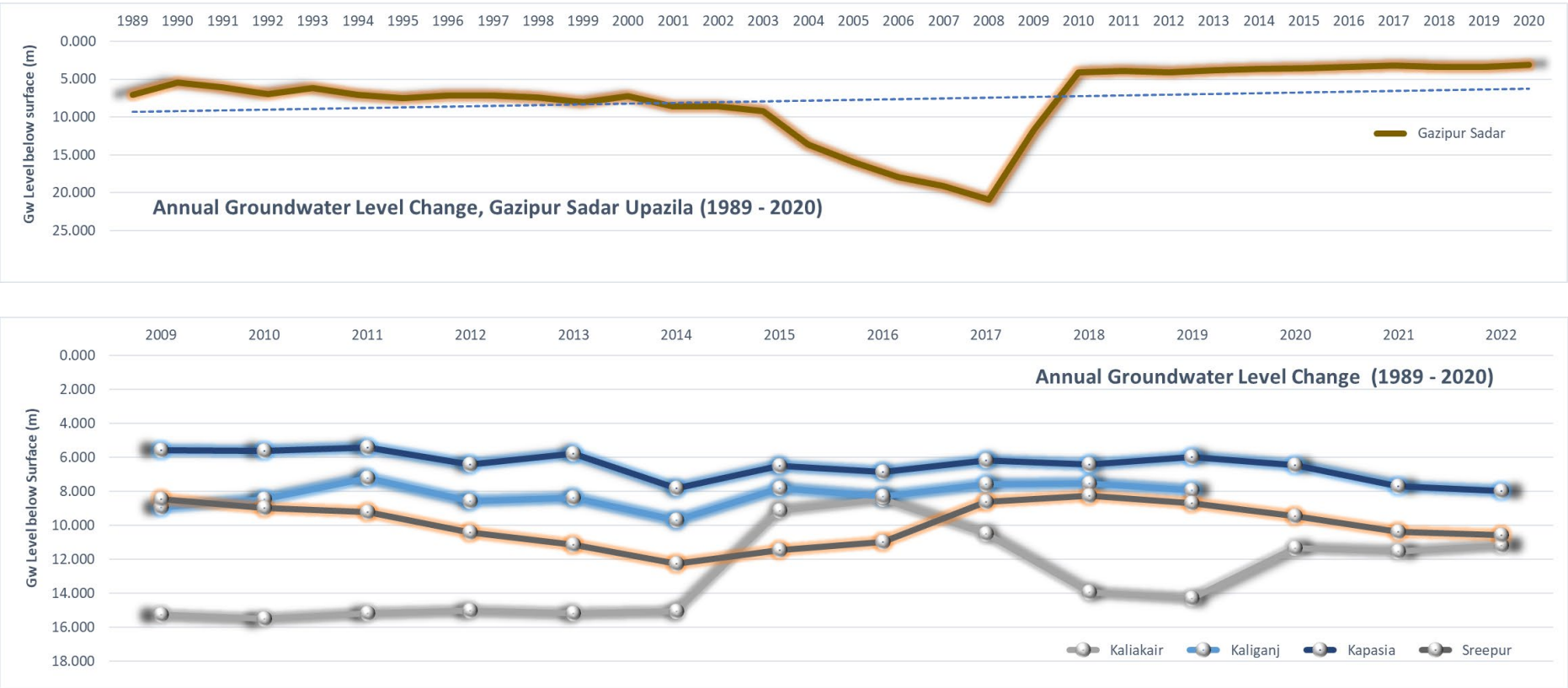

Figure 2.7:Annual groundwater level change at different Upazila of Gazipur District.

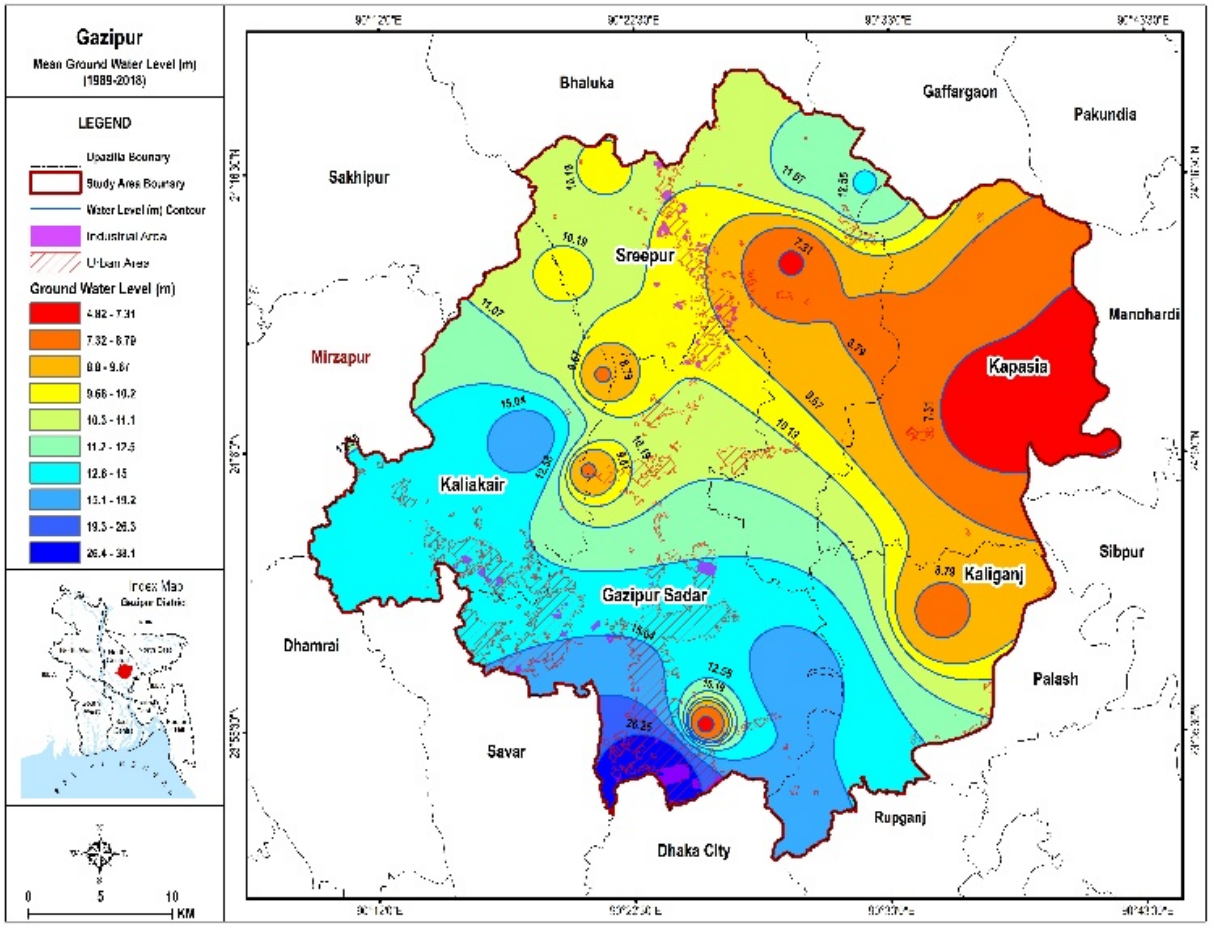

Figure 2.8: Water table contour maps mean Water Level (1989 -2018).

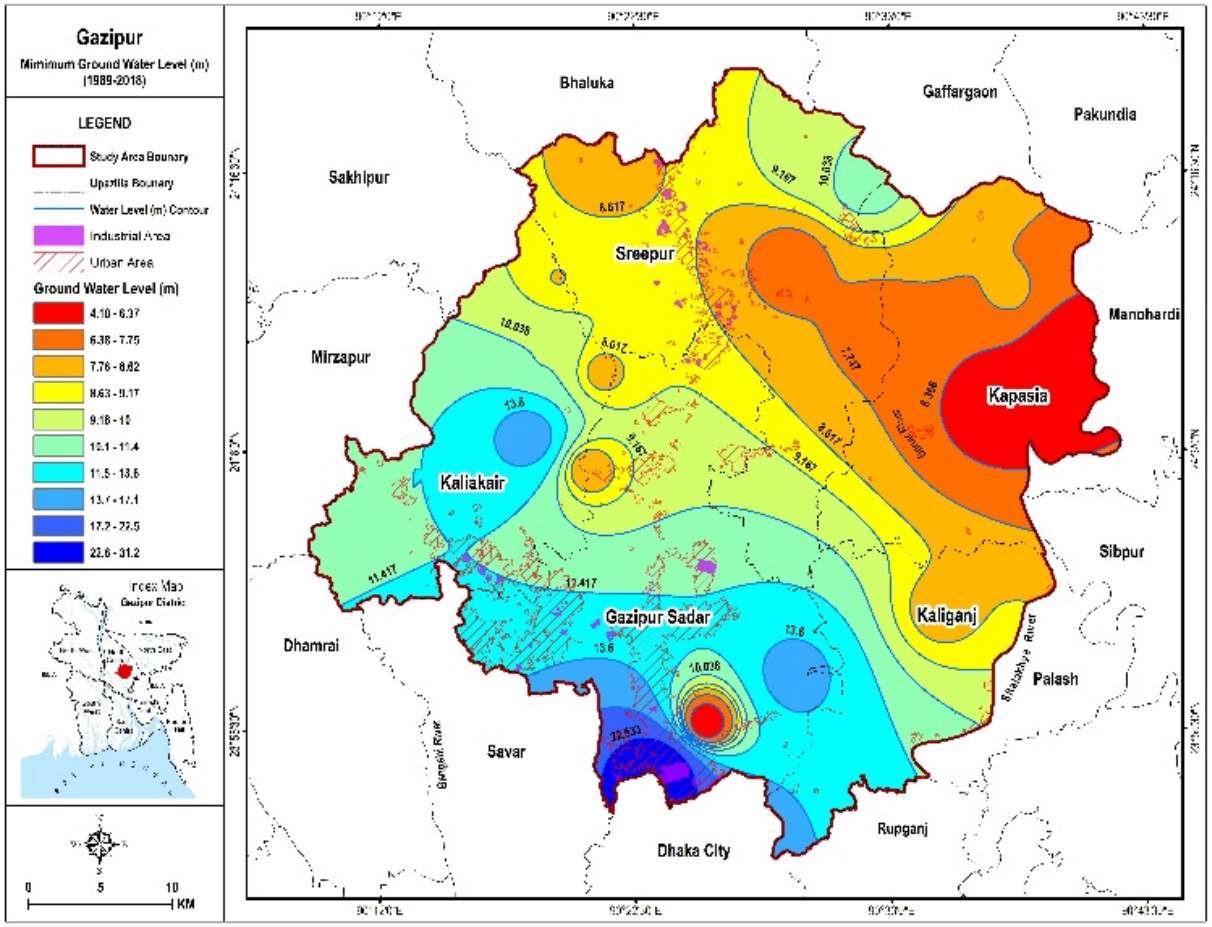

Figure 2.9:Water table contour maps Minimum Water Level (1989-2018).

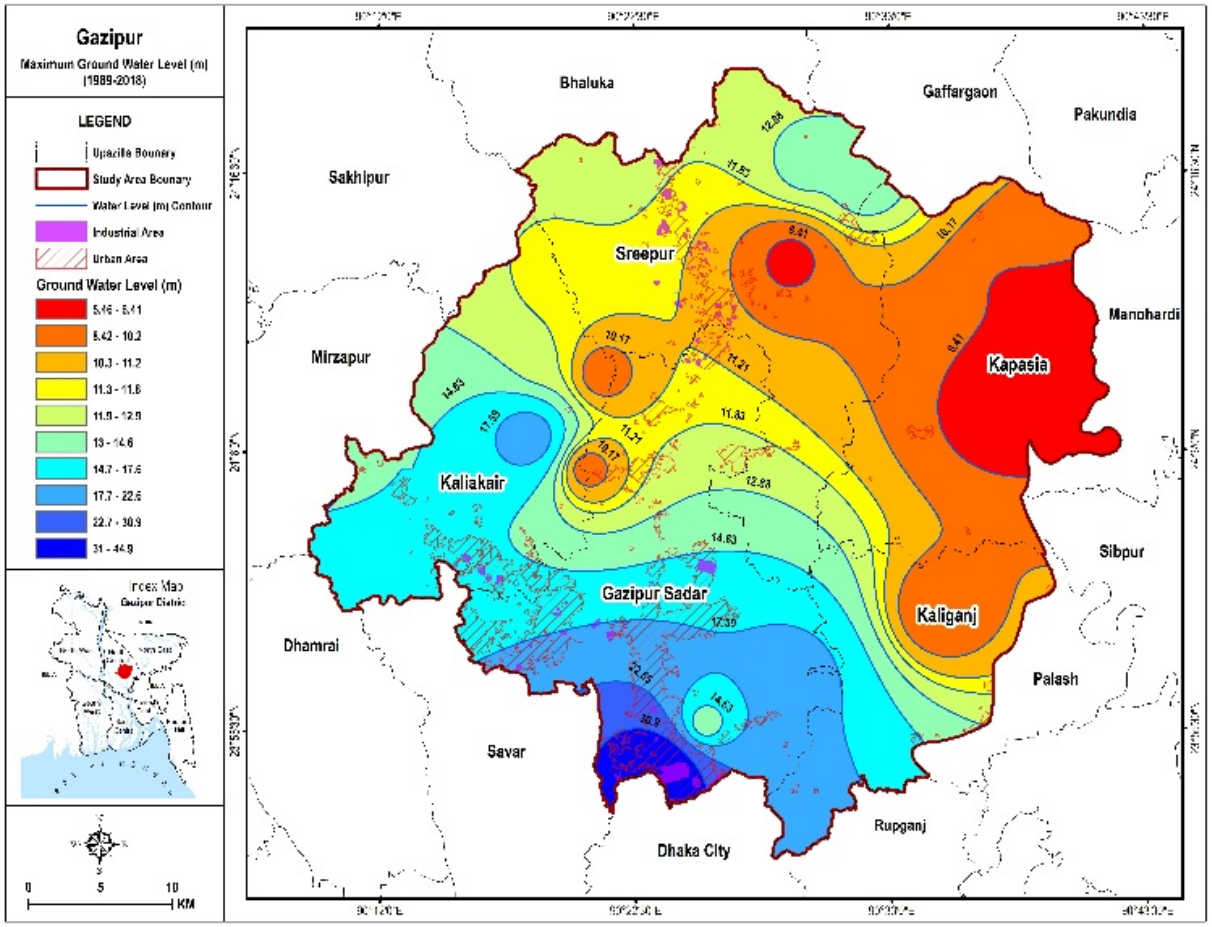

Figure 2.10: Water table contour maps Maximum Water Level (1989-2018).

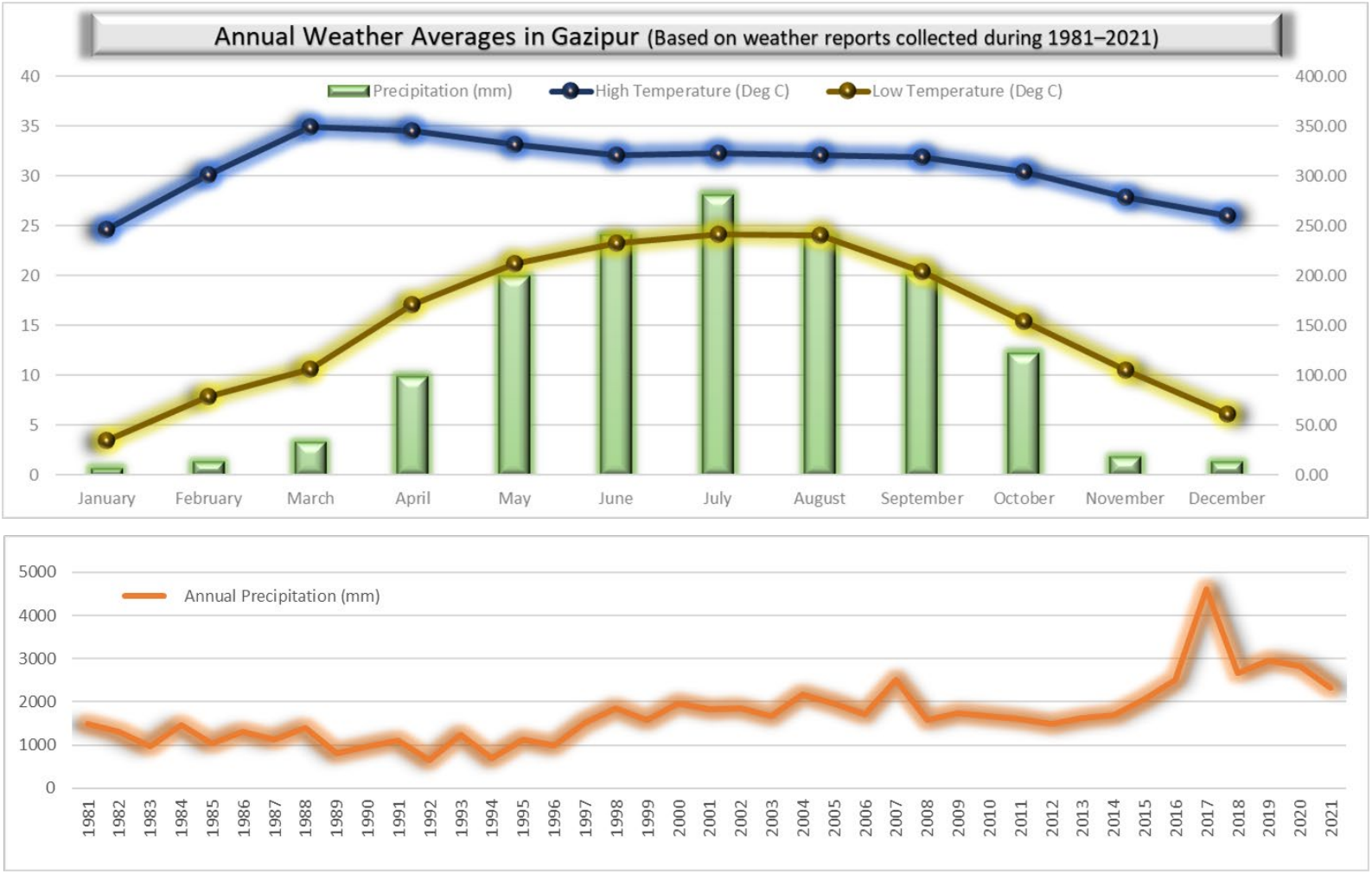

Figure 2.11: Annual weather variations for Gazipur district, based on data collected from BMD and Nasa Powers.

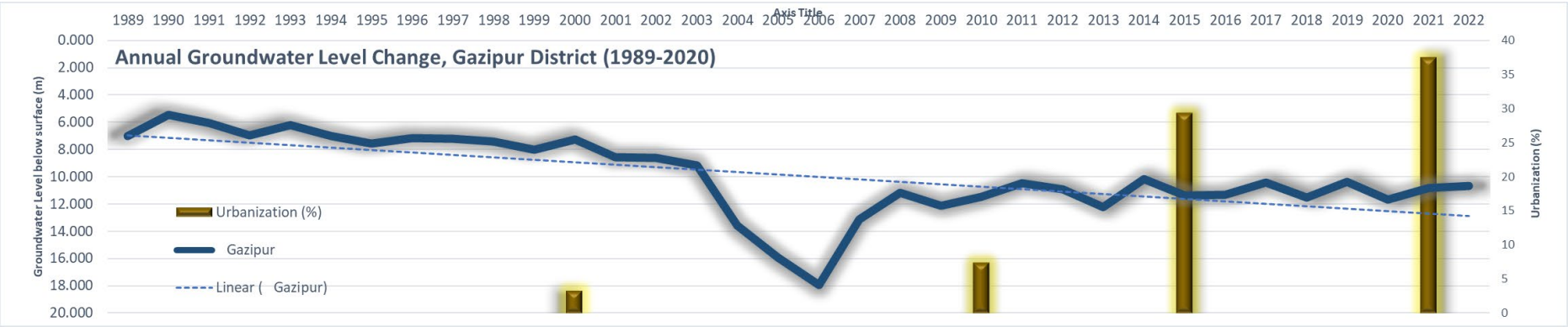

Figure 2.12: Comparative change between Groundwater Level (GWL) and Population Change (growth). This shows a strong relationship between the two factors, how urbanization is affecting groundwater resources, a growing trend.

The highest population densities are situated in the center of the central zone, while rural or semi-rural enclaves are located on the periphery. A few mechanical clusters, spontaneous urban private, and other urban periphery employments are dispersed over the rural hinterland. Horticulture and related occupations are burdened by spontaneous urban development. Consequently, the rural hinterland increasingly accommodates a large population of vagrants (BBS, 2014b; BBS, 2020). Other significant settlements in Gazipur include:

- Tongi: A rapidly growing industrial town located on the outskirts of Dhaka city. It is home to several large factories and serves as a major transportation hub for goods and people.
- Kapasia: A rural upazila (subdistrict) in Gazipur that is known for its natural beauty and agricultural productivity. It is home to several historical sites, including the Sreepur Zamindar Bari and the Bhawal National Park.
- Kaliakair: Another rural upazila in Gazipur that is known for its agricultural productivity. It is home to several large markets and serves as a hub for trade in agricultural goods.
- Pubail: A small town in Gazipur that is known for its textile industry. It is home to several large textile mills and serves as a hub for the production and export of textiles.

Gazipur is a rapidly growing industrial and commercial hub, home to a number of noteworthy organizations, including Bangladesh Rice Investigate Organized (BRRI), Bangladesh Agrarian Investigate Organized (BARI), CERDI, Seed Certifying Office, Security Printing, Machine Devices Production line, Bangladesh Arms Production line, Diesel Plant, Bangladesh Organized of Innovation (BIT), BRAC Dairy Cultivate, Incineration Ghat, etc. Factories include an aluminum production line, material plants, the pharmaceutical industry, the cosmetics industry, a machine apparatus manufacturing plant, a diesel plant, a security printing press, an arms manufacturing plant, a ceramics manufacturing plant, the packaging industry, the brick field, and the clothing industry. House Businesses incorporate weaving, goldsmith, metalworker, earthenwares, bamboo and cane work, fitting, bidi, and woodwork. Various caps, bazaars, and fairs are within the zone. Caps and bazaars number 36, the most famous of which are Tongi, Pubail, Mirzapur, Kasimpur, Joydebpur, Baruni Mela (Kaddar), and Rath Mela (Joydebpur) (BBS, 2020; BWP, 2019).

1.8. Forests and Natural Habitats

Gazipur district has a significant portion of forest cover, several protected areas, including wildlife sanctuaries and national parks. Some of the notable forests and parks in Gazipur district are described below. The district has a significant amount of forest cover, which helps to maintain the ecological balance of the region and provides habitat for various species of flora and fauna.

- **Bhawal National Park**: Bhawal National Park is located in the northeastern part of Gazipur district and is one of the largest national parks in Bangladesh. The park covers an area of 1,600 hectares and is home to various species of plants and animals, including deer, monkeys, wild boars, and numerous bird species. The national park was built in

1974 and formally pronounced in 1982 in the Bangladesh Natural life Act, 1974 (Sarker & Huq, 1985).

- **Gazipur Safari Park**: Gazipur Safari Park is a wildlife park located in the southeastern part of the district. It covers an area of 1,600 acres and is home to numerous species of mammals, reptiles, and birds. The park is divided into two sections, the Herbivore section, and the Carnivore section.
- **Muktijoddha Park**: Muktijoddha Park is a park located in the center of Gazipur city. The park covers an area of 20 acres and has a significant amount of greenery and trees.
- **Joydevpur Reserve Forest**: Joydevpur Reserve Forest is a protected forest area located in the southwestern part of Gazipur district. The forest covers an area of approximately 300 hectares and is home to various species of flora and fauna, including the Indian cobra, barking deer, and pythons.
- **Tongi Park**: Tongi Park is a small park located in the northwestern part of Gazipur district. The park covers an area of 5 acres and has a small pond and a significant amount of greenery and trees.

1.9. Aquifer Mapping

Aquifer mapping is the process of identifying, delineating, and characterizing underground layers of water-bearing permeable rock, sediment, or soil, known as aquifers. The main purpose of aquifer mapping is to understand the distribution, extent, and properties of these subsurface water resources. Aquifers of the study area are part of the Bengal Basin aquifer system, which is one of the largest groundwater systems in the world. The aquifer is composed of layers of sand and gravel, which are able to store and transmit water. This has led to a decline in water quality. The thickness of the Gazipur aquifer varies across the region. The Gazipur aquifer is an important source of water for irrigation, drinking, and other uses. The aquifer supplies water to over 2 million people in Gazipur district and surrounding areas (BBS, 2014, Parvin, 2017; Jamil & Ahmed, 2015).

The aquifer system Gazipur District area has four aquifers and four aquitards (Akhter & Hussain, 2017). But Individual logs and cross sections indicate the presence of only the Upper Aquitard (Madhupur Clay) and the Upper Aquifer (Aquifer 1) throughout the study area. the lower layers are discontinuous and are separated by clay lenses occasionally. These subunits are again hydraulically connected by vertical leakages at certain extent (Hasan, 1999). Previous studies suggest that the lower system might be a multi-layered leaky aquifer system and classifying them into layers will result into an overcomplicating aquifer system.

Thus, for this study a simpler subdivision of the aquifer system has been adopted – an aquitard (clay unit) underlain by an aquifer unit (Dupi Tila unit), which is overlying an aquitard unit. Both continuous and present through-out the aquifer system of the study area.

3 LITERATURE REVIEW

LITERATURE REVIEW

A detail and extensive literature review was conducted for this research to identify theoretical frameworks and methodologies to assist in designing research questions and hypotheses. This review helped in identifying the gaps and explaining how the research will contribute to the field. It will provide context for the research by placing it within the larger academic discourse.

A detail and extensive literature review was conducted for this research to identify theoretical frameworks and methodologies to assist in designing research questions and hypotheses. This review helped in identifying the gaps and explaining how the research will contribute to the field. It will provide context for the research by placing it within the larger academic discourse. In various regions of the Gazipur District, many researchers have undertaken major scientific and technical studies. These activities included a geochemical assessment of water resources, and evaluation of water resource vulnerability, a Land Use Suitability report, and a groundwater flow system. Most projects involved the Greater Dhaka Division or a portion of the Gazipur District. Very few were performed throughout the entire District.

Studies were done by Simu et al. (2017), Anannya et al. (2012), BBS (2014a), BBS (2014b)BBS (2013), Begum et al. (2009), Hasan et al. (2019), Al-Ferdous (2012), LGRD (2006), ICDDRB (2016), Islam et al. (2020), Islam et al. (2017), Simu et al. (2018), Sultana (2019), Shapla et al. (2015), Parvin (2018), Hassan and Southworth (2017), and others.

Gazipur is one of the districts of the Dhaka division. It is bordered north by Mymensingh and Kishoreganj, east by Narsingdi, south by Naranyanganj and Dhaka, and west by Tangail. On January 16, 2013, Gazipur City Corporation, the largest city corporation in Bangladesh, was founded. It consists of 57 wards and a total of 329.53 square kilometers. The population density of the Gazipur City Corporation is 1,884 inhabitants per square kilometer. It is located in an area with an average annual precipitation of 2,376 millimeters. The residents of the Gazipur City Corporation obtain their water from the municipal supply or their source. The pipeline water supply of the Gazipur City Corporation covers around 98 square kilometers. Because most people lack access to municipal water, they are forced to rely on their resources, primarily groundwater (WaterAid, 2018).

1.10. Hydrogeology and Groundwater Conditions

Shamsudduha et al. (2010) explained that Bangladesh occupies much of the Bengal Basin, one of the largest sedimentary basins in the world and the major depocenter of sedimentary fluxes from the Himalayan and Indo-Burman mountain ranges which are drained by the Ganges-Brahmaputra-Meghna (GBM) river system. This river system forms the world's largest delta, the Ganges-Brahmaputra- Meghna (GBM) Delta that covers almost all of Bangladesh. (Shamsudduha and Uddin, 2007)

The Pleistocene terrace deposits, Madhupur Tracts, located in slightly elevated (10–20 m above sea level) central parts of Bangladesh and covering almost entire of Gazipur District, are generally brown or tan colored, highly weathered, and more compacted than floodplain and deltaic deposits that are generally young (Holocene age), gray colored, and composed of sand, silt, clay, and occasional peat deposits. soil composition in Pleistocene terraces, Madhupur clay formation, are mainly clayey. Surface geology and soil composition which generally characterize shallow aquifers in Bangladesh largely control the timing and pathways of groundwater recharge to aquifers (MPO 1987; UNDP 1982; BARC, 1988; WARPO 2000; BGS & DPHE, 2001).

Groundwater in Bangladesh generally occurs at shallow (<10 mbgl) depth within widespread alluvial deposits (MPO, 1987). Shallow groundwater levels essentially follow surface topography. Groundwater levels are higher in northwestern parts of the country but generally low in the south. Aquifers that occur within the upper 80–100 mbgl of the stratigraphic sequence are generally identified as the shallow aquifer, and the deep aquifer occurs at >100 mbgl (Ravenscroft 2003).

1.11. Groundwater Geochemistry

According to Begum et al. (2009), the Madhupur tract consists of a diverse variety of soils produced over the Madhupur clays that are deficient in weatherable minerals. The floodplain transports an abundance of sediments from their origins. These sediments are mineral-rich and rapidly erode under high temperatures and seasonal wet and dry conditions, releasing Ca, Mg, K, Fe, Mn, Cu, Zn, P, etc. According to the results, the overall content of Fe, Mn, Cu, and Zn increases. All analyzed regions had abundant micronutrients (Fe, Mn, Cu, and Zn). Despite this, Bangladesh's chemical research, fertilizer tests, and field surveys have identified a wide region of soils deficient in accessible micronutrients. In the future, micronutrient insufficiency is projected to increase as crop intensification continues.

Al-Ferdous et al. (2012) claimed that rural farming in Bangladesh has been evolving from a robust agro-based business, from the backyard poultry rearing system to a commercial intensive one, over the past two decades.

The investigation conducted by Al-Ferdous et al. (2012) in Sreepur Upazila, Gazipur District, revealed that birds slaughtered, eviscerated, and dressed under local conditions are contaminated from the point of slaughtering to the point of consumption. There are biomagnifications at all stages of handling, transportation, and retailing. Contaminants may include feces, offal, carriage vehicles, cages, chicken feed, and waste. Escherichia coli is an essential contaminant during the slaughtering, handling, packaging, and washing processes. In any environment, the use of antimicrobials generates selective forces that promote the survival of antibiotic-resistant bacteria.

In the Gazipur City Corporations, over fifty percent of rubbish is placed in open spaces outside a residence, while 47.2% is disposed of on the premises. In addition, waste is collected daily in at least 40 percent of regions, whereas garbage is never collected in 37 percent of situations.

Sultana (2009) described the groundwaters in Sreepur Upazila, Gazipur District, as Ca-Na-HCO3-Cl. Potassium is more rapidly taken from solution by plants and clay minerals than sodium. Hence sodium concentrations are substantially higher than potassium concentrations. Again, Ca concentrations are greater than Mg concentrations because the sedimentary carbonates calcite, dolomite, and gypsum are the most soluble minerals in the study area. CaSO4 constitutes the primary source of sulfate.

Islam et al. (2020) determined that the waste material had a measurable effect on the soil quality, with the samples containing more available sulfur (S) but less total nitrogen (N), available phosphorus (P), and organic matter (OM). Iron (Fe) > zinc (Zn) > lead (Pb) > copper (Cu) > cadmium (Cd) was found to have the highest concentrations of heavy metals in soils, followed by zinc (Zn) > lead (Pb) > copper (Cu) > cadmium (Cd). This could be related to the waste leachates that percolated. The metal species were found to be somewhat lower at the accumulation site for solid waste and greater at the accumulation location for industrial effluents. Due to the fact that these heavy metals are eventually absorbed by developing plants and enter the food chain, this condition may be deemed hazardous. Therefore, reckless trash disposal should be discouraged, and a waste management and treatment policy for waste dumping and disposal should be implemented.

Industrial wastewater negatively influences the soils downstream more than solid waste. The soil pH was neutral and agriculturally appropriate (Al-Shaibani & Raza, 2004; Islam et al., 2020).

Simu et al. (2018) explained that soil samples from the industrial region of Gazipur reveal a neutral pH, which is optimal for nutrient uptake. For plant growth, moisture content, organic carbon, and organic matter are enriched in the soil. Al>Fe>K>Mg>Ca>Rb>Mn>Si>P is the tendency observed in the concentrations of the various species, as determined by analyses of occurrence. Most elements are used as fertilizer for soil nutrient supplementation and as raw materials in industrial processes. Industrial activities and agrochemicals primarily cause Gazipur district's degrading trace element situation. The contamination factor shows heavy metal contamination in the Gazipur region. Analyses of the pollution load index reveal that the locations are polluted by trace elements, whose origins are primarily industrial activities and agrochemicals.

A vast number of water quality criteria might make it challenging to evaluate water quality. Traditional water quality evaluation approaches compare experimentally established parameter values to an existing local normative, which does not give a global overview of spatial and temporal changes in the total water quality (Debels et al., 2005; Kannel et al., 2007; Edmund &

Shand, 2008). Numerous water quality indices were developed to provide a global perspective on the spatial and temporal changes in water quality to integrate complex water quality data and provide a simple and understandable tool for informing managers and decision-makers about the overall water quality status. An early water quality index was proposed by Horton (1965), and then developed by Brown et al. (1970), Dojlido et al. (1994), and Pesce & Wunderlin (2000).

It is possible to assess the water quality of any specific region or source using physical, chemical, and organic criteria. If the values of these parameters exceed the permitted limits, they are detrimental to human health. Water Quality Index (WQI) is one of the most persuasive measures of water quality that may determine if water sources are suitable for human use. The WQI can describe the water quality state across a vast area (Tyagi et al., 2013).

WQI employs water quality data and contributes to revising regulations developed by various environmental monitoring agencies. It has been determined that individual water quality variables cannot be used to characterize water quality (Tyagi et al., 2013).

The WQI illustrates the combined effect of many water quality measures and conveys water quality information to the public and policymakers. A typical WQI methodology is founded on the most prevalent elements, presented in three steps: Parameter Selection, Determination of Quality Function (curve) for Each Parameter Considered as the Sub-Index, and Sub-Index Aggregation with Mathematical Expression (Yogendra & Puttaiah, 2008; Terrado et al., 2010; Abbasi & Abbasi, 2012; Tyagi et al, 2013).

Multiple water quality indices have been developed to assess the water quality. Typically, these indices are calculated by comparing the amount and types of water quality measures measured to regional norms. Certified water quality indicators can rapidly reveal annual cycles, regional and temporal water quality changes, and water quality trends, even at low concentrations. Based on the number of water quality criteria utilized, existing indices contain significant variations and limits that are not widely recognized (Chaturvedi & Bassin, 2010; Brown et al., 1970).

Several water quality indicators have been developed to evaluate an area's water quality. They are based on the amount and types of water quality measurements. Even at low concentrations, water quality indicators are approved to rapidly reveal annual cycles, regional and temporal changes, and trends in water quality. The existing indices contain significant differences and limits (Tyagi et al., 2013).

Various WQI determination methods include the US National Sanitation Foundation Water Quality Index, the Canadian Water Quality Index, the British Columbia Water Quality Index, and the Oregon Water Quality Index. Weight Arithmetic Water Quality Index (WAWQI), National Sanitation Foundation Water Quality Index (NSFWQI), Canadian Council of Ministers of the Environment Water Quality Index (CCMEWQI), Oregon Water Quality Index (OWQI), etc. have

been formulated by several national and international organizations. A comparative overview of several methods has been explained in Table 3.1.

1.12. Vulnerability Assessment

DRASTIC is one of the most used groundwater vulnerability estimation tools, . Since Margaret introduced the concept of groundwater vulnerability in 1968, a variety of definitions have been presented. The sum of the ratings and weights given to each of the parameters results in the DRASTIC Vulnerability Index (DVI). We were able to identify three classifications, ranging from very low to very high, by examining the vulnerability map. It is a model that takes into account the primary geological and hydrological aspects that could have an effect on aquifer pollution. Its initials stand for depth to groundwater, recharge rate, aquifer, soil, topography, impact of the vadose zone, and hydraulic conductivity of the aquifer (Margat et al., 1968).

The inherent sensitivity of water to various pollutants (independent of their form) is caused by diverse human activities. Because different aquifers react differently to the same contaminant due to physicochemical differences, each situation has its vulnerability signature, which is determined by the pollutant's properties, taking into account the time of impact, the intensity of effects, and the interaction between the intrinsic vulnerability components and the contaminant. (Doerfliger et al., 1999; Gogu and Dassargues, 2000; Barbulescu, 2020). Different types (Table 3.2) of vulnerability approaches can be grouped into three categories which are;

- Category 1: The index-based methods consider soil and unsaturated zone characteristics. They are divided into the followings (Foster, 1987);
    - Hydrogeological Complex and Settings methods (HCS);
    - Matrix Systems approaches are based on combining two parameters and Rating Systems.
- Category 2: The statistical approaches that assess the groundwater vulnerability through statistical analysis or regression models (Masetti et al., 2009).
- Category 3: The Methods are based on simulation techniques for forecasting the processes related to contaminant transport (Neukum et al., 2008).

An approach based on an index is independent of data availability and similarity. The first and second types of methods are utilized to examine the intrinsic vulnerability of expansive areas (Kumar et al., 2015). The most used index methods for studying groundwater vulnerability are explained in Table 3.2, a brief overview of different methods, emphasizing their usage differences.

Table 3.1: Overview and review of different types of Water Quality Index (WQI) methods and rating systems.

Methods	Equation	WQI Value	WQI Rating	Advantages	Disadvantages
National Sanitation Foundation (NSF) WQI	$WQI = \sum_{i=1}^{n} Q_i . W_i$	91-100 71-90 51-70 26-50 0-25	Excellent WQ Good WQ Medium WQ Bad WQ Very Bad WQ	• Summarizes data in the index value. • Evaluation between areas & values. • Index value relates to using. • Facilitates communication.	• Loss of data during data handling. • Lack of dealing with uncertainty and subjectivity.
Canadian Council of Ministers of the Environment (CCME) WQI	$WQI = 100 - \frac{\sqrt{F_1^2 + F_2^2 + F_3^2}}{1.732}$	95-100 80-94 60-79 45-59 0-44	Excellent WQ Good WQ Fair WQ Marginal WQ Poor WQ	• Represent a variety of variables • Flexible • Adaptable • Suitable for evaluation • Easy to calculate	• Loss of information. • Manipulative. • Similar importance to all variables. • Only partial diagnostic.
Oregon WQI	$WQI = \sqrt{\frac{n}{\sum_{i=1}^{n} \frac{1}{SI_i^2}}}$	90-100 85-89 80-84 60-79 0-59	Excellent WQ Good WQ Fair WQ Poor WQ Very poor	• Un-weighted harmonic square means to allow impacted parameter influence • Acknowledge parameters' differing significance • Equation sensitive to changes & impacts	• Does not consider changes. • Cannot infer quality outside the network. • It cannot be used to provide definitive information about water quality.
Weight Arithmetic WQI	$WQI = \frac{\sum Q_i . W_i}{\sum_i}$	0-25 26-50 51-75 76-100 > 100	Excellent WQ Good WQ Poor WQ Very Poor WQ Unsuitable WQ	• Incorporate multiple parameters • Less number of parameters required • Useful for data presentation • Reflects the composite influence	• may not carry enough information. • Over validation of parameters.

(modified from Raza, 2008; Yogendra & Puttaiah, 2008; Terrado et al., 2010; Abbasi & Abbasi, 2012; Tyagi et al, 2013).

Table 3.2: Overview of different types of groundwater vulnerability assessment methods. (Modified from Raza, 2008; Jahromi et al., 2020; Kumar et al., 2013; Machiwal et al., 2018; Al-Adamat and Al-Shabeeb, 2017; Barbulescu, 2020; Kirlas et al., 2022; Tziritis et al., 2020)

Approaches	Proposed / Introduced by	Parameters										Type / Purpose
		Depth to Water	Net Recharge	Hydraulic conductivity	Soil	Topographic Slope	Hydrogeological features	Unsaturated Zone	Stream Network	Aquifer thickness	Land use	
DRASTIC	Aller et al., 1987	■	■	■	■	■	■	■				most widely used
GOD	Foster, 1987	■					■	■				classical system for quick assessment
SINTACS	Civita, 1994	■	■	■	■	■	■	■	■	■	■	surface waters and aquifer interactions
RIVA	Zwahlen, 2003		■				■	■				compares hydrogeological systems
EPIK	Doerfliger et al., 1999		■		■	■	■	■				developed especially for karst areas
COP	Andreo et al., 2009		■		■	■		■	■		■	flow, overlying layer, and precipitation
PI	Goldscheider et al., 2000	■	■		■	■	■	■	■		■	consideration of karst aquifers
AVI	Van Stempvoort et al., 1993		■	■			■			■		based on two physical parameters
SI	Ribeiro, 2000	■	■			■				■	■	pollution potential of agricultural groundwater environments

1.12.1. DRASTIC-based vulnerability assessment

Aller et al. (1987) prepared the DRASTIC vulnerability assessment system to assist in identifying the relative vulnerability areas. Only a basic understanding of hydrogeology and the processes that cause groundwater contamination govern. The DRASTIC methodology is based on hydrogeological settings and relative ranking of hydrological parameters (Table 3.3). DRASTIC dimensions do not constitute a method or a model but a framework. Contrary to most understanding and misconception, the DRASTIC method was never introduced specifically for unconfined aquifers. Instead, the approach clearly stated that different practices should be taken while using it for Confined and Unconfined aquifers based on the nature of the impermeable layer.

Aller et al. (1987) explicitly explained that the treatment of confined aquifers only differs from the unconfined aquifer by three data layers: the depth to water, aquifer media, and impact of the vadose zone. The water table is the water surface below the ground level. The water table may remain fixed at any specific level or fluctuate seasonally. Aquifer media is the consolidated or unconsolidated medium that serves as an aquifer (such as sand, gravel, or limestone). An aquifer is a rock formation that will yield sufficient water for use. The pollution potential of soil is influenced by its type, shrink/swell potential, and grain size. The attenuation characteristics between the water table and soil horizon are defined as the vadose zone.

The number of control parameters sets the type of the catastrophe function, which is determined by the appropriate classification number. This numerical approach, known as DRASTIC, was designed to assess ground water. The system contains three significant parts: weights, ranges, and ratings (Dee et al., 1973; Aller et al., 1987).

Jamil and Ahmed (2016) conducted a groundwater pollution risk assessment study, considering the contamination source as the industrial area on the banks of Tongi River. This area facilitates the largest and oldest industries in the country, consisting of almost 200 industries. Their study revealed that the low-lying area near riverbanks is the riskiest zones.

1.12.2. Applicability in unconfined aquifer

For an unconfined aquifer, depth to water refers to the top of the water surface. The term 'net recharge' refers to the quantity of water per unit area of land that percolates through the soil, transporting surface contaminants to the aquifer. Recharge to unconfined aquifers occurs more readily, and the pollution potential is comparatively greater than in confined aquifers. For a confined aquifer, the influence of the vadose zone is extended to include both the vadose zone and any saturated zones that exist above the aquifer (Aller et al., 1987).

Table 3.3: Ranges, ratings, and relative weights used for the indicators in the DRASTIC model (Some units in this table are converted to SI units, where applicable. (Modified from Aller et al., 1985; Raza, 2008).

	HYDROGEOLOGIC PARAMETERS	RANGE		RATING	WEIGHT	
					GMIP*	AP**
D	Depth to Water	**ft**	**m**		5	5
		0-5	0 – 1.52	10		
		5-10	1.52 – 3.05	9		
		15-30	3.05 – 9.14	7		
		30-50	9.14 – 15.24	5		
		50-75	15.24 – 22.86	3		
		75-100	22.86 – 30.48	2		
		100+	30.48+	1		
R	Net Recharge	**in**	**mm**		4	4
		0-2	0 – 50.8	1		
		2-4	50.8 – 101.6	3		
		4-7	101.6 – 177.8	6		
		7-10	177.8 – 254	8		
		10+	254+	9		
A	Aquifer Media	Massive Shale		2	3	3
		Metamorphic / Igneous		3		
		Weathered Meamorphic / Igneous		4		
		Thin bedded Sandstone, Limestone, Shale Sequences		6		
		Massive Sandstone		6		
		Massive Limestone		6		
		Sand and Gravel		8		
		Basalt		9		
		Karst Limestone		10		
S	Soil Media	Thin or Absent		10	2	5
		Gravel		10		
		Sand		9		
		Shrinking and / or Aggregated Clay		7		
		Sandy Loam		6		
		Loam		5		
		Silty Loam		4		
		Clay Loam		3		
		Nonshrinking and Nonaggregated Clay		1		
T	Topography (%)	0-2		10	1	3
		2-6		9		
		6-12		5		
		12-18		3		
		18+		1		
I	Impact of Vadose Media	Silt / Clay		1	5	4
		Shale		3		
		Limestone		6		
		Sandstone		6		
		Bedded Limestone, Sandstone, Shale		6		
		Sand and Gravel with significant Silt and Clay		6		
		Metamorphic / Igneous		4		
		Sand and Gravel		8		
		Basalt		9		
		Karst Limestone		10		

1.12.3. Applicability in confined aquifer

Aller et al. (1987) stated that the depth of water for a confined aquifer is the top of the aquifer. Under normal conditions, a confined aquifer is protected by the impermeable layer as they retard water movement. But, at some confined aquifers, head distribution creates a flow condition that converts a confined to an unconfined layer. Therefore, many specified layers get water intake from recharge, causing the infiltration of contaminants. Recharge water is the reason for leaching and transporting solid or liquid contaminants. Thus, recharge rate becomes proportional to the potential pollution rate (Nadiri et al., 2018).

1.13. Land Cover and Land Use

Land use and land cover (LULC) aids in assessing the human impact on natural resources and the environment. The majority of LULC maps are generated using remote sensing images. Using Earth observation (EO) satellite photos, it is feasible to monitor huge areas on a local, national, and international scale (Giuliani et al., 2020; Saah et al., 2020; Zioti et al., 2022).

According to the Bureau of Statistics Census of 2001, the population of the Gazipur City area was 128,429. The people of Gazipur City were estimated to be 300,112 in 2005, with 156,586 men and 143,526 women. Migration enticed by employment opportunities created by the rise of commercial and industrial operations inside the City Corporation is primarily responsible for the significant proportional increase in population. (Raza et al., 2021).

Based on the national average growth rate of 3.3%, a conservative population estimate for 2010 is 353,008 people, and it is projected to reach 371,380 in 2015 and 422,530 in 2020. This is a growing pace that will continue to increase. In the future decade, it is anticipated that the population of the Gazipur District could exceed the average projection (BBS, 2014a; BBS, 2014 b).

Shapla et al. (2015) classified land in the district of Gazipur, located in the northern region of Dhaka. Landsat 4 - 5 TM and Landsat 7 ETM+ images acquired in 2001, 2005, and 2009, BNP, are identified using unsupervised classification with image segmentation. During the eight years, the paddy area rose from 30 percent to 37 percent, followed by the homestead area (55 percent to 57 percent) and the urban area (1 percent to 3 percent). These changes were accompanied by a decline in forest land cover (14 percent to 3 percent). In the category of the homestead, the presence of diverse types of vegetation makes it difficult to distinguish the category from the paddy field; however, paddy has a higher level of accuracy than other categories, ranging from 93.70 percent to 99.95 percent.

Simu et al. (2017) conducted a study encompassing the southern and southwestern regions of the Gazipur District. According to the 1992 land cover map the main varying pattern was vegetation, including farmland, forestland, and grass plain. The second land use category was a

settlement, which included dwellings, buildings, and markets. The 2003 land cover map analysis shows that the predominant LU change took place during 1992. The dominant land use type was settlement followed by it was vegetation. Then followed by bare ground and water bodies. But the volume of water bodies decreased dramatically as agricultural practices expanded into low-lying areas that were once water bodies. By analyzing the land use pattern of 2014, it can be determined that settlements were the predominant land use type, but water bodies were the predominant land cover in that region. Following the formation of the export processing zone, water bodies were gradually encroached upon. In that order, the remaining space is occupied by vegetation, barren terrain, and bodies of water. The interpretation of satellite images of the study area in 1992, 2003, and 2014 has revealed that the land use pattern has altered significantly. The study region's water bodies accounted for 19.53, 3.37, and 3.45 percent of the total area in 1992, 2003, and 2014, respectively. It is evident from this scenario that the water bodies in the research area are diminishing rapidly, with a significant decline between 1992 and 2003. The settlement area has steadily risen from 33.51 percent in 1992 to 47.78 percent in 2003 to 55.93 percent in 2014. Due to these alterations in land use patterns, a substantial quantity of water bodies has been filled and occupied due to industrial settlements, planned and unplanned urbanization, bare land, etc. After industrialization, the area of water bodies has shrunk drastically, while the population in the study area has exploded.

Anannya et al. (2012) Greater Dhaka faces insurmountable obstacles due to its uncontrolled growth, high levels of poverty and social vulnerability, inadequate infrastructure, lack of social services, poor physical and social environment quality, and incompetent urban management. Due to the high expense of food and the inability of the majority of families and households to purchase or supply an adequate quantity of nutritious food, they are subject to hunger and disease. Urban agriculture promotion and sustainability appear to overcome these issues while increasing income and employment in urban areas. Additionally, road accessibility has a substantial impact on urban and peri-urban agriculture.

The study by Sayed et al. (2015) examined the effects of industrial impact on land-use patterns and surface water quality of the Turag River and its associated wetlands next to Konabari, BSCIC region in Bangladesh's Gazipur district. Brickfields and industry expanded between 2004 and 2010, whereas water bodies, croplands, and vegetation shrank. The most considerable proportion of industry area incorporation came from croplands (49.44 percent; 356 acres), while the lowest proportion came from aquatic bodies (0.14 percent; 1 acre). Except for pH, all water quality parameters surpassed the permissible limits, showing that the water of the Turag River and its surrounding wetlands have been highly polluted. It should not be used to sustain human and animal life without adequate treatment.

Yesmin et al. (2014) assessed LULC variations over the past two decades in the Mirzapur Union of the Gazipur district using remote sensing and GIS technology. According to the conclusions of

this study, forest cover has dropped by 20.29 percent, settlement area has expanded by 28.64 percent, and water bodies have reduced by 6.25 percent. During the same period, bare land rose by 20.91 percent due to unplanted forest clearance. During this period, numerous new infrastructures were created, Sal's deforestation rate doubled. The most prominent aspects are the expansion of brickfields and various businesses.

1.14. Contamination Indicator

Various groundwater quality and quantity studies predict the electrical conductivity (EC) or total dissolved solids (TDS).

The US EPA has indicated that conductivity is a valuable indicator of water quality. Conductivity changes may suggest that a discharge or other pollutant source has reached an aquatic resource. Significant changes in conductivity (typically increases) may indicate that a discharge or other source of disturbance has degraded the state of health of the water body and its accompanying biota. Human activity generally increases the number of dissolved solids entering the water, increasing conductivity.

Naudet et al. (2004) employed the EC value of groundwater to map the geometry of contaminated plumes accurately. A map of EC offered information regarding the mineralization of the groundwater. They demonstrated that EC might be used as an indicator to determine the downstream trajectory of the contaminated plume.

Kheirandish et al. (2020) investigated groundwater quality and quantity to model the watershed's electrical conductivity (EC) and anticipate trends in EC changes using MT3DMS. Rajamanickam and Nagan (2010) utilized a similar method to forecast groundwater quality using five distinct MODFLOW and MT3DMS scenarios. Rahnama and Zamzam (2011) also used a model to simulate the quantity and quality of groundwater.

1.15. Groundwater Flow and Contaminant Transport Modeling

Bangladesh's aquifers are composed of unconsolidated, river-borne alluviums and semi-consolidated sedimentary layers.

Using present technology, high-quality water from the upper few hundred meters can be extracted at an economically viable cost. Major hydrogeological investigations sought to hydrostratigraphically characterize the sedimentary sequence. Furthermore, a geochronological characterization of Bangladesh's aquifers is essential. The classification should consider the depositional environment and geomorphology of the region.

According to Sultana (2019), all geologic formations are horizontal, and the aquifer has an undefined aerial extent. Influenced by the pumping test, the aquifer in their study area has a

homogeneous, isotropic, and uniform thickness. The density and viscosity of groundwater are constant. The potentiometric surface variations are a result of the local pumping wells.

There are three principal aquifers in the central region of Bangladesh:

- An upper (composite) aquifer, which can reach depths of 50 m and is covered with an upper silty clay layer of less than 20 m;
- A middle (main) aquifer of fine to heavy sands, which is generally 10 m to 60 m thick and in most areas is hydraulically connected with the composite aquifer above; and
- A deep aquifer of medium, medium-to-fine, or medium-to-coarse sand is generally found at depths below 100 m.

Groundwater exists at shallow depths in Bangladesh's enormous alluvial aquifers and supplies most of the country's drinking and agricultural water needs. Until recently, 97% of the population drank groundwater, and groundwater sources serve more than 70% of the entire irrigated area. More than 10 million shallow hand-pumped wells, often known locally as hand tube wells (HTWs), provide potable water to nearly all rural and urban areas without a piped water supply (Akhter & Hossain, 2017; Hasan et al., 2007).

Population growth in Dhaka and Gazipur, as determined by Parvin (2018), has resulted in an increase in resource demand and drastic alterations in the groundwater level's diagonal pattern since 2000. The most important result of this study is the identification of the decreasing groundwater level in the Gazipur and Dhaka Districts. The report also reveals a growing tendency of drought due to rising demand. The unsustainable drop of groundwater levels in Dhaka and Gazipur can be attributed to drought periods, which are a direct result of increasing population pressure.

MODFLOW/MT3DMS approach provides accurate solutions for problems involving variable-density ground water flow and solute transport. The interaction of social and environmental processes can be better understood through the modeling of social-ecological systems. The complexity and unpredictability of both underlying subsystems impact the quantitative social-ecological models. Groundwater quality can be related land use variations and GIS can be used to conduct spatial analysis of LCLU data. Thus, can be incorporate with MT3DMS processing for better understanding of the spatial and temporal variations (Langevin and Guo, 2005; Zhang et al., 2013).

1.16. Groundwater, Urbanization, and Industrialization

Currently, more than 74% of irrigated land is covered by groundwater, growing yearly. The majority of the nation's industries obtain their water needs from groundwater. The desire for water has several origins (Foster et al., 2011). In addition to natural evapotranspiration, water is

consumed by water supply, irrigation, fisheries and livestock, industry, navigation, and the environment (where salinity control is essential). The National Water Management Plan (NWMP) of Bangladesh forecasts that in 2025, the proportions of total water demand will be as follows: instream, 56%; agricultural, 32%; environment, 9%; and water supply, 3% (Zahid et al., 2013).

The first comprehensive classification of Bangladesh's aquifer systems was undertaken by UNDP (1982). In accordance with this three-tiered classification, the country's aquifers were divided into the top or composite aquifer, the main aquifer, and the deep aquifer to a depth of around 140 meters (Hassan, 2004; LGRD, 2006).

During the National Water Plan development, the Master Plan Organization (MPO) suggested two aquifer sequences, Upper and Lower, for the Miocene–Pliocene and Holocene deposits. Based on the isotopic composition of groundwater, the IAEA proposed four isotopic water types at different depths and suggested a modified three-fold classification: First Aquifer (70–100 m), Second Aquifer (200–300 m), and Third Aquifer (>300 m).

BGS & DPHE (2001) used the UNDP three-fold classification with new nomenclature to divide the aquifers into the Upper Shallow Aquifer, the Lower Shallow Aquifer, and the Deep Aquifer. The Ground Water Task Force provided a geological classification of the major aquifers in their 2002 report. According to this classification, the significant aquifers are the Upper Holocene Aquifer, the Middle Holocene Aquifer, the Late Pleistocene–Early Holocene Aquifer, and the Plio-Pleistocene Aquifer (MPO, 1985; Aggarwal et al., 2000; Zahid et al., 2004; Ahmed, 2011).

Due to the natural expansion and rural migration, cities and towns' growing size and population are key elements in environmental change (Salaj, et al., 2018). The world's rural population doubled over the 20th century, whereas the urban population increased by over 10. The subsurface is vital to providing water, sanitation, and drainage and managing this ever-changing urban environment. Consequently, the combination of water supply sources is likely to change as water demand increases. Cities can encroach and encircle their peri-urban wellfields, degrading their water supply (Konikow & Mercer, 1978; Foster et al., 1998; Morris et al., 2003a).

Urbanization affects the quantity and quality of groundwater by substantially altering recharge patterns and rates, introducing new abstraction regimes, and negatively affecting groundwater quality. Increases in groundwater abstraction beneath significant cities can be substantial, long-lasting, and locally oriented (Morris et al., 2003b; Xu & Usher, 2006; Raza et al., 2020).

Depending on the aquifer's vulnerability to contamination and its susceptibility to the impacts of excessive abstraction, urbanization activities may impact the underlying groundwater. Not all hydrogeological ecosystems are equally susceptible to contamination or extraction-related consequences. The concept of aquifer vulnerability is already well-established, and approaches

for its assessment and mapping at various scales have been developed, particularly for metropolitan areas (Foster et al., 1998; Morris et al., 2003b; Xu & Usher, 2006).

The study completed by Parvin (2019) indicated a very alarming condition of Groundwater level in Gazipur. She compared population growth to groundwater level fluctuation. Her comparative study indicated a drastic water level drop as the population multiplied over the years, reaching a peak by 2019.

4 METHODOLOGY

METHODOLOGY

The research methodology is a strategic or scientific approach to organizing and analyzing the study's scattered ideas and views. It also expresses collecting, processing, and analyzing data and information techniques. This study has maintained a systematically arranged methodology to achieve the desired output. The workflow of this research work is presented in Figure 4.1.

To understand the status of the groundwater condition, 17 well data were collected from BWDB. Daily Water level data for years from 2008 to 2018 were used. Unfortunately, few blank values were identified. Each station's water level data were taken as a mean monthly and yearly to represent groundwater conditions. Mean monthly datasets for the selected reference period (2008-2018) were processed for assessment.

Annual mean groundwater levels (below ground) for ten locations within Dhaka and Gazipur districts were plotted against time to understand GWL fluctuation. The changes indicated the depletion rate. It is necessary to determine the maximum depletion period for the Dupi Tila aquifer.

1.17. Groundwater Sample Collection, Analysis, and Interpretation

Water quality samples were collected at different sites to understand quality impact and trends. Water quality data usually exhibit non-normal distribution, presence of outliers, missing values, values below detection limits (censored), and serial dependence. Appropriate statistical approaches were applied to analyze water quality data.

1.17.1. Groundwater sampling

The environment-sensitive Physico-chemical parameters are temperature (T^oC), electrical conductance (EC), and hydrogen-ion concentration (pH), which were measured at the sampling point and later at laboratory water samples were analyzed according to the standard methods.

Extensive groundwater sampling was conducted in 2018. A total of 143 groundwater samples were collected from hand tube wells (HTW), shallow tube wells (STW), and monitoring wells (MW) in January 2017, following standard protocol. Electrical conductivity (EC) was measured using a portable EC meter on the spot in the field. Nitrate ($NO3^-$) was determined by Ion Chromatography System (ICS), and chromium (Cr) was analyzed using Atomic Absorption Spectrometry (AAS), GBC Scientific Equipment at the Geochemical Laboratory, Geology Department, University of Dhaka.

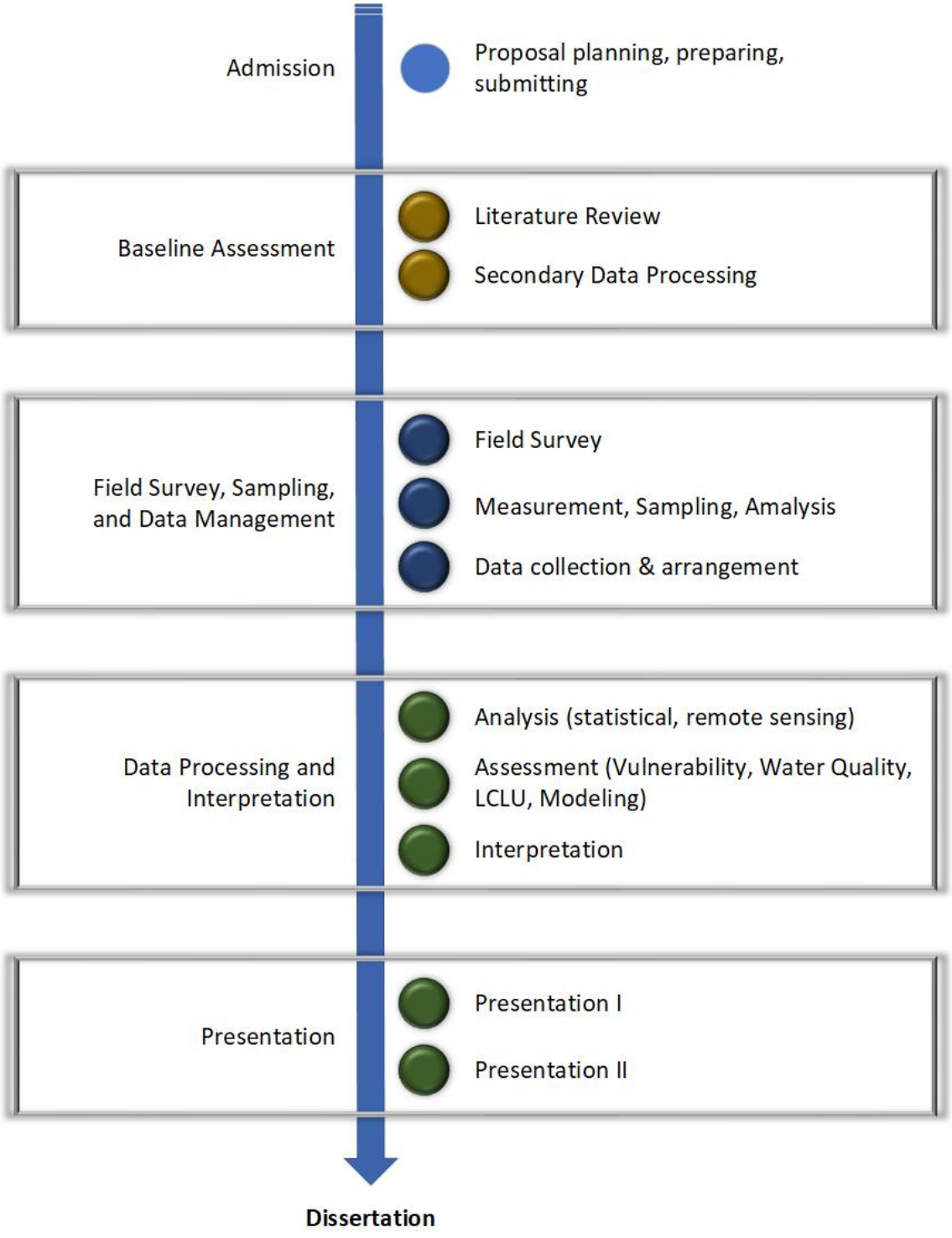

Figure 4.1: Methodology Workflow showing different stages of this research work.

Almost 145 samples were collected and sampling points measured at every sampling year throughout the district. Due to the restrictions and limitations, only Physico-chemical parameters were measured at the site during 2019, 2020, and 2021 (Figure 4.2).

1.17.2. Groundwater classification

Piper diagram and Durov Diagram for the Water samples collected across Gazipur District were prepared using Rockware2002. The Piper Trilinear diagram (Piper, 1953) is an effective tool in segregating analysis data for critical study with respect to the sources of the dissolved constituents in waters, modifications in the character of water as it passes through an area, and related geo-chemical problem. Langguth (1966) classified seven sectors within the piper diagram.

Major ions are plotted in the two base triangles of the diagram as cation and anion percentages of milli-equivalents per liter. Total cation and total anions are each considered as 100 percent. The respective cation and anion locations for analysis are projected into the rectangle, representing the total ion relationship. The diagram's central plotting field (diamond-shaped) is divided into nine areas, and water is classified into nine types depending on the area where the analyses fall. In this classification, alkali cations (Na^+ and K^+) are called primary constituents, and the alkaline earth cation (Ca^{2+} and Mg^{2+}) are called secondary constituents. The strong acid anions (SO_4^{2-}, Cl^- and NO_3^-) are treated as saline constituents, and CO_3^{2-} and HCO_3^- are termed weak acids. Mutual balancing of these anions and cations determines the chemical character of water (Domenico & Shcwartz, 1997; Aral &Taylor, 2011).

Durov diagram is based on the percentage of the significant ions' in meq/l. The cations are plotted on the left side and anions on the upper part of the diagram, from where the sample points are projected onto the central square. The Durov diagram allows displaying specific geochemical processes affecting water genesis. Lloyd & Heathcoat (1985) classified the main square into nine sectors, each signifying a certain process

Doneen's Permeability Index indicates the impact of soil from irrigation water due to soil permeability. It is influenced by soil's sodium, calcium, magnesium and bicarbonate contents. Doneen (1964) has evolved a criterion for assessing the suitability of water for irrigation based on the permeability index (PI) as given below.

$$PI = \frac{Na + \sqrt{HCO_3}}{Ca + Mg + Na} \times 100 \qquad \text{----- (Eq. 1)}$$

where Na, Ca, etc., values are in on meq/l.

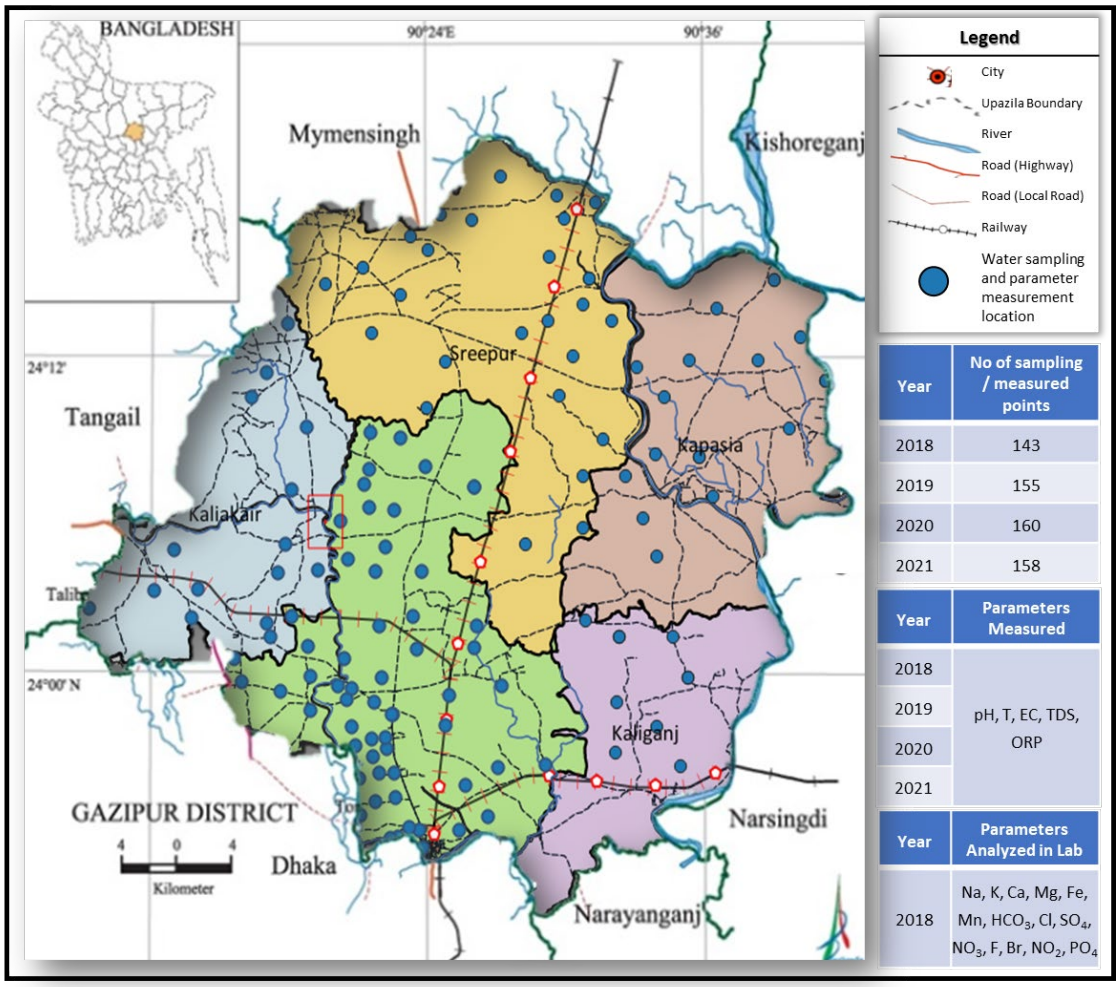

Figure 4.2: Groundwater sampling points for the Hydrochemical study of the Gazipur District. Samples were collected from the Upper Dupi Tila Aquifer. The same sampling points were used for 2018, 2019, 2020, and 2021 to ensure proper impact and trend assessment. Sample collection for over the years was disrupted due to the global pandemic situation.

1.17.3. Statistical interpretations

1.17.3.1. Arithmetic Mean

The mean is the most familiar used statistical approach. The confidence intervals for the mean provide a range of values around the mean where the "true" mean can be expected. Calculating the Arithmetic Mean involves dividing the number of data elements by the total number of data elements. (Helsel et al., 2020) Symbolically, the arithmetic mean is expressed as,

$$\bar{x} = \frac{\sum x_i}{n} \qquad \text{----- (Eq. 2)}$$

where is the arithmetic mean for a sample (dataset), and ∑is summation notation. xi refers to each data set element as i ranges from 1 to n. n is the number of elements in the data set.

1.17.3.2. Standard Deviation

The Standard deviation calculates the dispersion of the data. This is also a widely used parameter as it indicates the average deviation of each element value from the mean. The formula for sample standard deviation is as follows (Helsel et al., 2020).

$$S = \sqrt{\frac{\sum(\bar{x} - x_1)^2}{n - 1}} \qquad \text{----- (Eq. 3)}$$

1.17.3.3. Skewness

Shapiro et al. (1968) simulated samples to detect non-normality. Based on their results, the skewness test is the most appropriate for use in groundwater quality analysis.

The skewness coefficient measures the deviation of the distribution from symmetry (Harris et al., 1987). It is a measure of the symmetry of a distribution around its mean.

$$B_1 = \frac{m_3}{{m_2}^{\frac{3}{2}}} \qquad \text{----- (Eq. 4)}$$

where m2 and m3 are respectively the second and third moments of the distribution around the mean. In a normal distribution, B1 = 0 (i.e. a symmetrical distance). If the skewness is different from 0, that distribution is considered asymmetrical (Helsel et al., 2020).

Plots skewed to the right infer that they have a long tail to the right (i.e., mode<median<mean), and a left-skewed distribution infers a long tail towards the left. Any order is possible according to the dataset condition. A bell-shaped Gaussian distribution, 68% of the values lie within one SD of the mean (on either side) (Helsel et al., 2020).

1.17.3.4. Student's t-Test

Testing for the particular form of seasonality where one season differs from the others may be accomplished by a two-sample comparison of means. The most common test to compare two standards is the Student's t-test (Swan & Sandilands, 1995). This test allows comparing two samples against one another. The calculated statistic is compared to tabulated values of the t-distribution. The test assumes the data are independent and come from normally distributed populations with equal variances (Harris et al., 1995).

The t-score is the desired level of confidence based on the degrees of freedom and the estimated population. The degree of freedom can vary after certain restrictions on values.

The hypothesis of the t-test is (Davies, 2002);

$$H_0 : \mu_1 = \mu_2 \qquad \text{----- (Eq. 5)}$$

It refers to the mean of the population represented by the two representative sample groups being the same. At a level of significance (10%; α = 0.10), the test statistics can be expressed as follows;

$$t = \frac{\bar{X} - \overline{X_2}}{S_e} \qquad \text{----- (Eq. 6)}$$

The standard error of the mean is calculated from the following equation:

$$s_e = s_p \sqrt{\frac{1}{n_1} + \frac{1}{n_2}} \qquad \text{----- (Eq. 7)}$$

where, sp is a pooled estimate of the standard deviation estimated from the variances of the two data sets

$$s_p^2 = \frac{(n_1 - 1)s_1^2 + (n_2 - 1)s_2^2}{n_1 + n_2 - 2} \qquad \text{----- (Eq. 8)}$$

The process of pooling the two sample variances creates an additional degree of freedom. The degrees of freedom for the t-test of equivalency are (Davies, 2002):

$$v = n_1 + n_2 - 2 \qquad \text{----- (Eq. 9)}$$

the t-test is based on three basic assumptions: samples are collected randomly, populations of the sample source are normally distributed, and variances of the two populations are equal.

1.17.3.5. F-Test

The assumption of equal variances can be checked using the F-test (Pfaffenberger and Patterson 1977). The F-distribution is named after the statistician Sir Ronald Fisher. This is the theoretical distribution of values that would be expected by random sampling from a normal population. The test-statistics, F, is the ratio between two sample variances (Davies, 2002):

$$F = \frac{s_1^2}{s_2^2} \qquad \text{----- (Eq. 10)}$$

Under the null hypothesis, this ratio is distributed as the F-distribution with (n1-1) and (n2-1) degrees of freedom. If the null hypothesis is correct, the calculated F value should be less than a theoretical F value.

1.17.3.6. Correlation Matrix

The correlation coefficient (r) expresses the linear association of random variables. Its value ranges from -1 to +1. The positive (+) and negative (-) signs of r infer proportional and inverse proportional relationships between variables, respectively. A value close to -1 indicates a strong negative correlation, and a value close to +1 indicates a strong positive correlation between variables. The closer the value of r to zero indicates, the poorer the correlation (Voudouris et al., 2000).

1.17.4. Water quality index (WQI)

Water quality indices are used to quantitatively assess water quality (Brown et al., 1970). The Water Quality Index (WQI) is used to detect and evaluate pollution in any area. Its indices are based on the physico-chemical parameters in water samples. Calculating WQI was completed following the equation of Horton's method, as stated below.

$$WQI = \frac{\sum Q_i . W_i}{\sum W_i} \qquad \text{----- (Eq. 11)}$$

where W_i = weight associated with i^{th} water quality parameter, Q_i = *sub-index for* i^{th} *water quality parameter, and* N = the number of water quality parameters.

The quality rating scale (Qi) for each parameter is calculated by using this expression:

$$Q_i = 100\left[\frac{V_i - V_0}{S_i - V_0}\right] \quad \text{----- (Eq. 12)}$$

where Vi is the estimated concentration of ith parameter in the analyzed water, Vo is the ideal parameter in pure water, Vo = 0 (except pH =7.0 and DO = 14.6 mg/l), and Si is recommended standard value of ith parameter.

The unit weight (Wi) for each water quality parameter is calculated by using the following formula:

$$W_i = \frac{K}{S_i} \quad \text{----- (Eq. 13)}$$

where K = proportionality constant and can also be calculated by using the following equation:

$$K = \frac{1}{\sum\left(\frac{1}{S_i}\right)} \quad \text{----- (Eq. 14)}$$

The computed WQI values are categorized into five groups. GIS was used to generate a map containing the research area's water quality and distribution information. The GIS attribute table independently recorded each chemical parameter's location information, concentration values, and weight (Wi). Then, qi and Si were calculated using the preceding expression from the GIS functions menu. Finally, the WQI values were computed by adding all Si. These values were then interpolated using an inverse distance approach and a moving average algorithm to build a WQI value map.

The reasoning behind selecting the average inverse distance approach is that points adjacent to an output pixel receive large weights, while points further away receive small weights. Therefore, values of points that are close to an output pixel have a more significant impact on the value of the output pixel than values of points that are further away. The output pixel values are the weighted averages of the input point values. Lastly, slicing choices are applied using these ranges of values and four groups of water quality classes to build a map showing the spatial distribution of water quality (Chakraborty et al., 2007).

1.18. Numerical Rating Using the DRASTIC Method

DRASTIC was developed in the USA by Aller et al. (1987). Seven hydrogeological attributes establish the acronyms of the DRASTIC process (Hasan et al., 2019).

The DRASTIC method assigns weight for specific indicators applying the Delphi procedure. On a scale from 1 to 5, weights are applied to the indicators to represent their relative importance to the pollution potential. In addition, subclasses of particular indicators are ranked according to their contamination contribution. For instance, a relative value of 5 will be assigned to an indicator that substantially affects the model calculation and 1 to a modest contribution. An indicator is then divided into sub-classes (range) and ranked based on its distinctive qualities for a certain study area. However, the rank may vary from one area of study to the next. The subclasses are allocated on a scale from 1 to 10, indicating the lowest contamination and the most, respectively. Regardless of the fixed weight values for each indication in the model, each input can be adjusted based on the area of interest (Aller et al., 1987; Hassan et al., 2019; Goossens et al., 1987).

Index values prioritize the study area with respect to groundwater contamination vulnerability. The index is a quantitative ranking factor, the higher the index, the greater the groundwater pollution potential. However, it is a relative value used only for comparative purposes (Ehteshami et al., 1991). The DRASTIC Index, a measure of the pollution potential, is computed by summation of the products of rating and weights of each factor as follows (Aller et al., 1987):

$$DI = D_r.D_w + R_r.R_w + A_r.A_w + S_r.S_w + T_r.T_w + I_r.I_w + C_r.C_w \quad \textit{- (Eq. 15)}$$

Where, DI= DRASTIC Index, D_r = rating to the depth to the water table, D_w = weight assigned to the depth to the water table, R_r = rating for ranges of aquifer recharge, R_w = weight for the aquifer recharge, A_r = rating assigned to aquifer media, A_w = weight assigned to aquifer media, S_r = rating for the soil media, S_w = weight assigned for soil media, T_r = rating for topography (slope), T_w = weight assigned to topography, I_r = rating assigned to vadose zone, I_w = rating assigned to vadose zone, C_r = rating assigned to hydraulic conductivity, and C_w = weight assigned to hydraulic conductivity.

Higher DI values indicate greater susceptibility to groundwater contamination. Even though the apparent subjectivity in its calculation DI reflects a complex composite of implicit factors such as travel time, sorption, and dilution (Rosen, 1994).

There are limitations to the DRASTIC method's adaptation to specific environmental situations (Hrkal, 2001). While selecting and compiling data, the user's subjectivity can influence the process. DRASTIC is based on criteria as opposed to particular site characteristics. The overestimation of the susceptibility of porous media aquifers relative to fractured media aquifers is an example of the influence of neglecting site-specific data (Rosen, 1994; Meeks and Dean, 1990; Kim and Hamm, 1999). Nonetheless, the primary advantage of the DRASTIC method is its weights of evidence approach; descriptive variables may be utilized in the statistical analysis as categorical or hierarchical variables (Barber et al., 1993).

Vulnerability assessment includes (1) vulnerability mapping using data collecting from relevant sources, data preparation, and model calculation; (2) assessing indicator efficiency using sensitivity analysis; and (3) validation of the resulting vulnerability map. Relevant databases were consulted to acquire primary and secondary sources for this investigation.

There are a variety of vulnerability assessment methodologies. Most recent attempts at mapping vulnerability relied on geographic information systems (GIS). This permits the importation, manipulation, analysis, and combination of point and area (polygon) data (Barber et al., 1993). It is possible to generate consecutive variants of the vulnerability map to acquire the most precise depiction of the vulnerability in a given region. The GIS technique is time-consuming and expensive as all data must be converted to vector format (Hrkal, 2001).

This research was conducted using the overlay/index DRASTIC approach. In the overlay/index method, applications map the physiographic and anthropogenic characteristics of a region using a numerical index or rating. The ratings may be treated equally or weighted in accordance with their proportional effect over the area (Hammerlinck & Arneson, 1998). The evaluations are then merged to produce a composite level of vulnerability. When the layers are combined, these point values are added to the vulnerability map. DRASTIC-generated groundwater vulnerability maps aim to identify regions with the greatest risk for groundwater pollution (Rupert, 2001).

- **D:** This information was collected from bore log data. Thirty-three bore logs depicted the subsurface lithological description and were used to determine aquifer properties. Once all logs had been inspected and recorded for depth in each place, the depth attributes were transferred to an Excel spreadsheet containing the geographic coordinates of each bore log. A GIS-based point shapefile was subsequently produced. To observe the spatial distribution of D, inverse distance weighted (IDW) interpolation techniques were utilized in a GIS setting (Almasri & Kaluarachchi, 2007; Gogu and Dassargues, 2000; Table 4).
- **R:** It was initially assessed by the water table fluctuation (WTF) method. The method estimates groundwater recharge as the product of specific yield (Sy) and the annual rate of water level rise or fall (Δh), including the total groundwater draft (Sophocleous, 1991). The governing equation of net recharge is:

$$net\ recharge\ = \mathrm{Sy} \times \Delta \mathrm{h} \qquad \text{----- (Eq. 16)}$$

  Previous studies state that groundwater recharge levels range from 223 to 437 mm/year. (Table 4)
- **A:** For the calculation of D, the kind of aquifer material was derived using the bore log information received from BWDB. A's spatial distribution was mapped using a method

identical to that of D. The aquifers in the study area comprised three separate lithologies: fine sand, medium sand, and coarse sand.

- **S:** The current soil texture map with a representative fraction (RF) of 1:500,000 was digitized. The map was used to identify soil textures in the research area. (Table 03).
- **T**: Information was acquired using the digital elevation map (DEM). Using GIS spatial analyst tools, slope (in percentage) was generated. Due to the area's flat terrain, the slope percentage change is low in Gazipur District, ranging from 0 to 12 degrees. The entire slope map was divided into five categories: 1%, 1% to 3%, 3% to 5%, 5% to 10%, and greater than 10%. The steep slope permits faster runoff, minimizing contaminants' migration into the aquifer. In contrast, water can remain longer in flat terrain, making contaminants easier to filter into the aquifer. (Table 03)
- **I**: It was derived from lithological information using the same approaches as the indications D and A. Most of the vadose zone materials in the research area are clay and silty clay. Their ratings were determined based on a comparative evaluation of how well the given vadose zone materials might behave as an infiltrating or permeability potential medium. Due to clay's extremely low permeability, it was assigned a low rank of 2 compared to silty clay, which was assigned a rank of 3 due to its averaged greater permeability calculated using the given equations. The estimated average hydraulic conductivity rate varies between 12.71 and 24.68 meters per day. In this investigation, IDW was utilized to determine the spatial distribution of hydraulic conductivity. The entire study region was separated into two subclasses, 15 m/day, and >15 m/day, based on this range of hydraulic conductivity. (Table 03)
- **C**: Hydraulic conductivity is important because it controls the rate of groundwater movement in the saturated zone, thereby controlling the degree and fate of contaminants. Hydraulic conductivity values used in this study were taken from different pumping test data done by different studies. the C is neither very high nor very low in the study area, a moderate ranking was assigned to the subclasses.

The minimum and maximum DVI values of the different vulnerability maps usually vary in different ranges. Therefore, the study normalized the DVI values for comparison purposes. The advantage of taking normalization is to break down the relationships of anomalies to generate smaller, well-structured relationships among different DRASTIC maps. The value of DVI maps was converted to the range of 0 to 100 using the following formula:

$$X' = \frac{X - X_{min}}{X_{max} - X_{min}} \quad \text{----- (Eq. 17)}$$

where X’ is the normalized index value, and X is the original index value obtained from different DRASTIC models.

1.19. Image Segmentation and Classification

Image processing is the operating and processing remotely detected digital data to create an end product, such as a change detection map. It includes four major components:

- Pre-processing,
- Classification,
- Accuracy assessment
- Change detection techniques.

Land Cover Land Use (LCLU) has been utilized for generalized information extraction. It generates a standard set of diagnostic attributes to describe various classes. Classifiers serve as standard building blocks that can be assembled to define the complicated semantics of each class (Giri, 2012).

Three historical Landsat satellite images spanning the research area have been utilized to examine the municipality level's spatiotemporal LCLU changes. (Table 4.1)

Landsat pictures were pre-processed using georeferencing and geometric correction to prepare multitemporal satellite images for reliable change detection and analysis. The EPSG:4326 - WGS 84 coordinate system was utilized.

To stress spectrally focused land cover classification methodologies. In Supervised Classification, the image analyst "supervises" the pixel categorization process by providing numerical descriptors of the various land cover types present in a scene to the computer algorithm. This operation is carried out in two distinct steps. The primary distinction between these methods is that supervised classification requires training steps followed by a classification step. In the unsupervised method, image data are initially categorized by aggregating them into the scene's natural spectral groupings or clusters. The image analyst then identifies these spectral groupings' land cover by comparing the classified picture data to ground reference data.

1.19.1. Object-based change detection

Studies of land use and land cover structure change usually need development and definition of more or less homogeneous land use/land cover units before the analysis is started. These have to be defined and spatially differentiated using the available data sources (e.g. remote sensing) and any other relevant information and local knowledge.

Using ERDAS Imagine 9.1, classification and interpretation of images were done. They utilize reference photographs (for example, digital orthophotos) (1980, 1992, and 2002). Using land cover maps, ground control signatures for the supervised classification were created.

Table 4.1: Landsat Band wavelength (nm) used for image classification. (Modified from Shapla et al., 2015; https://www.usgs.gov/faqs/what-are-best-landsat-spectral-bands-use-my-research)

Band	Landsat 8/9 Operational Land Image (OLI) and Thermal Infrared Sensor (TIRS)			Landsat 4-5 Thematic Mapper (TM) and Landsat 7 Enhanced Thematic Mapper Plus (ETM+)		
	Intensity (color)	Wavelength	Useful for mapping	Intensity (color)	Wavelength	Useful for mapping
Band 1	coastal aerosol	0.43-0.45	Coastal and aerosol studies	blue	0.45-0.52	Bathymetric mapping, distinguishing soil from vegetation and deciduous from coniferous vegetation
Band 2	blue	0.45-0.51	Bathymetric mapping, distinguishing soil from vegetation and deciduous from coniferous vegetation	green	0.52-0.60	Emphasizes peak vegetation, which is useful for assessing plant vigor
Band 3	green	0.53-0.59	Emphasizes peak vegetation, which is useful for assessing plant vigor	red	0.63-0.69	Discriminates vegetation slopes
Band 4	Band 4 - red	0.64-0.67	Discriminates vegetation slopes	Near-Infrared	0.77-0.90	Emphasizes biomass content and shorelines
Band 5	Near Infrared (NIR)	0.85-0.88	Emphasizes biomass content and shorelines	Short-wave Infrared	1.55-1.75	Discriminates moisture content of soil and vegetation; penetrates thin clouds
Band 6	Short-wave Infrared (SWIR) 1	1.57-1.65	Discriminates moisture content of soil and vegetation; penetrates thin clouds	Thermal Infrared	10.40-12.50	Thermal mapping and estimated soil moisture
Band 7	Short-wave Infrared (SWIR) 2	2.11-2.29	The improved moisture content of soil and vegetation; penetrates thin clouds	Short-wave Infrared	2.09-2.35	Hydrothermally altered rocks associated with mineral deposits
Band 8	Panchromatic	0.50-0.68	15 meter resolution, sharper image definition	Panchromatic (Landsat 7 only)	0.52-0.90	15 meter resolution, sharper image definition
Band 9	Cirrus	1.36-1.38	Improved detection of cirrus cloud contamination			
Band 10 - TIRS 1	Band 10 - TIRS 1	10.60-11.19	100 meter resolution, thermal mapping, and estimated soil moisture			
Band 11 - TIRS 2	Band 11 - TIRS 2	11.50-12.51	100 meter resolution, improved thermal mapping, and estimated soil moisture			

Change detection can be measured using data from a single sensor and data from numerous sensors acquired at different times. Due to their identical spectral, spatial, and radiometric resolutions, multiple pictures obtained with the Landsat-5 TM sensor do not require extensive pre-processing (Read & Lam, 2002).

1.19.2. Accuracy assessment

Utilizing rectified digital orthophotos allowed for direct comparison of image and orthophoto features during the selection of training samples for use in image classification and accuracy assessment of classed maps. This image preprocessing was performed using ERDAS Imagine Version 9.1.

On the basis of 270 stratified random sampling locations, a comparison between each categorized image, and a comparison with a suite of orthophotos, Google Earth Imageries, and existing land cover maps, the classification accuracy was evaluated. After a picture accuracy review, each image was vectorized into polygons. As a Minimum Mapping Unit for spatial landscape analysis, these polygon coverages were preprocessed to remove areas smaller than 1 ha. (Congalton & Green, 1999).

Kappa statistics/index were calculated for each classed map to evaluate the results' precision. Landsat land use/cover maps for 1976, 1992, and 2001 were classified with Kappa statistics of 78.1 percent, 78.6 percent, and 83.4 percent, respectively. The Kappa coefficient is the proportional reduction in error caused by a classification procedure compared to a purely random classification error. Kappa accounts for all parts of the confusion matrix, excluding coincidental agreements. Consequently, it gives a more stringent evaluation of classification precision. The Kappa coefficient was calculated according to the formula given by Congalton & Green (1999):

$$K = \frac{N\sum_{i=1}^{r} X_{ii} - \sum_{i=1}^{r}(X_{i+} \times X_{+i})}{N^2 - \sum^{ri=1}(X_{i+} \times X_{+i})} \qquad \text{----- (Eq. 18)}$$

where,

r = the number of rows in the error matrix

X_{ii} = the number of observations in row i column i (along the diagonal)

X_{i+} = is the marginal total of row i (right of the matrix)

X_{+i} = the marginal total of column i (bottom of the matrix)

N = the total number of observations included in the matrix

Overall Accuracy = $\frac{a}{b} \times 100 = \frac{26}{35} \times 100 = 74.29\%$

where, a is the total number of correctly classified pixels (diagonal) and b is the total number of reference pixels.

$$\text{Kappa Coefficient (T)} = \frac{(TS \times TCS) - \sum(CT \times RT)}{TS^2 - \sum(CT \times RT)} \times 100 \qquad \text{----- (Eq. 19)}$$

where, TS is the total sample number, TCS is the total number of correctly classified sample, CT is the total number of columns, and RT is the total number of rows.

$$T = \frac{(30*26) - ((8*9)+(4*4)+(7*6)+(7*7)+(9*9))}{(30*30) - ((8*9)+(4*4)+(7*6)+(7*7)+(9*9))} \times 100 = \frac{780-260}{900-260} \times 100 = 81.25\%$$

1.20. Chloride Mass Balance (CMB)

The Chloride Mass Balance (CMB) method calculates regional groundwater recharge values. The method is based on the annual precipitation, chloride concentration in precipitation, and chloride concentration in groundwater of the aquifer. (Bazuhaira & Wood, 1996)

$$Q = \frac{R \times Cl_{wav}}{Cl_{gw}} \qquad \text{----- (Eq. 20)}$$

where, Q= recharge flux (LT^{-1})

R= average annual rainfall (LT^{-1})

Cl_{wav}= weighted average chloride concentration in rainfall (ML^{-3})

Cl_{gw}= average chloride concentration in groundwater (ML^{-3})

M= mass unit, L= length unit and T = time unit

The limitation of this method is that Cl^- can originate from different unknown sources or is difficult to quantify, such as from infiltration of atmospheric deposition of Cl^- and seawater intrusion of Cl^- along with coastal aquifers. It can only be applied to the saturated zone provided there is an assumption of no evapotranspiration losses, upward or downward leakage, irrigation, or recycled waste water (Somaratne & Smettem, 2014).

1.21. Flow and Contaminant Transport Modeling

A numerical computer model is a program containing equations representing groundwater flow between model cells. As the equations are solved, a groundwater flow model predicts the amount of water flowing horizontally and vertically between cells and any changes in the volume of water stored in each cell (Bartolini and Vincent, 2017).

The U.S. Geological Survey created MODFLOW to characterize and forecast the behavior of groundwater flow systems. The Darcy flow equation and the mass continuity equation serve as the basis for the code (Hassan, 1992; Kahsay, 2008).

MODFLOW is a well-known modeling program that has been validated in a number of settings and is frequently used. MODFLOW was selected for this study due to its simple compatibility with the solute transport modeling program MT3D.

MODFLOW uses block-centered finite differences to resolve three-dimensional flow equations numerically. It comprises a main program, modules, and autonomous subroutines (Hassan, 2000; McDonald and Harbaugh, 1988; Hassan, 1992). MODFLOW is selected for the following reasons:

- MODFLOW is one of the most widely used groundwater flow codes in hydrogeology and can simulate steady-state and transient flow conditions in one.
- The model can simulate recharge, flow to wells, flow to drains and flow through riverbeds.
- MODFLOW is extensively tested in various environments under different conditions.
- The theory behind the model is well documented and relatively easy to understand.

The partial differential equation on which MODFLOW is based is:

$$\frac{\partial}{\partial x}\left[k_{xx}\frac{\partial h}{\partial x}\right]+\frac{\partial}{\partial y}\left[k_{yy}\frac{\partial h}{\partial y}\right]+\frac{\partial}{\partial z}\left[k_{zz}\frac{\partial h}{\partial z}\right]-W=S_s\frac{\partial h}{\partial t} \qquad \text{----- (Eq. 21)}$$

Where kxx, kyy, kzz represent hydraulic conductivity along x, y, and z coordinate axes (LT^{-1}) parallel to the major axes of hydraulic conductivity, h represents the potentiometric level (L), W is flexternal inflows or outflows of water (T^{-1}), S_s represents the specific storage of the porous media (L^{-1}), and t is time.

As there is no change in storage over time under steady-state conditions, the right-hand side of the equation is set to zero.

The first step in building the model was defining the represented region and boundary conditions using natural physical features and restrictions. The model encompassed the whole UTM-defined study region. The model grid network was created using a variety of hydrogeological parameters and aquifer geometry-related data. The entire area of research is shown using grid reference. The grid reference is used to prepare the data needed for import into the model. It was constructed by repeatedly subdividing a square mesh. 2 km^2 is the area of a single square mesh.

The groundwater systems under the research region consist of the Dupi Tila sand formation and the Madhupur clay formation. The age of these sediments is Plio-Pleistocene. Although the formation is not exposed in any portion of the study area, it serves as the primary aquifer in numerous areas, including other regions of Bangladesh (Ahmed, 1994). The deeper aquifers beneath Greater Dhaka have not yet been thoroughly investigated. The hydro-stratigraphy of this region, up to an approximate depth of 350 meters, has been characterized based on lithological

data (please refer to chapter four). The layered hydro-stratigraphy of the region consists mostly of sands, silts, and clays. Based on bore-log likelihood, geo-electrical profiles, and lithological characterization, subsurface sediment production was categorized for various hydro-stratigraphic units.

Uniformity of lithological composition, textured sediments, and stratigraphic position were considered for distinguishing the Aquifer and Aquitard units and their diverse depth placements in the study area. Accordingly, eight hydro-stratigraphic units were determined up to the examined depth. A bore-log study revealed that the aquitard is not continuous; thus, the upper and lower aquifers are connected and exchange water.

Simplified hydraulic equivalents have approximated complex geological circumstances for the goal of creating a basic model. The lithological modeling of the aquifer system identified eight layers consisting of fine, medium, coarse, and clay sand. Various hydrogeological characteristics are assigned to each layer of the model.

Packages can be utilized to construct the GWF process. There are three packages in use: the Basic Package, the Hydrological package, and the Solver package. Internal flow packages and stress packages can further subdivide the hydrological packages. (Figure 4.3)

It is possible to merge many packages containing identical subroutines because each package contains similar subroutines. However, not every possible combination is possible. Two solver packages or internal flow packages cannot be utilized simultaneously.

The basic package includes the Stress (ST), Advance in time (AD), Output control (OC), and Output (OT) procedures, which are not included in the other packages. The basic package might thus be viewed as one that primarily addresses administrative responsibilities. The internal flow package is primarily responsible for calculating and prescribing conductance terms.

The stress package is the portion of the hydrological package that addresses boundary conditions. The stress package consists mostly of the five packages - Well, Recharge, River, General head, and Drain package. The General package and the River package address the identical feature in slightly different ways.

The River package was deemed a more accurate representation of a river's actual behavior than the generic head package, which is why it was utilized here. Recharge, General-head (north and south border), and Drain packages will also be used in the modeling process. The solver packages approximate the numerical model.

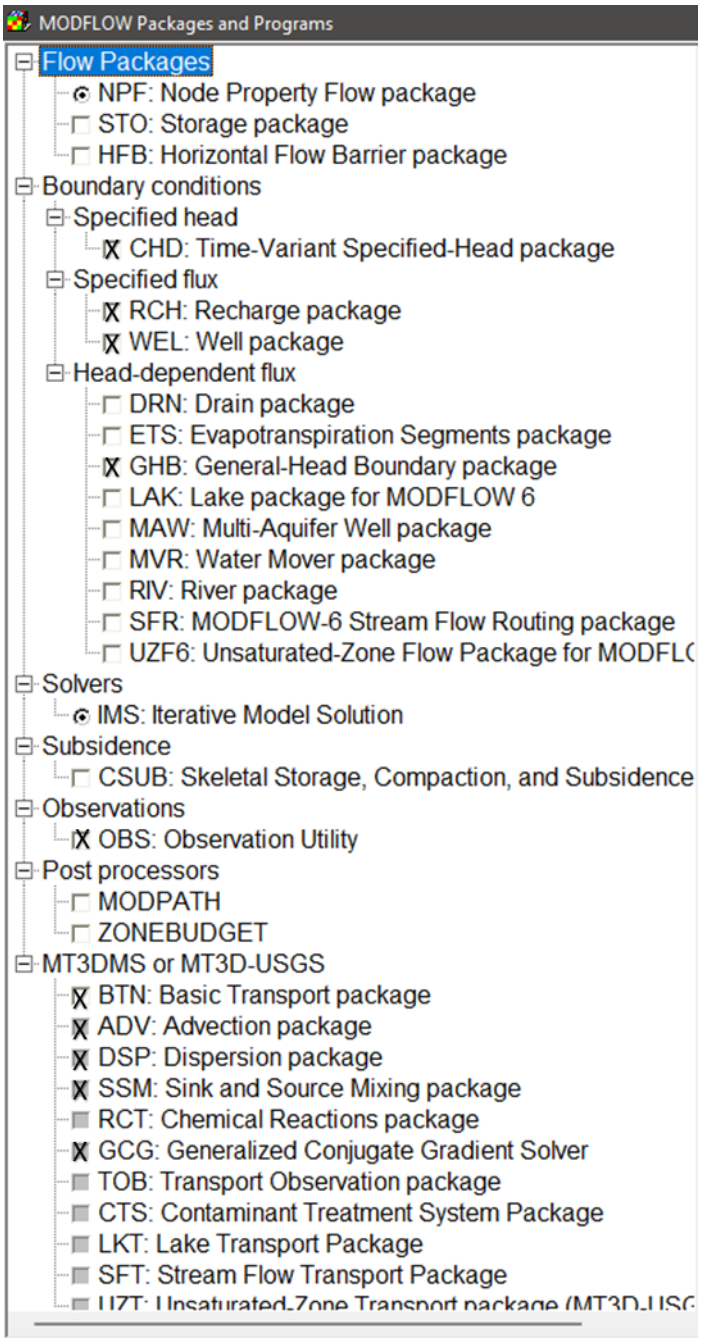

Figure 4.3: MODFLOW packages applied in this work.

MT3DMS is a three-dimensional model for solving pollutants' advection, dispersion, and chemical reactions in saturated groundwater flow systems. MT3DMS interacts directly with the finite-difference groundwater flow model MODFLOW of the U.S. Geological Survey for the flow solution and supports the hydrologic and discretization capabilities of MODFLOW. MT3DMS includes numerous transport solution strategies in a single code, which is often crucial, notably for model calibration. Since its initial release in 1990 as MT3D for modeling single-species mass transport, MT3DMS has been utilized in several research projects and field applications. The movement equation of a contaminant in 3-D groundwater (constant density) in a porous medium is expressed as follows (Schwartz & Zhang, 2003; Leake, 1997; Almasri & Kaluarachchi, 2007; Zheng et al., 2012):

$$\frac{\partial(\theta C^k)}{\partial t} = \frac{\partial}{\partial x_i}\left(\theta D_{ij}\frac{\partial C^k}{\partial x_j}\right) - \frac{\partial}{\partial x_i}(\theta v_i C^k) + q_s C_s^k + \sum R_n \quad \text{----- (Eq. 22)}$$

$$\text{also, } \frac{\partial(\theta C^k)}{\partial t} = \theta\frac{\partial C^k}{\partial t} + C^k\frac{\partial \theta}{\partial t} = \theta\frac{\partial C^k}{\partial t} + q_s' C^k \quad \text{----- (Eq. 23)}$$

Where, θ is the porosity of the substurface medium, C^k represents the dissolved concentration of k species (ML^{-3}), t represents time, xij is the distance along respective Cartesian coordinate axis (L), D_{ij} is the tensor of the hydrodynamic dispersion coefficient (L^2T^{-1}), V_i is the pore water velocity (LT^{-1}), q_s is the volumetric flow rate per unit volume of the aquifer to reflect fluid sources (positive) or sinks (negative) (T^{-1}), C^k_s is the concentration of the source (ML^{-3}), and $\sum R_n$ is the chemical reaction term ($ML^{-3}T^{-1}$).

Two factors effectively transfer contamination in groundwater, namely, advection and dispersion.

Advection describes the transport of miscible contaminants at the same velocity as the groundwater. The advection transport equation is;

$$\partial\frac{(\theta v_i C)}{\partial x_i} \quad \text{----- (Eq. 24)}$$

To measure the degree of advection domination, a dimensionless Peclet number is usually used, which is defined as:

$$P_e = \frac{|v|L}{D} \quad \text{----- (Eq. 25)}$$

Where |v| is the magnitude of the seepage velocity vector, L is the length, commonly taken as the grid cell width, and D is the dispersion coefficient.

Dispersion in a porous medium refers to the distribution of contaminants over a larger area than predicted from the average groundwater velocity vectors alone (Anderson, 1984). Mechanical dispersion, resulting from differences in actual velocity on a microscale from the average groundwater velocity and molecular diffusion driven by concentration gradients, are the causes of dispersion. Compared to the effects of mechanical dispersion, molecular diffusion is typically secondary and minor and only becomes significant when groundwater velocity is very low.

Then projection system used for the model is EPSG:4326 - WGS 84. (Figure 9)

Geological materials in the area of research were represented using a two-layer model. Hydrogeological stratification of the system determines the number of model layers considered in the discretized domain of groundwater modeling. In a number of modeling methodologies, a single model layer can simulate the hydrogeological layers of an existing system. Based on geology logs and well-completion data, a layer with a constant average thickness of 30 meters is used to represent the aquifer system. Using the extracted DEM from the ASTER image and the lithologic logs, the top and bottom elevations of the aquifer system are determined.

The groundwater abstraction for irrigation has been designated as a cluster grid cell, while water supply to the industry has been designated as an individual grid cell.

A 15-meter-resolution DEM is produced from an ASTER. To evaluate the vertical accuracy of the DEM, ground control points are generated using topographic maps of the research area. The vertical accuracy of the DEM is evaluated by comparing the extracted elevation value at several checkpoints with those prepared from the topographic maps as ground control elevation points. The relationship between the ground elevation and the elevation from DEM.

The corrected Elevation from DEM is used to define the ground elevation of boreholes, the aquifer top, and bottom, and to construct cross-sections. In addition, the DEM plays a significant role in defining the model boundary during the construction of the conceptual model.

5 LAND COVER / LAND USE (LCLU)

MAPPING LAND COVER AND LAND USE CHANGE (LCLU)

It is essential to analyze the spatial and temporal features of land-use change to appreciate and assess the ecological implications of urbanization (Deng et al., 2009). Land Use Land Cover (LULC) change detection aids in understanding the dynamics of environmental change and its impact on land areas. Identification of LULC features is a reliable and precise method for land cover classification and proper user management. Land cover classification from open-source Landsat images has been extensively utilized to describe local to global-scale landscape changes and related human-caused disruptions (Yuang et al., 2005; NRC, 1993).

1.22. Data Acquisition

Two types of satellite images were used: Landsat 4-5 Thematic Mapper (TM) and Landsat 7 Enhanced Thematic Mapper Plus (ETM+). In both cases, cloud cover was kept at 0% or almost 0%. Landsat satellite images for 2000, 2005, 2010, 2015, 2019, and 2021 were downloaded from the United States Geological Survey (USGS) website. Gazipur is included within the Landsat path 137, row 44. Map projection of the images is UTM within Zone 46N WGS 84. The topographic feature was taken from DEM data based on SRTM. Wavelengths of the Landsat bands are given in table 5. Four land cover types were identified and used for classification. (Table 5.1)

1.23. Image Classification

This study used a modified version of the Anderson Scheme Level I approach to analyze LULC alterations (Anderson et al., 1976). In constructing the classification scheme, additional parameters such as the primary land use categories within the study area and discrepancies in the spatial resolution of the photos were taken into account. Prior to classification, all satellite data were analyzed using spectral and spatial profiles to determine the digital numbers (DNs) of various LULC groups. The training samples were chosen from the reference data and supplementary data.

Several classes were mistakenly classified in the supervised classification of LULC, with certain urban settlements misclassified as landfills due to their spectral similarities. Similarly, the wetland class was combined with the lowland class due to their comparable spectral features, and both the wetland/lowland category and the cultivated land category were misclassified.

Post-classification refinement was thus employed to increase the classification's precision, as it is a straightforward and efficient technique (Harris & Ventura, 1995). In addition, because the urban surface is heterogeneous and made up of a complex combination of elements (e.g., buildings, roads, grass, trees, soil, and water) (Jensen & Im, 2007), mixed pixels are a prevalent issue when employing medium-spatial resolution data such as Landsat (Lu &Weng, 2005).

Table 5.1: Land Cover nomenclature used for the classification of Gazipur District.

Cover type	**Description**
Water-Bodies	River, pond, lakes, canals, and reservoirs
Forest	Care covered with trees that form a canopy on the land, including hilly forest, bush, and shrubs, tree covers that are not exactly adjacent or part of houses
Agriculture	Areas representing agricultural or related activities, including paddy fields, vegetables, fruits, and other cultivable lands.
Urban and industries	Presence of houses, offices, buildings, shelters, and so. - primarily any feature representing urbanization and industrialization

In multiple approaches, the problem of messy pixels was handled. For instance, thematic information (such as water bodies, vegetation, and bare soil) was extracted from the Landsat data using the V–S–W index (Yamagata et al., 1997). Then a rule-based technique employing thematic information and GIS data (such as DEM, municipal maps, water bodies, etc.) was implemented in ERDAS spatial modeler to correct previously misclassified land cover categories.

1.24. Accuracy Assessment

The final step of the picture categorization process is the evaluation of accuracy. Accuracy evaluation compares a classification with the ground truth or credible sources. Using field data and the geographical features on land use maps, high-resolution images, and SOB topographic maps, LULC maps were reviewed. The classification accuracy was also assessed using a non-parametric Kappa test that considers all elements of the confusion matrix, not just the diagonal ones. The total accuracy of the Landsat LULC data was 85.6%, 89.6%, and 90%, with corresponding Kappa statistics of 82.7, 87.5, and 87.9% for MSS, TM, and ETM+, respectively. Standard LULC mapping precision is 85–90 percent (Anderson et al., 1976; Table 5.2).

1.25. Change Detection and Mapping

Individual precision has a significant impact on the accuracy of change detection. This research employed the post-classification change detection method to identify changes' kind, rate, and location (Hardin et al., 2007). To detect spatial changes, a GIS-based overlay technique was utilized. It involves superimposing photos to compare potential modifications. The cross operation enables the comparison of images with even temporal differences. However, this procedure is slow and laborious but highly accurate (Hassan & Southworth, 2017).

1.26. LCLU Changes

The spatial and temporal developments of the Gazipur District over nearly two decades have been evaluated. (Figure 5.1)

In 2000, lowlands, agricultural land, and aquatic bodies were the predominant land use types, and urban expansion was moderate. By 2005, the transformation had begun to accelerate at a regulated and moderate rate, with declining water bodies and accelerated settlement or urbanization. In 2010, the replacement of aquatic bodies gained prominence. Urbanization became dominant and began to border agricultural fields. In 2019, a radical shift in land usage became apparent, and the replacement of water bodies grew so aggressive as to be irreversible. Urban and industrial constructions started to predominate, while agricultural lands became, at times, seasonal features - alternating as seasonal sources of water.

Table 5.2: Image classification accuracy assessment.

	Water-Bodies	Forest	Agriculture	Urban and industries	Total
Water-Bodies	9	0	0	0	9
Forest	0	3	3	0	6
Agriculture	0	3	5	0	9
Urban and industries	0	1	0	7	7
Total	9	6	9	7	35

Years	Gazipur Sadar	
	Overall Accuracy	Kappa Coefficient
1995	80%	81.25%
2000	82.22%	77.19%
2015	82%	77.33%
2020	76%	69.31%

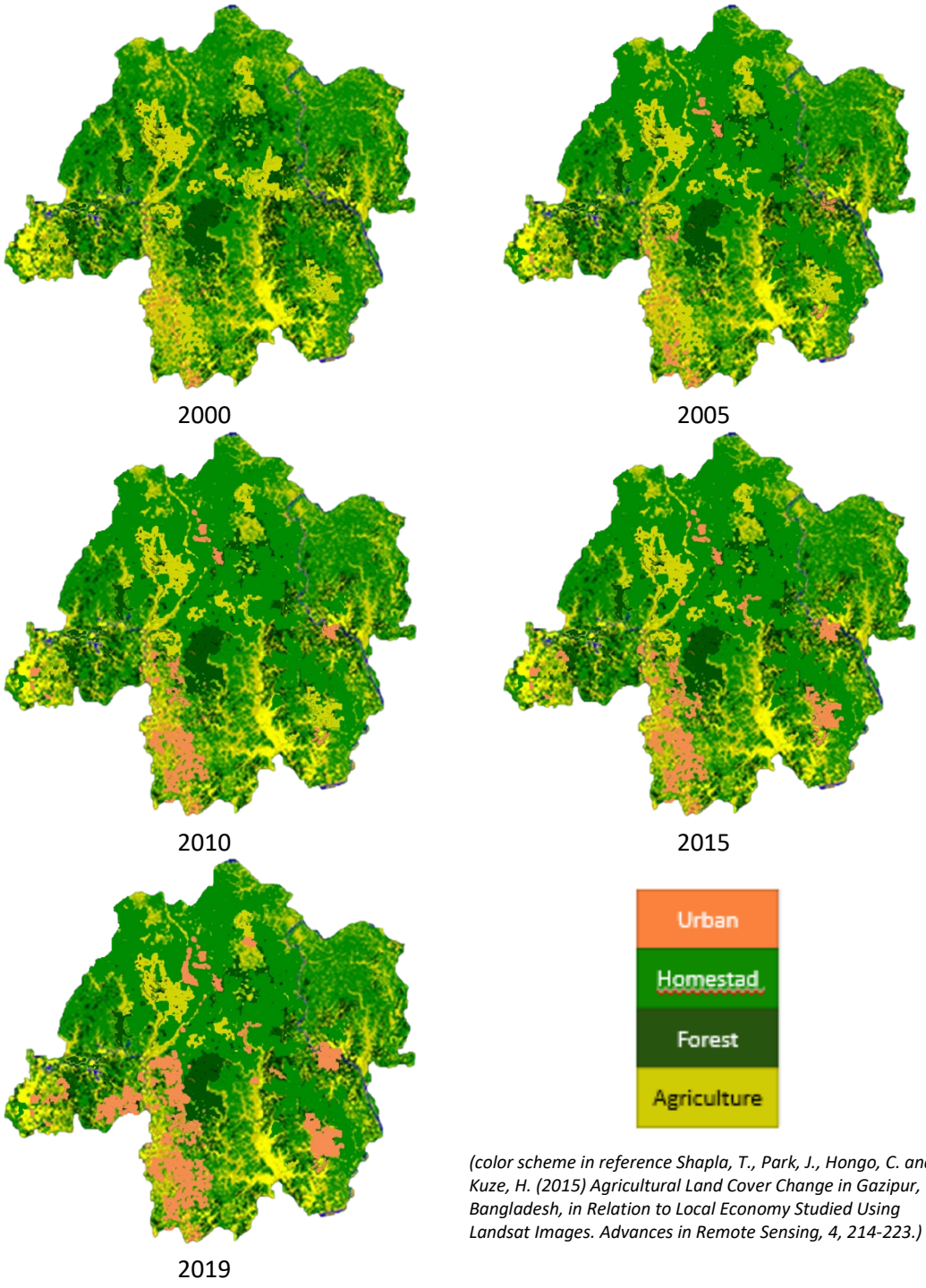

(color scheme in reference Shapla, T., Park, J., Hongo, C. and Kuze, H. (2015) Agricultural Land Cover Change in Gazipur, Bangladesh, in Relation to Local Economy Studied Using Landsat Images. Advances in Remote Sensing, 4, 214-223.)

Figure 5.1: LCLU classification of Gazipur District showing Spatio-Temporal changes of 2000, 2005, 2010, 2015, and 2019.It is very evident that Urbanization increased rapidly throughout the Gazipur District. This expansion is taking place especially along the main highway and around the growing industrial areas. The main Agricultural zones are hard hit by the expansion.

Urban area changes varied from 1 percent in 2000 to nearly 30 percent in 2021. This transformation was most pronounced in Gazipur Sadar, followed by Kaliakair. Considerable urbanization has happened in the Gazipur-Sadar subdistrict in the Dhaka metropolitan region. Importantly, a portion of the fertile agricultural land has to be shifted to other uses as a result of rising urbanization.

Such dramatic shifts generate severe environmental repercussions. Generally, deforestation is irreversible, causing permanent harm to habitats and biodiversity. In Sreepur, the forest cover decreased by about 30 percent, Kaliakair by 14 percent, Kapasia by 20 percent, and Gazipur Sadar by more than 40 percent. (Figure 5.2)

Although improvements began along significant routes, particularly the Dhaka-Mymensingh Highway, in 2015, they began growing in an unintended direction. The south of the Gazipur Sadar Upazila is about 80 percent urbanized, according to the 2021 picture categorization. (Table 5.3)

1.27. Spatial and Temporal Changes in Urban and Industrial Growth

Urbanization also affects the regional ecology in its entirety. In regions downwind of large industrial complexes, precipitation, air pollution, and the frequency of days with thunderstorms all rise. Not only can urban areas influence weather patterns, but also water runoff patterns. Generally, urban areas create more precipitation but reduce water penetration and lower water tables. This indicates that runoff happens faster when peak flows are bigger. As flood levels increase, so do downstream flooding and water pollution. Populations in urban areas interact with their environment. The consumption of food, energy, water, and land by urban residents alters the ecosystem. In turn, the urban environment's pollution impacts the urban population's health and quality of life.

Many of the environmental effects of metropolitan areas are not always linear. More significant urban populations inevitably generate more environmental issues. The magnitude of environmental consequences is largely determined by urban populations' consumption and lifestyle patterns, not just their numbers. Urban areas consume far more energy for power, transportation, cooking, and heating than rural settlements. Per capita, urban populations have significantly more automobiles than rural people. In the areas of the Gazipur district, including Gazipur Sadar, Sreepur, and Kaleakair, the impact of urbanization and urbanization patterns on the local thermal environment and precipitation is examined.

Among the most irrevocable human influences on the global ecosystem is the conversion of land for urban activities. It accelerates the loss of highly productive farmland, alters the temperature, varies hydrologic and biogeochemical cycles, fragments habitats, and decreases biodiversity (Seto et al., 2011). These consequences are seen on various levels. Future urbanization will pose direct challenges to high-value ecosystems.

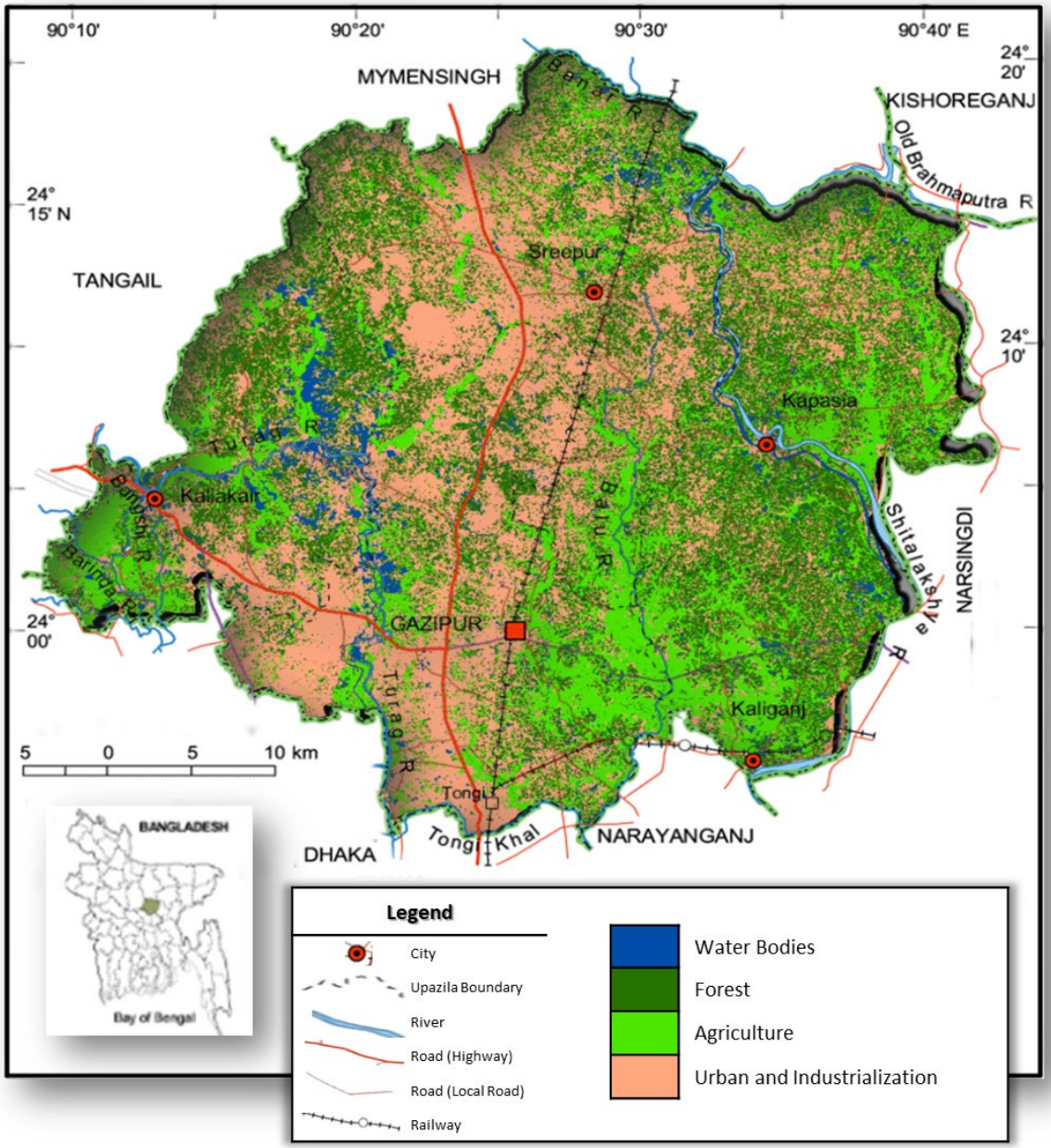

Figure 5.2: LCLU classification map of Gazipur District for the year 2021, showing Spatial variation of water bodies forests, agricultural areas, and Urban & Industrialization settings.

Table 5.3: Urbanization trend in Gazipur District over the last two decades.

	Urbanization (%)			
	2000	2010	2015	2021
Gazipur District	3.4	7.48	29.38	37.41
Gazipur Sadar	6.4	12.56	34.38	48.23
Kaliakair	1.6	7.28	35.64	57.33
Sreepur	1.8	6.35	29.87	43.71
Kapasia	0.8	3.62	4.73	9.36
Kaliganj	0.6	6.54	17.13	15.35

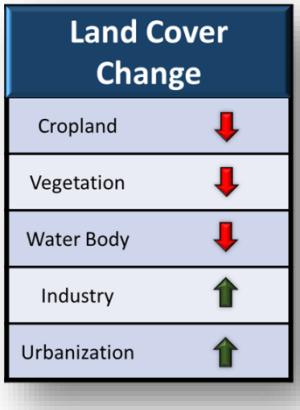

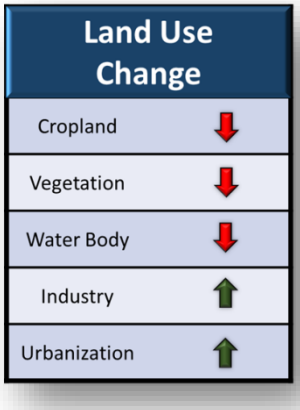

For instance: the fastest rates of land conversion over the next few decades will likely occur in biodiversity hotspots that were relatively unaffected by urban development in 2000. (Seto et al., 2012). The type of urban expansion is a key factor in the susceptibility of urban residents to environmental stress (Seto & Shepherd, 2009). The environmental effects of urban growth extend far beyond city limits. Agriculture intensifies on remaining undeveloped land and is projected to expand into new areas in fast urbanizing areas, placing pressure on land resources (Guneralp & Seto, 2008).

Moreover, urban environments alter precipitation patterns over hundreds of square kilometers (Kaufman et al., 2007). Urban growth will also impact the world climate. It is projected that roughly 5 percent of total emissions from tropical deforestation and land-use change are attributable to direct loss of vegetation biomass in areas with a high potential for urban growth (Seto et al., 2012). The extent and magnitude of these effects have yet to be thoroughly investigated. Although numerous studies have characterized the impact of urbanization on CO2 emissions and heat budgets, the consequences on the movement of water, aerosols, and nitrogen in the climate system are just beginning to be comprehended (Seto & Shepherd, 2009).

The rural-to-urban migration frequently leads to overpopulation, pollution, and inadequate sanitation – all of which are detrimental to the environment. Unfortunately, bringing people out of poverty and into more industrialized nations frequently comes at the expense of the local ecosystem. It has potential environmental effects if not guided by sustainable and intelligent policies. If poorly planned, massive urban sprawl can increase deforestation, habitat degradation, and greenhouse gas (GHG) or carbon emissions. Urbanites also tend to consume more food and energy than those living in rural regions, which places a greater demand on natural resources, which are finite and will eventually be depleted.

6 GROUNDWATER QUALITY ASSESSMENT

GROUNDWATER QUALITY ASSESSMENT OF GAZIPUR DISTRICT

Understanding groundwater quality is essential for sustainable water resource management. This study was carried out to understand the hydro-geochemical condition and its relation with the Urbanization and industrialization of the Gazipur District. The hydrochemical interpretation process of the data includes conventional graphical plots and multivariate analysis. The Interpretation is based on the observed water types, hydrochemical facies, and factors controlling groundwater quality.

Hydrogeochemical processes aid in understanding the contributions of rock-water interaction and anthropogenic impacts on groundwater quality. These geochemical processes are accountable for the regional differences in groundwater chemistry.

The chemical equilibrium of groundwater is based on the relative rate of groundwater flow and water/rock interaction as the water moves through the aquifer and alters its chemistry. Human activities, livestock production, and agriculture contribute significantly to environmental contamination. High amounts of ammonia nitrogen, organic and inorganic nitrogen compounds, and harmful microorganisms are found in animal effluent (Toth, 1984; Freeze and Cherry, 1979; Vissers, 2005).

1.28. Groundwater Quality Assessment

Ions are described on a sample-by-sample basis. The water samples were categorized using graphical methods. These methodologies include the diagrams of Piper, Durov, and Wilcox. Geochemical analysis results are given in Appendix 1. In reference to the drinking water standards considered by Bangladesh and WHO (Table 6.1), values received in this work are not extremely high, with certain exceptions. (Figure 6.1)

Statistical interpretation of the geochemical results has been included in determining groundwater quality condition. The statistical tools used to interpret water quality are analysis of arithmetic mean, standard deviation, coefficient of skewness, T-test, F-test, and correlation matrix.

1.28.1. pH and ORP

The pH scale determines how acidic or basic water is. The range is 0 to 14, with 7 representing neutrality. Acidity is indicated by pH values below 7, whereas baseness is shown by pH values above 7. In reality, pH is a measurement of the proportion of free hydrogen and hydroxyl ions in water. While water with more free hydroxyl ions is basic, water with more free hydrogen ions is acidic. Since chemicals in the water can change pH, pH is a crucial sign that the chemical composition of the water is changing.

Table 6.1: WHO and Bangladesh standards for drinking purposes.

SI No.	Water quality parameter	Unit	WHO standard		Bangladesh standard	
			Max. accept. limit	Max. allow. limit	Max. recom. limit	Max. allow. limit
1.	pH		6.5	8.5	6.5	8.5
2.	TDS	ppm	500	1500	–	1500
3.	Calcium	ppm	75	200	–	–
4.	Magnesium	ppm	50	150	–	–
5.	Potassium	ppm	–	–	12	–
6.	Sodium	ppm	–	200	200	–
7.	Iron	ppm	0.3	1.0	1.0	5.0
8.	Bicarbonate	ppm	–	–	–	–
9.	Chloride	ppm	200	600	600	1000
10.	Sulfate	ppm	200	400	–	400
11.	Nitrate	ppm	10	–	45	50
12.	Total Hardness	mg/l	100	500	200	500

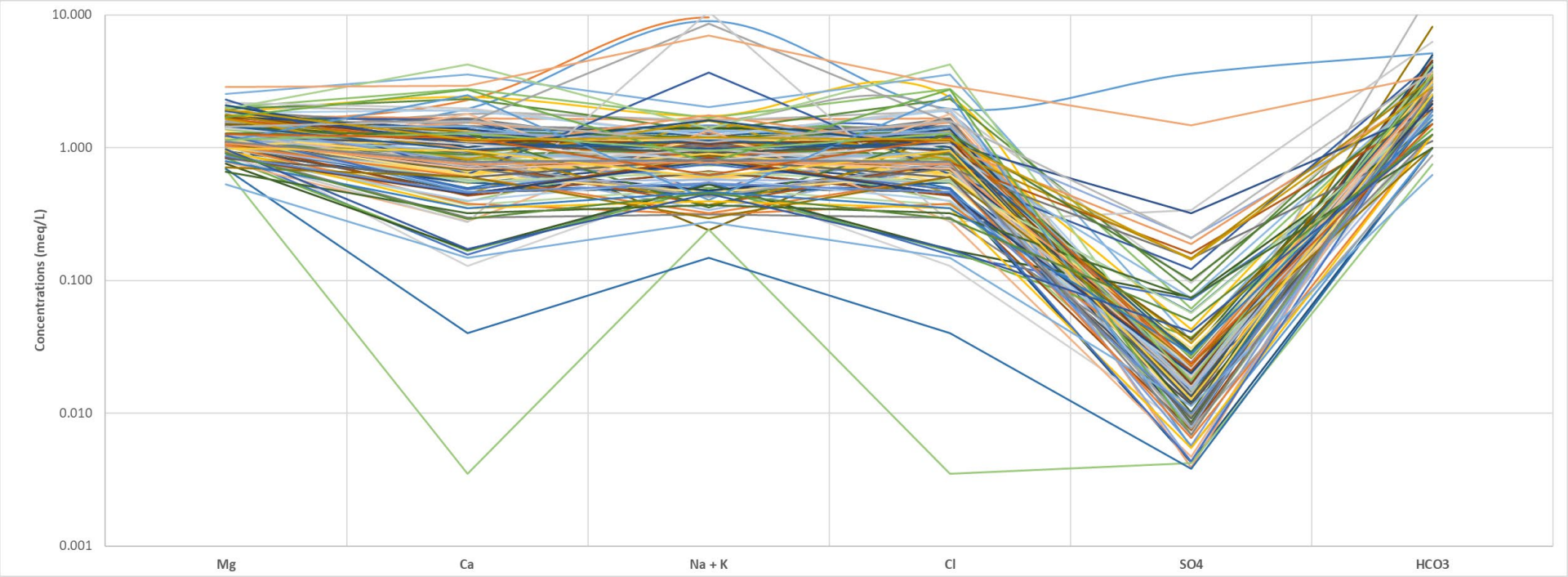

Figure 6.1: Schoeller diagram showing Groundwater quality variation of different samples across Gazipur District. most samples are within limit, with some spiking and breaking trend.

The pH of water controls the biological availability (amount that can be consumed by aquatic life) and solubility (amount that can be dissolved in the water) of chemical components such nutrients (phosphorus, nitrogen, and carbon) and heavy metals (lead, copper, cadmium, etc.).

ORP is the amount of energy in water in terms of electrons. It is measured in millivolts. Drinking water should have a rating of least -50 millivolts. Groundwater quality is influenced by ORP due to its metallic pollutants. pH and ORP values in Gazipur District ranges 4.7 to 9.7 and from -100 to 300, respectively. Spatial distribution (Figure 6.2; Figure 6.3) for 2018 indicates that pH and ORP concentration are high in highly dense urban/industrial areas.

1.28.2. Electrical Conductance (EC) and Total Dissolved Solid (TDS)

Higher EC in the study area indicates the enrichment of salts in the groundwater. The value of electrical conductivity may be an approximate index of the total content of dissolved substance in water. It depends upon temperature, concentration and types of ions present (Hem 1985). Because TDS measurement is time-consuming, it is often estimated from electrical conductivity (EC) assuming dissolved solids are predominantly ionic species of low enough concentration to yield a linear TDS-EC relationship:

$$TDS\ (mg/L) = ke \times EC\ (\mu S/cm) \quad \text{----- } (Eq.\ 26)$$

where ke is a constant of proportionality.

EC ranges from 91 to 1590 µS/cm and TDS varies between 45 and 792 (mg/l). Values have high concentration in urban and industrial settings (Figure 6.4; Figure 6.5).

1.28.3. Calcium (Ca^{2+}) and Magnesium (Mg^{2+})

The range of calcium concentration of all analyzed groundwater samples is 0.7-84 mg/l. The range of magnesium concentration over all analyzed groundwater samples is 6.4-34.68 mg/l. concentration levels are within the limit. Spatial distribution map shows that comparatively higher concentration can be seen along the urban and industrial area of Gazipur Sadar Upazila (Figure 6.6: Figure 6.7). Calcium and Magnesium dissolved in natural water are alkaline earth metals commonly found in drinking water. Calcium is the most abundant alkaline-earth metal and a significant component of numerous common rock minerals. It is an essential ingredient for plant and animal life and a significant component of most natural water solutes. Magnesium is also a common element in plant and animal nutrition. In specific facets of water chemistry, calcium and magnesium may be thought to have similar effects, such as their contributions to the hardness property (Hem, 1989; WHO, 2022).

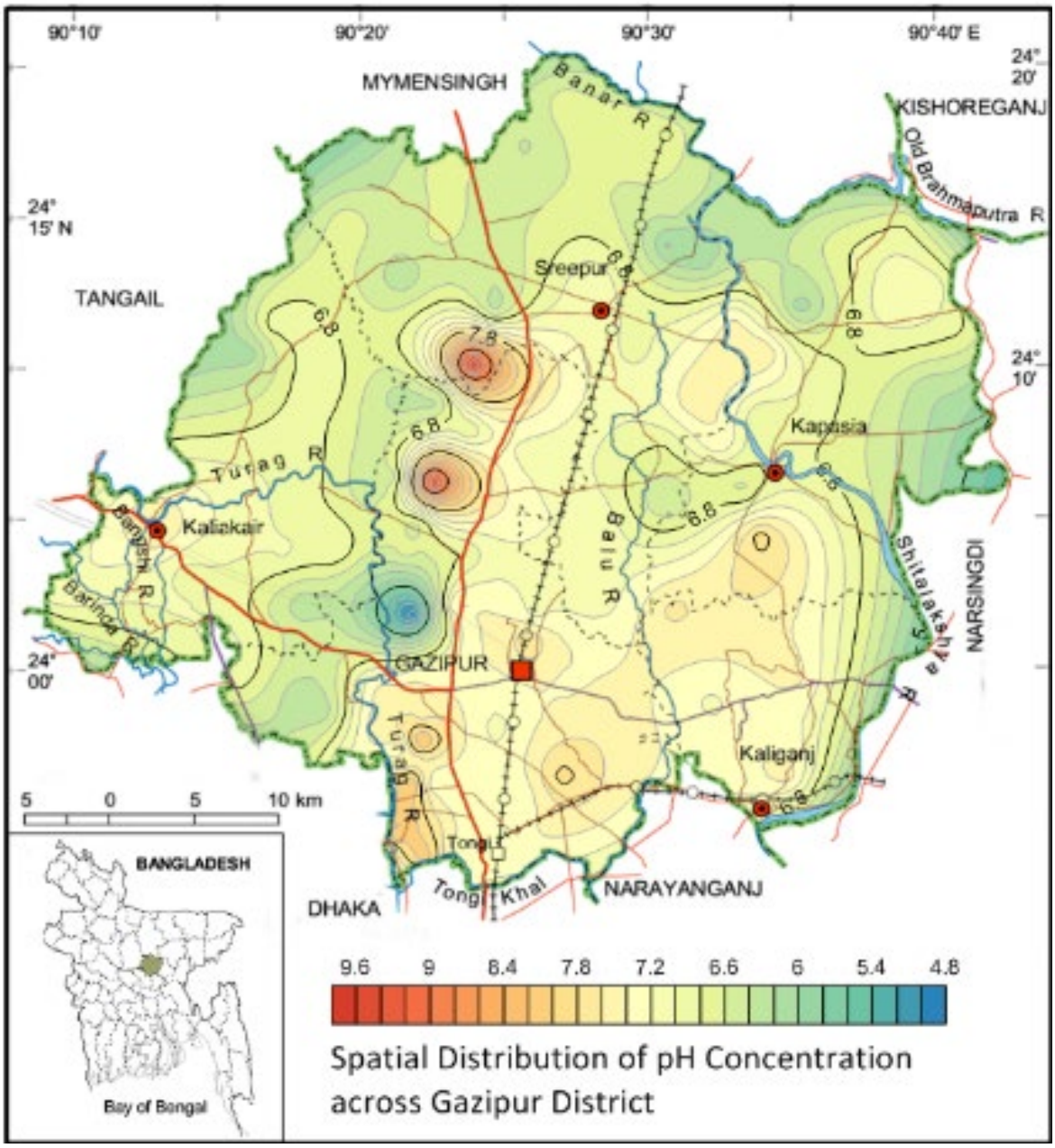

Figure 6.2: Spatial variation of pH concentration across Gazipur District, showing concentration level concentric and comparatively high at urban or settlement areas.

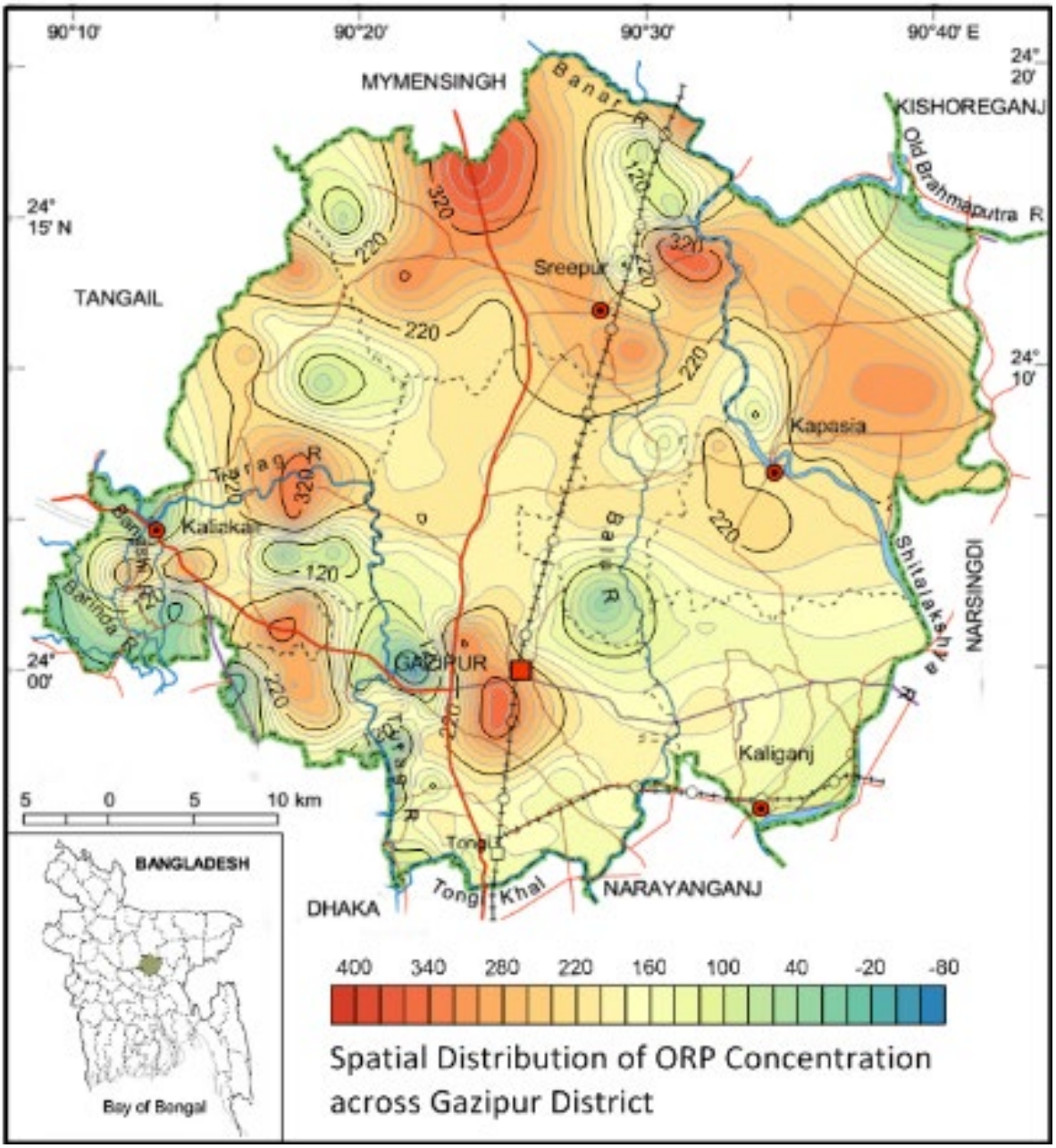

Figure 6.3: Spatial variation of ORP concentration across Gazipur District, showing concentration level concentric and comparatively high at urban or settlement areas.

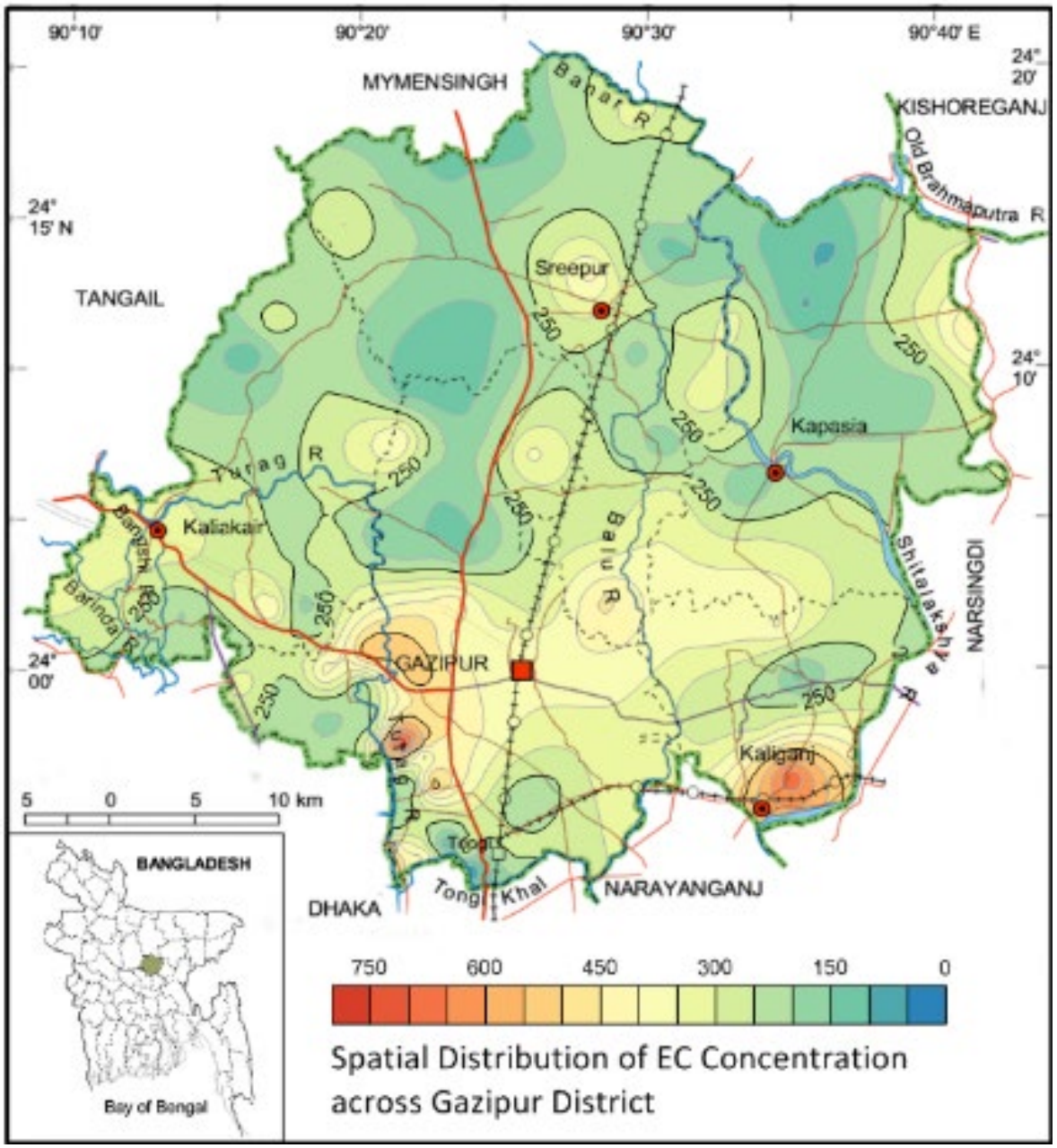

Figure 6.4: Spatial variation of EC value across Gazipur District, showing concentration level concentric and comparatively high at urban or settlement areas.

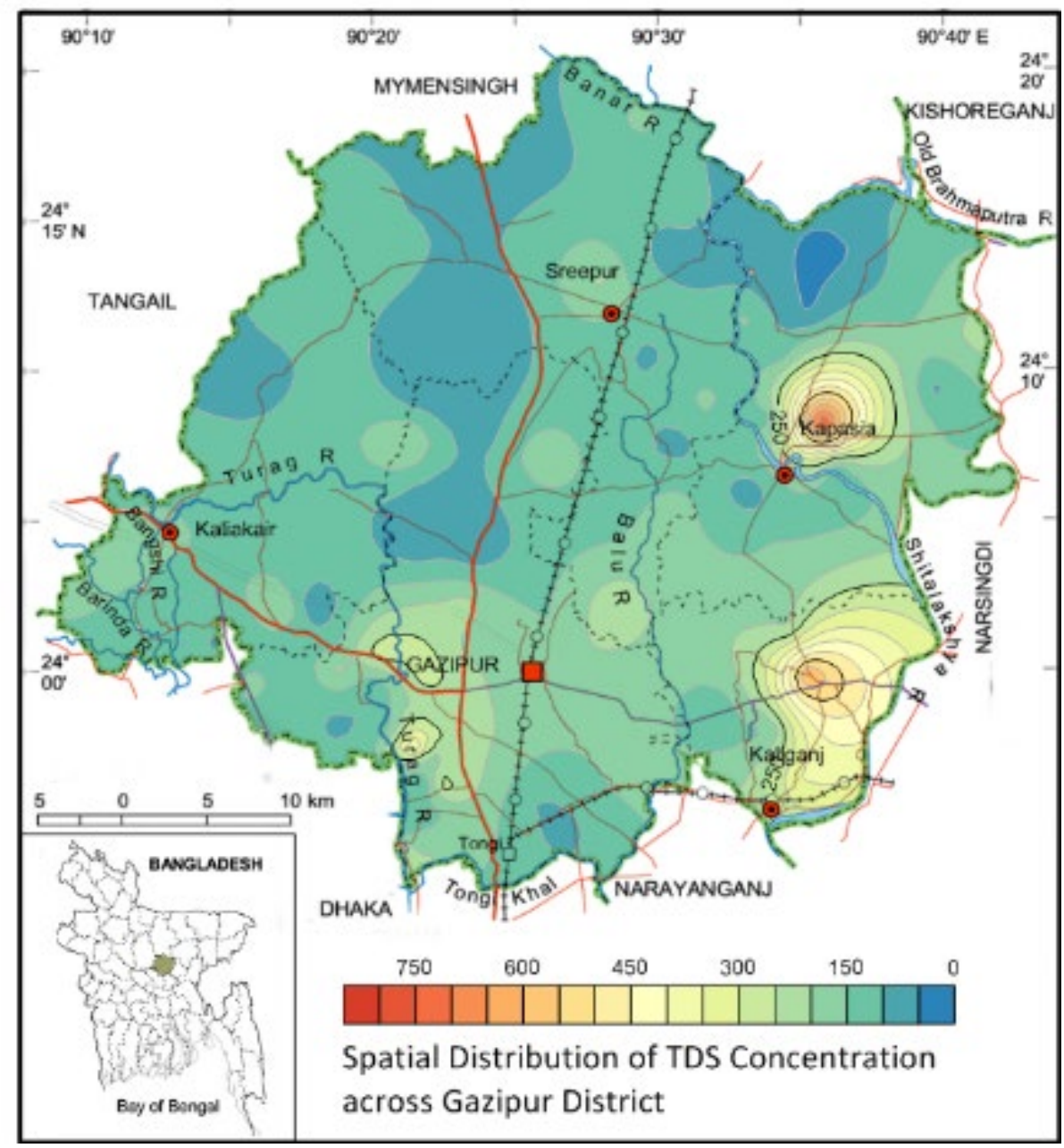

Figure 6.5: Spatial variation of TDS values across Gazipur District, showing concentration level concentric and comparatively high at urban or settlement areas.

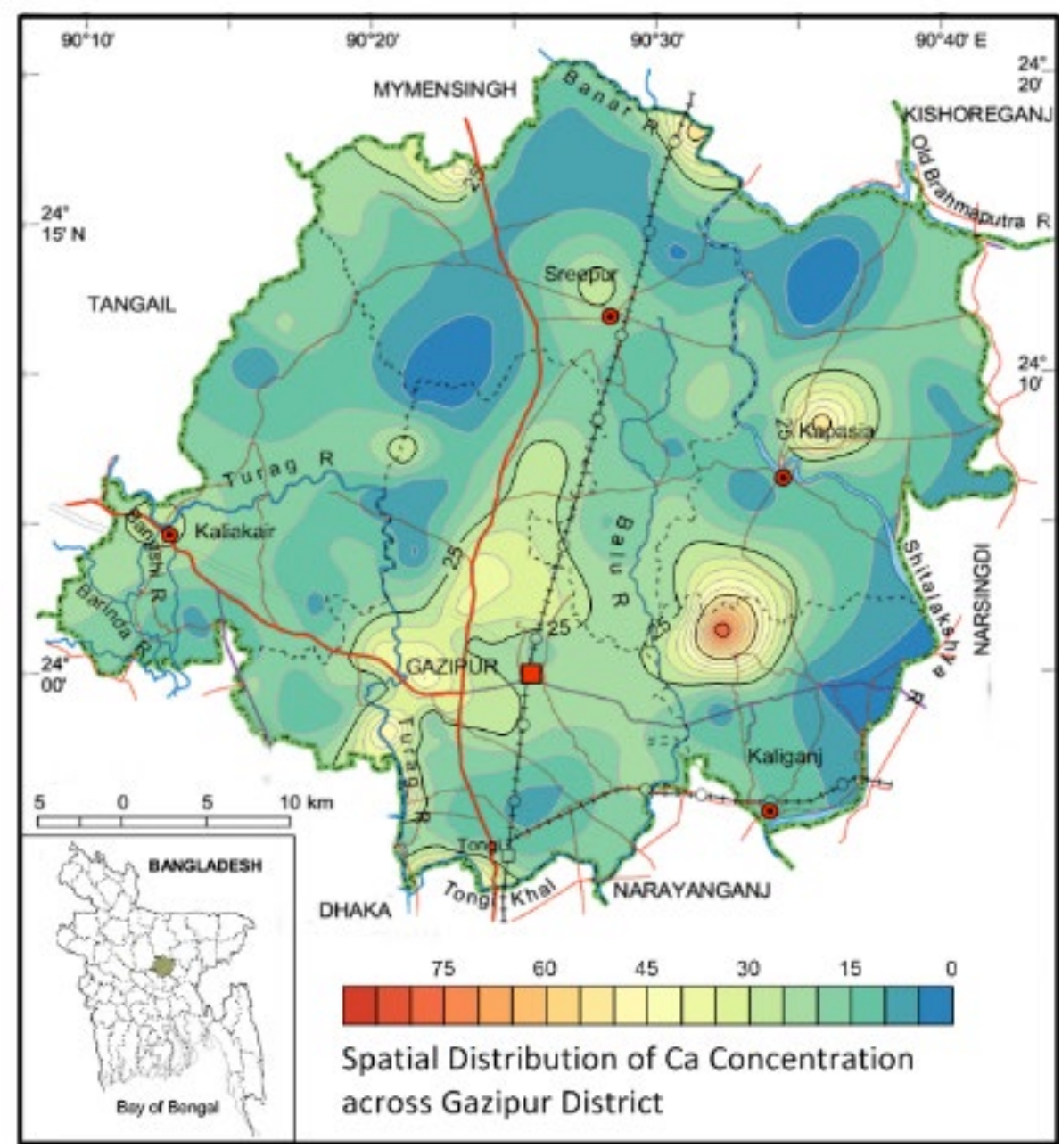

Figure 6.6: Spatial variation of Ca^{2+} concentration across Gazipur District, showing concentration level concentric and comparatively high at urban or settlement areas.

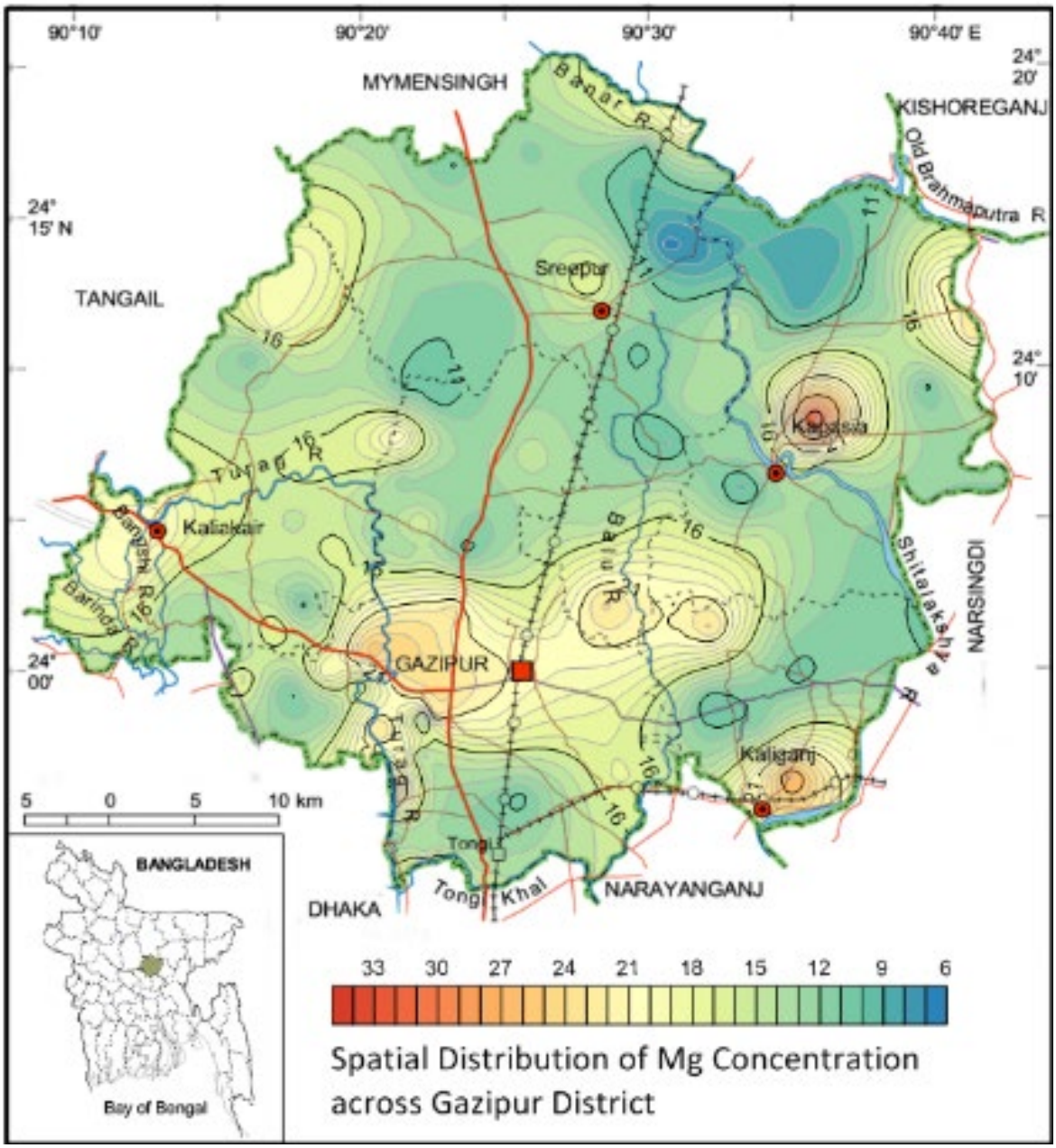

Figure 6.7: Spatial variation of Mg^{2+} concentration across Gazipur District, showing concentration level concentric and comparatively high at urban or settlement areas.

It is an essential ingredient for plant and animal life and a significant component of most natural water solutes. Magnesium is also a common element in plant and animal nutrition. In specific facets of water chemistry, calcium and magnesium may be thought to have similar effects, such as their contributions to the hardness property (Hem, 1989; WHO, 2022).

1.28.4. Sodium (Na^+) and Potassium (K^+)

The range of sodium concentration over all analyzed groundwater samples is 2.9-243 mg/l. The range of Potassium concentrations over all analyzed groundwater samples is 0.1-14.3 mg/l. Concentration levels are below water quality standards. (Figure 6.8; Figure 6.9)

Groundwater often contains a higher concentration of sodium and potassium and is the most prevalent alkali metal. Potassium-bearing minerals degrade significantly more slowly than those with sodium, resulting in a higher sodium concentration. The abundance of sodium and potassium in groundwater is mostly due to the chemical breakdown of feldspar, feldspathoid, and some micas. Other sources of sodium and potassium in groundwater are contamination by agricultural by-products and industrial effluents (Hem, 1989). The concentration of these elements in water confirms the above-stated condition for the study area. High sodium concentration may be due to the chemical decomposition of many sodium-bearing feldspars and the contamination of agricultural by-products.

1.28.5. Bicarbonate (HCO_3^-)

The range of bicarbonate concentration over all analyzed groundwater samples is 85.24-4749.133 mg/l. (Figure 6.10)

Bi-carbonate and carbonate are usually present in groundwater because of the weathering of carbonate minerals and the presence of CO_2, which helps dissolve these elements (Rain Water and Thatcher, 1960). The dissolved carbon-dioxide species, bicarbonate, and carbonate produce alkalinity. Bicarbonate concentration of more than 200 mg/l is not uncommon in groundwater, and higher concentrations can result in carbon dioxide being produced within the aquifer and mixed with organic matters (Lubello & Gori, 2001). A high bicarbonate concentration may be due to the presence of much organic matter in the aquifer and their reaction with carbon-di-oxide (Hem, 1989).

1.28.6. Chloride (Cl^-)

The range of chloride ion concentration over all analyzed groundwater samples is 1.8-262 mg/l. (Figure 6.11)

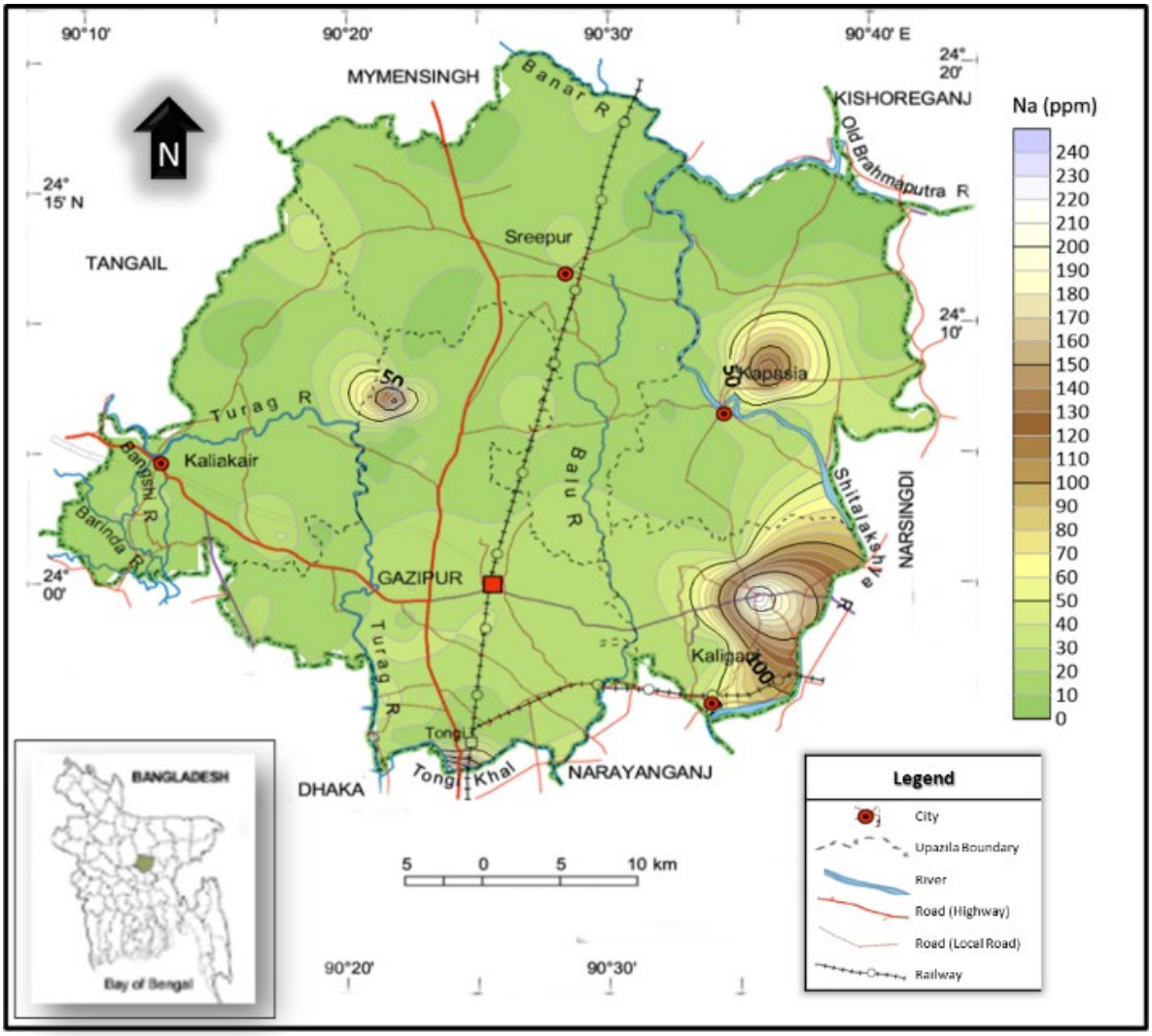

Figure 6.8: Spatial variation of Na^+ concentration across Gazipur District, showing concentration level concentric and comparatively high at urban or settlement areas.

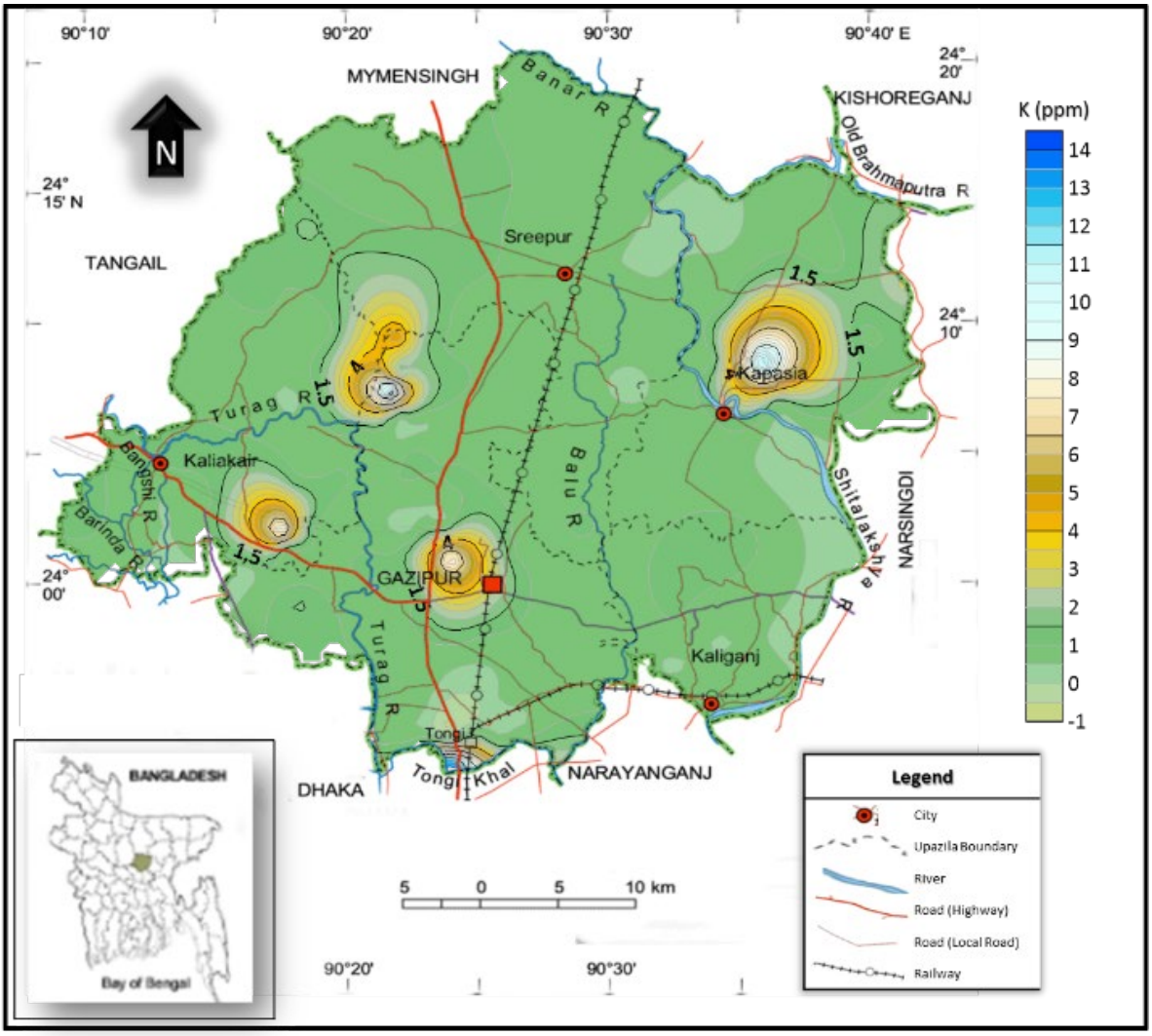

Figure 6.9: Spatial variation of K+ concentration across Gazipur District, showing concentration level concentric and comparatively high at urban or settlement areas.

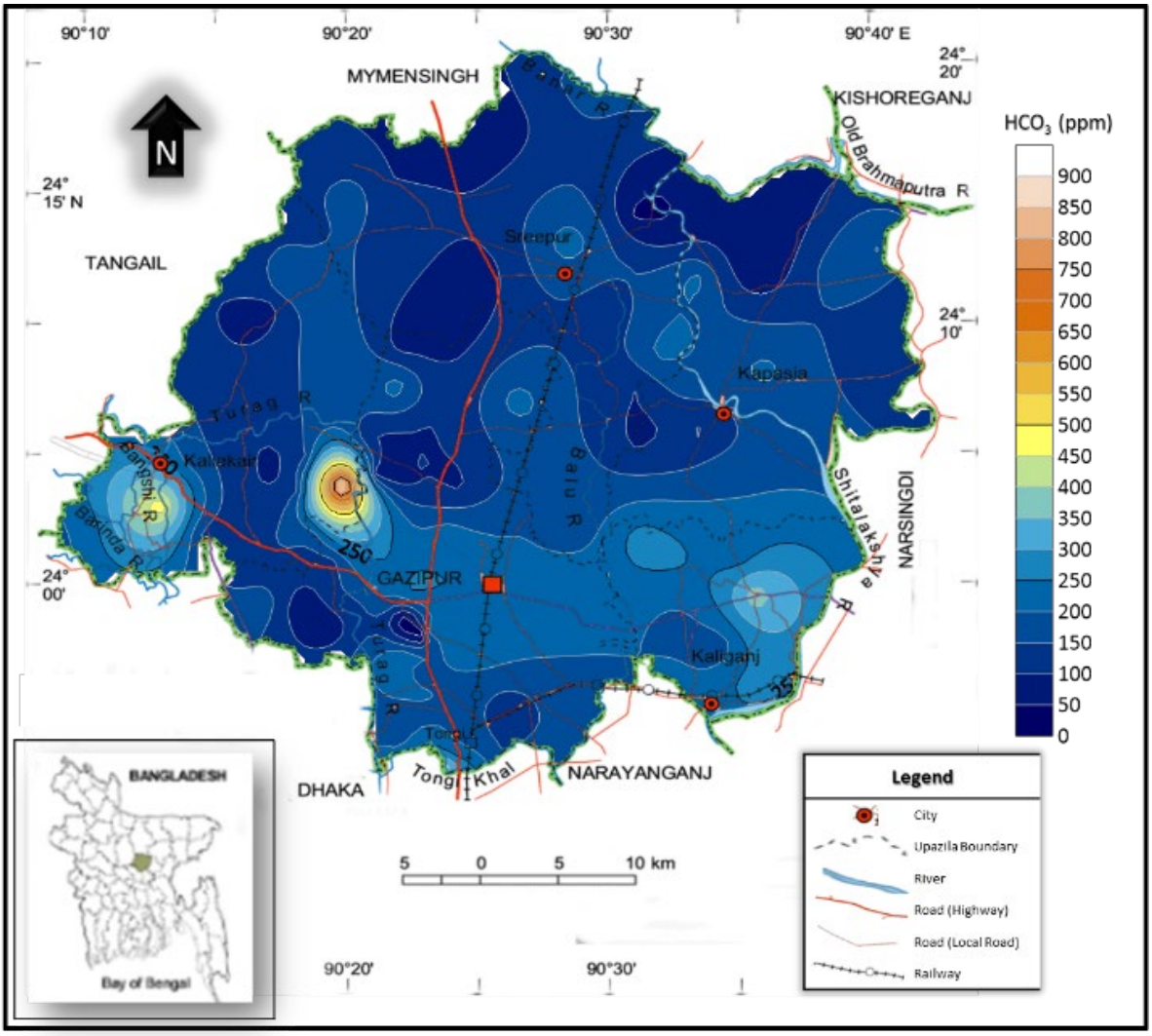

Figure 6.10: Spatial variation of $HCO3^-$ concentration across Gazipur District, showing concentration level concentric and comparatively high at urban or settlement areas.

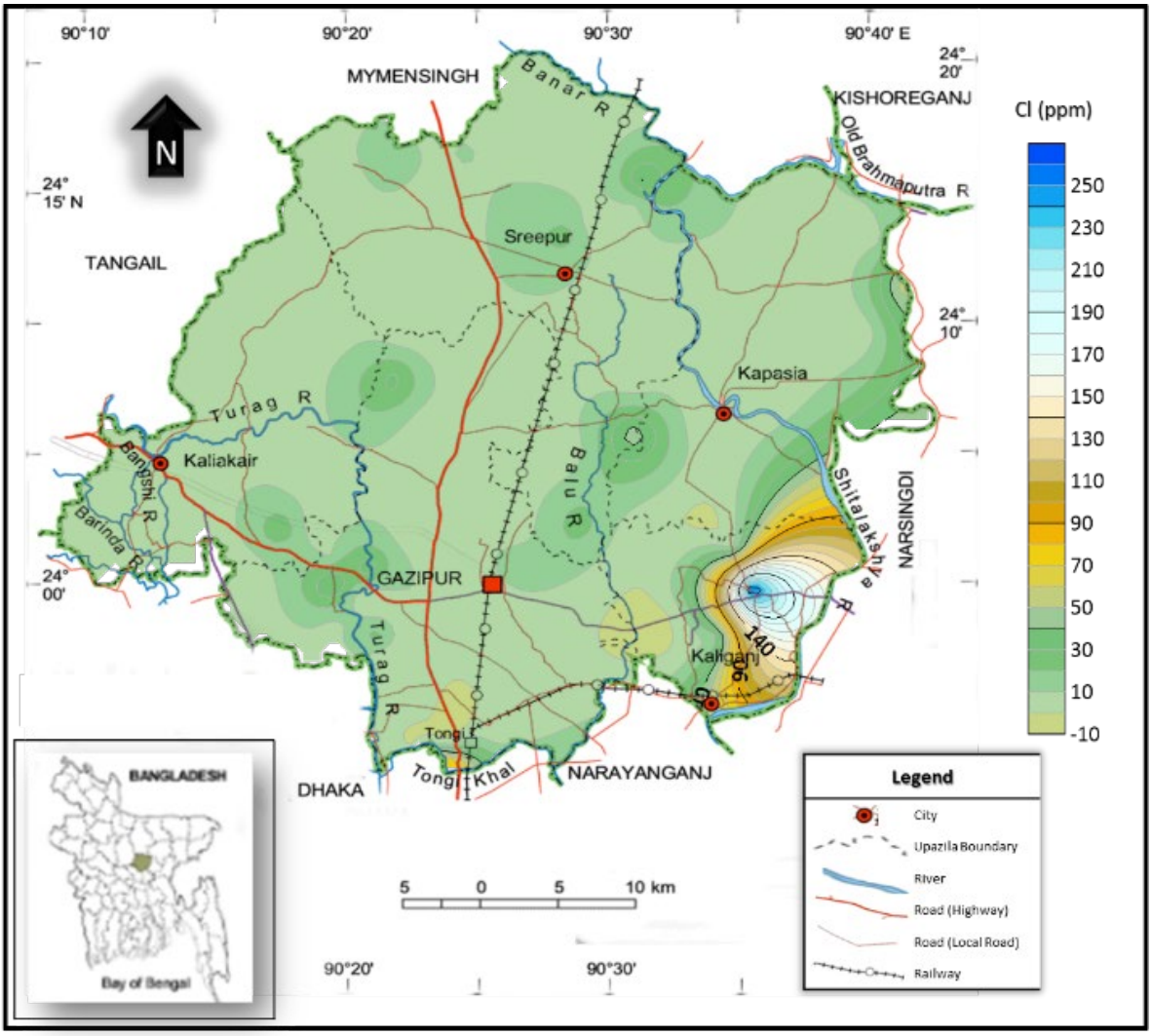

Figure 6.11: Spatial variation of Cl^- concentration across Gazipur District, showing concentration level concentric and comparatively high at urban or settlement areas.

Chloride is an indication of salinity in water. It is one of the significant important constants of natural water. At concentrations above 250mg/l, water tastes salty (Sawyer et al., 2003). Most chloride in groundwater comes from evaporated salted connate water. Surface water in the humid region is usually low in chloride (Hem, 1989). High chloride concentration may be due to the effects of human activities (pollution), connate water, or the presence of shale that has lost chloride by leaching as a result of near-surface exposure. The spike can be attributed to the effect of human activities (pollution).

1.28.7. Nitrate ($N0_3^-$)

The range of nitrate concentration over all analyzed groundwater samples is 0-1.9 mg/l. There are few samples showing concentrations of nitrate. (Figure 6.12)

In water, nitrogen may occur in several forms depending on its level of oxidation. Nitrate is the most prevalent form of nitrogen in groundwater. The residences of nitrogen compounds indicate the presence of organic matter. Nitrogen fixing plants (legumes) and bacteria, chemical fertilizers, sewage, and decaying organic matter are the principal sources of nitrate in water. The nitrate content of undiluted water rarely exceeds 10mg/l, this could be a concern, specially while using it for drinking or irrigation water. High concentration is normally due to human and animal accretions, and chemical fertilizers percolate into the aquifer (Hem, 1989).

1.28.8. Sulfate (SO_4^{-2})

The range of sulfate concentration over all analyzed groundwater samples is 0-174 mg/l. The concentration level is insignificant. (Figure 6.13)

Naturally occurring sulfate in groundwater results from the oxidation of sulfur in igneous rock, sulfate oxidation within sedimentary rocks, particularly the organic shale, or leachable sulfate in fertilizers and from other human influence. It seems like groundwater in the area has no Sulphate contamination.

1.29. Assessment for Irrigation

Main source of water for irrigation in Bangladesh is local groundwater, affecting plants, and agricultural soils directly (Aghazadeh & Mogaddam, 2010). Therefore, a water quality assessment for irrigation is very important. The following parameters are used here to evaluate the water quality suitability for irrigation.

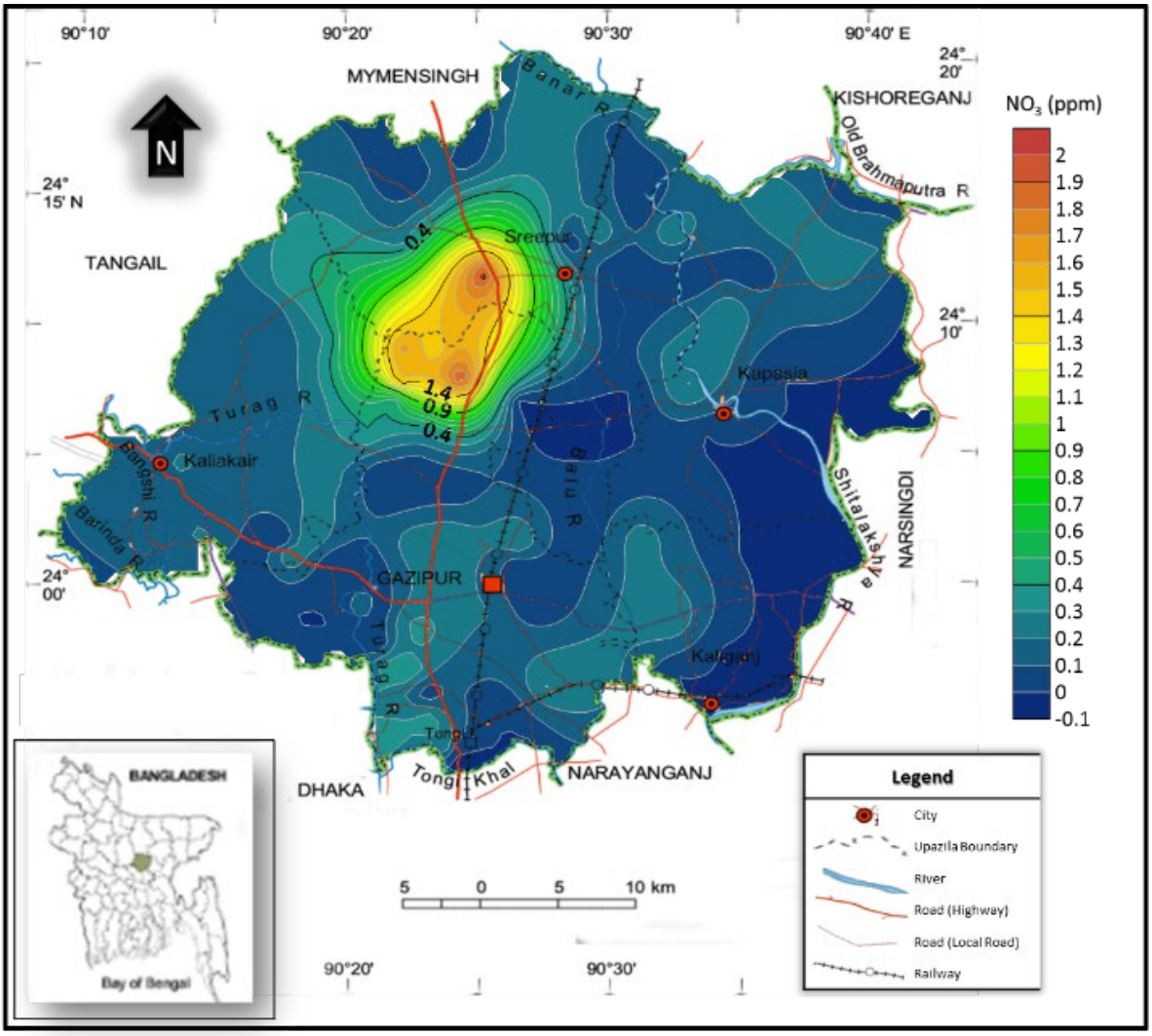

Figure 6.12: Spatial variation of NO_3^- concentration across Gazipur District, showing concentration level concentric and comparatively high at urban or settlement areas.

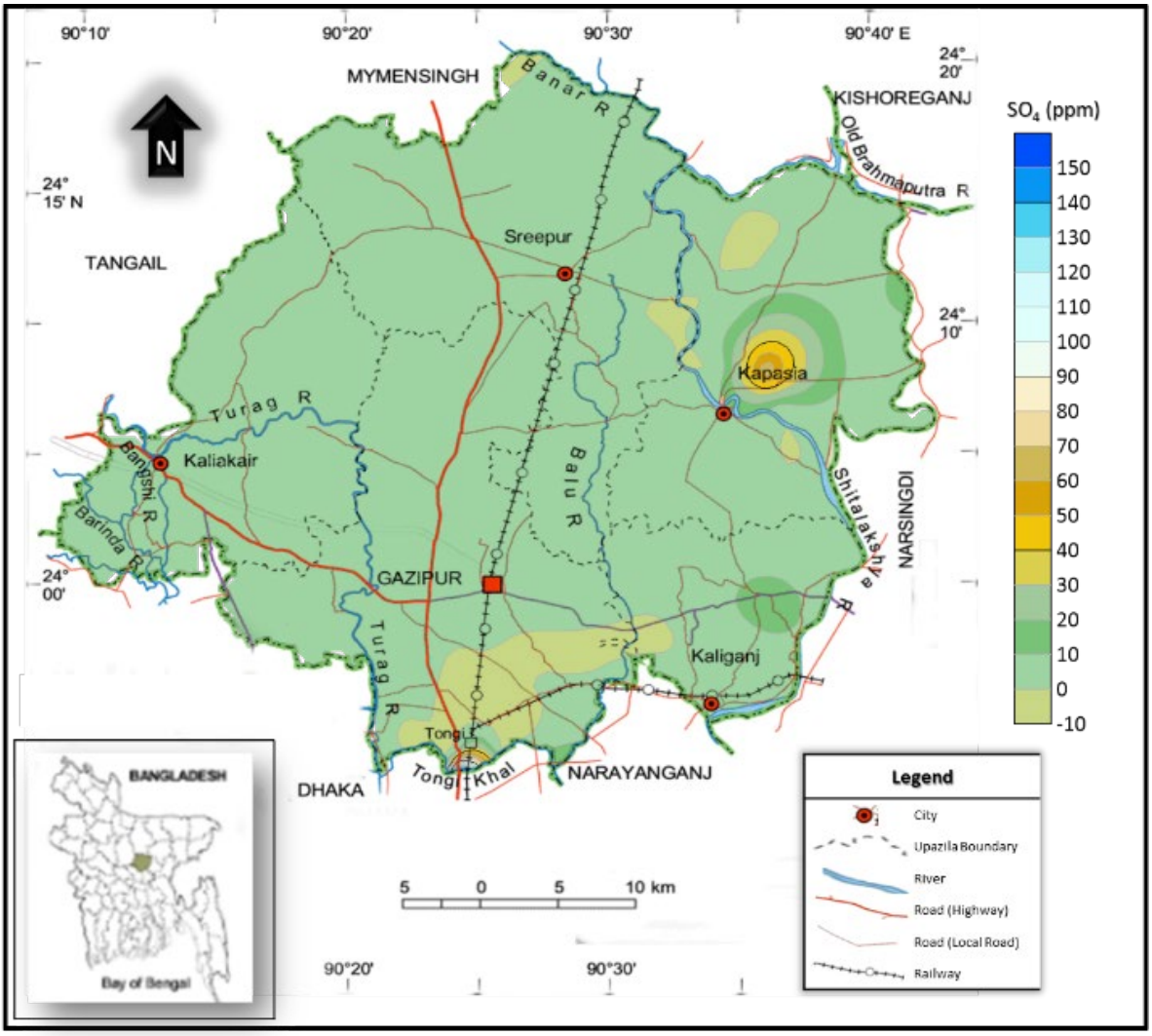

Figure 6.13: Spatial variation of SO_4^{-2} concentration across Gazipur District, showing concentration level concentric and comparatively high at urban or settlement areas.

1.29.1. Sodium adsorption ratio (SAR)

Sodium Adsorption Ratio (SAR) is calculated using the following equation. It should be noted that SAR values classifies water as excellent (less than 10), good (10 to 18), doubtful (18 to 26), and unsuitable (more than 26) for irrigation (Aziane et al, 2020; Gonzalez-Acevedo et al., 2020).

$$SAR = \frac{Na^{+}}{\sqrt{\frac{(Ca^{2+} + Mg^{2+})}{2}}} \text{ meq/L} \qquad \text{----- (Eq. 27)}$$

Spatial distribution of SAR values over Gazipur district indicate that south eastern side exhibit high concentration values (Figure 6.14). This area is a growing industrial zone with dense urbanization.

1.29.2. Magnesium adsorption ratio (MAR)

Magnesium Adsorption Ratio (MAR) is calculated using the following equation. It should be noted that MAR values with more than 50 indicates the water is unsuitable for irrigation (Aziane et al., 2020; Gonzalez-Acevedo et al, 2020).

$$MAR = \left(\frac{Mg^{2+}}{Mg^{2+} + Ca^{2+}}\right) \times 100 \text{ meq/L} \qquad \text{----- (Eq. 28)}$$

Spatial distribution of MAR values over Gazipur district indicate that over values are high throughout the study area. higher concentrations can be seen north- central areas where agricultural activities are high. (Figure 6.15)

1.29.3. Permeability index (PI)

Permeability index (PI) is calculated using the following equation. It should be noted that PI values classifies water as excellent (less than 20), good (20 to 40), injurious (40 to 80), unsatisfactory (more than 80) for irrigation (Aziane et al., 2020; Gonzalez-Acevedo et al., 2020).

$$PI = \left(\frac{Na^{+} + \sqrt{HCO_3^{-}}}{Na^{+} + Ca^{2+} + Mg^{2+}}\right) \times 100 \text{ meq/L} \qquad \text{----- (Eq. 29)}$$

Spatial distribution of PI values over Gazipur district indicate no major hotspots. (Figure 6.16). Two concentric high values at urban areas can be seen.

1.29.4. Soluble sodium percentage (SSP)

Soluble Sodium Percentage (SSP) is calculated using the following equation. It should be noted

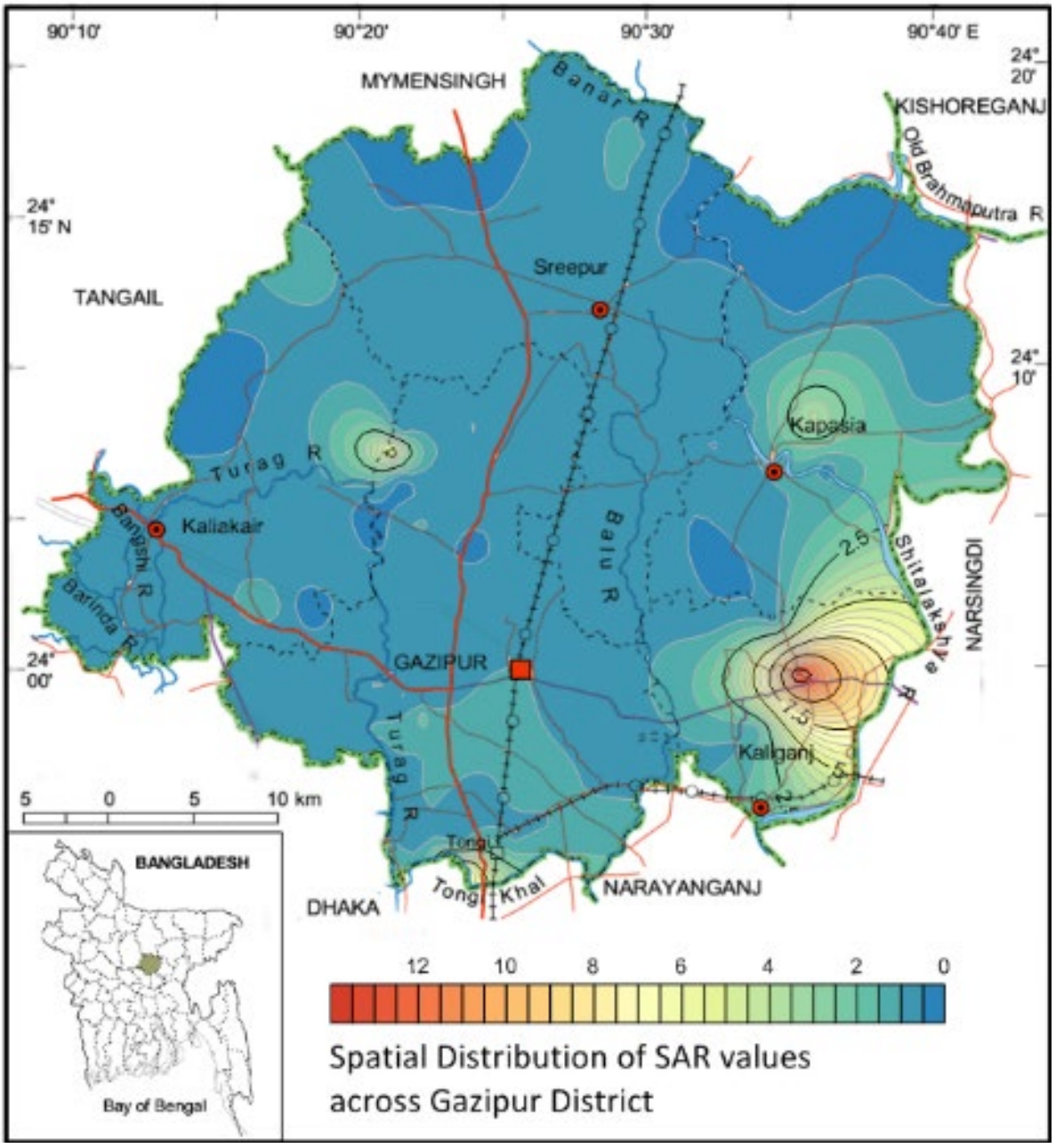

Figure 6.14: Spatial variation of Sodium Adsorption Ratio (SAR) values of groundwater samples collected across Gazipur District, showing increased values along urban settings but excessive spike on south-eastern corner of the district.

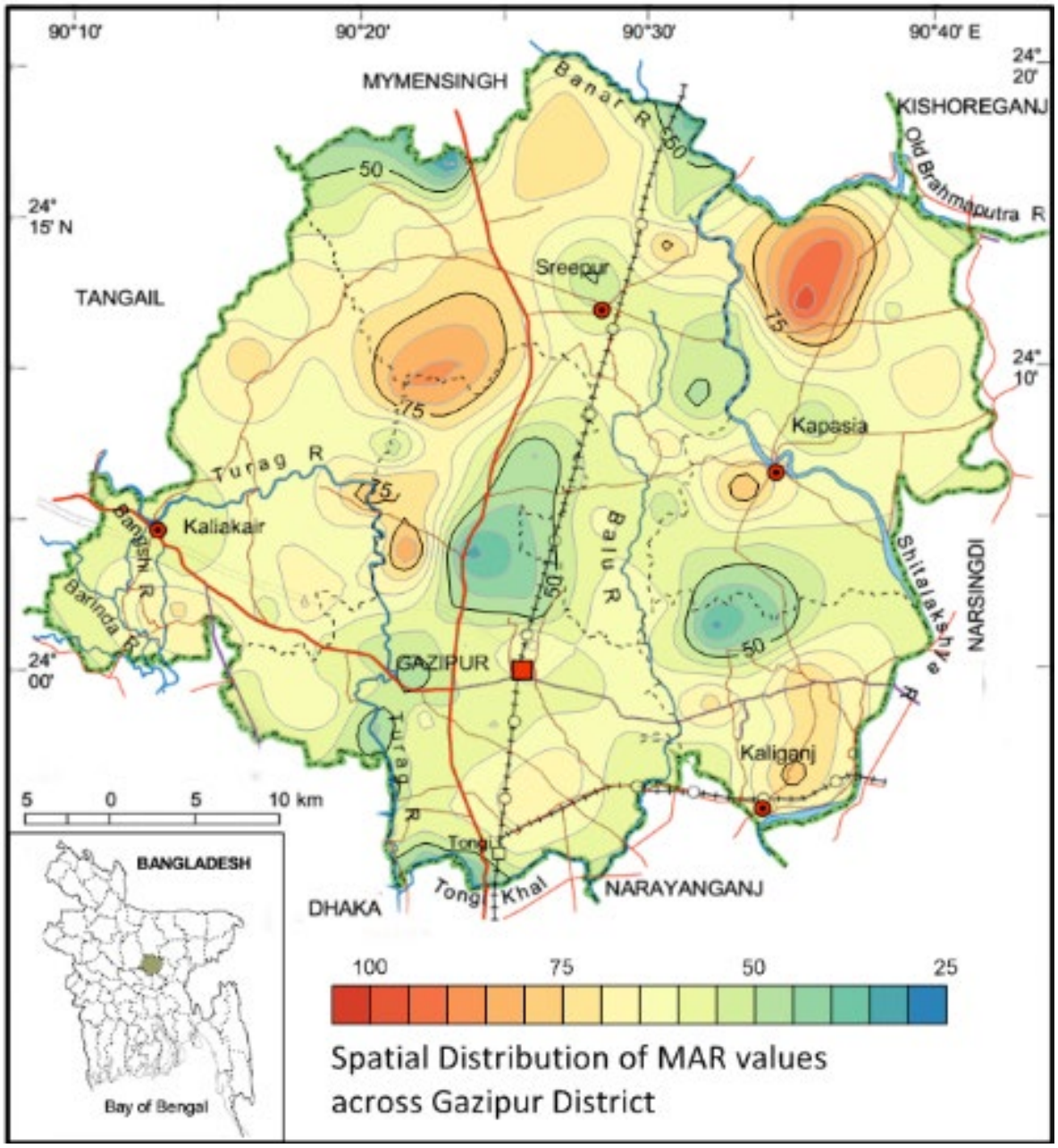

Figure 6.15: Spatial variation of Magnesium Adsorption Ratio (MAR) values of groundwater samples collected across Gazipur District, showing increased values along urban settings but excessive spike on south-eastern corner of the district.

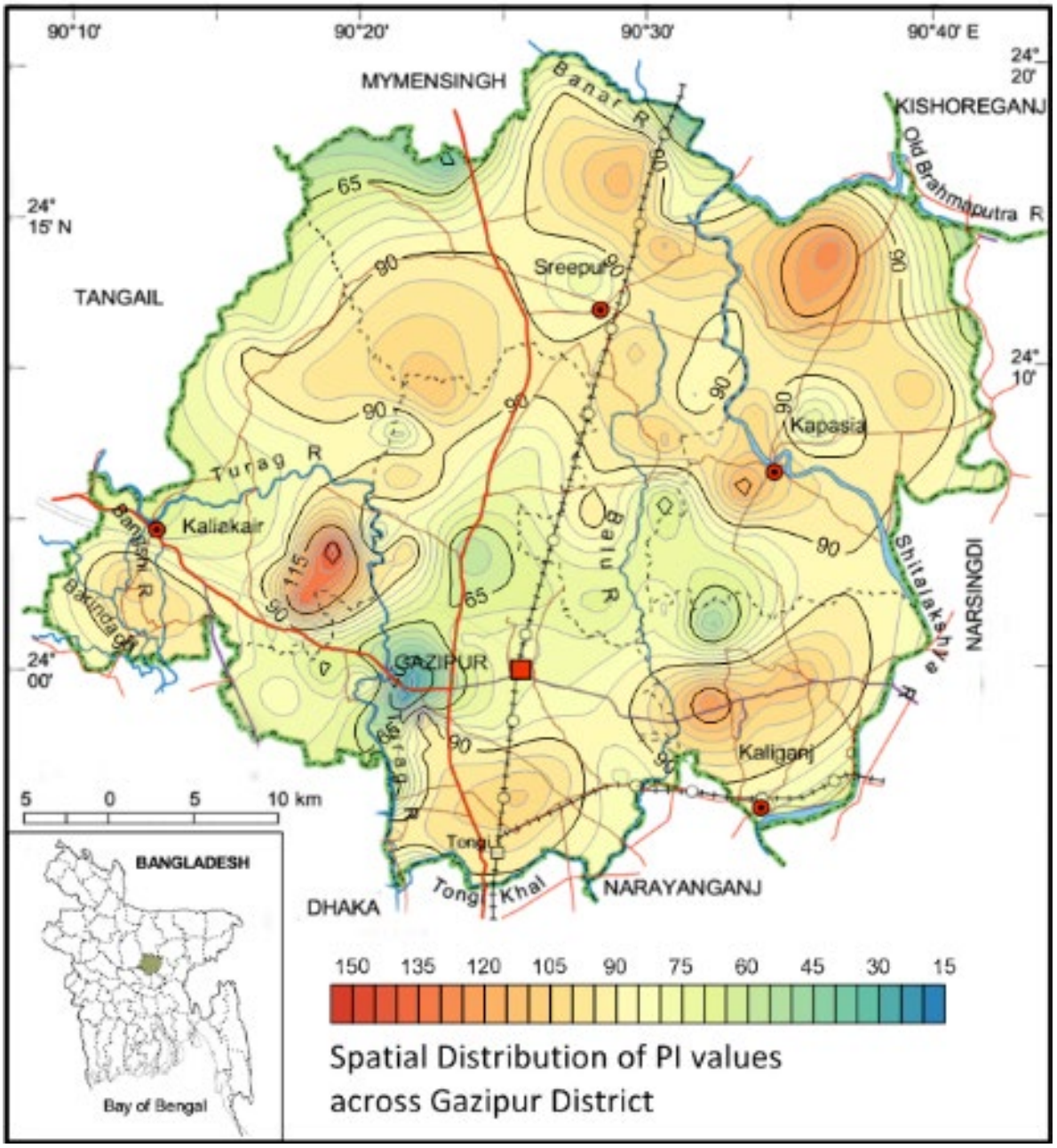

Figure 6.16: Spatial variation of Permeability Index (PI) values of groundwater samples collected across Gazipur District, showing increased values along urban settings. It is evident that most of the groundwaters in the district are not completely suitable for irrigation, especially along areas where urbanization and industrialization development are rapidly growing.

that SSP values classifies water as excellent (less than 50) and bad (more than 50) for irrigation (Aziane et al., 2020; Gonzalez-Acevedo et al., 2020).

$$SSP = \left(\frac{Na^{+}}{Na^{+} + Ca^{2+} + Mg^{2+}}\right) \times 100 \text{ meq/L} \qquad \text{----- (Eq. 30)}$$

Spatial distribution of SSP values over Gazipur district indicate that south eastern side exhibit high concentration values (Figure 6.17). This area is a growing industrial zone with dense urbanization. Thus, water from high concentration area shouldn't be used for irrigation as it may cause soil salinization.

1.30. Water Classification

The characteristic geochemical behavior of groundwater is important in a hydrogeological study. This behavior gives a classification of water and states its suitability level. Irrigation suitability of groundwater was evaluated based on widely accepted guidelines, namely, Piper trilinear diagram, Wilcox diagram, USSL classification diagram, and Doneen diagram.

From the Piper trilinear diagram, it can be determined that alkaline earths exceed alkalies in this sample. Although the diagram is effective, many problems need to be answered by intensive studies of critical analytical data by other methods (Piper, 1944; Figure 6.18).

From the Durov Diagram, groundwater samples show a more concentric pattern at the g-sector of the Langgurth division. According to Lloyd & Heathcost, groundwater samples taken during the dry season are of simple dissolution or mixing with no dominant anion or cation (sector 5). But groundwater samples exhibit a more end-point grade with Cl and Na dominance. Increased mixing of Na and Cl Water Is related to reverse ion exchange of Na-Cl waters Indicative of Cement pollution. Hem (1989) stated that a high level of Na and Cl within water indicates contamination of human activities, agricultural by-products, and industrial effluents. (Figure 6.19)

The Wilcox plot is used to determine the viability of water for irrigation purposes (Wilcox, 1955). It is a semi-log scatter plot of the "sodium hazard" (sodium adsorption ratio [SAR]) against the "salinity hazard" (electrical conductivity) to evaluate the irrigation suitability of groundwater. All the concentration values are expressed in equivalents per million.

U.S. Salinity Laboratory diagram (1954) interpretation is given in Figure 6.20. The two most significant parameters of sodium and salinity hazards indicate usability for agricultural purposes.

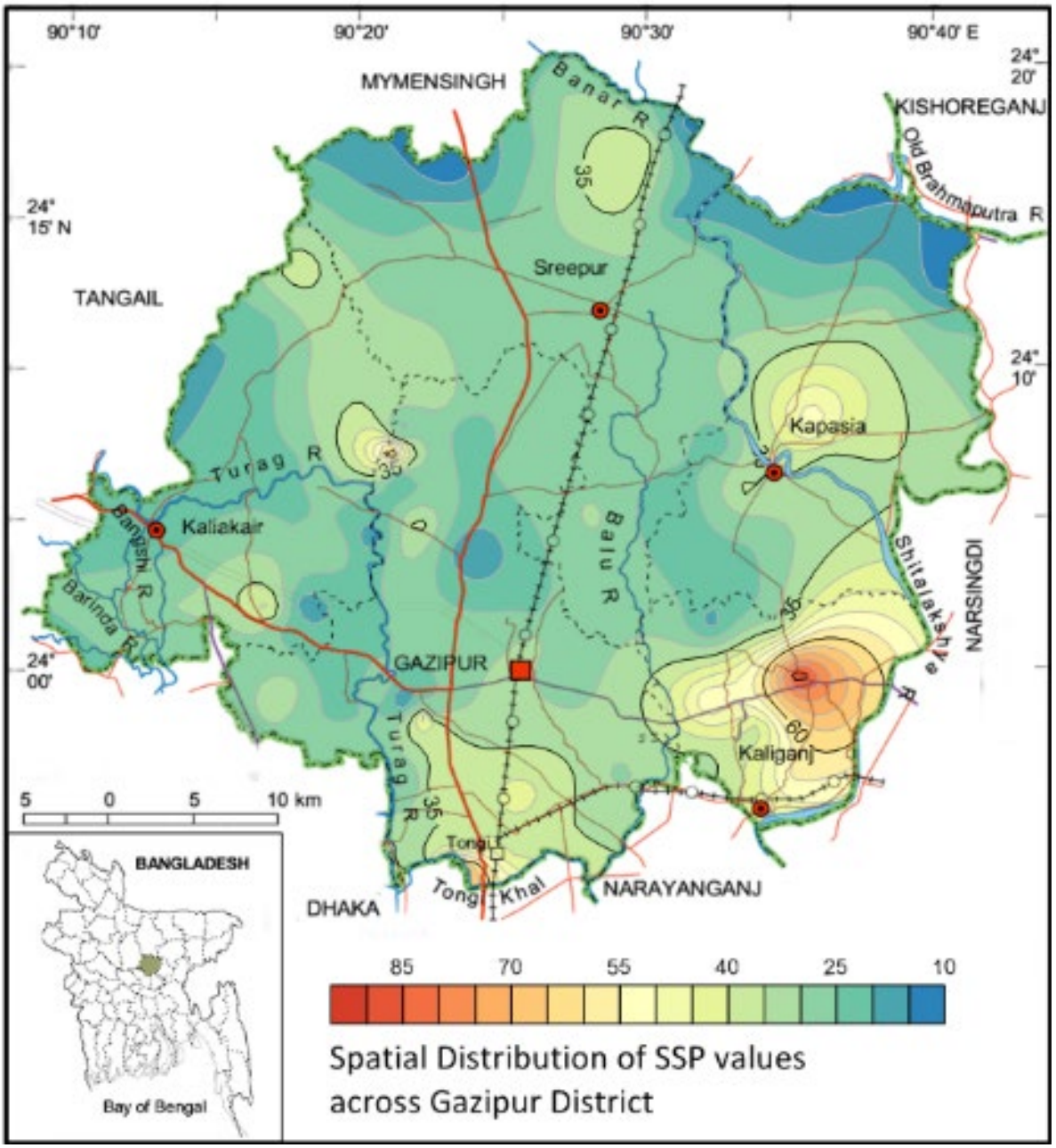

Figure 6.17: Spatial variation of Soluble Sodium Percent (SSP) values of groundwater samples collected across Gazipur District, showing increased values along urban settings. It is evident that most of the groundwaters in the district are not completely suitable for irrigation, especially along areas where urbanization and industrialization development are rapidly growing.

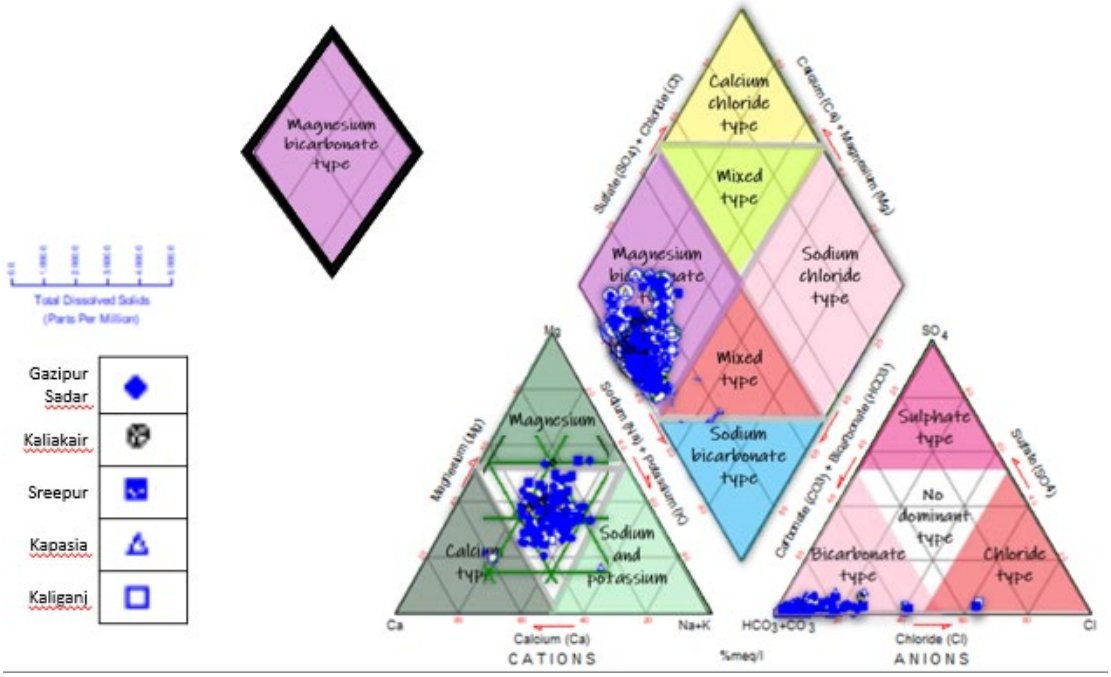

Figure 6.18: Piper Diagram of groundwater samples collected from Gazipur District with index diagram showing standard Piper Diagram classification proposed by Langguth (1966). It is evident that groundwater throughout Gazipur District are similar and are generally of Magnesium-bicarbonate type.

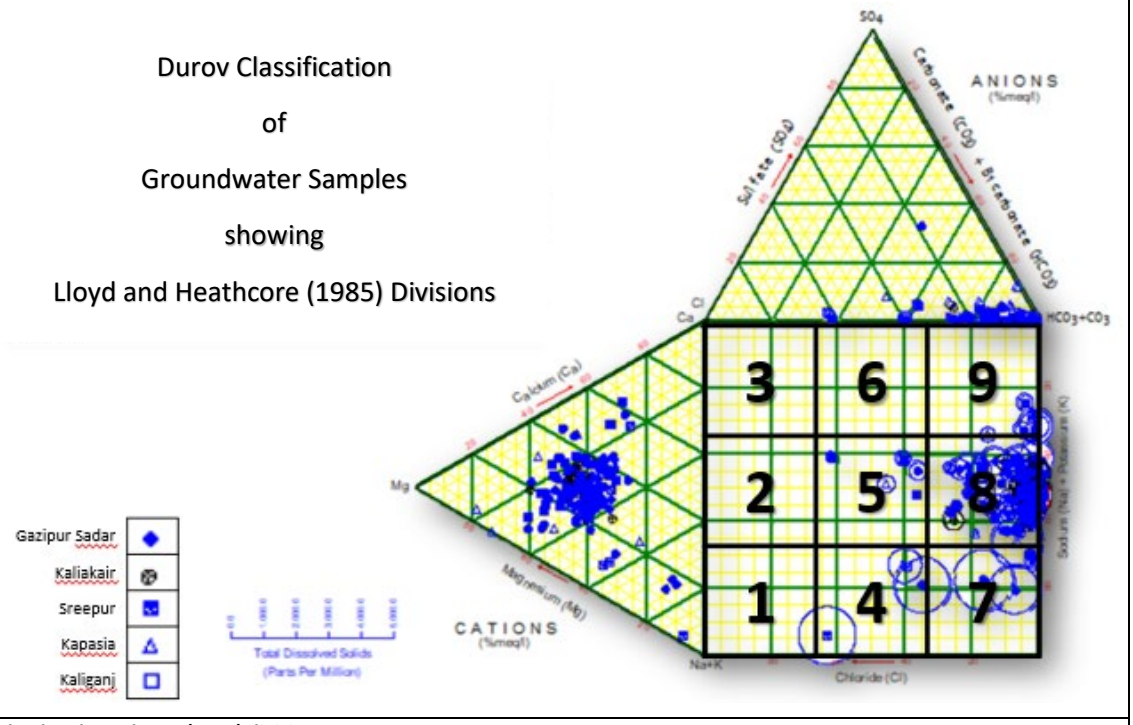

Lloyd and Heathcote (1985) divisions

(1) HCO3- and Ca- are dominant, frequently indicates recharging water in limestone, sandstones, and other aquifers.
(2) HCO3- and Ca- are dominant, association with dolomite. If Na+ is significant, an important ion exchange is presumed.
(3) HCO3- and Na+ are dominated, indicates ion exchange water.
(4) Ca+2 and SO4-2 are dominant, frequently indicates a recharge water in lava and, otherwise mixed water.
(5) no dominant anion or cation, indicates water exhibiting dissolution or mixing.
(6) SO2-2 and Na+ are dominated, water type is not frequently encountered and indicates probable mixing influence.
(7) Cl- and Na- dominant frequently encountered unless current pollution is present. Otherwise, the water may result from reverse ion exchange of Na-Cl waters.
(8) Cl- and Na- are dominant cation, indicate that the groundwater can be related to reverse ion exchange of Na-Cl waters.
(9) Cl- and Na- dominant frequently indicate end point waters

Figure 6.19: Durov Diagram of groundwater samples collected from Gazipur District with index diagram showing standard Durov Diagram classification proposed by Lloyd and Heathcoat (1985). Groundwater of the Gazipur district is mostly of Cl^- and Na^- dominant, with few samples indicating end point waters.

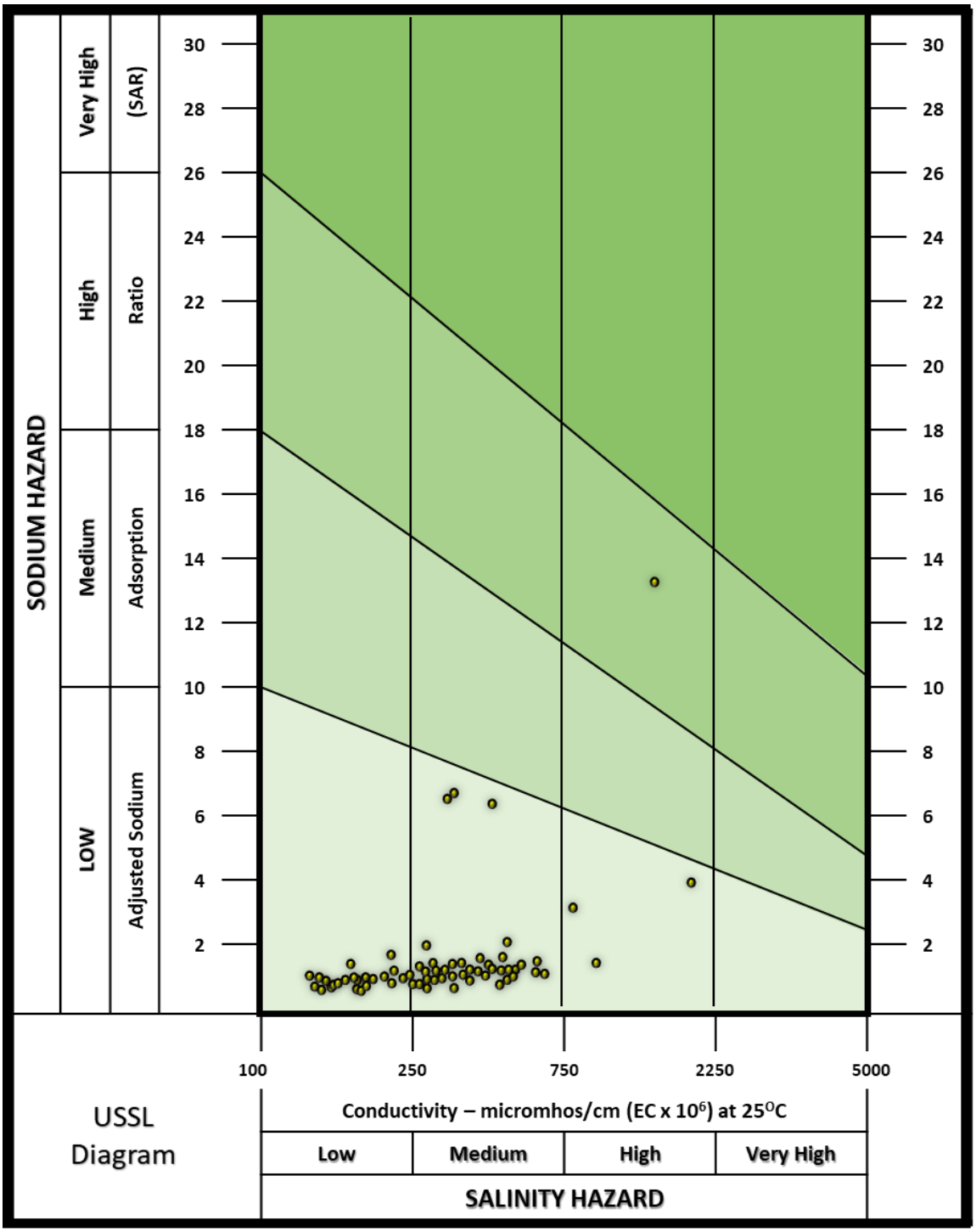

Figure 6.20: Groundwater Quality classification using USSL Diagram (USSL, 1954) for irrigation purpose of samples collected from Gazipur District. Though most are indicating low to moderate salinity hazard with low sodium hazard, yet there is a trend of growing levels. Samples show high sodium hazard with high salinity Hazard.

USSL diagram indicates that the samples are concentric and range from low salinity with medium sodium to medium salinity with low sodium. The Doneen diagram plots (Figure 3.21) indicate that Gazipur district groundwater is generally suitable for irrigation. Groundwater of the Gazipur District is excellent for irrigation, aside from a few spiked spots, probably localized contamination.

Thus, the spiked samples may result/ from localized point source contamination that made its way to groundwater. This may be due to effluents from the industries and domestic sewage.

Gibbs plot indicates the dominating process that controls groundwater chemistry. Figure 6.22 demonstrates that groundwater samples from the Gazipur District are regulated mainly through rock weathering and evaporation and particle precipitation to a lesser extent. Thus, we might conclude that groundwater is of poor quality. The quantities of ions created by the chemical weathering of the rock may increase salinity when evaporation increases.

1.31. Statistical Interpretation of Geochemical Data

The purpose of applying statistics was to interpret the geochemical results and have a comparative understanding of samples affected by spatially varying factors. The statistical parameters used for the study are analysis of arithmetic mean, analysis of standard deviation, analysis of T-test, correlation matrix, and Cluster analysis.

EC, TDS, Na, and Ca have comparatively higher standard deviation values than the parameters. (Table 6.2). This infers that the EC level varies from one sampling point to another due to contamination sources and spatial distribution.

Chloride is an indicator of industrial waste (Hem, 1985). Chloride is primarily present in low concentrations. The analytical data were analyzed using the correlation technique to investigate inter-elemental associations. The results of the correlation suggested a strong ($p < 0.05$) association among all the major and minor ions in water samples (Figure 6.23). Correlation analysis shows the strongest association between TDS - EC (r=0.99), which infers that the measured value of EC will heavily influence the TDS level. Besides very strong association is also present for K-Na (r=8.421), Mg-Ca (r=0.7), and Cl-Na (r=0.6). All these parameters are associated with agricultural pesticides, sewage, and industrial effluents. Their strong association indicates the probable impact condition of urbanization and industrialization contamination. (Table 6.3)

Cluster analysis shows a number of small cluster units that belong under two major cluster groups. These groups differ significantly from each other. Using the complete amalgamation linkage rule and Euclidean distances criteria, it was observed that the number of variables used is 13, the number of cases identified is 132, and the number of linkage distances is 16. The Dendrogram clearly shows the presence of three major clusters (Figure 6.24).

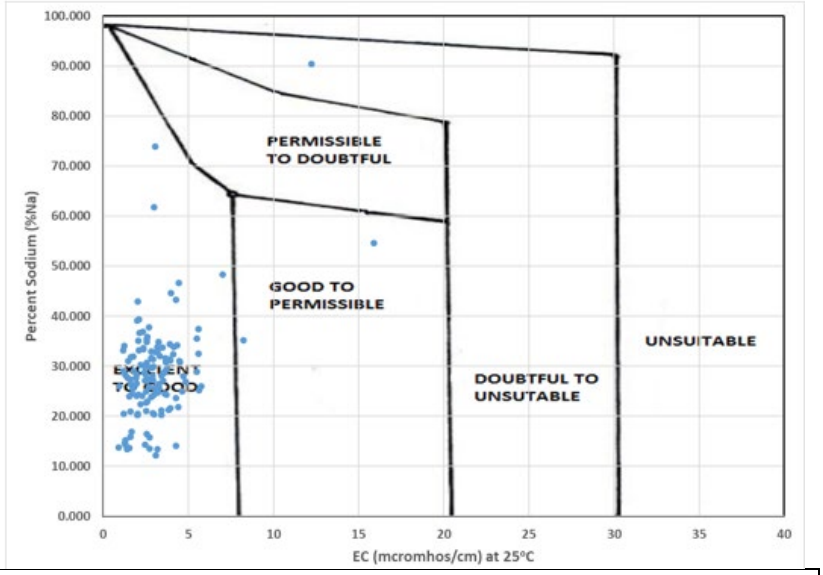

Wilcox Diagram

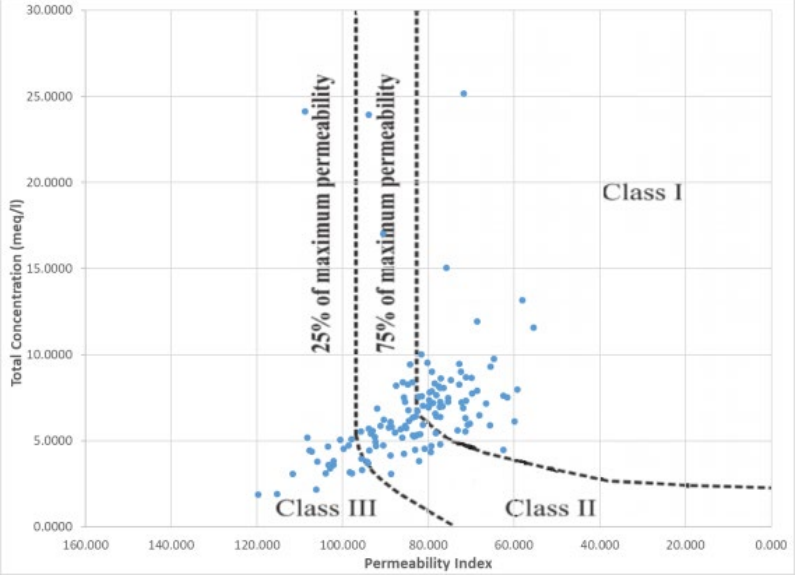

Doneen Diagram

Figure 6.21: Groundwater quality classification for irrigation use of samples collected from Gazipur District.

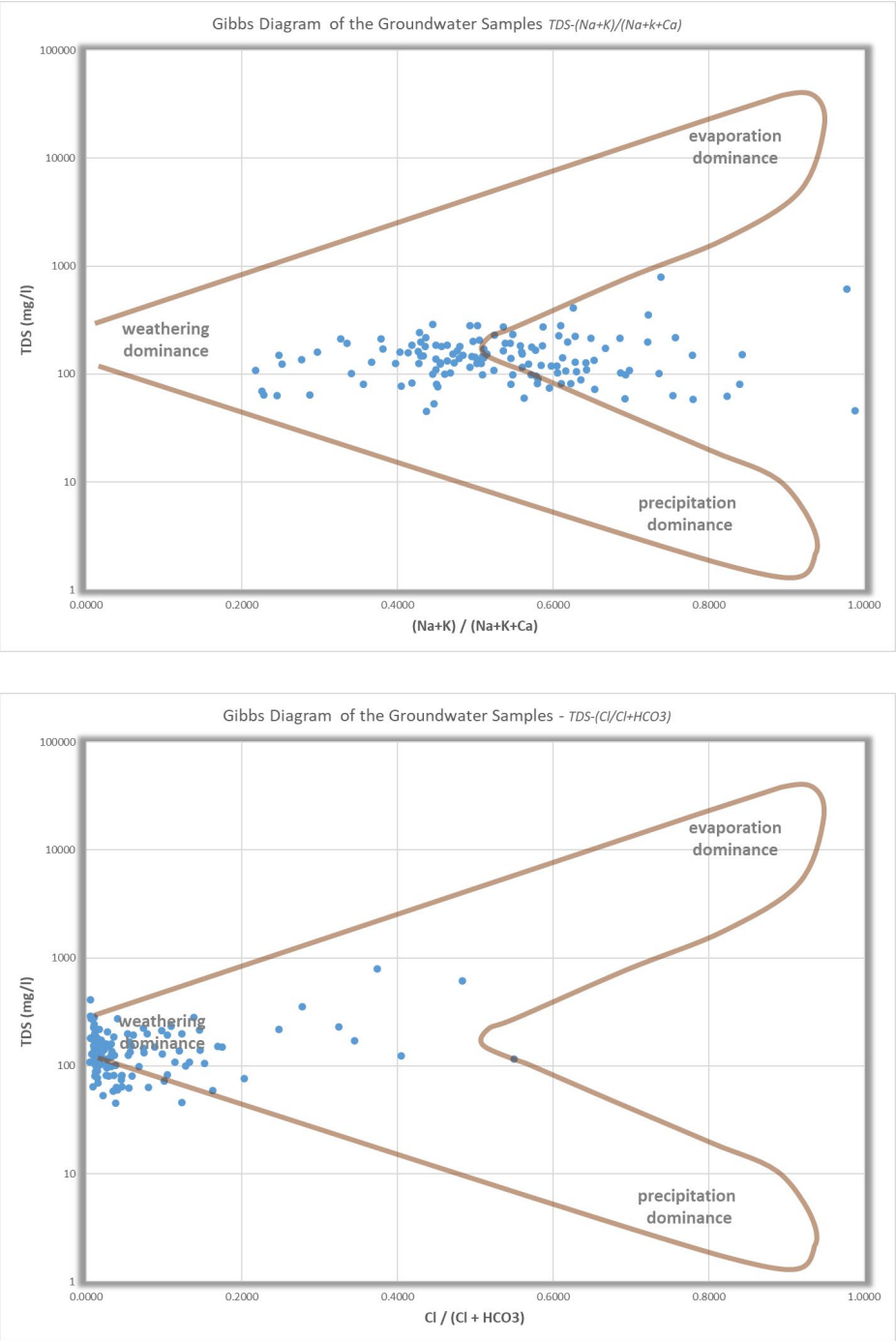

Figure 6.22: Gibbs plot showing major processes controlling groundwater chemistry samples collected from Gazipur District.

Table 6.2: Statistical analysis results of groundwater samples collected from Gazipur District.

	pH	T	EC	TDS	ORP	Na	K	Ca	Mg	Fe	Mn	HCO3	Cl	SO4	NO3	F
		oC	us/min	mg/L		mg/L	mg/L	mg/L	mg/L	mg/L	mg/L	mg/L	mg/L	mg/L	mg/L	mg/L
Minimum	4.74	23.00	91.00	45.00	-100.00	2.99	0.13	0.07	6.44	0.00	0.00	41.13	1.08	0.00	0.00	0.02
Maximum	9.78	31.80	1590.00	792.00	390.00	243.01	14.37	65.03	34.68	8.06	2.51	373.63	262.86	173.33	31.54	2.25
Mean	7.04	26.90	273.50	136.00	194.00	18.84	0.81	20.13	14.28	0.12	0.08	169.44	3.91	0.85	0.00	0.26
Average	7.06	26.90	308.76	153.20	188.56	24.23	1.44	20.44	15.41	0.44	0.15	177.56	13.62	3.77	0.64	0.34
Std Deviation	0.64	1.17	185.53	93.22	99.96	29.84	2.40	11.31	4.59	0.92	0.27	67.75	31.39	16.23	3.03	0.35
Variance	0.41	1.38	34685.85	8755.75	10068.87	897.50	5.79	128.92	21.25	0.85	0.07	4625.41	992.80	265.52	9.23	0.12
Skewness	0.85	0.38	3.66	3.60	-0.20	5.35	4.36	1.21	0.97	5.22	5.85	0.53	5.55	9.28	8.52	3.63
Kurtosis	4.26	3.72	20.46	19.88	-0.10	32.03	18.64	2.98	1.50	36.49	46.76	0.44	36.69	92.96	83.47	15.30

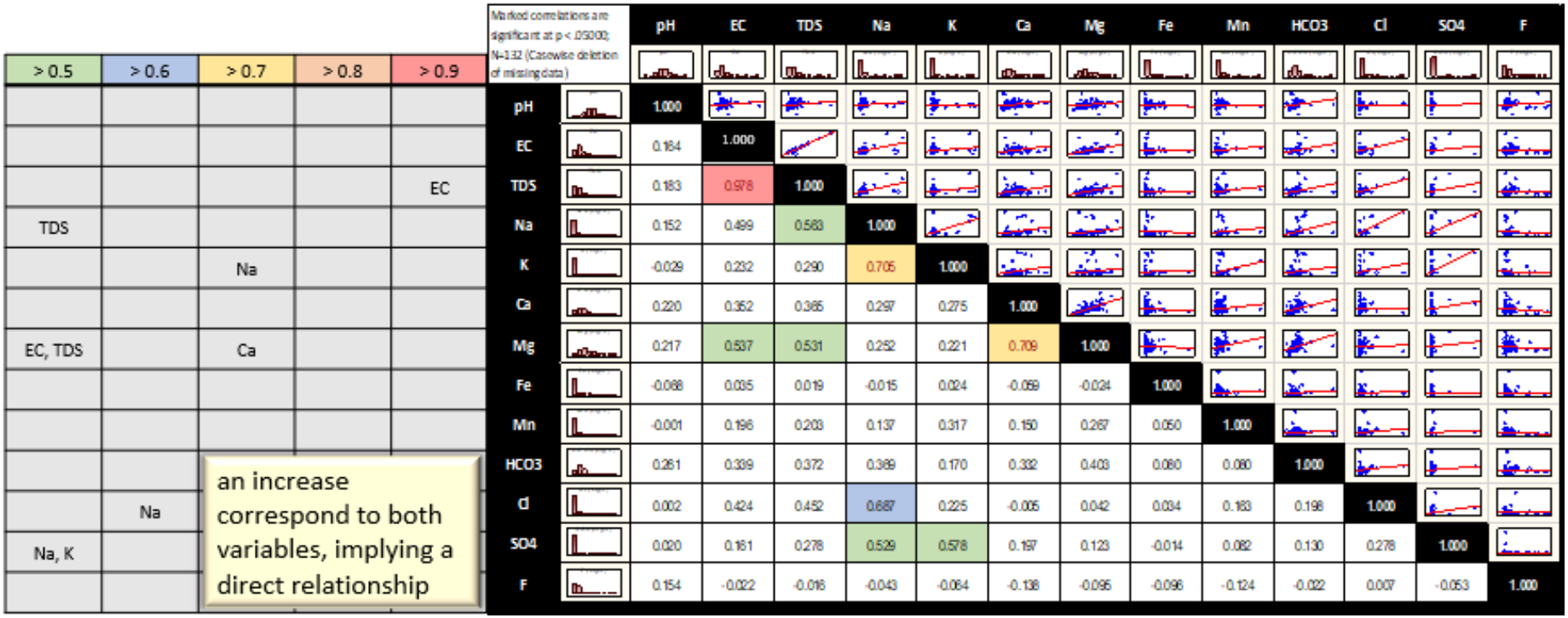

Figure 6.23: Pearson correlation to determine p-values to understand the significance of pair-parameters and joint effect variables of groundwater samples collected from Gazipur District.

Table 6.3: Correlation Matrix results to determine the significant difference between the means, which may be related to certain features. The relationship between EC-TDS is expected. A strong relationship between Na-K indicates strong influence of agricultural activities and sewage mixing. Mg-Ca is evident.

Correlation Coefficient	Parameters		T-Stat	Confidence		
				Value	Interval	
					(+95%)	(-95%)
> 0.9	TDS	EC	18.173	16.506	169.558	136.545
> 0.7	K	Na	8.421	5.917	31.338	19.505
> 0.7	Mg	Ca	4.903	1.845	6.462	2.771
> 0.6	Cl	Na	6.703	4.520	166.066	157.027

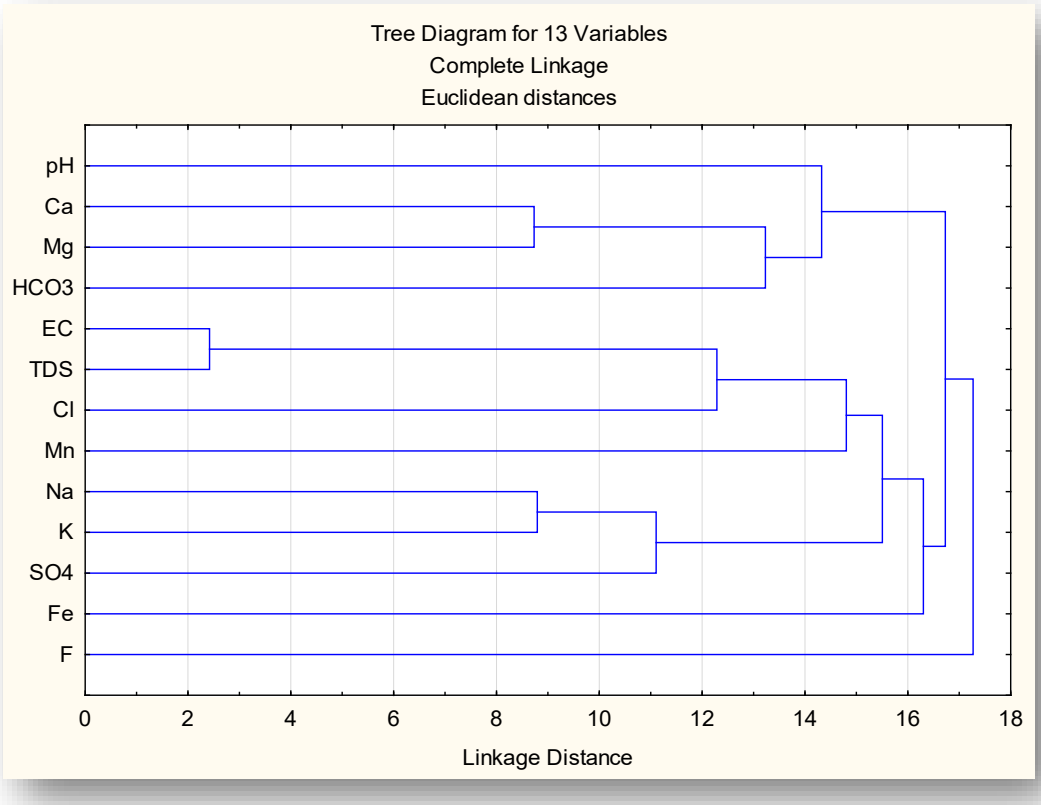

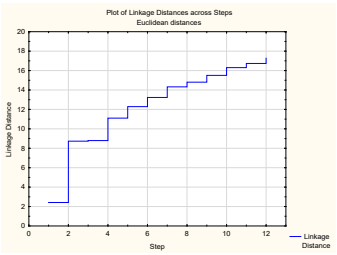

Amalgamation Schedule: Complete Linkage

linkage distance	Euclidean distances												
	Obj 1	Obj 2	Obj 3	Obj 4	Obj 5	Obj 6	Obj 7	Obj 8	Obj 9	Obj 10	Obj 11	Obj 12	Obj 13
2.418954	EC	TDS											
8.731194	Ca	Mg											
8.794804	Na	K											
11.10572	Na	K	SO4										
12.28616	EC	TDS	Cl										
13.23105	Ca	Mg	HCO3										
14.32315	pH	Ca	Mg	HCO3									
14.80463	EC	TDS	Cl	Mn									
15.50502	EC	TDS	Cl	Mn	Na	K	SO4						
16.30356	EC	TDS	Cl	Mn	Na	K	SO4	Fe					
16.73062	pH	Ca	Mg	HCO3	EC	TDS	Cl	Mn	Na	K	SO4	Fe	
17.27021	pH	Ca	Mg	HCO3	EC	TDS	Cl	Mn	Na	K	SO4	Fe	F

Figure 6.24: Classifying variables based on the degree of association to understand the relationship of parameters of groundwater samples collected from Gazipur District.

The dominating group being of TDS-EC. Clusters 2 and 3 are Ca-Mg-HCO_3, and Mn-Na-K-SO_4, respectively. Thus, it can be stated that EC and TDS maintain a strong presence over the water quality condition, or the quality changes heavily impact them.

1.32. Water Quality Index (WQI)

Water Quality Index (WQI) has been used to assess groundwater conditions and its vulnerability to contamination based on hydrochemical data. (Table 6.4; Appendix 2)

WQI is commonly used for detecting and evaluating water pollution and may be defined as a reflection of the composite influence of different quality parameters on the overall quality of water (Horton, 1965). It may be defined as a rating reflecting the composite influence of varying water quality parameters on the overall quality of water. (Table 6.5)

The main objective of computing the water quality index (WQI) is to turn the complex water quality data into easily understandable and usable information. A parameter has to be selected based on its impact on the overall quality of water and its health effects.

Thirteen parameters were considered to calculate WQI: pH, TDS, sodium, potassium, calcium, magnesium, iron, manganese, bicarbonate, chloride, sulfate, nitrate, and fluoride. The computed WQI shows that 48% of the water sample falls in excellent and 48% in good water categories. Spatially, WQI values exceed the limit in areas with high urbanization and industrialization setups. Thus, inferring an impact of population density on groundwater resources. (Figure 6.25)

1.33. EC Variation

EC parameter assesses the capacity of water to conduct electrical current. It could be influenced by temperature and by the presence of inorganic dissolved solids such as nitrate, chloride, sulfate, and phosphate anions (EPA, 2020).

EC is useful as a general measure of water quality. USEPA (2020) states that Significant changes in conductivity can be an indicator of pollution of aquatic resources. Significant changes (usually increases) in conductivity may indicate that a discharge or some other disturbance source has decreased the water body's relative condition or health and its associated biota. Anthropogenic activities tend to increase the number of dissolved solids, subsequently increasing conductivity. The most desirable limit of EC in drinking water is 1,500 µmhos/cm (WHO 2004).

Total dissolved solids (TDS) also presented similar Spatio-temporal variation over the district.

EC and TDS were measured four years in the same month to obtain a trend. Over the years, from 2018 to 2021, both parameters have increased gradually.

Table 6.4: Calculation of Water Quality Index (WQI) of the groundwater samples collected across Gazipur District.

Parameter		Observed Values	Standard Values	Unit Weights	Quality Rating	$w_i q_i$
		v_i	s_i	w_i	q_i	
pH		7.54	8.5	0.00578	0.36000	0.00208
EC	uS/cm	990	500	0.00010	1.98000	0.00019
TDS	mg/l	520	1000	0.00005	0.52000	0.00003
Na	mg/l	159.503	200	0.00025	0.79752	0.00020
K	mg/l	16.395	12	0.00409	1.36625	0.00559
Ca	mg/l	38.29	75	0.00065	0.51053	0.00033
Mg	mg/l	15.42	35	0.00140	0.44057	0.00062
Fe	mg/l	0.029	0.10	0.49124	0.29000	0.14246
Mn	mg/l	0.024	0.10	0.49124	0.24000	0.11790
HCO3	mg/l	251.625	600	0.00008	0.41938	0.00003
Cl	mg/l	87.861	600	0.00008	0.14644	0.00001
SO4	mg/l	157.804	400	0.00012	0.39451	0.00005
NO3	mg/l	19.229	10	0.00491	1.92291	0.00945
F	mg/l	0.231	1.000	0.049	0.23110	0.01135

Table 6.5: Classification of water quality-based weighted arithmetic WQI methods. (Modified from Brown et.al., 1970; Chaturvedi & Bassin, 2010)

WQI	STATUS	POSSIBLE USAGES
0 - 25	Excellent	Drinking, Irrigation and Industrial
26 - 50	Good	Domestic, Irrigation and Industrial
51 - 75	Fair	Irrigation and Industrial
76 - 100	Poor	Irrigation
101 - 150	Very Poor	Restricted use for Irrigation
150	Unsuitable for drinking	Proper treatment required before use.

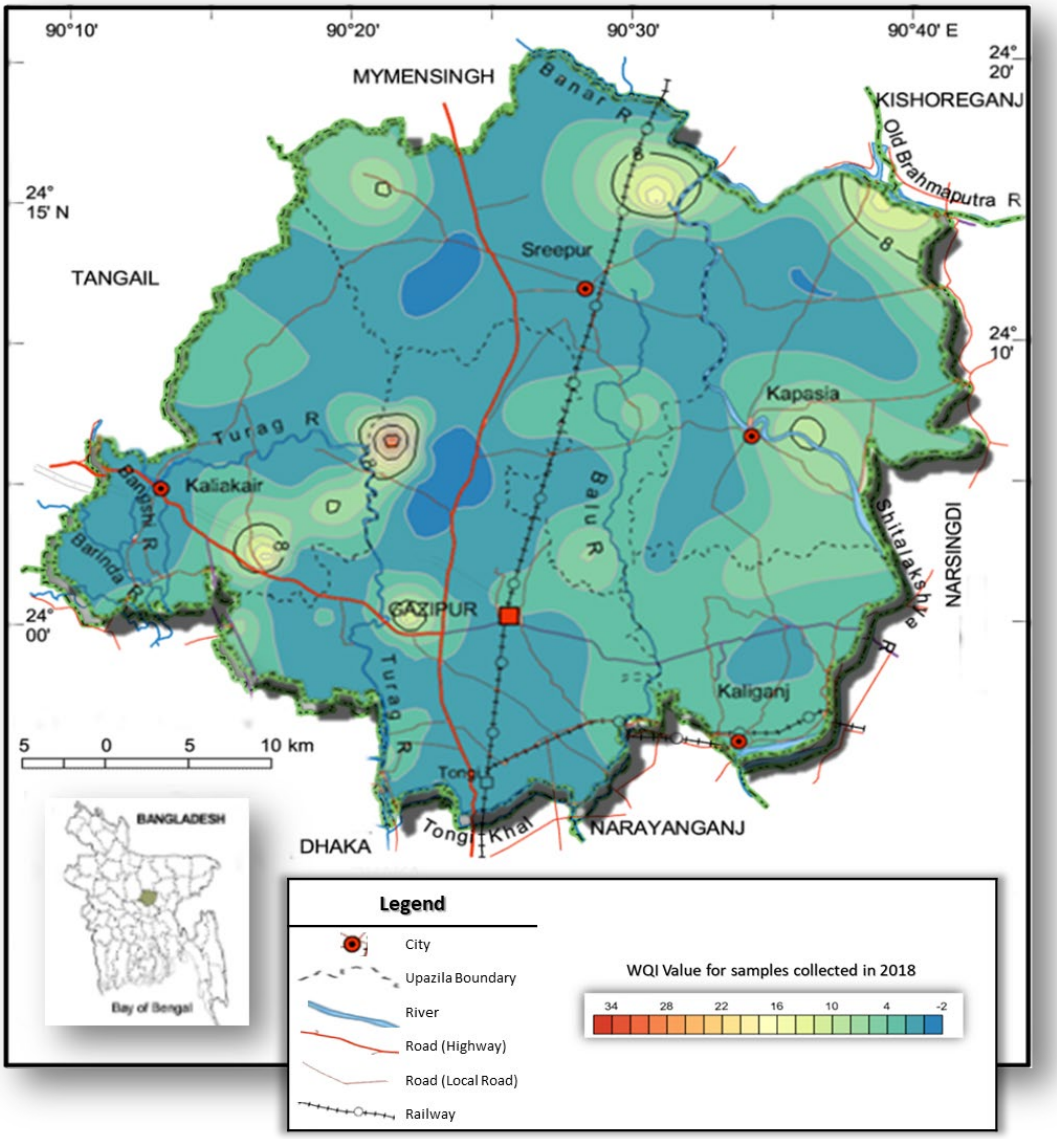

Figure 6.25: Spatial Variation of Water Quality Index (WQI) of measured samples across Gazipur District. High concentration is at Gazipur Sadar, Sreepur, southern Kaliakair, and Kapasia. All densely populated, rapidly growing urbanization and industrialization area.

A similar comparative increasing trend can be observed with historical measurements. EC and TDS level variation is presented in Table 6.5. Figure 6.26 shows that EC value has increased over time, especially in urban and industrial areas in Gazipur District.

Thus, a high concentration of EC is observed in the study area. This spike can be due to domestic/anthropogenic activities. The spatial distribution of EC indicates that both are increasing in density population and industrialized arears. As Gazipur is on a thick clay layer, contaminant infiltration perhaps took place along cracks and fractures on the surface or leaks along various ill-planned and improperly maintained wells.

Table 6.6: EC and TDS value distribution over the years in Gazipur district.

	EC (µmhos/cm)			TDS (ppm)		
	Maximum	Average	Minimum	Maximum	Average	Minimum
2018	1430	438	119	991	310	79
2019	1777	432	117	1067	265	72
2020	1955	553	129	1243	261	78
2021	2150	612	142	1350	263	85

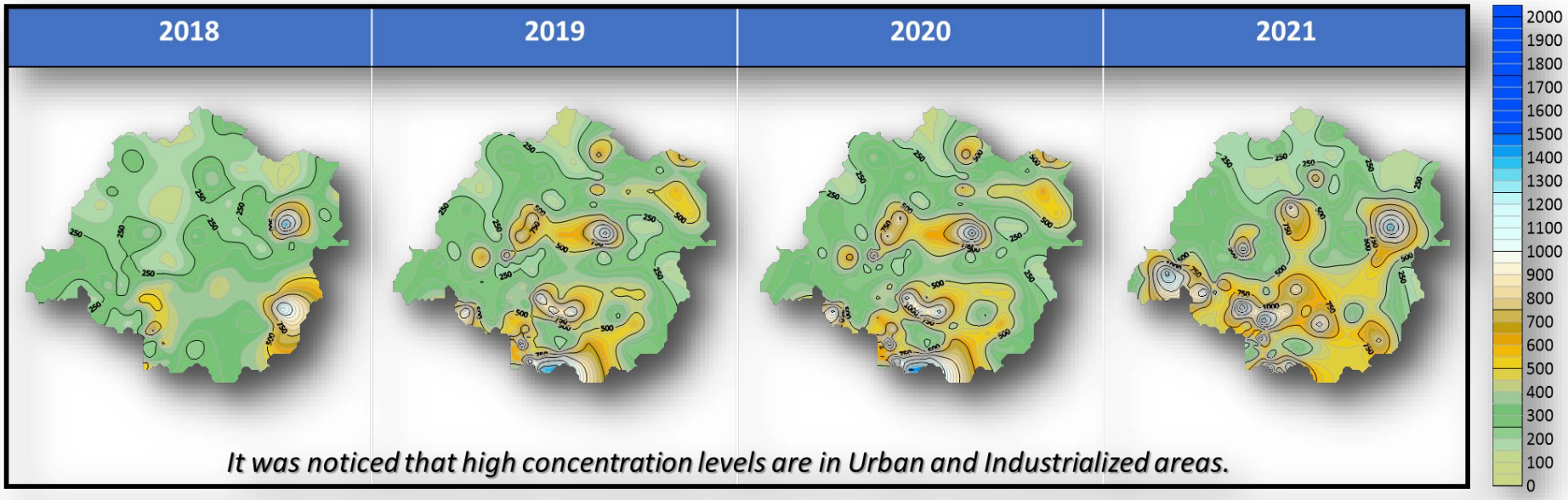

Figure 6.26: Groundwater EC variation across Gazipur District. Over the years concentration has been increasing with growing urban and industrial developments.

7 GROUNDWATER VULNERABILITY ASSESSMENT

GROUNDWATER VULNERABILITY ASSESSMENT USING A MODIFIED DRASTIC MODEL

1.34. Intrinsic Aquifer Vulnerability Mapping Using DRASTIC Method

Assessing groundwater's vulnerability does not quantify the exact contamination level but indicates the likelihood of groundwater contamination. There are numerous methods for assessing vulnerability, among which the DRASTIC Index approach is one of the most used and straightforward (Albinet & Margat, 1970; Abdeslam et al., 2017).

The key objective of this research work is to assess the anthropogenic effect on groundwater and how it makes it vulnerable to contamination. Human-caused activities must be carefully observed as growing population, increasing population density, and social development to sustain population growth are having their impact on land and resources. It is expected that at Gazipur that the low-permeability clay layer will protect the underlying aquifer from surface contamination. Nonetheless, extensive pumping and lowering of the water table might increase vertical leakage into the aquifer.

DRASTIC parameters are processed under the GIS environment to detect the low-, moderate- and high-vulnerable zones. The assigned weights, ranges, ratings, and index used for the DRASTIC parameters has been presented in Table 3.3. A standard vulnerability assessment to understand the modification required to ensure the applicability of the DRASTIC method for an Urban and industrial area above a confined aquifer.

1.34.1. Depth to groundwater (D)

Depth to water is defined as the distance (in meters) from the ground surface to the water table. For this research work, 18 BWDB water wells have been used to assess and measure the water level for 2018. Well, locations were plotted in an ArcGIS project. Using the GIS extrapolation method, a contour map was prepared, masking it by the Gazipur shape file. Groundwater level fluctuates between 9 to 80 m. The lower values (< 3 m) were observed in the northwest and the highest values along the southern part. (Figure 7.1)

1.34.2. Net recharge (R)

Net recharge is the total quantity of water infiltrating from the ground surface to an aquifer annually. Higher the recharge rate, the rating is higher. A groundwater recharge map is prepared based on standard and conventional understanding for the study area, which will be clarified later on in this research work. For this stage of the study, recharge has been calculated by the CMB method. The recharge value ranges between 10.7mm to 51mm/day. The analysis shows that the minimum value of net recharge lies in Gazipur Sadar.

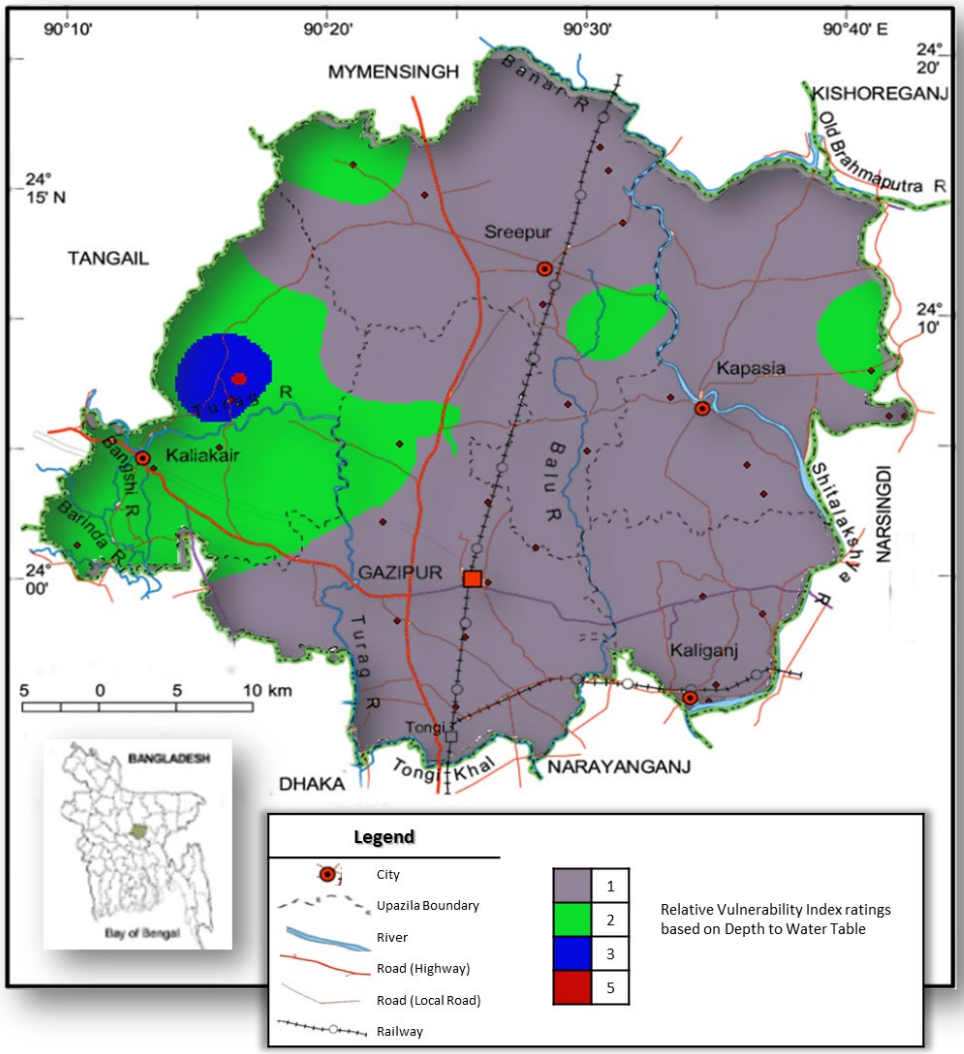

Figure 7.1: DRASTIC parameter map – showing spatial distribution of the depth to aquifer media vulnerability index values, essentially referring to the water table level. Highest depth can be seen at the western part and consistent almost throughout the district.

It also indicates that 21.5% (1602 sq. km.) of the total study area possesses a net recharge above 92 mm/year. It can be noted that net recharge is moderately responsive to aquifer vulnerability. (Figure 7.2)

1.34.3. Aquifer media (A)

Aquifer media refers to the consolidated or unconsolidated rock which serves as an aquifer. The aquifer considered for this study Is confined. Its overlain by a thick clay layer known as the Madhupur Clay. Aside from narrow strips to the east and west side of the district, Gazipur is situated on the southern extension of the Madhupur Clay layer.

There are five distinctive characteristics of the aquifer system beneath Gazipur. The aquifer systems are: (1) Very Fine Sand, (2) Fine Sand, (3) Fine Sand and Medium Sand, (4) Medium Sand, and (5) Medium and Coarse Sand. Aquifers consisting of medium sand cover approximately 86% of the study area; aquifers comprised of fine sand cover about 9% (a few patches in the Sreepur, Kaliakair, Kaliganj, Gazipur Sadar, and Kapasia upazilla); and aquifers consisting of coarse sand cover approximately 5% of the study area. (Figure 7.3)

1.34.4. Soil media (S)

Soil considerably impacts the quantity of recharge that may permeate into the ground and, consequently, the ability of contaminants to flow vertically into the vadose zone. The soil ingredients determine the vertical movement of pollutants via the vadose zone and the recharge potential (Lee, 2003). Clay characteristics, such as its shrink/swell potential and grain size, significantly impact the soil's contamination potential. From the soil map, it can be inferred that clay, silty lay, and sandy clay are the three dominant soil types in the study area, covering around 37% and 36% of the total study area, respectively. The other soil types are clay loam, sandy clay loam, and loamy sand, representing around 16%, 8%, and 3% of the total study area. (Figure 7.4)

1.34.5. Topography (T)

Topography refers to the slope variation of the land's surface. The degree of the slope will impact the extent of pollutant runoff and its ability to settle and penetrate. Tthe geography of the research region is relatively flat, with slopes ranging from 0 to 12 degrees. Most of the center portions of the Gazipur Sadar, Sreepur, and Kapasia Upazillas, as well as parts of the Kaliakair and Kaliganj Upazillas, have steeper slopes than eight degrees. Figure 3 illustrates the topography of the research area (e). The slope was generated from the digital elevation model (DEM) of the area of investigation. According to the study, the slope of the majority of the studied region is less than 1 percent. Therefore, there is a strong likelihood that water will accumulate on the top and percolate into the aquifer. Less than 1 percent slope is scored as a 10. In this scenario, the research area is extremely topographically fragile. (Figure 7.5)

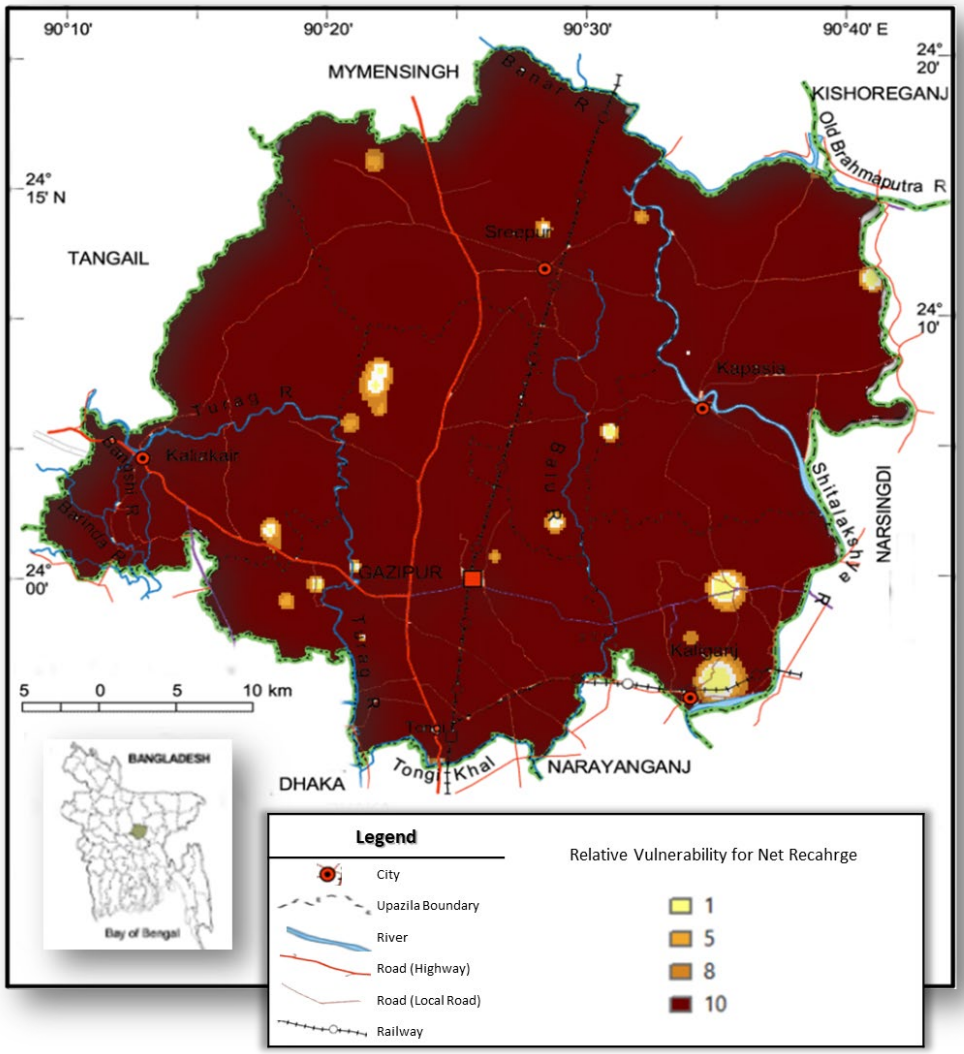

Figure 7.2: DRASTIC parameter map – showing spatial distribution of the net-recharge values across the study area. High recharge is evident along the forest and green areas of the district, which contradicts the fact that the district is underlain by thick Madhupur Tract clay layer. Commonly practiced and used data were applied.

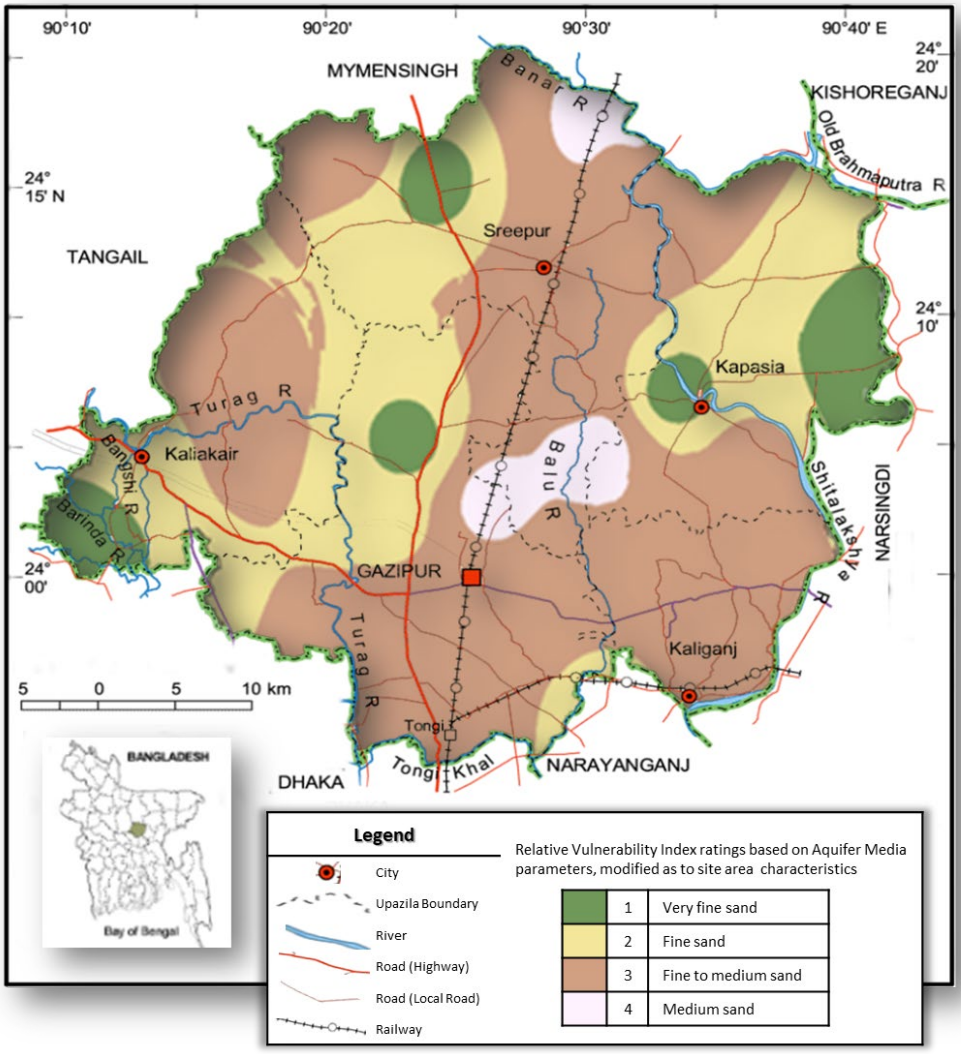

Figure 7.3: DRASTIC parameter map – showing spatial distribution of the aquifer media across the study area.

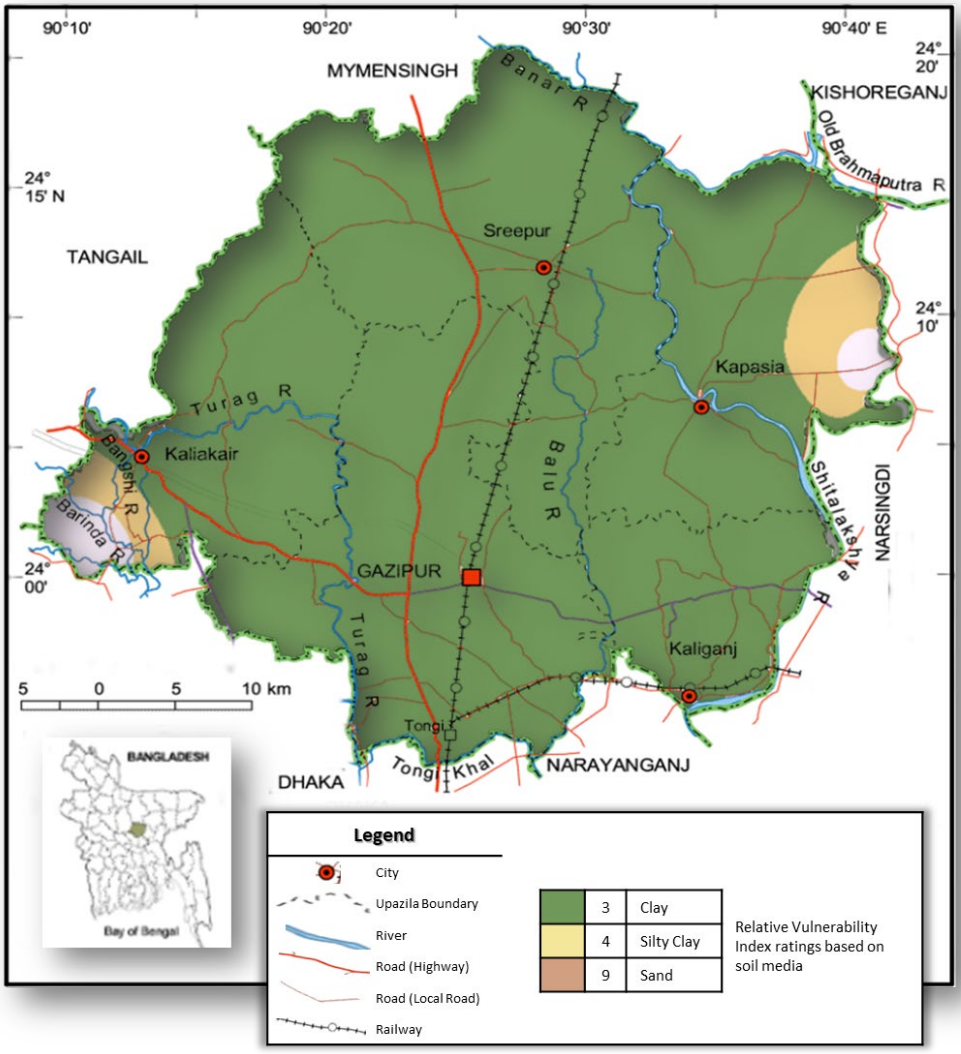

Figure 7.4: DRASTIC parameter map – showing spatial distribution of the soil media across the study area. The clay layer is the thick Madhupur Clay. Most of the district is covered by the clay unit. Along the eastern and the western edges exposure of sand and silty clay can be seen. The generalization is due to lack of available detail data.

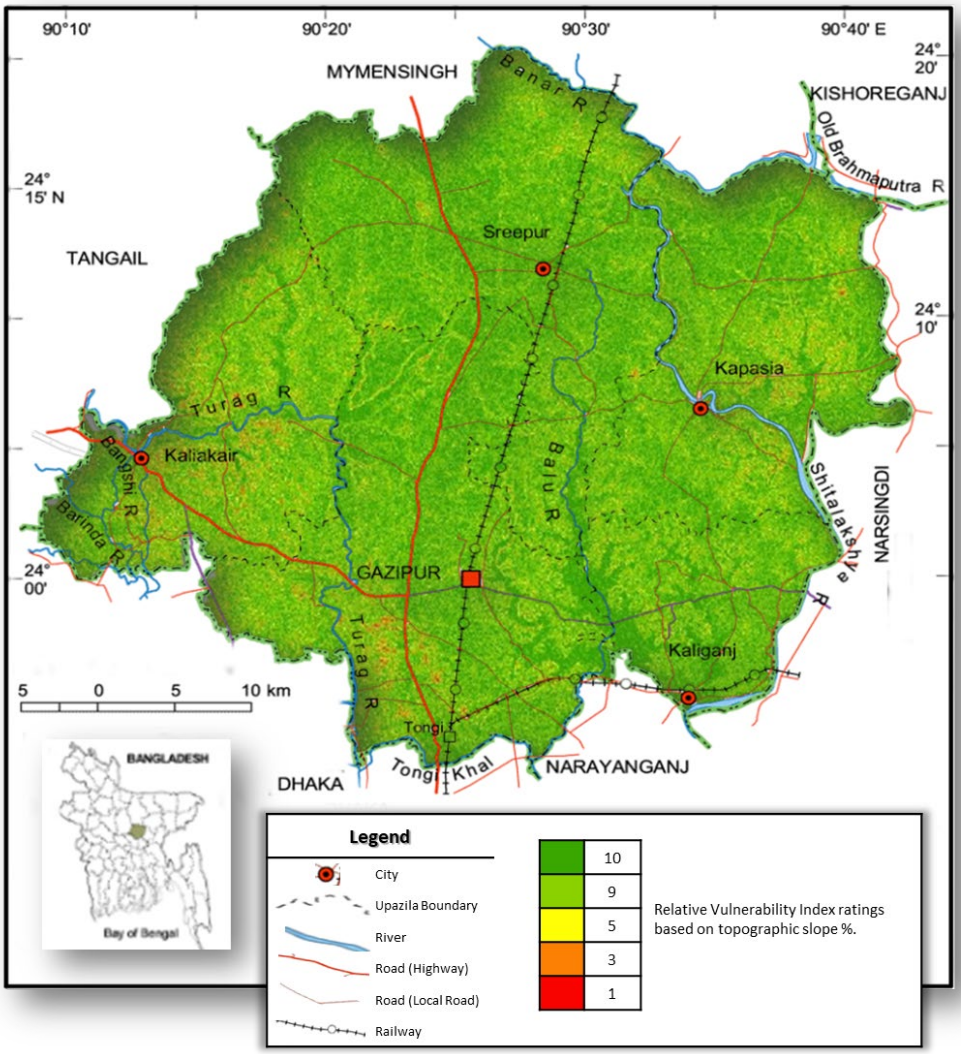

Figure 7.5: DRASTIC parameter map – showing spatial distribution of topographic slope (%) across the study area. Inclination is along north to south, and clearly marks out the surface flow systems.

1.34.6. Impact of vadose zone (I)

The vadose zone is described as the unsaturated zone above the water table. In the plains, the vadose zone consists of unconsolidated clayey gravel and sand, but in the mountains, it consists of igneous rocks and limestone. Figure 34 illustrates the map of vadose zone impact. Clay, fine sand, and silty clay are the three unique vadose-zone materials in the research region. Fine sand occupies the largest area, around 55 percent of the whole, followed by clay at approximately 25 percent and fine sand at roughly 20 percent, primarily in small patches in the Sreepur, Kapasia, and Kaliakair Upazillas; Gazipur Sadar; and in a few areas of Kaliganj. (Figure 7.6)

1.34.7. Hydraulic conductivity (C)

Hydraulic conductivity is crucial because it regulates the pace of groundwater movement in the saturated zone, consequently influencing the concentration and fate of contaminants.

The hydraulic conductivity (C) relates to the aquifer's capacity to transfer water and consequently regulates the migration and dispersion of contaminants from the injection site within the saturated zone and the plume concentration inside the aquifer. According to the investigation, the moderate Gazipur region has a greater hydraulic conductivity value than the higher Gazipur region. (Figure 7.7)

1.34.8. DRASTIC vulnerability index

The vulnerability map was obtained using the seven hydro-geological data layers in the ArcView GIS software environment. DRASTIC scores ranged from 58 to 177, considering the determined ratings and weightings. These values were reclassified into three classes using the Natural Breaks (Jenks) classification method. The study area’s vulnerability was classed as low (<100), medium (100-140), and high (>140) according to data obtained from hydrogeological investigations.

Figure 7.8 depicts the DRASTIC-generated groundwater vulnerability map for the research area. The model yielded vulnerability ratings with a unimodal distribution ranging from 79 to 137. The estimated DRASTIC scores were classified into three vulnerability classes using an equal-area interval (EI): low (79–97), moderate (97–117), and high (117–137). The region corresponding to each class of vulnerability.

The resulting vulnerability map indicates that the greater part of Gazipur is moderately vulnerable, and south eastern parts are of low category vulnerable. The concern with this approach is that it has taken into consideration the following factors;

- Despite being a confined aquifer, the recharge is constant and has no such impact on the urban and industrial settings. Due to the development, they have created a concrete covering of the surface area.

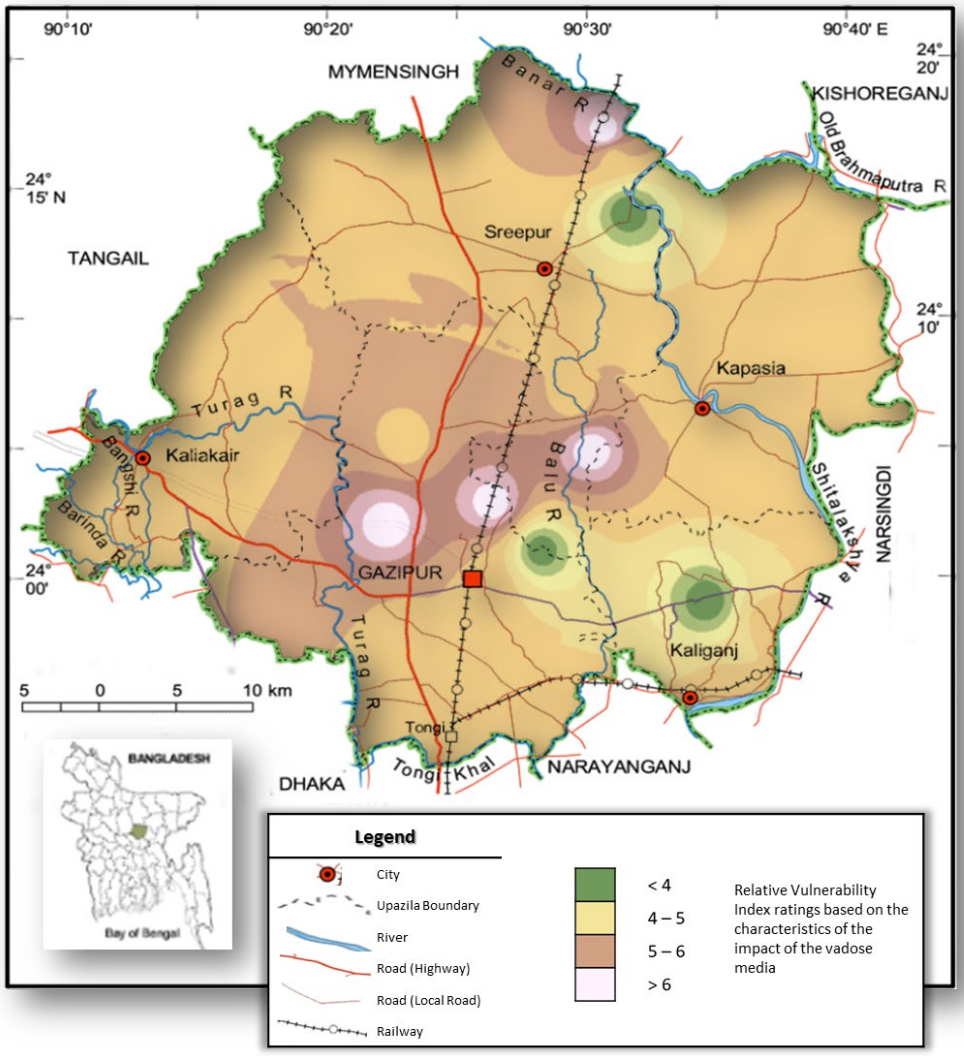

Figure 7.6: DRASTIC parameter map – showing spatial distribution of the vadose media across the study area. Values are the DRASTIC factor value with 6 as the highest. This indicates the influence of the unsaturated zone above the water table, controlling the attenuation of the contaminants into the aquifer, diminishing groundwater pollution, in the case of Gazipur district it is evident that highest influence would be along the developing urban and industrial areas.

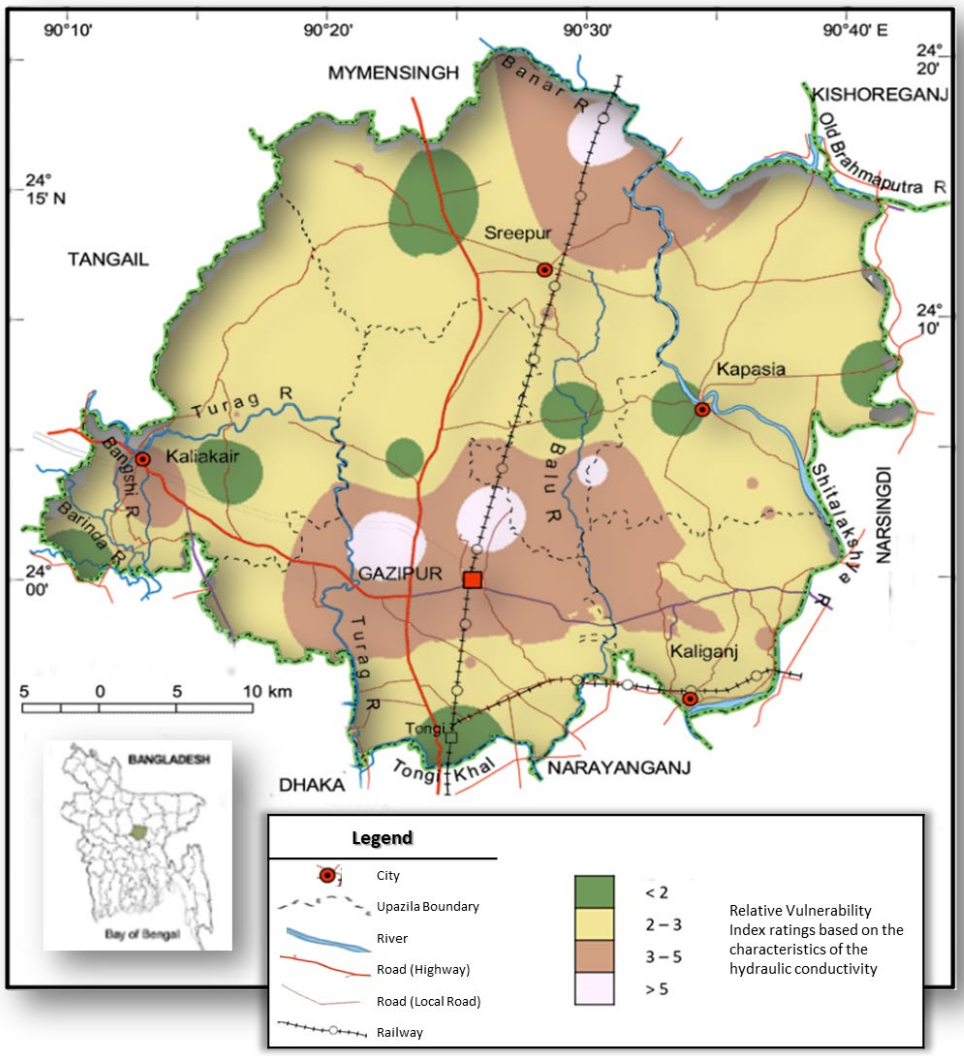

Figure 7.7: DRASTIC parameter map – showing spatial distribution of the hydraulic conductivity of the study area.

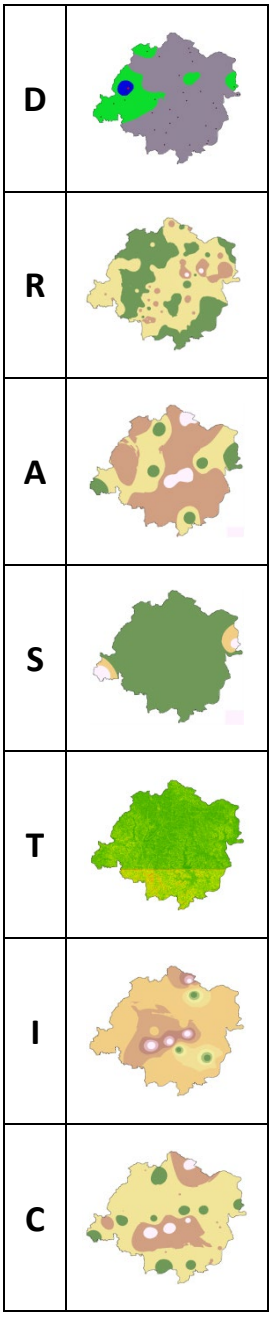

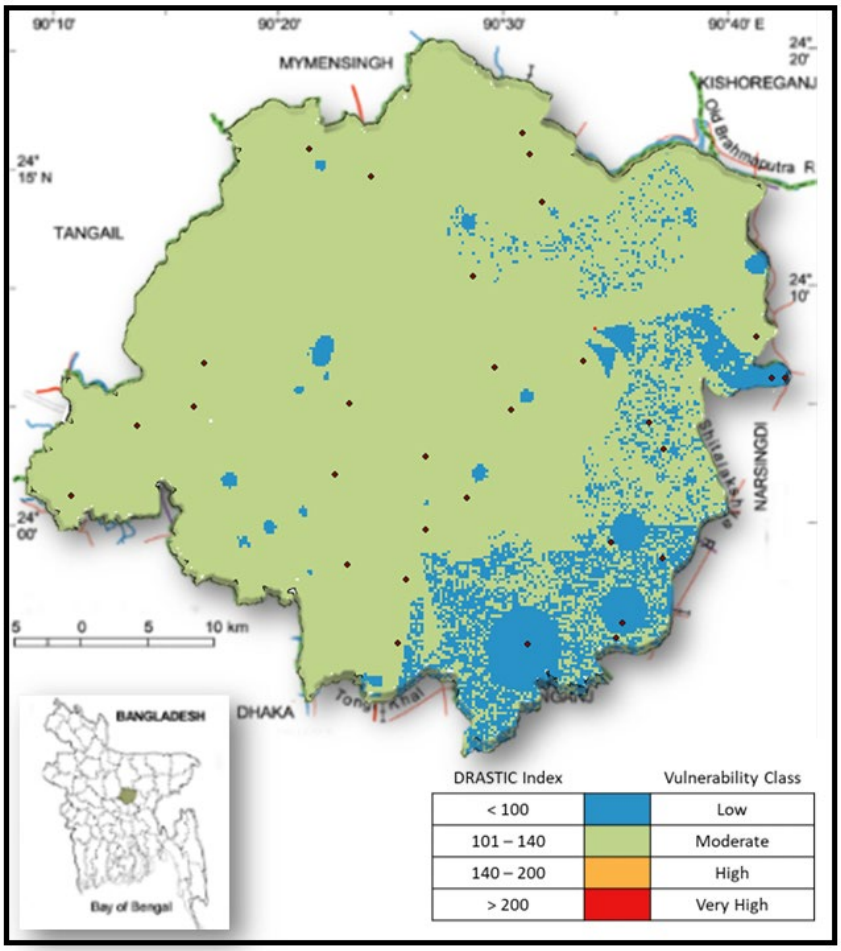

Figure 7.8: DRASTIC vulnerability map of Gazipur district. Considering the standard parameter values vulnerability condition of the entire district can be classified as moderately to low. Contradicting the fact that in increasing industrial areas the condition is low and no effect of rapidly increasing urbanization.

- It doesn’t take into account the impact of water abstraction.
- It doesn’t consider the impact of water contamination from the random installation of pumping wells and deep tube wells and that they expose the aquifer to seepage and leakages.
- The DRASTIC model does not consider the anthropogenic influence

1.35. Proposed Modification of DRASTIC Model

Considering the above-mentioned limitations and concerns, this research work believes a modification of the DRASTIC method is required to incorporate and introduce a new parameter.

1.35.1. Urbanization and industrialization factor – population density

Due to the natural expansion and rural migration, cities and towns' growing size and population are key elements in environmental change. Despite the fact that agriculture is almost always the largest user of groundwater, the water demands of urban communities and their economic activities and companies continue to rise. Urbanization affects the quantity and quality of groundwater by substantially altering recharge patterns and rates, introducing new abstraction regimes, and negatively affecting groundwater quality (Foster et al., 1998).

An evaluation of the threat to groundwater posed by urban activities must consider the relationship between recharge and discharge pressures and the consequent pollutant loading (Schmoll et al., 2006). Depending on the aquifer's vulnerability to pollution and the impacts of excessive abstraction, urbanization activities may potentially impact the underlying groundwater. a) The ease with which water and pollutants can flow to the underlying groundwater, and b) the attenuation capacity of the intervening material determines the vulnerability to pollution. Both are determined by the qualities and attributes of the soil and aquifer, which vary depending on the hydrogeological context (Al-Zabet, 2002; Vrba and Zaporozec, 1994; Foster et al., 2002; Schmoll et al., 2006; Xu and Usher, 2006).

Increases in groundwater abstraction beneath significant cities can be substantial, sustained, and locally focused. To maintain the water quality in the watershed for bathing and drinking, the population density should be less than 2,375 and less than 2,672 for fish and other aquatic organisms (Liyanage & Yamada, 2017; Hassan et al., 2019).

Taking into consideration of the above technical aspects and research observations mentioned in previous chapters, the followings can be stated for the study area;

- Due to increasing urbanization, the impervious surface area is growing.
- Gazipur District is experiencing extremely fast urbanization and industrialization process.
- The urban recharge component of groundwater is more than ten times greater than the natural recharge, which is questionable as a thick clay layer covers the Gazipur aquifer.

- Urbanization and industrialization are negatively impacting the groundwater resource due to excessive pumping or high abstraction rate.

Gazipur's urbanization and industrialization are a direct result of rural and urban migration, as evidenced by the rise in population density in the district, as shown by BBS (2012) and the following data cited above. The notion of Push-Pull Migration has an impact on population growth. More Industries will necessitate more People, and more people will require a more densely populated environment, which will increase water abstraction and the likelihood of groundwater contamination. The quality of groundwater is governed by its physical, chemical, and biological composition, with population density, urbanization, and industry having an effect. (Table 11)

This research proposes a modified method for including urbanization and industrialization factors in vulnerability assessment work. This additional inclusion can be labeled P, referring to the change in Population Density brought on by urbanization and industrialization. Consequently, the new vulnerability assessment is known as DRASTIC-P. (Figure 30)

Consequently, population density can be used to measure urbanization and industrialization. It would be prudent to select 2300 people per km2 as the effect threshold figure. As a result, this will directly impact all other aspects and affect them. The scale for weight value is 7, with a grade of 5 for low and 10 for high ranges. Consequently, the Population density Index is either 35 or 70.

1.35.2. DRASTIC-P vulnerability index

As urbanization and industrialization are causing Land cover changes, recharge calculation should also consider the concrete coverage factor while calculating water seepage to the aquifer. Thus, before r-mapping vulnerability, the net recharge should also be re- calculated.

A new net- recharge map (Figure 7.9) and Population Density Map (Figure 38) have been prepared for the modified DRASTIC vulnerability map.

The new factor was included, and a Vulnerability assessment using the DRASTIC method as a base, DRASTIC-P, was prepared (Figure 7.10).

The new DRASTIC Map clearly states that urbanization and industrialization are putting the aquifer in a vulnerable situation and impacting the overall water resources of the Gazipur District (Figure 7.11).

Table 7.1: Population density change over the years in Gazipur district.

	Area (km2)	Population (person)	Density (person/km^2)
1981	1,741.53	1,173,000	674
1991	1,741.53	1,618,000	929
2001	1,741.53	2,031,891	1,167
2011	1,806.36	3,403,912	1,884
2016	1,806.36	3,809,000	2,109
2020	1,806.36	4,159,000	2,303
			Not accounting for temporary migrants

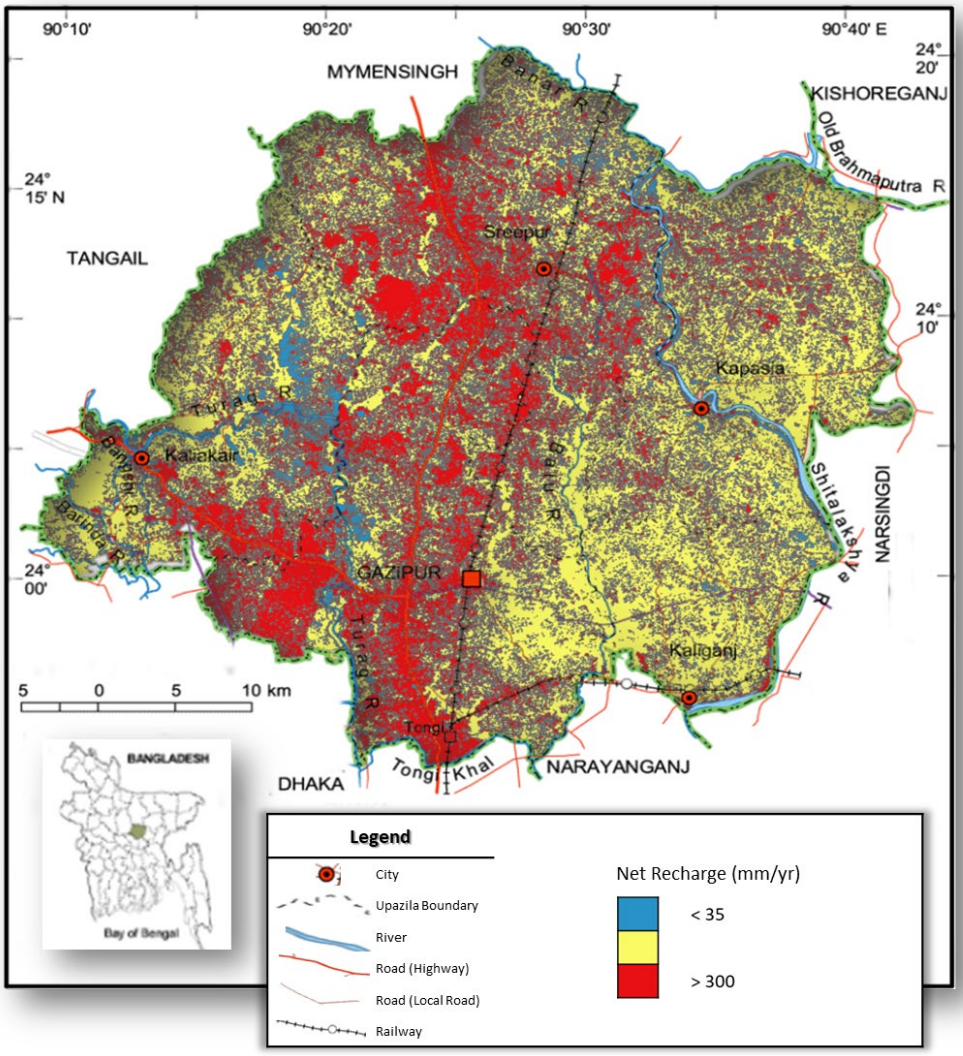

Figure 7.9: Revised net-recharge map. It's evident that though recharge is almost improbable due to thick Madhupur clay layer, yet for the cracks from urban settlement with growing industrial establishment a strong recharge along these areas is very high.

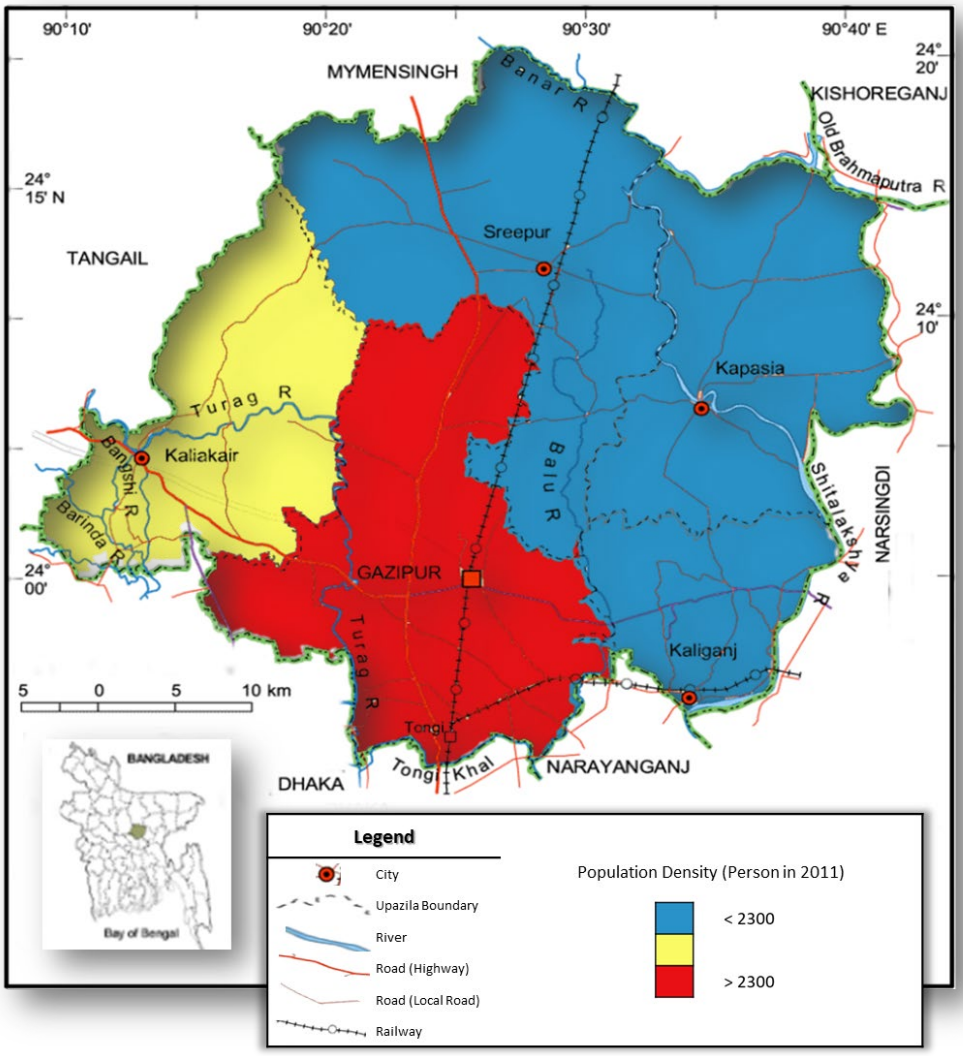

Figure 7.10: New Population Density Map. Taking 2300 person per square kilometer as a cutoff value it is evident that the prospect of that concentration is clearly in Gazipur Sadar area, where urbanization and industrialization is growing at alarmingly increasing rate.

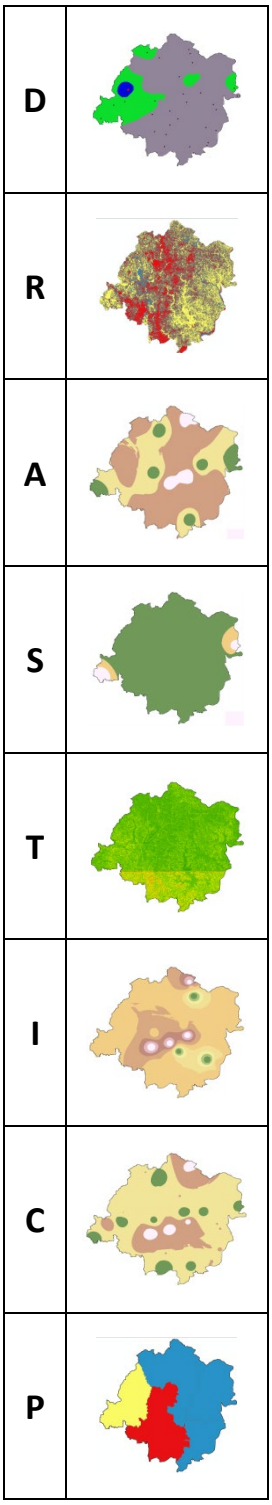

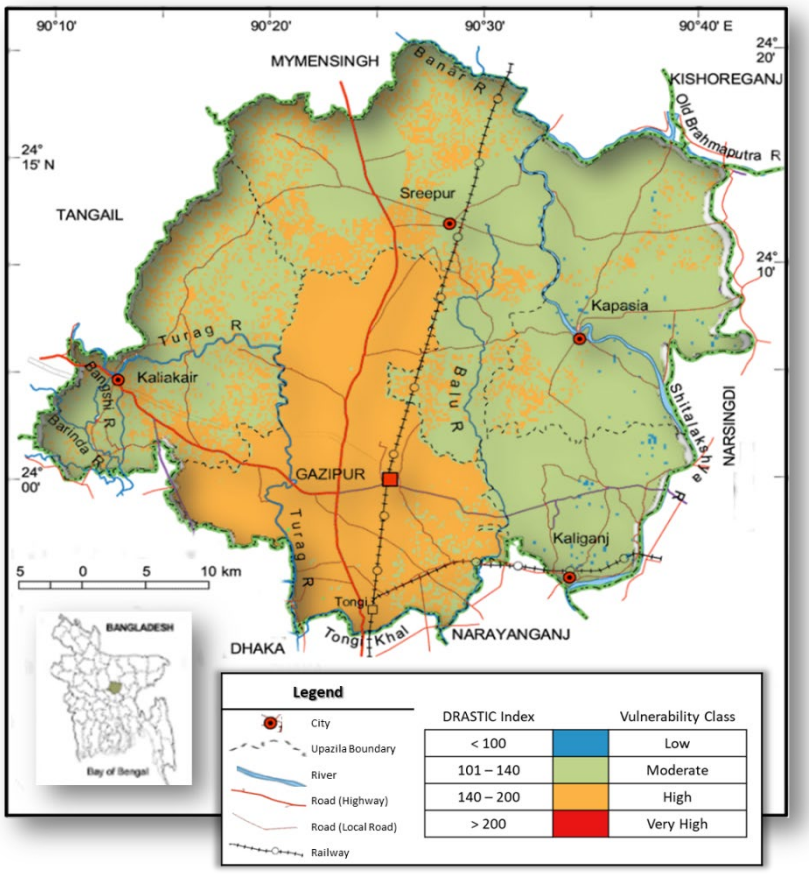

Figure 7.11: Modified DRASTIC-P map for Gazipur district. The modified vulnerability map single outs the urbanization and industrialization effect on the district.

8 GROUNDWATER FLOW AND CONTAMINANT TRANSPORT MODELING

GROUNDWATER FLOW AND CONTAMINANT TRANSPORT MODELING

1.36. Conceptual Model

The conceptual model provides an understanding of the approach plan and a simplified description of the problem's characteristics. The conceptual model describes a hydrogeologic framework, groundwater flow, recharge, evapotranspiration, stream discharge, water consumption, and hydraulic features (Davies et al., 2015).

A conceptual model of the region is constructed using the available data on hydrostratigraphy, well logs, geologic maps, and geologic cross-sections.

1.36.1. Geologic Settings

Gazipur is located at the southernmost tip of the Madhupur Tract. The older sediment sequence of the study area consists of sandstone from the Dupi Tila Formation, which is unconformably positioned above the Madhupur Formation. Recent Alluvium occurs on top of the Madhupur Formation (Jamil and Ahmed, 2015).

The Madhupur Clay sits above the fine to coarse-grained micaceous, quartzofeldspathic sands of the Dupi Tila Formation. This region's sands have a thickness of around 140 meters. At the top of the Dupi Tila Formation are fine silty sands, fine/medium-grained sands, medium/coarse-grained sands, and gravels at the base. As a result of the mafic minerals' exposure to the elements, considerable quantities of iron oxides and secondary clays are present. Clay lenses are occasionally discovered within the Dupi Tila Formation.

Within the study area, the Dupi Tila Formation acts as a confined aquifer. The Madhupur Clay encloses the major aquifer in the region, composed of Dupi Tila Formation sand units. In many regions, the total thickness of the aquifer units surpasses 200 meters. Its average thickness is approximately 140 meters. Composite is the name used to describe the Dupi Tila aquifer (Hasan, 1999).

1.36.2. Hydrogeologic Settings

The shape of the aquifer system is determined using data extracted from the pertinent literature. For modeling purposes, simpler hydrogeological equivalents were utilized to approximate the complex geological conditions deduced from drill logs. Four layers make up a simplified aquifer system: two aquifer layers and two aquitard levels (Hasan, 1999; Figure 2.5).

As there are problems with verifying missing data and an absence of detailed studies, this research has considered the broad observation of prior work. Based on grain size, hydraulic qualities, and geological occurrence, it has been considered a single Upper Aquifer for ease of correlation, overlain by an Upper aquitard, Lower aquitard, and Lower Aquifer. In light of the research purpose, which was to quantify the vulnerability of the aquifer to the effects of urbanization and industrialization made it reasonable to calculate groundwater flow exclusively for the upper aquifer. (Table 8.1)

1.36.3. Water Level

The contours in the region's central and southern portions are widely separated, showing the permeability of the sedimentary formation near the surface. There is evidence of inflow in the region's extreme western and eastern portions, where Madhupur Clay does not cover the surface runoff. In 2000, a considerable change in water level was observed, which is exceedingly unusual considering the absence of evidence of violent or rapid weather changes. At 65 meters above sea level, the GWL revealed a larger and deeper depression cone in 2013. The eastern side, between 12 and 19 m above sea level, extracts less groundwater (Hoque et al., 2007; Islam et al., 2017).

The water level measurements were calibrated using records from 18 observation wells (Figure 43) in the modeled area. Observation wells were provided with weekly water level data received from BWDB. Some of these boreholes have histories of twenty to thirty years of monitoring. Since 1986, however, only monitoring data for the upper aquifer are available.

The model's estimation of groundwater head distribution was in reasonable agreement with the regional groundwater contour map rebuilt from a small number of wellhead data. Unfortunately, the East, Northeast, and West lack piezometric data, making comparisons in these locations difficult. The estimated contours of groundwater level depict the observed water level trend. It is evident that water level drop has extensively taken place in urban settling areas. It s highly affected at Gazipur Sadar Pourosova area, south central part of the Gazipur District. Major changes took place during 2009 and 2018 compared to the previous decade (Figure 8.1).

1.36.4. Recharge

The properties of the soil affect the quantity of recharge that percolates into the ground, the amount of potential dispersion, and the purification process of contaminants as they move vertically into the deeper zone. Though certain previous studies refer to recharge usage, the presence of a thick clay layer contradicts the vertical or surficial recharge of the Gazipur district. Thus, Gazipur district groundwater is recharged by subsurface inflow along with the aquifer layer. This research work for modeling purposes did not consider vertical recharge.

Table 8.1: Hydrostratigraphy of Gazipur district.

Age	Stratigraphy	Lithology	Hydrogeology	Average thickness	Kx	Ky	Kz	Ss	Sy	Total Porosity
				(m)	m/s	m/s	m/s	1/m		
Recent	Lowland Alluvium	Swamp, levee & riverbed deposit	Connected to Surface drainage							
Pleistocene	Madhupur Clay Formation	Silty clay with fine sand	Aquitard		2e-08	2e-08	2e-08	0.0001	0.035	0.5
Plio-Pleistocene	Dupi Tila Formation	Fluvio-deltaic sand	Aquifer		0.0002	0.0002	0.0002	0.00001	0.15	0.2
		Dupi Tila claystone	Aquitard		5.8e-07	5.8e-07	5.8e-07	0.00015	0.05	0.48

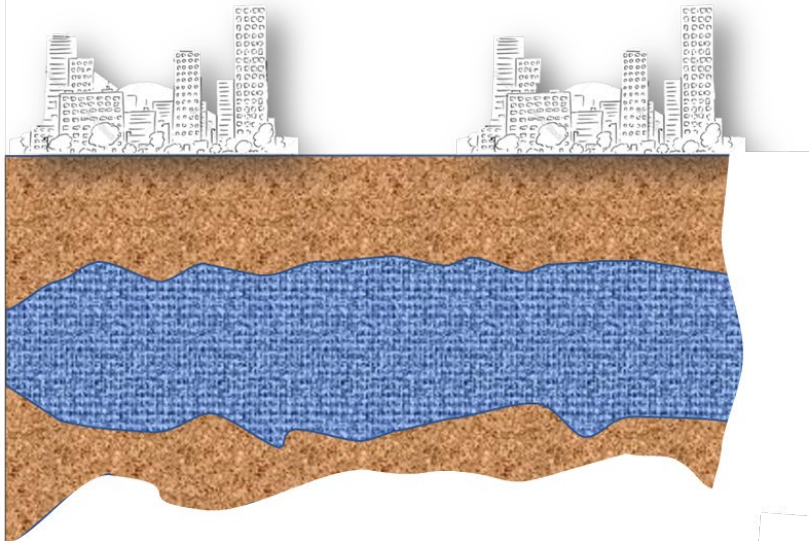

1999 - 2008	*Water level drop below surface (m)*	2009 - 2018
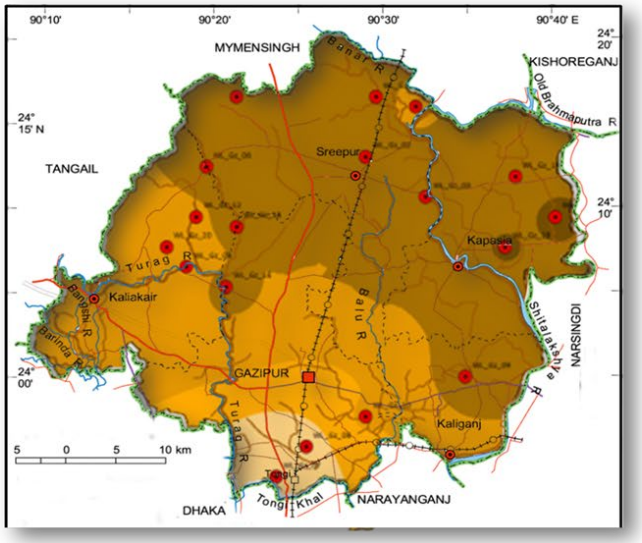	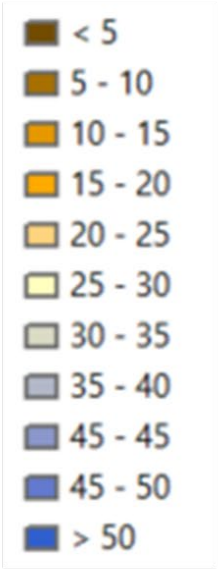	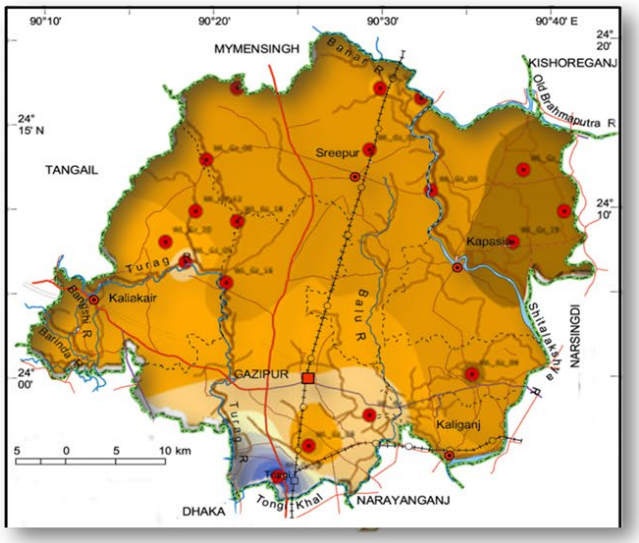

Figure 8.1: Water level drop over the last two decades across Gazipur district. It is clear that comparatively over the decade water level drop increased greatly more towards the south and mainly along the increasing urbanizations areas.

1.36.5. Abstraction

Groundwater abstraction for the Gazipur district cannot be specified. Previous studies hypothesized the values and generalized the rates, but they cannot be properly regulated. It is difficult to properly account for the total number of wells operated within the Gazipur district. Many undocumented private wells are working in the area. Therefore, this research has considered the abstraction rate generalized based on area coverage calculated from LCLU classification and standard abstraction for agricultural and urban settings. (Table 8.2)

1.36.6. Calibrations

By adjusting input parameters, groundwater model calibration seeks to achieve an acceptable agreement between the modeled response and the aquifer system's known equivalent response. Model calibration typically consists of two stages. The first phase is a steady-state calibration, wherein stable, time-independent conditions are reproduced by the model and compared to actual system conditions under constant inflow/outflow conditions. In the second step, the model's reaction to a historical record of recharge and abstraction data is compared with the observed response of the aquifer system. To avoid the uncertainty created by model parameter estimations, the values for several parameters already calibrated in the literature were taken into account in this work.

A first steady-state simulation was done to confirm the model parameters derived from previous research and establish a suitable head distribution for the subsequent transient calibration.

1.36.7. Model

The model covers an area of approximately 1,800 km^2. The grid of the model was based on a network of 30 rows and 40 columns, generating a mesh of squares with a resolution of 500*500m. The model grid network and boundaries are shown in Figure 48. Although the calibrated groundwater flow model should be viewed in the context of these limitations, it may be used as a basis for the three-dimensional solute transport model MT3D.

1.37. Groundwater Flow Model

Using steady-state and quasi-transient numerical groundwater flow models, the hypothesized groundwater-flow systems of the Gazipur District have been simulated. A three-dimensional finite-difference numerical model was developed to simulate groundwater flow using the US Geological Survey (USGS) program MODFLOW 2006 (Harbaugh 2005; Harbaugh et al., 2000; Poeter et al. 2005).

Table 8.2: Abstraction rate calculation for urban settings in Gazipur district. (Modified from Akhter & Hossain, 2017; Islam et al, 2017)

	Population (million)	Abstraction (million m^3/d)	Area (m^2)	Abstraction per unit area (million m^3/d)
Gazipur Sadar	2.09	0.25	662.67	$3.7x10^{-4}$
Kaliakair	0.48	0.057	776	$1.91x10^{-4}$
Sreepur	0.83	0.10	303.03	$1.291x10^{-4}$

The steady-state model depicts unpumped natural conditions. Twelve stress periods were determined using monthly averages from 1982 to 2013 to generate the transient model. To analyze the long-term monthly variation of groundwater level and to illustrate the long-term seasonal variation (i.e., dry and wet conditions) throughout the entire region, it was chosen to apply quasi-transient simulation to long-term monthly data. The model region of approximately 1,741 km2 was discretized using a finite-difference grid with 40 columns and 30 rows and a uniform cell size of 500 m 500 m. (Figure 49)

Outflow occurs over the eastern and western fronts (where the major rivers are) and from the production wells; hence, the boundary conditions are governed by the geography and geology of the region. The model's top is the DEM image of the land surface topography acquired from SRTM. The boundary conditions along the modeled area for the target aquifer are stated. A survey of the relevant literature indicates that the river depth does not extend into the aquifer. It is surrounded by a thick layer of Madhupur Clay (Table 8.3). Therefore, neither river recharge nor river outflow has been considered.

Depending on the region, the seasonal change of the groundwater level from dry to wet varies between 3 and 5 meters, demonstrating the natural pattern of the climate system dominated by monsoons. Transient calculations with groundwater abstraction demonstrate that the creation of depression cones caused by pumping has disrupted the typical regional flow patterns in the southern portion of the metropolitan area of Gazipur Sadar. Fall is greatest during the dry season.

The depression cone within and surrounding the district suggests that abstraction surpasses recharging. The changes in water level between the wet and dry seasons indicate that the Dupi Tila aquifer can recover, with a 5 m rise in water level from the dry circumstances as a result of recharging during the monsoon season in the surrounding areas, particularly in the northern portion. It implies that additional abstraction beyond the existing storage will exacerbate the aquifer's permanent depletion. (Figure 8.3)

1.38. Contaminant Transport Model

Using MODFLOW and the solute transport algorithm (MT3D), the current study created a groundwater flow model and modeled the transportation of pollutants in the basin. MT3D is widely recognized as an appropriate method for evaluating the transport of solutes in groundwater. It includes advection, dispersion, and chemical interactions of dissolved elements in groundwater systems (Zheng & Wang, 1999). Using MT3D, a three-dimensional transport model was used to simulate point and non-point source contamination and to investigate the range of expected concentrations at various depths, locations, and times for a number of potential contaminating sources.

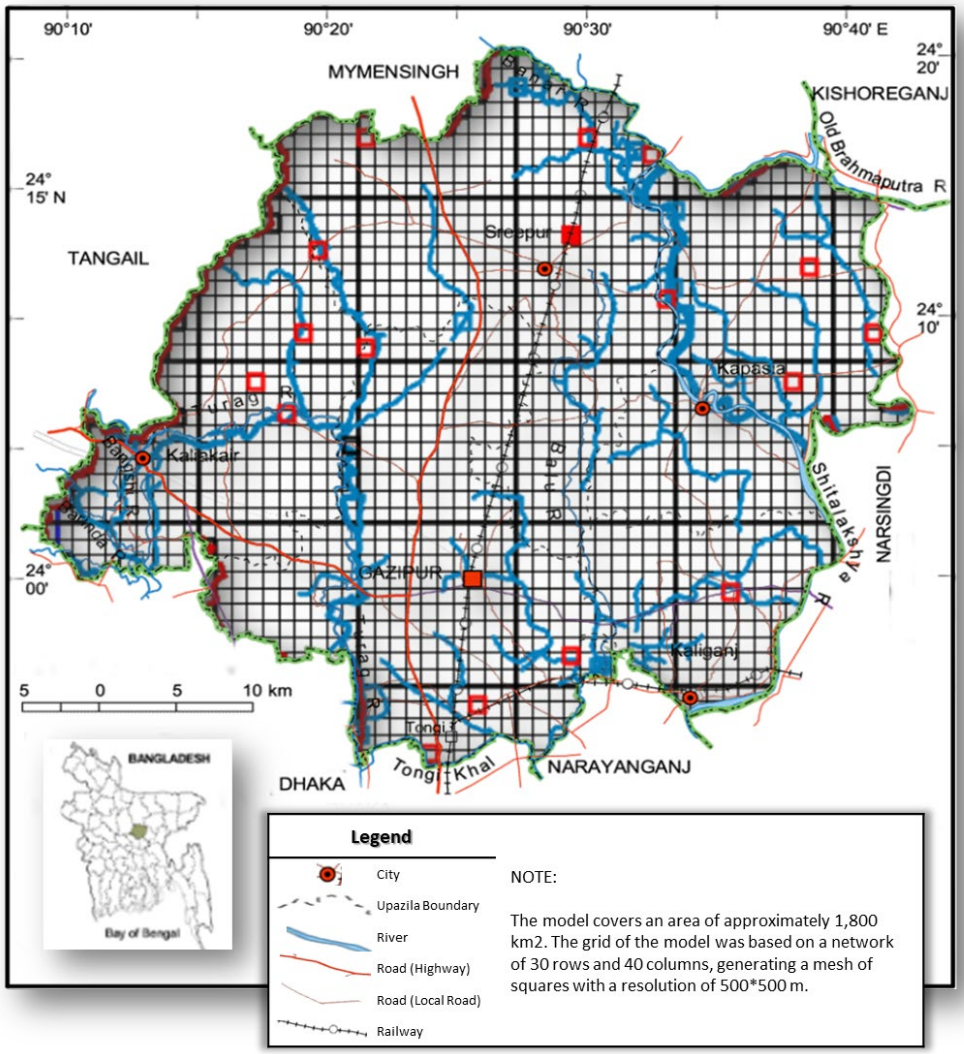

Figure 8.2: Model grid details showing network and boundaries, network of 30 rows and 40 columns, generating a mesh of squares with a resolution of 500*500m.

Table 8.3: Comparison between the river base levels and the top of the upper aquifer.

Name of the River	Channel Base level (m PWD)	The base of Upper Aquitard (m PWD)	Penetration of Upper Aquifer	Wet Season Width (m)	Dry Season Width (m)
Turag	0.6 to -10.0	-12.3 to -22.5	No	170	80
Balu	0.5 to -3.5	-5.5 to -12.0	No	100	70
Tongi	0.5 to -2.5	-22.0 to -32.0	No	100	60

(Data from BWDB; Modifies from Hasan, 1999).

Extensive groundwater abstraction within the district's urban areas creates a localized depression point.

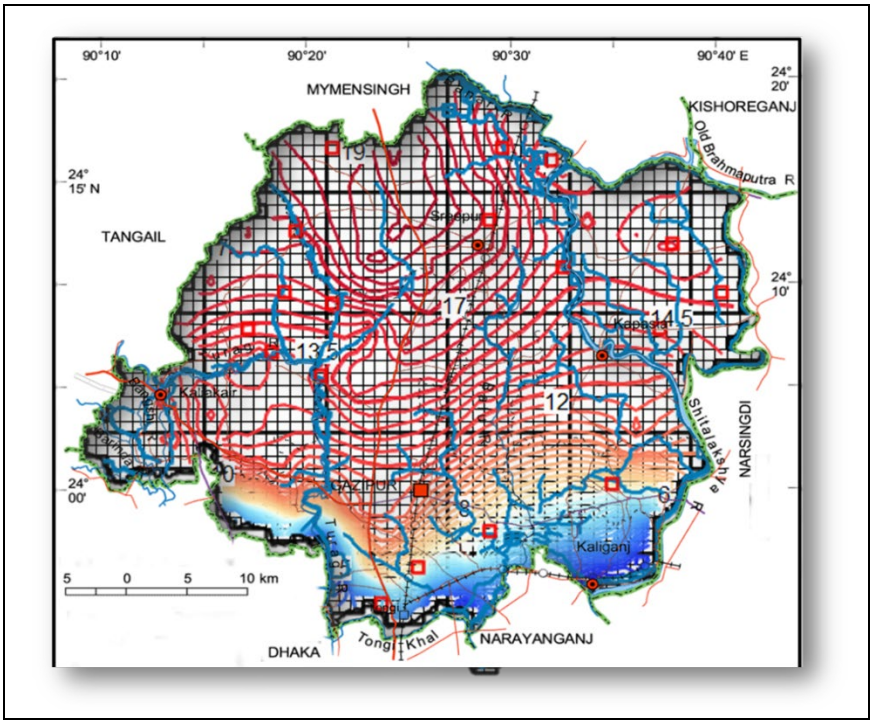

Heavy abstraction along the southern part of the district is growing rapidly

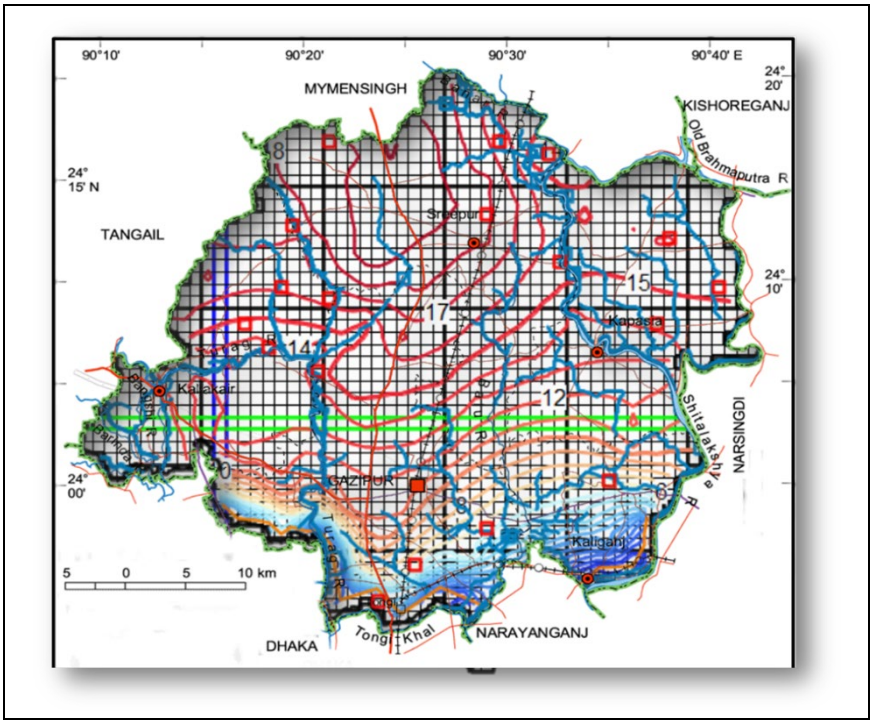

Figure 8.3: Groundwater flow condition indicating flow direction dictated by urban abstraction, causing localized depression of water level.

The primary objectives of solute transport modeling in this thesis are to investigate the relative significance of the various contaminant sources identified by the field survey and to determine the extent to which heavy groundwater abstraction from the Dupi Tila aquifer over the past two decades has contributed to the spread of contaminants in the aquifer and the size of the contaminated groundwater plume.

The value of the model parameters used in the MODFLOW simulations remained the same for the contaminant transport modeling. The model estimates a 10 percent effective porosity for the top Madhupur Clay layer. The estimated effective porosity for all remaining strata is 15% based on published values for similar (sand) lithologies.

Dispersion relates to the dispersion of pollutants due to aquifer heterogeneities and mixing, an essential phenomenon incorporated in MT3D but not in MODPATH. Mixing along the flow path occurs because the invading solute-containing water does not all travel at the same speed. Both longitudinal and transverse dispersion is possible (Fetter, 1993).

In the solute transport model of the groundwater system, the longitudinal dispersity of all strata was assumed to be 20m, corresponding with reported values for alluvial sediments and the size of contaminant migration (Spitz & Morneo, 1996).

In addition, a solute in water will travel from a region of higher concentration to a region of lower concentration in accordance with the chemical potential gradient. This process is called diffusion or molecular diffusion.

Transport equations cannot be solved without initial and boundary conditions. In general, three types of boundary conditions are employed in transport models: (1) Concentrations along a boundary are specified (Dirichlet condition or concentration type boundary); (2) concentration gradients across a boundary are specified (Neumann condition); and (3) both concentrations along a boundary and concentration gradients across a boundary are specified, resulting in the Cauchy condition. A Dirichlet boundary is a specified-head boundary in flow modeling; a boundary condition of this type works as a source supplying water to the domain or a sink removing water from the domain. Similarly, a specified-concentration border in a transport model functions as a source through which solute mass enters the domain or as a sink through which solute mass exits the domain. As the Cauchy condition for this study, urban and industrial concentrations have been studied. The transient simulations under MT3D began with zero initial concentrations due to a lack of data.

The transport of contaminants was modeled using MT3D under three distinct situations. As the top layer (the Madhupur Clay) was already dry at these flow conditions, the particles were deposited near its base. The particles were then tracked to their discharge locations. The initial background average TDS concentration was estimated to be 500 mg/L, and the allowable limit

for EC in drinking water was determined by WHO as 400 S/cm. At the modeling of the groundwater table, TDS concentrations of 4,000 mg/L and EC concentrations of 2,500 S/cm were assigned to represent the urban source loading. Between 2015 and 2020, the pollutant movement was initially simulated for five years 2015 and 2020. The urban setting has remained unchanged for more than ten years and has been forecasted for 30 years using MODFLOW simulations of transient groundwater flow. (Figure 8.4)

First Scenario: The first MT3D scenario is localized point-source contamination with a concentration of 4,000 mg/l in the Upper aquifer. Two urban and industrial regions were evaluated, namely Sreepur and Gazipur Sadar.

Second scenario: MT3D simulations were again run for 30 years to demonstrate how the contaminant concentration in groundwater changes over time under these various contamination source settings.

Third Scenario: The third scenario involves thirty years of citywide urban contamination.

During the first five years, contamination will spread southward up to approximately 125 meters (Figure 40). Observable is the quick downgradient pollution migration from the peri-urban area of interest. In ten years, the estimated EC plume might migrate a distance of 250 meters towards the downstream region (Figure 40). Consequently, if the migration of the EC plume is not prevented in the early phases, it is expected to amplify and further contaminate the groundwater reservoirs in the Gazipur District, posing a severe hazard to the entire aquifer. In 30 years, the estimated EC plume will be dispersed throughout the district due to continual pollution infiltration from surface urban and industrial environments.

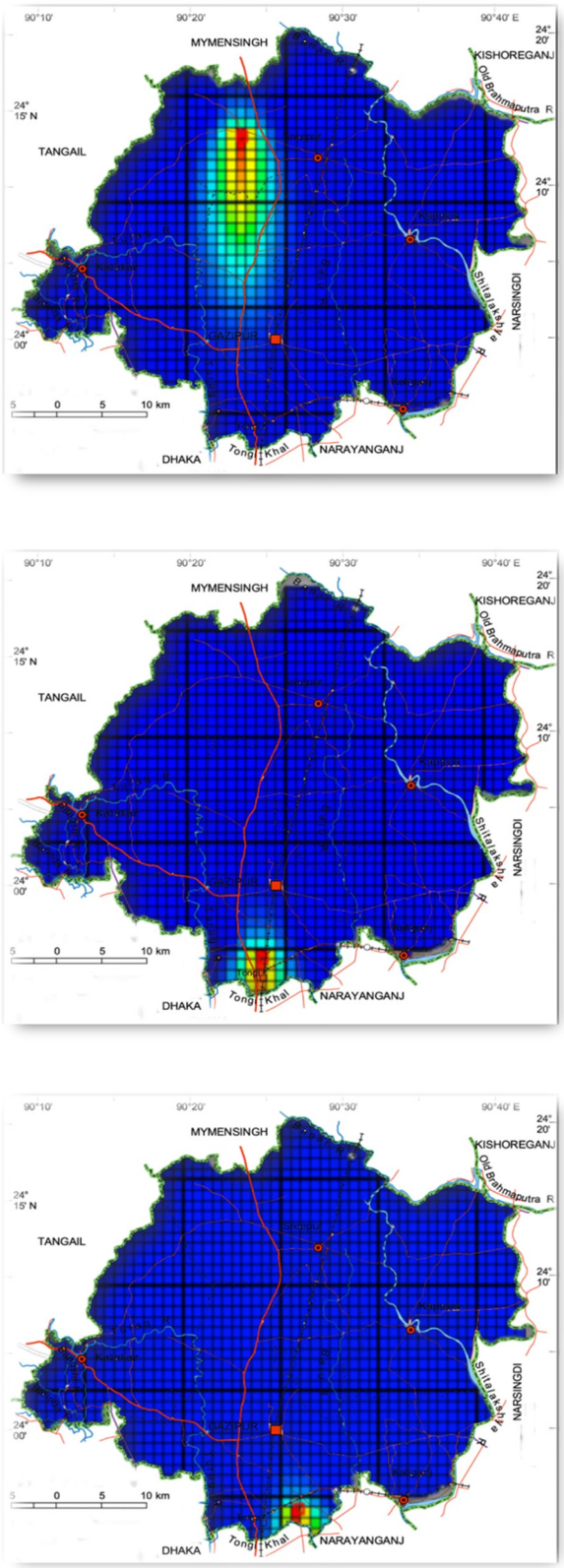

Figure 8.4: Contamination plume movement showing probable migration direction in different scenarios. Plume movement is southwards, irrespective of initiation point.

9 CONCLUSION

CONCLUSION AND RECOMMENDATION

1.39. Conclusion

Using the results of the groundwater modeling exercise, a system for early warning might be developed; for instance, the impacts of dumping hazardous materials at industrial sites could be easily monitored, allowing for the prediction of the first arrival and peak concentration times.

TDS and EC concentrations are higher in the research area due to domestic effluents, agriculture, and local human activities that enter the groundwater. This would have increased the ion concentration in the water. Consequently, it might be stated that EC significantly impacts the water quality condition or that they are greatly affected by the quality change. The groundwater in the research region is contaminated by domestic effluents and local human activities, resulting in a high concentration of EC. In densely populated and industrialized areas, the prevalence and incidence of EC are on the rise.

According to the estimated WQI, 48 percent of water samples are excellent, while 48 percent are good. In locations where urbanization and industrialization are dominant, WQI levels exceed the limit allowed. Consequently, population density affects groundwater resources. EC is a useful water quality parameter that can be used to assess contamination. According to the USEPA (2020), significant increases in conductivity may indicate contamination in aquatic resources. Substantial fluctuations in conductivity (usually increases) may suggest that a discharge or other source of disturbance has damaged the health of a water body and its associated biota. The dissolved solids' concentration grows due to human activities, increasing conductivity.

This research offers a revised methodology for including urbanization and industrialization in vulnerability evaluations. This addition is labeled P to indicate the change in Population Density brought about by urbanization and industry. Consequently, the new vulnerability assessment is known as DRASTIC-P. According to the new DRASTIC Map, urbanization and industrialization are putting the aquifer in a hazardous situation and impacting the district's water resources. According to the generated vulnerability map, most of Gazipur is somewhat exposed, whereas the southeastern section is not vulnerable.

Depending on the vulnerability of the aquifer to contamination and the effects of excessive abstraction, urbanization activities may impact the groundwater beneath.

Domestic and industrial sectors consume the most water in the Gazipur District, with 85 percent of the urban water demand being met by groundwater and 15 percent by surface water. Groundwater reserves are in peril due to uncontrolled groundwater abstraction and chronically reduced recharge, resulting in a constant decline of >2 meters per year in the average groundwater level. Changes in hydrogeological factors have a negligible effect on the projected

flow pattern, whereas recharge and uneven abstraction has a substantial impact. The spatial maps of groundwater levels during wet and dry periods for the averaged condition reveal that the groundwater level can rise by 5 meters from dry to wet under the current environmental conditions. Urbanization and industrialization in Gazipur are direct results of rural and urban migration, as seen by the increasing population density of the district.

In less than ten years, however, the model forecasts that pollution will spread to surrounding regions. Flow is not linear across the system; instead, it is more rapid in areas with high abstraction rates, depending on abstraction rates. Fundamentally, this research suggests that the depression cone can spread beyond the model's boundaries; as a result, future modeling efforts should focus on a larger area and more exact measurements of in-situ hydrogeological parameters. Urbanization and industrialization are causing land cover changes. According to the new DRASTIC Map, urbanization and industrialization are putting the aquifer in a hazardous situation and impacting the district's water resources.

1.40. Recommendation

Different economic characteristics, such as those related to agriculture, exist in any research area. Due to the diversity of operations, contamination levels vary. Thus preventive measures should be a priority. The social and economic growth of the studied areas should also be considered. Important to remember is the fact that vulnerability maps cannot substitute actual field surveys and investigations. These maps are solely applicable for prioritizing field investigations, and supporting field surveys should be conducted.

The following points summarize the proposed improvements;

- EC and TDS should be utilized as an indicator more frequently and before any geochemical research.
- The influence of urbanization and industrialization on groundwater is an increasing cause for worry. A proper impact and vulnerability assessment should be conducted for each major city.
- Modeling procedures, in general, demand more detail and calculated data.
- The absence of geophysical log data was felt when defining the aquifer layer heterogeneity; hence, petrophysical modeling of aquifers is necessary.
- Piezometers and water quality monitoring wells should be strategically placed to increase well control.
- Urgently required is a comprehensive investigation to identify a possible measurable element connecting urbanization, industrialization, water quality, and groundwater level in the district.

10 REFERENCES

REFERENCE

1. Abbasi, T. & Abbasi, S.A. (2012). Water quality indices. Elsevier, Amsterdam, The Netherlands. 2012.
2. Abdeslam, I., Fehdi, C., & Djabri, L. (2017). Application of drastic method for determining the vulnerability of an alluvial aquifer: Morsott-El Aouinet north east of Algeria: using ArcGIS environment. Scie Direct Energy Proceed 119(2017):308–317.
3. Aggarwal, P.K., Basu, A. R., Poreda, R. J., Kulkarni, K.M., Froehlich, K., Tarafdar. S.A., Ali, M., Ahmed, N., Hussain, A., Rahman, M., & Ahmed, S.R. (2000). A Report on Isotope Hydrology of Groundwater in Bangladesh: Implications for Characterization and mitigation of Arsenic in Groundwater. IAEA TC Project BGD/8/016.
4. Aghazadeh, N. & Mogaddam, A.A. (2010). Assessment of Groundwater Quality and Its Suitability for Drinking and Agricultural Uses in the Oshnavieh Area, Northwest of Iran. Journal of Environmental Protection, 1, 30-40. https://doi.org/10.4236/jep.2010.11005
5. Ahmed, K.M. (1994). The Hydrogeology of the Dupi Tila Sands Aquifer of the Barind Tract, NW Bangladesh. Thesis Submitted for the degree of Doctor of Philosophy in Hydrogeology Department of Geological Sciences, University College London, London University.
6. Ahmed, K.M. (2011). Water Resources Planning and Management, eds. R. Quentin Grafton and Karen Hussey. Published by Cambridge University, Press. © R. Quentin Grafton and Karen Hussey 2011.
7. Akhter, S. & Hossain, M.S. (2017). Groundwater Modeling of Dhaka City and Surrounding Areas and Evaluation of the Effect of Artificial Recharge on Aquifers. World Journal of Research and Review (WJRR) ISSN:2455-3956, Volume-5, Issue-3, September 2017 Pages 54-60.
8. Alam, M.K. (1988). Geology of Madhupur Tract and its adjoining area in Bangladesh. Records of Geological Survey of Bangladesh (GSB), v. 5, pt. 3, Dhaka, Bangladesh.
9. Al-Adamat, R. & Al-Shabeeb, A.R. (2017) A Simplified Method for the Assessment of Groundwater Vulnerability to Contamination. Journal of Water Resource and Protection, 2017, 9, 305-321.
10. Albinet, M. & Margat, J. (1970). Groundwater Pollution Vulnerability Mapping. Bull. Bur. Res. Geol. Min. Bull BRGM 2nd Ser. 1970, 3, 13–22.
11. Al-Ferdous, T., Hossain, K.M.M., Kabira, S.M.L., & Amin, M.M. (2012). Characterization of Escherichia coli isolates obtained from washing and rinsed water of broilers in pluck shops at Sreepur of Gazipur district in Bangladesh. Scientific Journal of Microbiology (2012) 1(5) 126-132.

12. Aller, L., Bennett, T., Lehr, J., & Petty, R., (1987). DRASTIC: a standardized system for evaluating groundwater pollution using hydrogeologic settings. US EPA/Robert S. Kerr Environmental Research Laboratory. EPA/ 600/2–85/018.
13. Almasri, M.N. & Kaluarachchi, J.J. (2007) Modeling nitrate contamination of groundwater in agricultural watersheds. J Hydrol 343:211–229.
14. Al-Shaibani, A.A. & Raza, J. (2004). Influence of Wastewater Projects on Groundwater Quality in a shallow Aquifer. 4th Specialty Conference on Environmental Progress in the Petroleum and Petrochemical Industry.
15. Al-Zabet, T. (2002). Evaluation of aquifer vulnerability to contamination potential using the DRASTIC method. Environ Geol 2002(43):203–208.
16. Ananya, T.H., Mahid, Y., Shanta, A.S., & Hafiz, R. (2012). Urban Agriculture in DMDP Area: A Case Study of Gazipur, Kaliganj, Rupganj and Narayanganj Upazilas. Journal of Bangladesh Institute of Planners, Vol. 5, December 2012, pp. 69-77, ISSN 2075-9363.
17. Anderson, M.P. (1984) Movement of contaminants in groundwater: groundwater transport—advection and dispersion, groundwater contamination. National Academy Press, Washington, DC, pp 37–45.
18. Anderson, R., Hardy, E.E., Roach, J.T., & Witmer, R.E. (1976). A land use and land cover classification system for use with remote sensor data. USGS Professional Paper 964. Washington, DC.
19. Aral, M.M. & Taylor, S.W. (2011). Groundwater Quantity and Quality Management. American Society of Civil Engineers (ASCE), 1801 Alexander Bell Drive, Reston, Virginia, 20191-4400.
20. Arifeen, H.M., Phoungthong, K., Mostafaeipour, A., Yuangyai, N., Yuangyai, C., Techato, K., & Jutidamrongphan, W. (2021). Determine the Land-Use Land-Cover Changes, Urban Expansion, and Their Driving Factors for Sustainable Development in Gazipur Bangladesh. Atmosphere 2021, 12, 1353. https://doi.org/10.3390/atmos12101353.
21. Aziane, N., Khaddari, A., Ebn-Touhami, M., Zouahri, A., Nassali, H., & Elyoubi, M.S. (2020). Evaluation of groundwater suitability for irrigation in the coastal aquifer of Mnasra (Gharb, Morocco). Mediterranean Journal of Chemistry 2020, 10(2), 197-212.
22. Bangladesh Water Partnership (BWP) (2019). Rapid Assessment of the Groundwater Sustainability of Greater Dhaka Area. BWP is the country partnership of the Global Water Partnership Organization (GWPO), supported by 2030 Water Resources Group (2030 WRG) and funded by H&M.
23. Banglapedia (2021). National Encyclopedia of Bangladesh. https://en.banglapedia.org.
24. BARC (Bangladesh Agricultural Research Council) (1988) Agro Ecological Zones (AEZ) inventory map, scale: 1:250,000. Bangladesh Agricultural Research Council, Dhaka.
25. Barber, C., Bates, L.E., Barron, R., & Allison, H. (1993). Assessment of the relative vulnerability of groundwater to pollution: a review and background paper for the

conference workshop on vulnerability assessment AGSO Journal of Australian Geology & Geophysics, 14 (2/3), p. 147-154

26. Barbulescu, Alina (2020). Assessing Groundwater Vulnerability: DRASTIC and DRASTIC-Like Methods: A Review. Water 2020, 12, 1356; doi:10.3390/w12051356.
27. Bartolino, J.R. and Vincent, S. (2017). A Groundwater-Flow Model for the Treasure Valley and Surrounding Area, Southwestern Idaho U.S. Geological Survey Fact Sheet 2017–3027.
28. Bazuhaira, A.S., & Wood, W.W. (1996). Chloride mass-balance method for estimating ground water recharge in arid areas: examples from western Saudi Arabia. Journal of Hydrology, Volume 186, Issues 1–4, 15 November 1996, Pages 153-159.
29. BBS (2012). Statistical Yearbook of Bangladesh-2011. Dhaka: Bangladesh Bureau of Statistics.
30. BBS (2013). District Statistics 2011, Gazipur. Bangladesh Bureau of Statistics (BBS), Statistics and Informatics Division (SID), Ministry of Planning; 1st edition (January 1, 2013), ISBN-13: 978-984-51-9056-5.
31. BBS (2014)a. Bangladesh Community and Housing Census 2011 Community Report, Zila Gazipur. Bangladesh Bureau of Statistics (BBS), Statistics and Informatics Division (SID), Ministry of Planning; 1st edition (January 1, 2013), ISBN-13: 978-984-33-8578-9.
32. BBS (2014)b. Population & Housing Census-2011 Community Report: Gazipur. Bangladesh Bureau of Statistics (BBS), Statistics and Informatics Division (SID), Ministry of Planning; 1st edition (November 2014), ISBN-978-984-33-8578-9.
33. BBS, (2015) Statistical Yearbook of Bangladesh. Bangladesh Bureau of Statistics, Statistics Division, Ministry of Planning. Government of the People's Republic of Bangladesh, Dhaka.
34. BBS (2020). Bangladesh Statistics 2019. Bangladesh Bureau of Statistics (BBS), Statistics and Informatics Division (SID), Ministry of Planning.
35. Begum, K., Jahan, I., Rahman, M.H., Chowdhury, M.S., & Elahi, S.F. (2009). Status of some Micronutrients in Different Soils of Gazipur District as Related to Soil Properties and Land Type. Bangladesh Journal of Scientific and Industrial Research, 44(4), 425-430, 2009.
36. BGS & DPHE (2001). Arsenic contamination of groundwater in Bangladesh. Kinniburgh, D.G. and Smedley, P.L. (Editors), Volume 2; Final Report, British Geological Survey Report WC/00/19, British Geological Survey, Keyworth. ISBN 0852723849.
37. Brown, R. M., McClelland, N. I., Deininger, R. A. & Tozer, R. G. (1970). A water quality index: Do we dare? Water and Sewage Works, 117, 339–343.
38. Burgess, W.G., Hasan, M.K., Rihani, E., Ahmed, K.M., Hoque, M.A., & Darling, W.G. (2011). Groundwater quality trends in the Dupi Tila aquifer of Dhaka, Bangladesh: sources of contamination evaluated using the modeling and environmental isotopes. Int J Urban Sustain Dev 3(1):56–76. doi:10.1080/19463138.2011.554662.

39. Chakraborty, S., Sikdar, P.K., & Paul, P.K. (2007). Hydrogeochemical Framework of Quaternary Aquifer of English Bazaar Block, Malda District, West Bengal. The Icfai J. Earth Sci., 1, 61–74.
40. Chaturvedi, M.K. & Bassin, J.K. (2010). Assessing the water quality index of water treatment plant and bore wells, in Delhi, India. Environ. Monit. Assess., 163. 449-453. 2010.
41. Congalton, R.G. and Green, K. (1999). Assessing the Accuracy of Remotely Sensed Data Principles and Practices. Lewis Publishers, Boca Raton.
42. Curray, J. R. (1994). Sediment volume and mass beneath the Bay of Bengal. Earth and Planetary Science Letters, v. 125, p. 371-383.
43. Davies, J. (1994). The Hydrogeochemistry of alluvial aquifers in central Bangladesh. In: Nash, H. and McCall, G. J. H. (ed), Groundwater Quality, Chapman and Hall, London, 9-17.
44. Davies, R.B. (2002). Hypothesis Testing When a Nuisance Parameter Is Present Only Under the Alternative: Linear Model Case. Biometrika, 89 (June), 484-489.
45. Davis, K.W., Putnam, L.D., & LaBelle, A.R. (2015). Conceptual and numerical models of groundwater flow in the Ogallala and Arikaree aquifers, Pine Ridge Indian Reservation area, South Dakota, water years 1980–2009: U.S. Geological Survey Scientific Investigations Report 2014–5241, 68 p., http://dx.doi.org/10.3133/sir20145241.
46. Debels, P., Figueroa, R., Urrutia, R., Barra, R., & Niell, X. (2005). Evaluation of Water Quality in the Chillán River (Central Chile) Using Physicochemical Parameters and a Modified Water Quality Index. Environmental Monitoring and Assessment, 110(1-3), 301–322. doi:10.1007/s10661-005-8064-1
47. Dee, N., Baker, J., Drobny, N., Duke, K., Whitman, I., & Fahringer, D. (1973). An environmental evaluation system for water resource planning; Water Resources Research, Vol. 9, No. 3, pp. 523- 535.
48. Deng, J.S., Wang, K., Hong, Y., Qi, & J. G. (2009) Spatio-temporal dynamics and evolution of land use change and landscape pattern in response to rapid urbanization. Landscape and Urban Planning 92 (2009) 187–198.
49. Dewan, A.M. & Yamaguchi, Y. (2009). Land use and land cover change in Greater Dhaka, Bangladesh: Using remote sensing to promote sustainable urbanization. Applied Geography, 29(3), 390–401.
50. Doerfliger, N., Jeannin, P.Y., & Zwahlen, F. (1999). Water vulnerability assessment in karst environments: A new method of defining protection areas using a multi-attribute approach and GIS tools (EPIK method). Environ. Geol. 1999, 39, 165–176.
51. Dojlido, J., Raniszewski, J., & Woyciechowska, J. (1994). Water quality index applied to rivers in the Vistula river basin in Poland. Environmental Monitoring and Assessment, 33(1), 33–42. doi:10.1007/bf00546659

52. Domenico, P.A. & Schwartz, F.W, (1997). Physical and chemical hydrogeology. 2nd Edition, John Wiley & Sons, Inc. 506p.
53. Doneen, L.D. (1964) Water Quality for Agriculture. Department of Irrigation, University of California, Davis, 48 p.
54. Edmunds, W.M. & Shand, P. (2008). Groundwater Baseline Quality. Natural Groundwater Quality Edited By W. Mike Edmunds and Paul Shand,© 2008 Blackwell Publishing Ltd. ISBN: 978-14051-5675-2.
55. Ehteshami, M., Peralta, R.C., Eisele, H., Deer, H., & Tindell, T. (1991). Assessing Pesticide Contamination to Groundwater, A Rapid Approach; GroundWater, vol. 29, no. 6, Rosen, 1994
56. Environmental Protection Agency (EPA) (2020). Conductivity: What is Conductivity, and Why is it Important? Available from: https://archive.epa.gov/.
57. Fetter, C.W. (1993) Contaminant Hydrogeology. Macmillan Publishing Company, New York.
58. Foster, S.S.D. & Chilton, P.J. (2003). Groundwater: the processes and global significance of aquifer degradation. Philosophical Transactions of the Royal Society of London, B, 358, 1957-1972.
59. Foster, S., Hirata, R., & Howard, K. (2011). Groundwater Use in Developing Cities: Policy Issues Arising from Current Trends. Hydrogeol. J., 19, 271–274.
60. Foster, S. (1987). Fundamental concepts in aquifer vulnerability, pollution risk, and protection strategy. Hydrol. Resour. Proc. Inf. 1987, 38, 69–86.
61. Foster, S.S.D., Hirata, R., Gomes, D., D'Elia, M., & Paris, M. (2002). Groundwater quality protection: a guide for water utilities municipal authorities and environment agencies. World Bank, Washington DC.
62. Foster, S.S.D., Lawrence, A.R., & Morris, B.M. (1998). Groundwater in urban development. World Bank Technical Paper no 390, Washington DC.
63. Freeze, R.A. & Cherry, J.A. (1979). Groundwater. Prentice-Hall, Englewood Cliffs, p 604
64. Giri, C.P. (2012). Remote Sensing of Land Use and Land Cover – Principles and Applications. CRC Press, ISBN-13: 978-1-4200-7075-0.
65. Giuliani, G., Mazzetti, P., Santoro, M., Nativi, S., Van Bemmelen, J., Colangeli, G., & Lehmann, A., (2020). Knowledge generation using satellite earth observations to support sustainable development goals (sdg): A use case on land degradation. Int. J. Appl. Earth Obs. 88, 102068. https://doi.org/10.1016/j.jag.2020.102068.
66. Gogu, R.C. & Dassargues, A. (2000). Current trends and future challenges in groundwater vulnerability assessment using overlay and index methods. Environ. Geol. 2000, 39, 549–559.
67. Gonzalez-Acevedo, Z.I., Padilla-Reyes, D.A., & Ramos-Leal, J.A. (2016). Quality assessment of irrigation water related to soil salinization in Tierra Nueva, San Luis Potosi, Mexico. Revista Mexicana De Ciencias Geologicas, volume 33, number 3, p. 271-285.

68. Goossens, M. & Van Damme, M. (1987). Vulnerability mapping in Flanders, Belgium. In Vulnerability of Soil and Groundwater to Pollutants International Conference; van Duijvenbooden, W., van Waegeningh, G.H., Eds.; Proceedings and Information 38; TNO Committee on Hydrological Research: The Hague, The Netherlands, 1987; pp. 355–360.
69. Güneralp, B. and Seto, K.C. (2008). Environmental Impacts of Urban Growth from an Integrated Dynamic Perspective: A Case Study of Shenzhen, South China. Global Environmental Change, 18, 720-735. https://doi.org/10.1016/j.gloenvcha.2008.07.004
70. Haq, K.A. (2006). Water Management in Dhaka. Int. J. Water Resour. Dev. 2006, 22, 291–311.
71. Hammerlinck, J.D. & Arneson, C.S. (1998). Wyoming Groundwater Vulnerability Assessment Handbook, Spatial Data and Visualization Report, Wyoming State Engineers Office, Wyoming, US.
72. Harbaugh, A.W. (2005). MODFLOW-2005, The U.S. Geological Survey modular groundwater model: the ground-water flow process. US Geol Surv Techniques Methods 6-A16.
73. Harbaugh, A.W., Banta, E.R., Hill, M.C. & McDonald, M.G. (2000). The US geological survey's modular ground water flow model e user guide to modularization concepts and the ground water flow process. US Geological Survey. Open-File Report 00e92
74. Hardin, P.J., Jackson, M.W., & Otterstrom, S.M. (2007). Mapping, measuring, and modeling urban growth. In Jensen, R.R., Gatrell, J.D. & McLean, D. (Eds.), Geo-spatial technologies in urban environments: Policy, practice, and pixels (2nd ed.). (pp. 141–176) Heidelberg: Springer-Verlag.
75. Harris, P.M., & Ventura, S.J. (1995). The integration of geographic data with remotely sensed imagery to improve classification in an urban area. Photogrammetric Engineering & Remote Sensing, 61(8), 993–998.
76. Hasan, M.A., Ahmed, K.M., Sracek, O., Bhattacharya, P., von Brömssen, M., Broms, S., Fogelström, J., Mazumder, M.L., & Jacks, G. (2007). Arsenic in shallow groundwater of Bangladesh: investigations from three different physiographic settings. Hydrogeol. J. 15, 1507–1522.
77. Hasan, M.K. (1999). The Vulnerability of the Dupi Tila Aquifer, Dhaka, Bangladesh. Thesis Submitted to the University of London for the Degree of Doctor of Philosophy, Department of Geological Sciences, University College London, July 1999.
78. Hasan, M., Islam, M.A., Hasan, M.A., Alam, M.J., & Peas, M.H. (2019). Groundwater vulnerability assessment in Savar Upazila of Dhaka district, Bangladesh — A GIS-based DRASTIC modeling. Groundwater for Sustainable Development 9, April 2019, 100220.
79. Hasan, M.K. (1999). The Vulnerability of the Dupi Tila Aquifer, Dhaka, Bangladesh. A Thesis Submitted to the University of London for the Degree of Doctor of Philosophy. Department of Geological Sciences University College London, July 1999.

80. Hassan, M.Q. (1992). Saline Water Intrusion and Hydrogeological Modeling in Southwest Bangladesh. GeoWissenschaftliche Texte 9, Scheltzky & Jeep, Berlin 1992.
81. Hassan, M.Q. (2000). Three-dimensional Groundwater Modeling in Unsteady-State Condition of Two Layered Aquifer System: A Study from the Ganges Delta Region, SW Bangladesh. Dhaka University, Dhaka, ISBN 984-31-0904-9, Bangladesh, 120p.
82. Hassan, M.Q. (2004). Water Resources Management and Development in Dhaka City, (Editor) Published by German Cultural Centre Dhaka, ISBN no. 984-32-1341-6, Dhaka,133p.
83. Hassan, M.Q., Raza, J., Karim, M. F., & Khandaker, N. I. (2019). Using Water Quality Index to Assess Groundwater Suitability at Gazipur District, Bangladesh. Geological Society of America Conference.
84. Hassan, M.M. & Southworth, J. (2017). Analyzing land cover change and urban growth trajectories of the mega-urban region of Dhaka using remotely sensed data and an ensemble classifier. Sustainability, 10(1), 10.
85. Helsel, D.R., Hirsch, R.M., Ryberg, K.R., Archfield, S.A., & Gilroy, E.J. (2020). Statistical methods in water resources: U.S. Geological Survey Techniques and Methods, book 4, chapter A3, 458 p.
86. Hem, J.D. (1989). Study and Interpretation of the Chemical Characteristics of Natural Water. U.S Geological Survey Water-supply Paper 2254.
87. Hoque, M.A., Hoque, M.M., & Ahmed, K.M. (2007). Declining groundwater level and aquifer dewatering in Dhaka metropolitan area, Bangladesh: causes and quantification. Hydrogeol J 15(8):1523–1534. doi:10.1007/s10040-007-0226-5.
88. Horton, R. K. (1965). An index-number system for rating water quality. Journal of Water Pollution Control Federation, 37(3), 300-306.
89. Hrkal, Z. (2001). Vulnerability of groundwater to acid deposition, Jizerské Mountains, northern Czech Republic: construction and reliability of a GIS-based vulnerability map. Hydrogeology Journal, 9(4), 348–357.
90. ICDDRB (2016). Baseline Population and Socioeconomic Census Slums of Dhaka (North and South) and Gazipur City Corporations, 2015-16. Urban Primary Health Care Services Delivery Project, Local Government Division, Ministry of Local Government, Rural Development & Cooperatives; conducted by International Centre for Diarrhoeal Disease Research, Bangladesh (ICDDRB).
91. Islam, M.B., Firoz, A.B.M., Foglia, L., Marandi, A., Khan, A.R., Schüth, C., & Ribbe, L. (2017). A regional groundwater-flow model for sustainable groundwater-resource management in the south Asian megacity of Dhaka, Bangladesh. Hydrogeology Journal, 25(3), 617–637. doi:10.1007/s10040-016-1526-4.
92. Islam, M.S. & Alam, M.J., (2009). Geological Aspects of Soil Formation of Bangladesh. Conference: Bangladesh Geotechnical Conference 2009.

93. Islam, M.S, Tusher, T.R., Mustafa, M., & Mamun, S.A. (2020). Investigation of soil quality and heavy metal concentrations from a waste dumping site of Konabari industrial area at Gazipur in Bangladesh. IOSR Journal of Environmental Science, Toxicology and Food Technology (IOSR-JESTFT), ISSN: 2319-2402, ISBN: 2319-2399. Volume 2, Issue 1 (Nov. - Dec. 2012), PP 01-07, www.Iosrjournals.org.
94. Islam, M.T., Croll, D., Gladieux, P., Soanes, D. M., Persoons, A., Bhattacharjee, P. (2016). Emergence of wheat blast in Bangladesh was caused by a South American lineage of Magnaporthe oryzae. BMC Biol. 14:84. doi: 10.1186/s12915-016-0309-7.
95. Jahromi, M.N., Gomeh, Z., Busico, G., Barzegar, R., Samany, N.N., Aalami, M.T., & Kazakis, N. (2020). Developing a SINTACS-based method to map groundwater multi-pollutant vulnerability using evolutionary algorithms. Environmental Science and Pollution Research.
96. Jamil, N.B. and Ahmed, K.M. (2016). Vulnerability Assessment and Groundwater Resources Planning for Tongi Industrial Area, Bangladesh Dhaka University Journal of Earth and Environmental Sciences, Vol. 4, December 2015.
97. Jensen, J.R., & Im, J. (2007). Remote sensing change detection in urban environments. In R. R. Jensen, J. D. Gatrell, & D. McLean (Eds.), Geo-spatial technologies in urban environments: Policy, practice, and pixels (2nd ed.). (pp. 7–30) Heidelberg: Springer-Verlag.
98. Kabir, A.S.M.S., Hossain, D. & Abdullah, R. (2011). 2-D Electrical Imaging in Some Geotechnical Investigation of Madhupur Clays, Bangladesh. Journal Geological Society of India, Vol.77, January 2011, pp.73-81.
99. Kahsay, G.H. (2008). Groundwater resource assessment through distributed steady-state flow modeling, Aynalem wellfield, Mekele, Ethiopia. Master of Science, International Institute for Geo-Information Science and Earth Observation Enschede, the Netherlands.
100. Kannel, P.R., Lee, S., Lee, Y.S., & Khan, S.P. (2007). Application of Water Quality Indices and Dissolved Oxygen as Indicators for River Water Classification and Urban Impact Assessment. Environ Monit Assess 132, 93–110 (2007). https://doi.org/10.1007/s10661-006-9505-1.
101. Kaufman, R.K., Seto, K.C., Schnieder, A., Liu, Z., Zhou, L., & Wang, W. (2007). Climate response to rapid urban growth: Evidence of a human-induced precipitation deficit. Journal of Climate 20, no. 10 (2007): 2299-2306.
102. Khandoker, R.A. (1989). Development of major tectonic elements of the Bengal Basin - A plate tectonic appraisal. Bangladesh Journal of Scientific Research, v. 7, p. 221-232.
103. Kheirandish, M., Rahimi, H.R., Kamaliardakani, M., & Salim, R. (2020). Obtaining the effect of sewage network on groundwater quality using MT3DMS code: Case study on Bojnourd plain. Groundwater for Sustainable Development, 100439.

104. Kim, Y.J. & Hamm, S.Y. (1999). Assessment of the potential for groundwater contamination using the DRASTIC/EGIS technique, Cheongju area, South Korea, Hydrogeology Journal, 7: 227-235
105. Kirlas , M.C., Karpouzos, D.K., Georgiou, P.E., & Katsifarakis, K.L. (2022). A comparative study of groundwater vulnerability methods in a porous aquifer in Greece. Applied Water Science (2022) 12:123
106. Kolokotroni, M., & Giridharan, R. (2008). Urban heat island intensity in London: An investigation of physical characteristics' impact on outdoor air temperature changes during summer. Solar Energy, 82(11), 986–998. doi:10.1016/j.solener.2008.05.00
107. Konikow, L.F. & Mercer, J.W. (1978). Groundwater flow and transport modeling. Journal of Hydrology, Volume 100, Issues 1–3, 1988, Pages 379-409, ISSN 0022-1694. https://doi.org/10.1016/0022-1694(88)90193-X.
108. Kumar, P., Bansod, K.S., Debnath, K.S., Thakur, P.K., & Ghanshyam, C. (2015) Index-based groundwater vulnerability mapping models using hydrogeological settings: Acritical evaluation. Environ. Impact Assess. Rev. 2015, 51, 38–49.
109. Kumar, S., Thirumalaivasan, D., Rdhakrishnan, N., & Mathew, S. (2013). Groundwater vulnerability assessment using SINTACS model. Geomatics, Natural Hazards, and Risk, 2013, Vol. 4, No. 4, 339-354.
110. Langguth, H.R. (1966). Groundwater verhaltisse in Bereiech Des Velberter. Sattles. Der Minister Fur Eraehrung, Land Wirtsch Forste (pp. 127). Duesseldorf: NRW.
111. Langevin, C.D., & Guo, W. (2006). MODFLOW/MT3DMS-Based Simulation of Variable-Density Ground Water Flow and Transport. Ground Water, 44(3), 339–351. doi:10.1111/j.1745-6584.2005.00156.x.
112. Leake, S.A. (1997). Modeling groundwater flow with MODFLOW and related programs: U.S. Geological Survey Fact Sheet 121–97, 4 p.
113. Lloyd, W., & Heathcote, A. (1985). Natural Inorganic Hydrochemistry in Relation to Groundwater, an Introduction. Oxford: Clarendon Press.
114. LGRD (2006). Final Report on Development of Deep Aquifer Database and Preliminary Deep Aquifer Map (First Phase). Published by the Department of Public Health Engineering (DPHE), Government of the People's Republic of Bangladesh (GoB), Arsenic Policy Support Unit (APSU), and JICA Bangladesh (JICA).
115. Liyanage, C.P. and Yamada, K. (2017) Impact of Population Growth on the Water Quality of NaturalWater Bodies. Sustainability 2017, 9, 1405; doi:10.3390/su9081405.
116. Lloyd, J.W. & Heathcoat, J.A. (1985). Natural Inorganic Chemistry in Relation to Groundwater. Clarendon Press, Oxford.
117. Lu, Q., & Weng, D. (2005). Urban classification using the full spectral information of Landsat ETM+ imagery in Marion County, Indiana. Photogrammetric Engineering & Remote Sensing, 71(11), 1275–1284.

118. Lubello, C. & Gori, R. (2001). Agricultural Water Reuse: A Review Water Pollution., edited by C. A. Brebbia, WIT Press, 544p
119. Machiwal, D., Jha, M.K., Singh, V.P., & Mohan, C. (2018). Assessment and mapping of groundwater vulnerability to pollution: Current status and challenges. Earth-Science Reviews.
120. Margat, J. (1968). Ground Water Vulnerability to Contamination; Bases de la Cartographie, Doc. 68 SGC198 HYD; BRGM: Orleans, France, 1968. (In French)
121. Masetti, M., Sterlacchini, S., Ballabio, C., Sorichetta, A., & Poli, S. (2009). Influence of threshold value in the use of statistical methods for groundwater vulnerability assessment. Sci. Total Environ. 2009, 407, 3836–3846.
122. McDonald, M. and Harbaugh, A.W. (1988) A Modular Three-Dimensional Finite Difference Ground-Water Flow Model. In: Techniques of Water-Resources Investigations, Book 6, U.S. Geological Survey, 588.
123. Meeks, Y.J. & Dean, J.D. (1990). Evaluating groundwater vulnerability to pesticides, Journal of water Resources Planning and Management, 116, 693-707
124. Mitchell, V. G., Duncan, H., Inman, M., Rahilly, M., Stewart, J., Vieritz, A., Holt, P., Grant, A., Fletcher, T.D., Coleman, J., Maheepala, S., Sharma, A., Deletic, A., & Breen, P. (2007). State of the art review of integrated urban water models. In: Novatech Lyon, France, pp.1–8.
125. Morgan, J.P. & McIntire, W.G. (1959). Quaternary geology of the Bengal Basin, East Pakistan, and India. Geol. Soc. Amer. Bull. v. 70, p. 319-342.
126. Morris, B. L., Lawrence, A. R.., Chilton, P. J., Adams, B., Calow, R., & Klinck, B. A. (2003). Groundwater and its susceptibility to degradation: A global assessment of the problems and options for management. Early Warning and Assessment Report Series, RS, 03-3. UNEP, Nairobi, Kenya.
127. Morris, B.L., Seddique, A.A., & Ahmed, K.M. (2003). Response of the Dupi Tila aquifer to intensive pumping in Dhaka, Bangladesh. Hydrogeology Journal, 11(4):496–503. doi:10.1007/s10040-003-0274-4.
128. MPO (1985). Geology of Bangladesh, Technical Report No.4. Master Plan Organization, Ministry of Irrigation, Water Development and Flood Control, Government of Bangladesh.
129. MPO (Master Plan Organisation) (1987). Groundwater Resources of Bangladesh. Technical Report no 5. Master Plan Organization, Dhaka. Hazra, USA; Sir M MacDonald, UK; Meta, USA; EPC, Bangladesh.
130. Nadiri, A.A., Sedghi, Z., Khatibi, R., & Sadeghfam, S. (2018). Mapping the specific vulnerability of multiple confined and unconfined aquifers by using artificial intelligence to learn from multiple DRASTIC frameworks. Journal of Environmental Management.

131. National Research Council (NRC) (1993). Groundwater vulnerability assessment, contamination potential underconditions of uncertainty. National Academy Press, Washington, DC, p 2005.
132. Naudet, V., Revil, A., Rizzo, E., Bottero, J.Y., & Bégassat, P. (2004). Groundwater redox conditions and conductivity in a contaminant plume from geoelectrical investigations. Hydrology and Earth System Sciences, 8(1), 8–22. doi:10.5194/hess-8-8-2004.
133. Neukum, C., Hotzl, H., & Himmelsbach, T. (2008). Validation of vulnerability mapping methods by field investigations and numerical modeling. Hydrogeol. J. 2008, 16, 641–658.
134. Parvin, M. (2018). Characteristics and occurrence of drought and its role in triggering over-exploitation of groundwater resources Dhaka and Gazipur districts, Bangladesh. MSc Thesis WSE-HERBD.18-18, the Master of Science degree at the UNESCO-IHE Institute for Water Education, Delft, the Netherlands.
135. Parvin, M. (2019). The Rate of Decline and Trend Line Analysis of Groundwater underneath Dhaka and Gazipur City. Journal of Water Resource and Protection, 2019, 11, 348-356.
136. Pesce, S.F. & Wunderlin, D.A. (2000). Use of Water Quality Indices to Verify the Impact of Córdoba City (Argentina) on Suquía River. Water Research, 34, 2915-2926. http://dx.doi.org/10.1016/S0043-1354(00)00036-1.
137. Poeter, E.P., Hill, M.C., Banta, E.R., Mehl, S., & Christensen, S. (2005). UCODE_2005 and six other computer codes for universal sensitivity analysis, calibration, and uncertainty evaluation. US Geol Surv Techniques Methods 6-A11.
138. Piper, A.M. (1944). A Graphic Procedure in the Geochemical Interpretation of Water-Analyses. Eos, Transactions American Geophysical Union, 25, 914-928. http://dx.doi.org/10.1029/TR025i006p00914
139. Qureshi, A., Ahmed, Z., & Krupnik, T. (2014). Groundwater Management in Bangladesh: An Analysis of Problems and Opportunities; Cereal Systems Initiative for South Asia Mechanization and Irrigation Project (CSISA-MI) Project; Research Report No. 2; CIMMYT: Dhaka, Bangladesh, 2014.
140. Rahman, M.A., Wiegand, B.A., Badruzzaman, A.B.M., & Ptak, T. (2013). Hydrogeological analysis of the upper Dupi Tila Aquifer, towards the implementation of a managed aquifer-recharge project in Dhaka City, Bangladesh. Hydrogeol J 21(5):1071–1089. doi:10.1007/s10040-013-0978-z.
141. Rahman, M.M., Al Thobiani, F., Shahid, S., Virdis, S.G.P., Kamruzzaman, M., Rahaman, H., Momin, M.A., Hossain, M.B., & Ghandourah, E.I. (2022) GIS and Remote Sensing-Based Multi-Criteria Analysis for Delineation of Groundwater Potential Zones: A Case Study for Industrial Zones in Bangladesh. Sustainability 2022, 14, 6667. https://doi.org/10.3390/su14116667.

142. Rahnama, M.B., & Zamzam, A. (2011). Quantitative and qualitative simulation of groundwater by mathematical models in Rafsanjan aquifer using MODFLOW and MT3DMS. Arabian Journal of Geosciences, 6(3), 901–912. doi:10.1007/s12517-011-0364-x.
143. Rajamanickam, R. & Nagan, S. (2010). Groundwater quality modeling of Amaravathi River basin of Karur District, Tamil Nadu, using visual modflow. International Journal on Environmental Sciences. volume 1, pp 91-108.
144. Ravenscroft, P (2003). Overview of the hydrogeology of Bangladesh. In: Rahman AA, Ravenscroft P (eds) Groundwater resources and development in Bangladesh: background to the arsenic crisis, agricultural potential and the environment, chap. 3. Bangladesh Centre for Advanced Studies, Univ Press, Dhaka, pp 43–86.
145. Raza, J. (2008). Groundwater Quality Evaluation and Vulnerability Assessment of Wadi Al-Arj Alluvium Aquifer Using GIS and DRASTIC Method. Masters Dissertation submitted to the Earth Sciences Department, King Fahd University of Petroleum & Minerals.
146. Raza, J., Ahmed, K.M., Hasan, M.Q., & Zahid, A. (2020). Historical changes in land-use due to industrialization and resultant adverse impacts on groundwater of the Dupi Tila aquifer in Gazipur area, Bangladesh. International Conference on Earth and Environmental Sciences & Technology for Sustainable Development, 2020
147. Raza, J., Hassan, M.Q., Zahid, A., & Khandaker, N. (2021) Utilizing Remote Sensing and GIS technique to Assess the Spatiotemporal Dynamics of Land Cover and Land Use Changes of Gazipur District, Bangladesh. The Geological Society of America Connects 2021, Portland Oregon, USA.
148. Reimann, R.U. (1993). Geology of Bangladesh. Gebruder Borntraeger, Berlin-Stuttgart.
149. Rosen, L. (1994). A Study of the DRASTIC Methodology with Emphasis on Swedish Conditions. Ground Water, 32(2), 278–285. doi:10.1111/j.1745-6584.1994.tb00642.x.
150. Rupert, M.G. (2001). Calibration of the DRASTIC groundwater vulnerability mapping method, Ground Water, vol. 39, Iss. 4
151. Saah, D., Tenneson, K., Poortinga, A., Nguyen, Q., Chishtie, F., San Aung, K., Markert, K. N., Clinton, N., Anderson, E.R., & Cutter, P., (2020). Primitives as building blocks for constructing land cover maps. Int. J. Appl. Earth Obs. 85, 101979.
152. Salaj, S.S., Ramesh, D., Babu, D.S.S., & Kaliraj, S. (2018). Impacts of urbanization on groundwater vulnerability along the Kozhikode coastal stretch, Southwestern India using GIS-based modified DRASTIC–U Model. Journal of Coastal Sciences, Volume 5 Issue No. 2 - 2018 Pages 1-27, ISSN: 2348 – 6740.
153. Sarker, N.M. & Huq, A.K.M.F. (1985). Protected Areas of Bangladesh. In: Conserving Asia's Natural Heritage, Thornsell, J. W. (ed.) pp. 36–8. IUCN, Gland, Switzerland.
154. Sawyer, C.N., McCarty, P.L., & Parkin, G.F. (2003). Chemistry for Environmental Engineering and Science. Fifth Edition, McGraw-Hill, p752.

155. Sayed, A.F., Bhuiyan, M.A.H., Chowdhury, M.A.I., & Kabir, M.M. (2015). Effects of Industrial Agglomeration on Land-Use Patterns and Surface Water Quality in Konabari, BSCIC area at Gazipur, Bangladesh. International Research Journal of Environment Sciences, Vol. 4(11), 42-49, November (2015), ISSN 2319–1414.
156. Seto, K.C., & Shepherd, J.M. (2009). Global urban land-use trends and climate impacts. Current Opinion in Environmental Sustainability, 1(1), 89–95. doi:10.1016/j.cosust.2009.07.01210.1016.
157. Seto, K.C., Fragkias, M., Güneralp, B., & Reilly, M.K. (2011). A Meta-Analysis of Global Urban Land Expansion. PLoS ONE, 6(8), e23777. doi:10.1371/journal.pone.
158. Seto, K.C., Guneralp, B., & Hutyra, L.R. (2012). Global forecasts of urban expansion to 2030 and direct impacts on biodiversity and carbon pools. Proceedings of the National Academy of Sciences, 109(40), 16083–16088. doi:10.1073/pnas.1211658109.
159. Schmoll, O., Howard, G., Chilton, P.J. and Chorus, I. (eds). (2006). Protecting groundwater for health: managing the quality of drinking water sources. WHO/IWA, London.
160. Schwartz, F. and Zhang, H. (2003) Fundamentals of groundwater. Wiley, New York.
161. Shamsudduha M & Uddin A (2007). Quaternary shoreline shifting and hydrogeologic influence on the distribution of groundwater arsenic in aquifers of the Bengal Basin. J Asian Earth Sci 31:177–194.
162. Shamsudduha , M., Taylor, R.G. , Ahmed, K.M., & Zahid, A. (2011). The impact of intensive groundwater abstraction on recharge to a shallow regional aquifer system: evidence from Bangladesh. Hydrogeology Journal (2011) 19: 901–916.
163. Shapiro, S.S., Wilk, M.B., & Chen, H.J. (1968). A Comparative Study of Various Tests for Normality. Journal of the American Statistical Association, 63(324), 1343. doi:10.2307/2285889
164. Shapla, T., Park, J. Hongo, C., & Kuze, H. (2015). Agricultural Land Cover Change in Gazipur, Bangladesh, in Relation to Local Economy Studied Using Landsat Images. Advances in Remote Sensing, 2015, 4, 214-223.
165. Simu, S.A., Sikder, T., Uddin, M.J., Deeba, F., Kashem, M.A., Mondal, K.P., Akter, M., Rahman, M., Banik, S., & Kurasaki, M. (2017). Sustainable Water Resources Management Monitoring of heavy metal pollution and GIS derived land use changes in the major economic zone of Bangladesh. Sustainable Water Resources Management, ISSN 2363-5037, Sustainable Water Resource Management. Springer International Publishing. DOI 10.1007/s40899-017-0151-2.
166. Simu, S.A., Uddin, M.J., Majumder, R.K., Zaman, M.N., Rahman, M.A., & Kashem, M.A. (2016). Industrial Area, Bangladesh. All Rights Reserved Euresian Publication © 2016 eISSN 2249 0256
167. Simu, S.A., Uddin, M.J., Majumder, R.K., Zaman, M.N., Rahman, M.A., & Kashem, M.A. (2018). Speciation analysis of Elements of Soil Samples by XRF in Gazipur industrial area,

Bangladesh. International Journal of Modern Research in Engineering and Technology (IJMRET). www.ijmret.org Volume 3 Issue 3, March 2018.

168. Somaratne, N. & Smettem, K.R.J. (2014). Theory of the generalized chloride mass balance method for recharge estimation in groundwater basins characterised by point and diffuse recharge. Hydrol. Earth Syst. Sci. Discuss., 11, 307–332, 2014, www.hydrol-earth-syst-sci-discuss.net/11/307/2014/. doi:10.5194/hessd-11-307-2014.
169. Sophocleous, M.A. (1991). Combining the soil water balance and water level fluctuation methods to estimate Natural Groundwater recharge: Practical Aspects. Journal of Hydrology, 124 (3-4): 229-241.
170. Spitz, K. & Moreno, J. (1996). A Practical Guide to Groundwater and Solute Transport Modeling. John Wiley & Sons, Inc., New York.
171. Swan, A.R.H. & Sandilands, M. (1995). Introduction to geological data analysis. Blackwell Science, Oxford, 1995.
172. Sultana, T. (2019). Hydrogeology of Sreepur Upazila, Gazipur District. M.Sc. Thesis Dissertation, Department of Geology, Faculty of Earth Sciences, University of Dhaka.
173. Terrado, M., Barcelo, D., Tauler, R., Borrell, E., & Campos, S.D. (2010). Surface-water-quality indices for the analysis of data generated by automated sampling networks. Trends Anal. Chem., 29(1). 40-52. 2010.
174. Toth, J. (1984). The role of regional groundwater flow in groundwater's chemical and thermal evolution, in Canadian/American Conference on Hydrogeology, Alberta, 1984, Worthington, OH, National Water Well Association, p. 3-39.
175. Tyagi, S., Sharma, B., Singh, P., & Dobhal, R. (2013) Water Quality Assessment in Terms of Water Quality Index. American Journal of Water Resources, 2013, Vol. 1, No. 3, 34-38, © Science and Education Publishing, DOI:10.12691/major-1-3-3.
176. Tziritis, E., Pisinaras, V., Panagopoulos, A., & Arampatzis, G. (2020). RIVA: a new proposed method for assessing intrinsic groundwater vulnerability. Environmental Science and Pollution Research. doi:10.1007/s11356-020-10872-3 Universal Journal of Environmental Research and Technology.
177. UNDP (United Nation Development Programme) (1982). Groundwater survey: the hydrogeological conditions of Bangladesh. Technical Report DP/UN/BGD-74-009/1, UNDP, New York.
178. United States Salinity Laboratory (USSL) (1954) Diagnosis and Improvement of Saline and Alkaline Soils. US Department of Agriculture Handbook, No. 60, 160 p.
179. Vissers, M.J.M. (2005). Patterns of Groundwater quality. Nederlands Geographical Studies 335, Faculteit Geowetenschappen, Universiteit Utrecht. ISBN-13: 978-90-6809-375-9.
180. Voudouris, K., Panagopoulos, A., & Koumantakis, J. (2000). Multivariate Statistical Analysis in the Assessment of Hydrochemistry of the Northern Korinthia Prefecture Alluvial Aquifer System (Peloponnese, Greece). Natural Resources Res., 9 (2), 135–146.

181. Vrba, J. & Zaporozec, A. (1994). Guidebook on Mapping Groundwater Vulnerability—IAH International Contributions to Hydrogeology, 16. FRG, Heise Publication, Hannover, 131 p.
182. WARPO (Water Resources Planning Organization) (2000). National Water Management Plan Project, Draft Development Strategy. Main final, vol 2, WARPO, Dhaka.
183. WaterAid (2018). Gazipur City Corporation, Bangladesh. SFD Lite Report prepared by WaterAid Bangladesh.
184. WHO (2022). Guidelines for drinking-water quality: fourth edition incorporating the first and second addenda. Geneva: World Health Organization (WHO); 2022. ISBN 978-92-4-004506-4.
185. WHO (2004). The World Health Report 2004 - Changing history. World Health Organization (WHO). https://apps.who.int/iris/handle/10665/42891.
186. Wilcox, L.V. (1955). Classification and Use of Irrigation Water. US Department of Agriculture, Circular 969, Washington DC.
187. Xu, Y., and Usher, B. (eds). 2006. Groundwater pollution in Africa. Taylor and Francis, London, Leiden, New York.
188. Yamagata, Y., Sugita, S., & Yasuoka, Y. (1997). Development of Vegetation–Soil–Water Index algorithms and applications. Japanese Journal of Remote Sensing, 17(1), 54–64.
189. Yesmin, R., Mohiuddin, A.S.M., Uddin, M.J., & Shahid, M.A. (2014). Land use and land cover change detection at Mirzapur Union of Gazipur District of Bangladesh using remote sensing and GIS technology. IOP Conference Series: Earth and Environmental Science, 20, 012055. doi:10.1088/1755-1315/20/1/012055
190. Yogendra, K. & Puttaiah, E.T. (2008), Determination of water quality index and suitability of an urban waterbody in Shimoga Town, Karnataka. Proceedings of Taal2007: The 12th World Lake Conference, pp. 342-346. 2008.
191. Yuan, F., Sawaya, K.E., Loeffelholz, B.C., & Bauer, M.E. (2005). Land cover classification and change analysis of the twin cities (Minnesota) metropolitan area by multitemporal Landsat remote sensing. Remote Sens. Environ. 2005, 98, 317–328.
192. Zahid, A. (2008). Study on Aquifer Environment in the Arsenic Affected areas of Chandpur and Madaripur Districts of Southern Bangladesh, Thesis is presented for the Degree of Doctor of Philosophy (Ph.D.) in Hydrogeology in the Department of Geology under the Faculty of Earth and Environmental Sciences, University of Dhaka, Bangla
193. Zahid, A, Hassan, M.Q., Samad, Q. A., Islam, R., Khan, M.S., & Haque, R. (2013). (Joint Editor): Impact of Climate Change on Socio-Economic Conditions of Bangladesh. ISBN No. 978 984 33 7883-5, Dhaka, 227p
194. Zahid, A., Hossain, A., Uddin, M.E., & Deeba, F. (2004). Groundwater level declining trend in Dhaka city aquifer, Proceeding of the International Workshop on Water Resources Management and Development in Dhaka City, May 2004, 133p.

195. Zahid, A., Reaz, S., & Ahmed, U. (2006). Groundwater Resources Development in Bangladesh: Contribution to Irrigation for Food Security and Constraints to Sustainability. Groundw. Gov. Asia Ser. 2006, 1, 27–46.
196. Zhang, H., Xu, W. L., & Hiscock, K. M. (2013). Application of MT3DMS and Geographic Information System to Evaluation of Groundwater Contamination in the Sherwood Sandstone Aquifer, UK. Water, Air, & Soil Pollution, 224(2). doi:10.1007/s11270-013-438-z.
197. Zheng, C. & Wang, P. (1999). MT3DMS: a modular three-dimensional multispecies transport model for simulation of advection, dispersion, and chemical reactions of contaminants in groundwater systems, documentation, and user's guide. US Army Corps of Engineers, Washington, DC.
198. Zheng, C., Hill, M. C., Cao, G., & Ma., R. (2012). MT3DMS: Model Use, Calibration, and Validation. Transactions of the ASABE, 55(4), 1549–1559. Selected Publications.
199. Zioti, F., Ferreira, K.R., Queiroz, G.R., Neves, A.K., Carlos, F.M., Souza, F.C., Santos, L.A., & Simoes, R.E.O. (2022). A platform for land use and land cover data integration and trajectory analysis. International Journal of Applied Earth Observations and Geoinformation 106 (2022) 102655.
200.

11 APPENDICES

APPENDICES

1.41. Appendix 1: Geochemical Data.

ID	2018																	
	Location *(Upazila)*	**Depth** *Below Surface* (m)	**pH**	**T (°C)**	**TDS** (mg/L)	**EC** (us/cm)	**ORP**	**Na** (mg/L)	**K** (mg/L)	**Ca** (mg/L)	**Mg** (mg/L)	**Fe** (mg/L)	**Mn** (mg/L)	**HCO_3** (mg/L)	**Cl** (mg/L)	**SO_4** (mg/L)	**NO_3** (mg/L)	**F** (mg/L)
G.18.002	Gazipur Sadar	9	7.4	28.1	352	489	140	197.3	13.9	39.3	14.4	0.2	0.1	312.6	73.9	173.3	0	0.2
G.18.004	Gazipur Sadar	19	7.4	27.4	349	513	140	213.2	12.9	45.8	17.9	0.5	0.3	373.6	79.1	0	0	0.2
G.18.006	Gazipur Sadar	15	8.2	27.7	201	254	94	35	2.4	35.8	14.7	0.1	0	289.8	3.3	0.7	0	0.1
G.18.007	Gazipur Sadar	16	7.8	25.4	168	221	105	38.9	1.7	48.4	22.5	0.1	0.4	251.6	3.6	0.9	0.2	0.2
G.18.008	Gazipur Sadar	25	7.3	27.5	173	286	132	29.6	0.8	21.2	13.7	0.1	0.2	221.1	3.1	1.1	0	0.5
G.18.009	Gazipur Sadar	22	7.4	25.1	485	725	196	30.6	0.8	18.4	13.5	0.1	0.2	251.6	2.7	1	0.3	0.5
G.18.010	Gazipur Sadar	2	7.2	28.9	178	243	98	28	0.8	28.5	14.1	0.2	0.1	221.1	2.2	1	0.3	0.5
G.18.011	Gazipur Sadar	13	7.2	28.9	380	589	98	28.5	0.8	18.8	14.2	0.3	0.2	205.9	2.2	1	0	0.6
G.18.012	Gazipur Sadar	16	7.6	30.1	582	956	182	22.3	0.8	16.3	13.6	0.2	0.1	167.8	2.3	1.3	0.3	0.5
G.18.013	Gazipur Sadar	8	7.6	23.7	450	745	189	23.1	0.6	25.2	13.7	0.2	0.1	190.6	2.8	1.2	0.4	0.6
G.18.015	Gazipur Sadar	11	8.3	28	318	470	175	17.5	0.6	10.8	11.4	1	0.1	137.3	2.5	1.1	0.4	0.6
G.18.016	Gazipur Sadar	13	8.3	25.3	703	983	180	19.3	0.5	22.5	18.5	0.3	0.3	205.9	2.6	0.4	0.2	0.2
G.18.019	Gazipur Sadar	9	8.4	26.5	448	698	105	36.7	1	33.4	21.4	0.2	0.4	198.3	2.4	0.8	0.3	0.3
G.18.020	Gazipur Sadar	10	7.5	27.1	201	301	19	36	1.1	38.1	24.7	0.1	0.5	213.5	2.6	0.8	0.3	0.3
G.18.021	Gazipur Sadar	11	8.4	30.8	274	391	208	32.9	0.9	23.7	17.7	0.2	0.1	228.8	1.5	0.8	0.3	0.4
G.18.023	Gazipur Sadar	16	7.6	27.6	287	413	173	38.1	0.8	55.4	24.2	0.1	0.1	183	27	3	0	0.3
G.18.024	Gazipur Sadar	11	7.4	26.8	979	1306	150	24.6	0.8	27.4	19	0.1	0	221.1	1.6	0.7	0.4	0.5
G.18.025	Gazipur Sadar	17	7.3	26.8	887	1150	3	24.6	0.9	31.8	18.6	0	0	228.8	1.5	0.6	0.4	0.5
G.18.027	Gazipur Sadar	19	7.6	26.9	941	1236	119	30.7	1.1	29.1	23	0.1	0.3	205.9	2.2	0.5	0.3	0.4

ID	2018																	
	Location *(Upazila)*	**Depth** *Below Surface* (m)	**pH**	**T (°C)**	**TDS** (mg/L)	**EC** (us/cm)	**ORP**	**Na** (mg/L)	**K** (mg/L)	**Ca** (mg/L)	**Mg** (mg/L)	**Fe** (mg/L)	**Mn** (mg/L)	**HCO_3** (mg/L)	**Cl** (mg/L)	**SO_4** (mg/L)	**NO_3** (mg/L)	**F** (mg/L)
G.18.028	Gazipur Sadar	21	7.4	23	219	300	154	36.9	1.1	9	11.2	0.4	0.1	0	2.6	0.8	0.3	0.2
G.18.029	Gazipur Sadar	23	7.5	26.5	168	238	213	10	0.9	32.4	20.4	0.1	0.3	0	2.3	0.5	0.3	0.4
G.18.031	Gazipur Sadar	16	7.4	27	550	761	164	30.6	0.6	24.4	18.6	0.2	0.1	190.6	2.7	0.9	0	0.2
G.18.033	Gazipur Sadar	9	7.1	26.8	867	1101	66	13.1	0.6	16.8	14.5	0.1	0.2	152.5	1.4	0.8	0.2	0.3
G.18.034	Gazipur Sadar	8	6.6	27.4	511	687	81	27.4	1.4	39.6	26.4	0.2	0.1	228.8	36.6	4.6	0	0.1
G.18.035	Gazipur Sadar	14	6.6	31.8	249	389	235	12.7	0.9	16.8	15.2	0	0	129.6	8.5	0.4	0	0.1
G.18.036	Gazipur Sadar	17	6.5	27.7	517	764	249	18.3	0.8	24.7	20.7	0.1	0.5	137.3	45.2	10	0	0.1
G.18.037	Gazipur Sadar	12	6.3	26.2	198	296	273	10.8	1.1	11.5	12.1	0	0	76.3	7.9	0.7	0	0.1
G.18.038	Gazipur Sadar	18	6.4	27.3	205	319	303	13.9	1.7	9.2	10.3	0	0	61	16.3	0.2	0	0.1
G.18.040	Gazipur Sadar	11	7.1	27.8	201	313	221	11.2	0.2	9.3	12.4	0	0.2	106.8	2.8	0.6	0	0.3
G.18.042	Gazipur Sadar	19	6.9	26.7	174	287	311	18.5	0.7	18.4	15.6	0	0.2	183	4.1	0.6	0.1	0.3
G.18.043	Gazipur Sadar	22	7.1	28.7	253	389	293	21	0.5	26.3	20.6	0.2	0.2	495.6	2	0.6	0.1	0.3
G.18.044	Gazipur Sadar	15	7.7	26.5	237	316	1	18.4	1.2	27.7	20.9	0.2	0.1	205.9	2.7	0.9	0.2	0.2
G.18.046	Gazipur Sadar	21	6.6	27.2	633	852	348	18.7	0.7	29	17.5	0	0.2	137.3	13.5	0.9	0.3	0.3
G.18.047	Gazipur Sadar	23	6.6	26.3	214	291	250	34.7	9.2	20.1	15.6	1.2	2.5	167.8	31.9	9.1	0	0.2
G.18.048	Kaliakair	21	6.2	26.7	194	293	318	4.9	1.1	26.7	18.3	0	0	183	5.4	1	0.3	0.3
G.18.049	Kaliakair	12	7	26.1	567	756	56	21.3	1.2	17	17.1	1.8	0.1	953.1	3.7	0.7	0.2	0.2
G.18.050	Kaliakair	17	7	25.6	121	160	14	17.2	1.1	13	15.4	0.6	0.5	144.9	5.1	1.1	0.2	0.3
G.18.051	Kaliakair	26	6.9	26.6	215	312	340	13.8	0.6	14.7	14.6	0	0	152.5	4.1	0.8	0.2	0.2
G.18.052	Kaliakair	14	7	26.6	853	1230	335	16.5	0.6	16.6	16.8	0.1	0.2	167.8	6.3	1.3	0.2	0.3
G.18.053	Kaliakair	23	7	26.5	153	243	56	19.4	0.5	13.9	13.5	0.4	0	190.6	2.4	0.8	0.3	0.4
G.18.054	Kaliakair	31	6.9	25.7	243	394	160	19.1	1	21.9	20.1	0.1	0	190.6	4.8	1.1	0.4	0.2
G.18.055	Gazipur Sadar	32	6.1	25.9	113	159	255	6.6	1.1	6	11.2	0.8	0.1	76.3	3.6	0.9	0.1	0.1
G.18.056	Kaliakair	34	6.6	26.4	249	347	331	35.6	1.6	16.5	20.1	0.2	0	137.3	6.2	1.6	0.4	0.3

ID	2018																	
	Location *(Upazila)*	**Depth** *Below Surface* (m)	**pH**	**T (°C)**	**TDS** (mg/L)	**EC** (us/cm)	**ORP**	**Na** (mg/L)	**K** (mg/L)	**Ca** (mg/L)	**Mg** (mg/L)	**Fe** (mg/L)	**Mn** (mg/L)	**HCO_3** (mg/L)	**Cl** (mg/L)	**SO_4** (mg/L)	**NO_3** (mg/L)	**F** (mg/L)
G.18.057	Kaliakair	33	6.8	26.9	213	308	60	18.2	0.7	21.2	17	0.7	0.2	167.8	5.8	1	0.2	0.3
G.18.058	Kaliakair	36	6.4	25.7	243	306	204	10.2	0.6	12.6	14.3	1.8	0.2	99.1	16.1	1.5	0	0.1
G.18.059	Kaliakair	32	6.2	26.3	199	286	332	12.6	1.1	11.2	12.5	0	0	129.6	4.4	0.7	0.3	0.2
G.18.060	Kaliakair	33	6.7	25.9	296	413	302	14.5	0.7	11.1	14	0.1	0	114.4	3.6	2.7	0.2	0
G.18.061	Kaliakair	9	6.8	26.5	93	127	369	8.8	0.8	49.7	13.7	0	0	61	6.5	0.3	0.2	0.2
G.18.062	Kaliakair	6	7.2	26.9	219	343	343	21.3	8.7	22.4	21.2	0	0.2	244	1.7	0.4	0.3	0.3
G.18.063	Kaliakair	3	7.2	27.3	182	291	361	31	2.2	26.3	20.9	0	0	244	2	0.5	0.2	0.4
G.18.064	Sreepur	6	7.1	27.9	249	379	354	30	0.9	26.4	19.3	0.1	0.2	244	2.8	0.4	0.1	0.2
G.18.065	Sreepur	4	6.6	26	106	166	390	6.6	1.4	12.1	12.6	0.1	0	76.3	11.2	0.3	0	0.1
G.18.066	Sreepur	2	6.5	27.2	94	128	374	9	1.3	15.5	13.4	0	0	53.4	7.3	0.4	0	0.1
G.18.067	Sreepur	8	6.4	26.2	169	239	339	8.7	0.6	7	11.6	0	0	76.3	2.7	0.3	0.3	0.1
G.18.068	Sreepur	9	6.7	26.2	143	220	239	16.9	0.6	9.7	15.1	0	0.2	144.9	1.7	0.2	0.3	0.1
G.18.069	Gazipur Sadar	9	6.6	26.8	208	270	318	17.4	0.7	55	20.6	0	0.3	152.5	1.8	0.3	0.3	0.1
G.18.070	Gazipur Sadar	11	6.7	26.5	241	332	216	25.7	0.7	19.3	17.7	0.2	0.1	167.8	11.1	1.4	0.3	0.2
G.18.071	Gazipur Sadar	12	6.8	25.6	143	208	77	18.8	0.7	8.9	10.3	1	0.4	129.6	2.3	1	0	0.3
G.18.072	Sreepur	18	6.6	25.4	156	213	162	18.4	0.8	12	10	1.2	0.4	137.3	2.5	0.4	0.2	0.2
G.18.073	Sreepur	19	6.4	29.3	173	245	71	6.3	0.9	12.1	8.6	3.5	0	61	41.5	1.1	0	0.1
G.18.074	Sreepur	17	6.8	26.8	143	206	304	17.7	0.8	9	10.5	0.1	0.4	129.6	3.5	1	0.2	0.3
G.18.075	Sreepur	13	6.1	28.2	93	152	363	8.4	0.1	6.4	8	0	0	61	15.6	3.5	0.3	0.1
G.18.076	Sreepur	20	6	29.2	79	119	384	5.9	0.8	3	6.4	0.2	0	38.1	8	0.5	0	0.2
G.18.077	Sreepur	21	6.8	26.3	179	254	100	17.3	0.7	15.1	13.1	0.5	0.1	167.8	2.4	1.1	0.3	0.3
G.18.078	Sreepur	23	7.2	27.8	313	427	306	24.6	0.8	31.8	17.5	0.1	0.1	228.8	24.6	9.9	0	0.4
G.18.079	Sreepur	31	6.9	25.5	186	252	206	13.5	0.5	19.1	12	0.6	0.1	152.5	5.1	0.6	0	0.4
G.18.080	Sreepur	12	6.9	27.6	189	278	327	12	0.8	9.2	10.6	0	0	114.4	1.7	0.5	0	0.3

ID	2018																	
	Location *(Upazila)*	**Depth** *Below Surface* (m)	**pH**	**T (°C)**	**TDS** (mg/L)	**EC** (us/cm)	**ORP**	**Na** (mg/L)	**K** (mg/L)	**Ca** (mg/L)	**Mg** (mg/L)	**Fe** (mg/L)	**Mn** (mg/L)	**HCO_3** (mg/L)	**Cl** (mg/L)	**SO_4** (mg/L)	**NO_3** (mg/L)	**F** (mg/L)
G.18.081	Sreepur	17	7.4	27.2	459	608	218	20.4	0.7	21.3	14.7	0.2	0	213.5	3.5	0.6	0	0.5
G.18.082	Sreepur	6	7.6	27	418	685	195	19.6	0.7	13.6	12.8	0.1	0.1	144.9	1.6	1.7	0.3	0.4
G.18.083	Sreepur	7	7.6	27.8	254	325	203	21.2	0.8	25.5	13.9	0.2	0	213.5	2.7	0.8	0.2	0.5
G.18.084	Sreepur	3	7.4	27.5	635	879	256	10.5	0.8	14.4	13.2	0	0	167.8	5.7	1.1	0.3	0.4
G.18.085	Sreepur	9	6.8	27.1	113	160	122	10.5	0.4	7	9.6	1.1	0	99.1	1.1	1.3	0	0.2
G.18.086	Sreepur	8	6.5	27.7	113	183	220	11.8	0.6	3.4	9.2	0.2	0	91.5	2.8	3.6	0	0.1
G.18.087	Sreepur	9	6.4	27.9	271	342	220	14	0.7	23.8	15.4	0.4	0.2	91.5	48.1	1.1	0	0.1
G.18.088	Sreepur	4	7.2	24.5	225	350	220	18.2	0.6	15.7	13.5	0	0	167.8	2.5	0.3	0	0.1
G.18.089	Sreepur	7	7.1	27.5	285	453	190	25.8	0.9	30.9	14.7	0.6	0.1	221.1	2.6	0.2	0	0.2
G.18.090	Sreepur	6	6.8	27.1	640	810	314	18.8	1.4	16.9	12.3	0.2	0	122	2.8	0.4	0	0.1
G.18.091	Kapasia	7	7.9	28	548	757	239	17.4	0.7	18.7	15.1	0	0.2	183	3.6	3.6	0	0.3
G.18.092	Sreepur	4	6.9	25.5	724	973	302	152.6	12.6	58.5	34.7	0.5	0.4	213.5	2.9	71.1	0	0.1
G.18.093	Kapasia	3	7	26.1	341	489	232	21.8	0.9	14.4	15.3	0.1	0	167.8	1.8	0.8	0.3	0.3
G.18.094	Kapasia	9	6.8	25.6	429	579	108	20.3	0.8	12.5	12.1	0.4	0.2	190.6	1.1	1.1	0.3	0.2
G.18.095	Sreepur	10	7.1	27.8	162	263	252	18	0.6	15.5	17.7	0	0	175.4	1.8	0.3	0.3	0.3
G.18.096	Sreepur	32	6.1	27.7	246	393	295	5.1	0.8	0.1	8.3	0	0	45.8	6.4	0.2	0	0.1
G.18.097	Gazipur Sadar	19	6.7	28	345	491	223	3	0.7	0.8	8.4	0	0	61	2.4	0.2	0.3	0.1
G.18.098	Kapasia	11	6.7	23.5	189	256	46	7.8	1.2	15.5	13.4	2.8	0	114.4	12.4	7.7	0	0.1
G.18.099	Kapasia	14	6.3	26.6	146	231	231	8.8	1.9	14.1	12.4	0	0	68.6	18.4	7.1	0	0.1
G.18.100	Kapasia	6	7.1	28	201	317	130	7.4	1.9	19	21.5	1	0.6	205.9	6.8	7	0.2	0.2
G.18.101	Kapasia	16	6.8	28.4	341	463	177	21.1	2.7	21.6	23.1	0.1	1.2	117.4	56.5	15.4	0	0.1
G.18.102	Kapasia	18	6.7	26.6	240	307	117	7.7	0.8	25.7	15.5	0.4	0	149.5	14.5	4.8	0	0.3
G.18.103	Kapasia	6	6.3	26.4	288	376	322	13.2	0.7	8	10.5	0.1	0	114.4	1.4	0.9	0	0.1
G.18.104	Kapasia	3	6.8	24.8	163	243	205	17.8	0.6	14	13.9	1.8	0.2	167.8	1.8	0.9	0	0.3

ID	2018																	
	Location *(Upazila)*	**Depth** *Below Surface* (m)	**pH**	**T (°C)**	**TDS** (mg/L)	**EC** (us/cm)	**ORP**	**Na** (mg/L)	**K** (mg/L)	**Ca** (mg/L)	**Mg** (mg/L)	**Fe** (mg/L)	**Mn** (mg/L)	**HCO_3** (mg/L)	**Cl** (mg/L)	**SO_4** (mg/L)	**NO_3** (mg/L)	**F** (mg/L)
G.18.105	Kapasia	16	7.4	27.5	134	183	164	23.2	0.9	12.8	12.9	0	0	152.5	9.2	1.1	0	0.2
G.18.106	Kapasia	13	7.4	27.4	182	244	164	21.9	0.6	13.6	13.2	0	0	152.5	5.6	0.6	0	0.3
G.18.107	Kapasia	10	7.2	26.8	201	332	160	21.3	0.7	7.9	10.5	0	0	122	4.8	0.5	0	0.4
G.18.108	Kapasia	14	7.9	27.3	127	160	143	22.6	0.7	10	14.4	0	0	167.8	3.3	0.5	0.3	0.2
G.18.109	Kapasia	9	7.5	27.1	174	269	191	23.3	0.6	21.9	17.4	0.4	0.3	183	3.6	0.6	0.3	0.4
G.18.110	Kapasia	6	7.5	26.6	403	513	135	84	0.7	12.6	28	0	0.6	266.9	102.8	5.8	0	0.4
G.18.111	Kapasia	4	7.3	27.1	159	253	166	22.2	0.4	17.8	13.2	0	0.6	213.5	4.4	0.8	0	0.4
G.18.112	Gazipur Sadar	5	7.2	27.1	246	361	170	22.6	0.5	13.5	12.2	0.2	0.1	167.8	13.3	0.8	0	0.4
G.18.113	Gazipur Sadar	9	7.2	26.8	227	326	194	30.3	1.1	5.6	9.5	0.7	0.1	183	1.9	0.2	0.3	0.3
G.18.114	Gazipur Sadar	15	7.5	27.5	562	736	154	243	0.7	5.5	10.4	0.2	0.1	381.3	262.9	16.3	0	0.6
G.18.115	Gazipur Sadar	16	7.4	27.1	394	515	151	25.8	0.9	22.3	13	0.8	0	221.1	20	0.5	0	0.4
G.18.116	Gazipur Sadar	14	7.4	26.7	364	526	157	25.3	1.4	26.2	13	1.2	0.1	213.5	6	0.2	0	0.3
G.18.117	Kaliganj	7	7.5	26.7	236	371	136	31.5	1.2	84.6	23.7	0.6	0	259.3	3.2	0.7	0.1	0.1
G.18.118	Kaliganj	9	7.6	27	216	313	187	36.2	1.1	20.1	25.4	3.4	0	305	4.3	0.6	0	0.1
G.18.119	Kaliganj	10	7.7	26.3	281	366	143	24.4	0.8	22.7	20.7	0.2	0	274.5	1.5	0.8	0.3	0.5
G.18.120	Kaliganj	12	7.1	26.8	343	469	17.1	26.9	1.1	23	23.4	1.2	0.2	175.4	25.8	6.9	0	0.2
G.18.121	Kaliganj	9	7.1	27.2	144	234	198	22.4	0.7	33.1	17	0.1	0	205.9	3.6	0.4	0.3	0.2
G.18.122	Kaliganj	19	7.8	27	197	269	141	25.4	1.1	16.3	20.5	0.9	0	205.9	17.5	0.9	0	0.3
G.18.123	Kaliganj	16	7.4	27.3	185	240	204	23.9	0.8	24.3	21.4	0.1	0	244	8.9	0.7	0	0.4
G.18.124	Kaliganj	21	4.7	26.9	224	317	130	27.4	0.4	26.4	22.5	0	0.1	213.5	2	0.5	0.3	0.5
G.18.125	Kaliganj	23	7.4	27.3	225	310	151	27.8	0.5	38.3	22.1	0	0.1	228.8	2.1	1	0.3	0.5
G.18.126	Kaliganj	17	6.8	27.3	991	1430	194	9.5	1.1	36.1	10.3	0	0	91.5	1.7	0.8	0	0.2
G.18.127	Sreepur	31	6.7	26.8	680	865	156	12.4	1.1	2.6	13.2	0.1	0	99.1	6.2	0.4	0	0.1
G.18.128	Gazipur Sadar	33	6.5	26.7	977	1346	227	26.1	1.2	10.7	16.4	0.1	0	106.8	1.8	0.7	0.1	0.1

ID	2018																	
	Location *(Upazila)*	**Depth** *Below Surface* (m)	**pH**	**T (°C)**	**TDS** (mg/L)	**EC** (us/cm)	**ORP**	**Na** (mg/L)	**K** (mg/L)	**Ca** (mg/L)	**Mg** (mg/L)	**Fe** (mg/L)	**Mn** (mg/L)	**HCO_3** (mg/L)	**Cl** (mg/L)	**SO_4** (mg/L)	**NO_3** (mg/L)	**F** (mg/L)
G.18.129	Gazipur Sadar	17	6.7	27.2	721	956	194	7.3	0.7	14.6	13	1.4	0	76.3	6	0.5	0	0.1
G.18.130	Gazipur Sadar	33	9.7	27.2	182	236	198	11.1	0.5	7.4	12.3	0.1	0	99.1	4.8	1.3	0.4	0.4
G.18.131	Gazipur Sadar	27	6.5	27	243	364	230	11.4	1	9.3	14.5	0.1	0	106.8	16.3	1	0.4	0.3
G.18.132	Gazipur Sadar	11	6.6	25.5	208	289	186	6.8	0.6	7.6	12.5	8.1	0.1	122	15.7	0.8	0.4	0.3
G.18.133	Gazipur Sadar	29	6.7	27.6	299	411	195	190	14.4	31	19	1.2	0.3	205.9	31.8	0.9	0.4	0.2
G.18.134	Gazipur Sadar	33	6.6	26.3	279	363	201	18.9	1.3	26.8	21.5	0	0.1	213.5	32	2.1	1.5	1.4
G.18.135	Gazipur Sadar	36	6.3	25.9	162	243	126	9.6	5.1	3.1	11	0	0	76.3	4.5	3.4	1.6	1.2
G.18.136	Gazipur Sadar	31	6.3	26.7	258	364	216	10.8	1.2	3.4	10.1	0.1	0	83.9	3	1.8	1.4	1.6
G.18.137	Gazipur Sadar	28	9.8	25.7	163	228	209	9.9	0.7	3.5	11.8	0.1	0	76.3	6.6	2	1.6	1.8
G.18.138	Gazipur Sadar	29	6.3	27.4	172	244	199	9.8	1.1	5.8	11	0	0	76.3	8.5	2.4	2	2.2
G.18.139	Gazipur Sadar	26	6.8	26.6	188	265	205	9.5	1.1	11	12.4	0.1	0	114.4	3.4	2.8	2	2.3

ID	2019					2020					2021				
	pH	T (°C)	TDS (mg/L)	EC (us/cm)	ORP	pH	T (°C)	TDS (mg/L)	EC (us/cm)	ORP	pH	T (°C)	TDS (mg/L)	EC (us/cm)	ORP
G.001	5.7	20.9	403	606	97.0	5.8	21.3	407	887	126.1	5.9	21.7	411	514	163.9
G.002	6.0	16.0	740	1181	123.0	6.0	16.3	747	1849	159.9	6.2	16.6	755	2034	207.9
G.003	6.5	20.0	913	1280	136.0	6.6	20.4	922	913	176.8	6.7	20.8	1350	1985	229.8
G.004	7.0	21.1	200	320	31.0	7.1	21.5	202	1034	40.3	7.2	21.9	204	1137	52.4
G.005	6.7	21.8	493	784	180.0	6.7	22.2	498	1192	234.0	6.8	22.7	503	1312	304.2
G.006	6.6	23.4	212	324	89.0	6.7	23.9	214	906	115.7	6.8	24.3	216	997	150.4
G.007	7.3	17.2	135	220	415.0	7.4	17.5	136	298	539.5	7.5	17.9	138	328	701.4
G.008	7.1	18.1	253	371	85.0	7.2	18.5	256	557	110.5	7.4	18.8	258	612	143.7
G.009	7.2	19.6	104	164	86.0	7.3	20.0	105	231	111.8	7.5	20.4	106	254	145.3
G.010	7.0	18.0	361	540	256.0	7.0	18.4	365	1892	332.8	7.2	18.7	368	2081	432.6
G.011	7.3	17.2	210	310	75.0	7.4	17.5	212	1288	97.5	7.5	17.9	214	1417	126.8
G.012	7.2	19.4	835	1065	57.0	7.3	19.8	1243	1955	74.1	7.4	20.2	852	2150	96.3
G.013	7.1	18.1	437	706	65.0	7.2	18.5	441	997	84.5	7.4	18.8	446	1096	109.9
G.014	7.2	19.6	253	410	85.0	7.3	20.0	256	781	110.5	7.5	20.4	258	859	143.7
G.015	7.0	20.1	104	154	86.0	7.1	20.5	105	705	111.8	7.2	20.9	106	776	145.3
G.016	7.2	23.5	320	487	48.0	7.2	24.0	323	646	62.4	7.4	24.4	326	710	81.1
G.017	7.3	28.0	291	454	56.0	7.3	28.6	294	367	72.8	7.5	29.1	297	404	94.6
G.018	7.3	20.9	167	232	48.0	7.4	21.3	169	255	62.4	7.5	21.7	170	281	81.1
G.019	7.1	23.5	115	158	75.0	7.2	24.0	116	284	97.5	7.3	24.4	117	312	126.8
G.020	7.3	19.1	129	164	95.0	7.4	19.5	130	1245	123.5	7.5	19.9	132	1370	160.6
G.021	7.4	20.7	568	798	8.0	7.5	21.1	574	141	10.4	7.6	21.5	579	155	13.5
G.022	6.8	16.9	84	117	46.0	6.9	17.2	78	125	59.8	7.0	17.6	345	551	77.7
G.023	6.4	18.7	231	334	102.0	6.5	19.1	233	367	132.6	6.6	19.5	236	404	172.4

ID	2019					2020					2021				
	pH	T (°C)	TDS (mg/L)	EC (us/cm)	ORP	pH	T (°C)	TDS (mg/L)	EC (us/cm)	ORP	pH	T (°C)	TDS (mg/L)	EC (us/cm)	ORP
G.024	6.5	17.4	167	269	91.0	6.6	17.7	169	296	118.3	6.7	18.1	170	325	153.8
G.025	6.3	22.7	134	174	116.0	6.4	23.2	135	191	150.8	6.5	23.6	137	211	196.0
G.026	6.0	21.3	87	127	43.0	6.1	21.7	88	209	55.9	6.2	22.2	146	230	72.7
G.027	5.5	23.9	95	130	110.0	5.5	24.4	96	143	143.0	5.6	24.9	115	157	185.9
G.028	6.2	24.9	1065	1440	16.4	6.2	25.4	571	1584	21.3	6.3	25.9	1096	1742	27.7
G.029	6.5	22.5	220	329	121.0	6.6	23.0	222	563	157.3	6.7	23.4	224	620	204.5
G.030	6.6	22.8	484	742	141.0	6.7	23.3	489	816	183.3	6.8	23.7	494	898	238.3
G.031	6.4	25.8	248	389	361.0	6.5	26.3	250	538	469.3	6.6	26.8	252	592	610.1
G.032	6.6	22.5	359	512	354.0	6.6	23.0	363	783	460.2	6.8	23.4	366	862	598.3
G.033	6.5	22.3	221	309	332.0	6.6	22.7	223	479	431.6	6.7	23.2	225	526	561.1
G.034	6.6	23.6	325	424	213.0	6.7	24.1	328	707	276.9	6.8	24.6	331	778	360.0
G.035	6.8	23.3	219	319	464.4	6.8	23.8	221	474	603.7	7.0	24.2	223	522	784.8
G.036	6.7	24.2	459	659	517.6	6.8	24.7	464	1003	672.9	6.9	25.2	468	1104	874.7
G.037	6.5	22.7	448	690	478.0	6.6	23.2	452	979	621.4	6.7	23.6	457	1077	807.8
G.038	6.3	23.7	360	459	323.0	6.4	24.2	363	784	419.9	6.5	24.7	367	863	545.9
G.039	6.9	23.0	247	346	677.2	7.0	23.5	249	536	880.4	7.1	23.9	251	589	1144.5
G.040	6.7	22.7	271	371	730.4	6.7	23.2	274	590	949.5	6.9	23.6	276	649	1234.4
G.041	6.9	27.0	575	945	312.0	7.0	27.5	581	1040	405.6	7.1	28.1	587	1143	527.3
G.042	6.6	23.4	310	413	624.0	6.6	23.9	313	674	811.2	6.8	24.3	316	742	1054.6
G.043	6.3	23.0	301	410	436.0	6.4	23.5	304	656	566.8	6.5	23.9	307	721	736.8
G.044	6.3	23.1	360	529	570.8	6.4	23.6	364	785	742.0	6.5	24.0	367	864	964.7
G.045	6.8	22.6	274	424	141.0	6.8	23.1	276	595	183.3	7.0	23.5	279	655	238.3
G.046	7.0	22.5	160	254	204.0	7.1	23.0	161	322	265.2	7.2	23.4	163	355	344.8
G.047	7.1	22.9	141	231	361.0	7.2	23.4	142	304	469.3	7.4	23.8	144	334	610.1
G.048	7.3	20.3	625	839	67.0	7.4	20.7	631	1367	87.1	7.5	21.1	637	1504	113.2

ID	2019					2020					2021				
	pH	T (°C)	TDS (mg/L)	EC (us/cm)	ORP	pH	T (°C)	TDS (mg/L)	EC (us/cm)	ORP	pH	T (°C)	TDS (mg/L)	EC (us/cm)	ORP
G.049	6.4	22.9	143	231	160.0	6.4	23.4	144	285	208.0	6.6	23.8	145	313	270.4
G.050	6.4	22.4	162	231	354.0	6.4	22.8	164	343	460.2	6.6	23.3	165	378	598.3
G.051	6.6	22.9	155	245	143.0	6.7	23.4	157	328	185.9	6.8	23.8	158	361	241.7
G.052	7.1	23.3	251	324	191.0	7.2	23.8	253	538	248.3	7.3	24.2	256	592	322.8
G.053	7.3	22.0	263	369	164.0	7.4	22.4	265	564	213.2	7.5	22.9	268	621	277.2
G.054	6.5	22.3	133	218	110.0	6.6	22.7	134	279	143.0	6.7	23.2	136	307	185.9
G.055	6.4	22.4	117	158	82.0	6.5	22.8	118	243	106.6	6.6	23.3	119	267	138.6
G.056	6.3	22.3	156	256	164.0	6.4	22.7	158	315	213.2	6.5	23.2	159	346	277.2
G.057	7.3	23.2	254	325	199.0	7.3	23.7	257	798	258.7	7.5	24.1	259	877	336.3
G.058	7.0	23.0	129	198	183.3	7.0	23.5	130	267	238.3	7.2	23.9	131	294	309.8
G.059	6.5	23.0	308	506	198.0	6.6	23.5	311	648	257.4	6.7	23.9	314	713	334.6
G.060	7.1	22.9	397	512	200.8	7.2	23.4	401	1052	261.1	7.3	23.8	405	1157	339.4
G.061	7.4	22.7	343	498	132.0	7.5	23.2	346	820	171.6	7.7	23.6	349	901	223.1
G.062	6.4	22.6	248	401	213.0	6.5	23.1	250	517	276.9	6.6	23.5	253	569	360.0
G.063	6.5	23.0	396	583	253.3	6.5	23.5	400	1081	329.3	6.6	23.9	404	1189	428.1
G.064	7.3	23.0	258	328	235.8	7.4	23.5	261	552	306.6	7.5	23.9	263	607	398.6
G.065	6.9	23.6	249	358	270.8	6.9	24.1	251	768	352.1	7.1	24.6	253	845	457.7
G.066	6.2	22.5	160	251	305.8	6.3	23.0	161	331	397.6	6.4	23.4	163	364	516.9
G.067	6.4	23.0	205	391	88.0	6.4	23.5	207	430	114.4	6.6	23.9	209	473	148.7
G.068	6.6	22.8	245	463	323.3	6.6	23.3	247	509	420.3	6.8	23.7	249	560	546.4
G.069	6.4	23.1	220	413	34.0	6.4	23.6	222	454	44.2	6.6	24.0	224	500	57.5
G.070	6.8	23.2	634	1306	358.3	6.9	23.7	640	1437	465.8	7.0	24.1	647	1580	605.6
G.071	7.1	21.0	562	1150	213.0	7.2	21.4	568	1265	276.9	7.3	21.8	573	1392	360.0
G.072	7.3	20.9	698	1236	177.0	7.4	21.3	705	1360	230.1	7.5	21.7	712	1496	299.1
G.073	7.1	20.6	150	300	98.0	7.2	21.0	152	330	127.4	7.4	21.4	153	363	165.6

ID	2019					2020					2021				
	pH	T (°C)	TDS (mg/L)	EC (us/cm)	ORP	pH	T (°C)	TDS (mg/L)	EC (us/cm)	ORP	pH	T (°C)	TDS (mg/L)	EC (us/cm)	ORP
G.074	7.3	18.0	119	238	99.0	7.4	18.4	120	262	128.7	7.5	18.7	121	288	167.3
G.075	7.0	25.3	136	273	58.0	7.0	25.8	137	300	75.4	7.2	26.3	139	330	98.0
G.076	7.0	20.4	393	761	163.0	7.1	20.8	396	837	211.9	7.2	21.2	400	921	275.5
G.077	6.7	21.6	596	1101	298.0	6.8	22.0	602	1211	387.4	6.9	22.5	608	1332	503.6
G.078	7.4	23.2	327	1587	267.0	7.5	23.7	330	1746	347.1	7.7	24.1	333	1920	451.2
G.079	7.3	21.3	212	389	11.0	7.4	21.7	214	428	14.3	7.5	22.2	216	471	18.6
G.080	7.3	20.9	168	336	77.0	7.4	21.3	170	370	100.1	7.5	21.7	171	407	130.1
G.081	7.1	20.6	150	300	98.0	7.2	21.0	152	330	127.4	7.4	21.4	153	363	165.6
G.082	7.3	18.0	119	238	99.0	7.4	18.4	120	262	128.7	7.5	18.7	121	288	167.3
G.083	7.0	25.3	136	273	58.0	7.0	25.8	137	300	75.4	7.2	26.3	139	330	98.0
G.084	6.9	22.3	178	313	113.0	7.0	22.7	179	344	146.9	7.1	23.2	181	379	191.0
G.085	6.3	23.9	168	293	301.0	6.4	24.4	169	322	391.3	6.5	24.9	171	355	508.7
G.086	7.1	20.4	185	343	211.0	7.2	20.8	186	377	274.3	7.3	21.2	188	415	356.6
G.087	6.8	20.9	159	291	351.0	6.9	21.3	160	320	456.3	7.0	21.7	162	352	593.2
G.088	7.2	21.5	193	379	360.0	7.3	21.9	194	417	468.0	7.4	22.4	196	459	608.4
G.089	6.9	26.4	244	453	9.0	7.0	26.9	246	498	11.7	7.1	27.5	248	548	15.2
G.090	6.3	22.0	434	810	111.0	6.3	22.4	438	891	144.3	6.5	22.9	443	980	187.6
G.091	5.4	28.0	91	183	168.0	5.4	28.6	92	201	218.4	5.5	29.1	93	221	283.9
G.092	5.8	22.2	122	244	163.0	5.8	22.6	123	268	211.9	6.0	23.1	124	295	275.5
G.093	4.9	18.4	166	332	188.0	5.0	18.8	168	365	244.4	5.1	19.1	169	402	317.7
G.094	5.3	26.0	84	130	172.0	5.3	26.5	96	143	223.6	5.4	27.1	115	157	290.7
G.095	5.3	24.7	85	169	188.0	5.3	25.2	86	186	244.4	5.4	25.7	87	204	317.7
G.096	5.7	19.3	97	134	180.0	5.8	19.7	106	147	234.0	5.9	20.1	115	162	304.2
G.097	5.6	23.5	85	169	21.0	5.7	24.0	86	186	27.3	5.8	24.4	87	204	35.5
G.098	5.7	25.3	134	240	111.0	5.8	25.8	135	264	144.3	5.9	26.3	137	290	187.6

ID	2019					2020					2021				
	pH	T (°C)	TDS (mg/L)	EC (us/cm)	ORP	pH	T (°C)	TDS (mg/L)	EC (us/cm)	ORP	pH	T (°C)	TDS (mg/L)	EC (us/cm)	ORP
G.099	6.3	22.0	91	269	168.0	6.3	22.4	92	296	218.4	6.5	22.9	93	325	283.9
G.100	5.4	28.0	122	183	163.0	5.4	28.6	123	201	211.9	5.5	29.1	124	221	275.5
G.101	5.8	22.2	166	244	188.0	5.8	22.6	168	268	244.4	6.0	23.1	169	295	317.7
G.102	4.9	18.4	208	332	172.0	5.0	18.8	247	365	223.6	5.1	19.1	296	402	290.7
G.103	5.3	26.0	85	130	188.0	5.3	26.5	86	143	244.4	5.4	27.1	97	157	317.7
G.104	5.3	24.7	72	119	180.0	5.3	25.2	126	186	234.0	5.4	25.7	126	204	304.2
G.105	5.7	19.3	85	134	21.0	5.8	19.7	86	147	27.3	5.9	20.1	102	162	35.5
G.106	5.6	23.5	120	169	18.0	5.7	24.0	121	186	23.4	5.8	24.4	122	204	30.4
G.107	5.7	25.3	181	240	94.0	5.8	25.8	183	264	122.2	5.9	26.3	185	290	158.9
G.108	6.4	20.5	86	142	113.0	6.5	20.9	268	398	146.9	6.6	21.3	315	438	191.0
G.109	6.5	24.8	155	117	88.0	6.6	25.3	97	129	114.4	6.7	25.8	85	142	148.7
G.110	6.2	24.6	78	310	126.0	6.2	25.1	79	341	163.8	6.3	25.6	235	375	212.9
G.111	5.3	25.5	198	156	130.0	5.4	26.0	200	172	169.0	5.5	26.5	202	189	219.7
G.112	6.1	23.4	159	265	215.0	6.2	23.9	160	292	279.5	6.3	24.3	162	321	363.4
G.113	6.6	20.6	209	396	113.0	6.7	21.0	211	436	146.9	6.8	21.4	213	479	191.0
G.114	6.1	24.1	167	287	89.0	6.2	24.6	168	316	115.7	6.3	25.1	170	347	150.4
G.115	5.8	23.3	214	389	114.0	5.9	23.8	216	428	148.2	6.0	24.2	218	471	192.7
G.116	6.7	20.6	182	316	125.0	6.8	21.0	184	348	162.5	6.9	21.4	186	382	211.3
G.117	6.4	18.8	164	326	117.0	6.5	19.2	166	359	152.1	6.6	19.6	167	394	197.7
G.118	6.5	21.0	401	852	119.0	6.5	21.4	405	937	154.7	6.6	21.8	409	1031	201.1
G.119	6.6	21.8	145	291	99.0	6.7	22.2	146	320	128.7	6.8	22.7	148	352	167.3
G.120	6.5	25.0	328	756	47.0	6.6	25.5	331	832	61.1	6.7	26.0	335	915	79.4
G.121	5.8	25.0	80	160	72.0	5.9	25.5	81	176	93.6	6.0	26.0	124	194	121.7
G.122	6.5	24.0	189	312	67.0	6.6	24.5	191	343	87.1	6.7	25.0	193	378	113.2
G.123	6.3	24.5	813	1670	213.0	6.4	25.0	821	1837	276.9	6.5	25.5	829	2021	360.0

ID	2019					2020					2021				
	pH	T (°C)	TDS (mg/L)	EC (us/cm)	ORP	pH	T (°C)	TDS (mg/L)	EC (us/cm)	ORP	pH	T (°C)	TDS (mg/L)	EC (us/cm)	ORP
G.124	6.3	21.8	76	143	165.0	6.4	22.2	118	157	214.5	6.5	22.7	112	173	278.9
G.125	6.7	22.6	210	394	102.0	6.8	23.1	212	433	132.6	6.9	23.5	214	477	172.4
G.126	6.3	22.0	1067	1777	117.0	6.4	22.4	166	175	152.1	6.5	22.9	167	192	197.7
G.127	6.4	18.8	176	326	119.0	6.5	19.2	178	359	154.7	6.6	19.6	180	394	201.1
G.128	6.5	21.0	145	352	99.0	6.5	21.4	146	387	128.7	6.6	21.8	148	426	167.3
G.129	6.6	21.8	66	291	47.0	6.7	22.2	214	320	61.1	6.8	22.7	232	352	79.4
G.130	6.5	25.0	80	132	72.0	6.6	25.5	81	145	93.6	6.7	26.0	116	160	121.7
G.131	5.8	25.0	187	160	197.0	5.9	25.5	189	176	256.1	6.0	26.0	191	194	332.9
G.132	6.6	25.0	92	136	113.0	6.7	25.5	93	150	146.9	6.8	26.0	104	165	191.0
G.133	6.2	25.7	257	515	51.0	6.3	26.2	260	567	66.3	6.4	26.7	262	623	86.2
G.134	6.4	22.4	263	526	49.0	6.5	22.8	266	579	63.7	6.6	23.3	268	636	82.8
G.135	6.6	21.4	185	371	88.0	6.7	21.8	187	408	114.4	6.8	22.3	189	449	148.7
G.136	6.7	23.3	156	313	19.0	6.7	23.8	158	344	24.7	6.9	24.2	159	379	32.1
G.137	6.6	21.2	183	366	64.0	6.6	21.6	185	403	83.2	6.8	22.1	187	443	108.2
G.138	5.8	25.0	304	608	47.0	5.9	25.5	307	669	61.1	6.0	26.0	310	736	79.4
G.139	6.1	24.5	343	685	25.0	6.2	25.0	346	754	32.5	6.3	25.5	350	829	42.3
G.140	6.5	25.7	340	879	94.0	6.5	26.2	343	967	122.2	6.7	26.7	347	1064	158.9
G.141	6.3	25.5	92	183	64.0	6.4	26.0	93	201	83.2	6.5	26.5	134	221	108.2
G.142	6.7	20.5	257	515	24.0	6.8	20.9	260	567	31.2	6.9	21.3	262	623	40.6
G.143	6.2	25.7	263	526	51.0	6.3	26.2	266	579	66.3	6.4	26.7	268	636	86.2
G.144	6.4	22.4	185	371	49.0	6.5	22.8	187	408	63.7	6.6	23.3	189	449	82.8
G.145	6.6	21.4	156	313	88.0	6.7	21.8	158	344	114.4	6.8	22.3	159	379	148.7

1.42. Appendix 2: Ionic Balance acceptance of the samples analyzed.

Ionic Balance Acceptance Criteria	
TA (meq/l)	Acceptable difference
0 - 3.0	± 0.2 %
3.0 - 10.0	± 2 %
10 - 800	± 5 %

The analytical precision of the ions analyzed was determined by calculating the normalized ionic charge balance error

ID	TA	Ionic Balance
	meq/l	%
G.18.02	11.2	-3.97
G.18.04	13.4	-0.01
G.18.06	4.9	3.10
G.18.07	6.3	1.87
G.18.08	3.8	3.56
G.18.09	4.2	11.18
G.18.10	3.7	-1.12
G.18.11	3.5	1.46
G.18.12	3.0	0.28
G.18.13	3.3	-2.24
G.18.15	2.4	2.34
G.18.16	3.5	-0.78
G.18.18	8.4	1.49
G.18.19	5.4	2.74
G.18.20	5.6	0.54
G.18.21	3.9	-2.82
G.18.22	4.2	-3.13
G.18.23	5.8	-4.90
G.18.24	3.8	-2.79
G.18.25	3.9	-4.33
G.18.27	4.5	-2.80
G.18.28	3.1	1.18
G.18.29	4.1	4.19
G.18.30	5.6	-1.53
G.18.31	4.3	2.16
G.18.33	2.6	0.11
G.18.34	5.0	-4.05

ID	TA	Ionic Balance
	meq/l	%
G.18.35	2.4	-5.31
G.18.36	3.8	-0.23
G.18.37	2.0	-1.85
G.18.38	1.9	-2.27
G.18.39	3.5	-2.75
G.18.40	1.9	-1.78
G.18.48	3.2	1.76
G.18.62	4.1	0.76
G.18.63	4.4	-0.56
G.18.64	4.5	2.95
G.18.89	3.7	-2.61
G.18.90	2.7	-0.43
G.18.105	2.8	1.29
G.18.106	2.7	-0.72
G.18.107	2.3	1.35
G.18.108	2.9	3.45
G.18.109	3.4	-2.11
G.18.121	4.1	0.64
G.18.122	3.9	2.91
G.18.123	4.3	2.92
G.18.124	4.4	0.18
G.18.125	4.7	-3.11
G.18.126	2.9	-3.62
G.18.127	1.8	0.79
G.18.128	2.8	-3.97
G.18.129	2.2	0.45
G.18.130	1.8	-1.92

ID	TA	Ionic Balance
	meq/l	%
G.18.131	2.3	1.71
G.18.132	2.2	0.63
G.18.133	12.3	2.01
G.18.134	3.9	-0.34
G.18.135	1.5	-2.22
G.18.136	1.6	3.26
G.18.139	2.2	3.98
G.18.41	2.4	4.24
G.18.42	3.2	2.23
G.18.43	4.2	3.15
G.18.44	3.8	-2.08
G.18.45	3.8	3.44
G.18.46	3.7	-0.75
G.18.47	3.9	-4.29
G.18.49	3.8	6.14
G.18.50	2.6	-2.22
G.18.51	2.7	1.95
G.18.52	3.0	0.57
G.18.53	2.7	0.99
G.18.54	3.3	-4.47
G.18.55	1.5	-3.29
G.18.56	4.5	4.71
G.18.110	7.4	5.60
G.18.111	3.1	1.45
G.18.112	2.7	-0.53
G.18.113	2.5	0.44
G.18.114	12.0	1.25

ID	TA	Ionic Balance
	meq/l	%
G.18.115	3.2	-2.28
G.18.116	3.7	1.50
G.18.117	7.4	-1.58
G.18.118	5.1	2.59
G.18.119	3.6	-4.60
G.18.81	3.1	-0.85
G.18.82	2.5	-1.42
G.18.84	2.3	-0.46
G.18.86	1.4	-3.77
G.18.91	3.3	4.65
G.18.92	12.1	-2.85
G.18.93	2.9	-1.46
G.18.94	2.7	2.60
G.18.95	2.9	-1.35
G.18.96	0.9	0.66
G.18.97	0.9	-0.33
G.18.98	2.4	0.11
G.18.99	2.2	0.78
G.18.100	3.1	-0.60
G.18.101	3.8	-2.27
G.18.102	3.0	1.29
G.18.103	2.0	2.44
G.18.104	2.8	1.74
G.18.57	3.3	-0.02
G.18.58	2.2	-2.69
G.18.59	2.3	2.63
G.18.60	2.2	-2.66

ID	TA	Ionic Balance
	meq/l	%
G.18.61	4.2	2.26
G.18.65	1.9	-2.38
G.18.66	2.1	-4.77
G.18.67	1.7	1.11
G.18.68	2.4	-0.92
G.18.69	5.6	3.14
G.18.70	3.4	-1.75
G.18.71	2.2	0.65
G.18.72	2.3	0.48
G.18.73	1.9	2.78
G.18.74	2.3	3.37
G.18.75	1.3	-1.00
G.18.76	1.3	-5.05
G.18.77	0.9	4.65
G.18.78	2.9	3.97
G.18.79	4.5	2.02
G.18.80	2.7	2.03
G.18.83	2.0	3.70
G.18.85	3.6	0.94
G.18.87	1.7	3.59
G.18.88	3.3	3.83
G.18.120	2.9	4.41
G.18.137	4.8	0.81
G.18.138	1.6	3.71

1.43. Appendix 3: Computation of WQI for individual groundwater samples.

ID	Quality Rating (qn)														Σ (qn*Wn)	WQI
	pH	EC	TDS	Na	K	Ca	Mg	Fe	Mn	HCO_3	Cl	SO_4	NO_3	F		
G.18.02	86.59	60.60	15.20	98.65	115.56	52.37	41.17	196.00	109.00	52.10	12.32	43.33	0.00	16.87	144.66	144.66
G.18.04	87.06	59.40	14.90	106.61	107.72	61.01	51.06	513.00	270.00	62.27	13.19	0.00	0.00	16.51	368.45	368.45
G.18.06	96.47	82.60	20.10	17.50	20.21	47.75	41.89	64.00	41.00	48.29	0.55	0.17	0.00	12.76	50.48	50.48
G.18.07	92.00	72.40	18.10	19.46	14.41	64.53	64.34	106.00	356.00	41.94	0.60	0.22	1.98	16.68	217.82	217.82
G.18.08	85.88	65.00	16.30	14.80	6.28	28.31	39.17	79.00	197.00	36.85	0.52	0.28	0.00	49.53	132.13	132.13
G.18.09	87.41	73.60	18.50	15.30	6.63	24.59	38.51	89.00	231.00	41.94	0.45	0.24	3.11	47.01	152.64	152.64
G.18.10	84.94	112.00	28.00	14.02	6.51	37.96	40.17	188.00	83.00	36.85	0.37	0.25	3.32	52.73	129.97	129.97
G.18.11	84.94	112.00	28.00	14.26	7.08	25.01	40.60	330.00	179.00	34.31	0.37	0.26	0.00	59.98	241.72	241.72
G.18.12	89.18	63.40	18.20	11.13	6.82	21.72	38.97	157.00	133.00	27.96	0.39	0.32	3.48	51.56	138.81	138.81
G.18.13	89.65	59.00	15.00	11.53	4.90	33.55	39.09	209.00	140.00	31.77	0.47	0.31	3.84	56.63	166.68	166.68
G.18.15	97.29	47.20	11.80	8.75	5.05	14.43	32.69	1048.00	132.00	22.88	0.41	0.28	4.02	62.08	556.06	556.06
G.18.16	98.00	41.00	10.30	9.65	4.11	29.99	52.94	321.00	313.00	34.31	0.43	0.10	1.70	17.47	298.34	298.34
G.18.18	91.18	40.40	10.00	22.80	11.20	94.79	88.40	101.00	514.00	33.04	0.52	0.42	1.83	17.70	289.54	289.54
G.18.19	99.06	59.60	14.80	18.33	8.52	44.56	61.09	150.00	362.00	33.04	0.41	0.19	3.39	32.11	241.96	241.96
G.18.20	88.24	40.60	10.10	18.01	9.03	50.76	70.51	129.00	495.00	35.58	0.44	0.21	2.77	32.17	294.36	294.36
G.18.21	99.06	109.60	27.40	16.43	7.22	31.59	50.46	155.00	69.00	38.13	0.26	0.20	2.75	37.73	107.34	107.34
G.18.22	86.59	164.60	41.10	16.64	6.23	35.08	58.74	142.00	49.00	41.94	0.22	0.20	3.30	37.81	91.85	91.85
G.18.23	89.65	55.20	13.70	19.04	6.51	73.80	69.11	114.00	109.00	30.50	4.50	0.74	0.00	31.52	106.56	106.56
G.18.24	87.53	70.00	17.90	12.29	6.77	36.59	54.23	62.00	35.00	36.85	0.27	0.17	3.65	53.47	48.56	48.56
G.18.25	86.12	114.80	28.70	12.31	7.75	42.41	53.09	38.00	43.00	38.13	0.24	0.14	3.60	51.85	40.99	40.99
G.18.27	89.18	96.60	24.10	15.37	9.31	38.84	65.80	58.00	273.00	34.31	0.36	0.12	3.26	39.46	157.51	157.51
G.18.28	87.59	88.60	21.90	18.44	9.47	11.99	32.09	409.00	86.00	0.00	0.44	0.19	3.44	17.65	233.20	233.20
G.18.29	88.35	85.20	21.30	4.99	7.61	43.20	58.31	122.00	294.00	0.00	0.39	0.12	2.96	41.09	197.36	197.36

ID	Quality Rating (qn)														Σ (qn*Wn)	WQI
	pH	EC	TDS	Na	K	Ca	Mg	Fe	Mn	HCO_3	Cl	SO_4	NO_3	F		
G.18.30	86.24	109.60	27.40	15.27	4.14	62.44	68.11	2662.00	181.00	41.94	1.79	0.99	2.12	78.10	1335.50	1335.50
G.18.31	87.41	61.00	15.30	15.28	4.80	32.57	53.26	168.00	133.00	31.77	0.45	0.21	0.00	24.28	142.68	142.68
G.18.33	83.53	44.00	10.90	6.56	4.94	22.41	41.31	51.00	224.00	25.42	0.23	0.20	2.16	26.51	130.57	130.57
G.18.34	77.65	112.40	28.10	13.70	11.64	52.77	75.29	210.00	85.00	38.13	6.10	1.15	0.00	10.42	139.24	139.24
G.18.35	77.41	50.20	12.60	6.34	7.30	22.44	43.34	35.00	45.00	21.60	1.42	0.11	0.00	14.42	38.67	38.67
G.18.36	76.00	88.00	21.70	9.17	6.66	32.93	59.09	76.00	534.00	22.88	7.53	2.51	0.00	6.19	286.47	286.47
G.18.37	73.76	39.00	9.80	5.40	9.32	15.31	34.49	49.00	32.00	12.71	1.32	0.17	0.00	12.49	39.02	39.02
G.18.38	74.82	42.00	10.50	6.96	13.83	12.21	29.46	17.00	35.00	10.17	2.72	0.05	0.00	12.13	25.44	25.44
G.18.39	81.41	68.00	17.00	11.54	5.76	30.36	51.26	1475.00	91.00	34.31	0.51	0.20	0.00	21.63	734.84	734.84
G.18.40	83.65	34.40	8.20	5.62	1.67	12.36	35.43	39.00	232.00	17.79	0.47	0.14	0.00	26.92	128.68	128.68
G.18.48	73.41	34.00	5.30	2.43	8.91	35.56	52.34	1.00	43.00	30.50	0.89	0.24	3.11	26.81	22.41	22.41
G.18.62	84.35	71.80	17.80	10.63	72.83	29.85	60.57	15.00	169.00	40.67	0.28	0.09	2.50	28.60	88.37	88.37
G.18.63	85.18	73.00	18.20	15.48	18.62	35.01	59.77	16.00	46.00	40.67	0.33	0.12	2.07	42.32	31.68	31.68
G.18.64	83.88	77.20	19.30	14.99	7.74	35.25	55.00	71.00	156.00	40.67	0.47	0.09	1.46	20.69	107.87	107.87
G.18.89	83.29	74.20	18.50	12.91	7.48	41.17	42.03	559.00	83.00	36.85	0.43	0.05	0.00	18.00	302.03	302.03
G.18.90	80.35	56.00	14.00	9.42	11.70	22.47	35.06	193.00	36.00	20.33	0.47	0.09	0.00	14.43	108.46	108.46
G.18.105	86.59	53.60	13.40	11.59	7.67	17.08	36.71	11.00	21.00	25.42	1.53	0.28	0.00	24.80	16.72	16.72
G.18.106	87.29	51.20	8.20	10.93	5.21	18.13	37.60	25.00	14.00	25.42	0.93	0.15	0.00	26.04	20.05	20.05
G.18.107	84.71	40.60	10.10	10.66	5.61	10.49	30.00	7.00	3.00	20.33	0.80	0.12	0.00	39.06	7.05	7.05
G.18.108	92.82	50.80	12.70	11.28	6.13	13.29	41.03	44.00	5.00	27.96	0.55	0.12	3.10	19.26	24.47	24.47
G.18.109	88.24	69.80	17.40	11.67	5.14	29.25	49.60	400.00	289.00	30.50	0.60	0.15	2.77	43.57	325.27	325.27
G.18.121	83.88	57.60	14.40	11.19	6.14	44.13	48.43	123.00	44.00	34.31	0.60	0.10	3.17	20.48	79.76	79.76
G.18.122	91.41	78.60	19.70	12.68	8.96	21.72	58.63	945.00	9.00	34.31	2.92	0.21	0.00	32.94	448.88	448.88
G.18.123	86.47	74.00	18.50	11.97	6.42	32.39	61.26	71.00	4.00	40.67	1.49	0.17	0.00	36.14	37.43	37.43
G.18.124	55.76	89.40	22.40	13.68	3.69	35.23	64.34	8.00	127.00	35.58	0.33	0.12	2.77	49.08	65.97	65.97

ID	Quality Rating (qn)														Σ (qn*Wn)	WQI
	pH	EC	TDS	Na	K	Ca	Mg	Fe	Mn	HCO_3	Cl	SO_4	NO_3	F		
G.18.125	87.18	89.80	22.50	13.88	3.85	51.03	63.26	20.00	125.00	38.13	0.35	0.24	2.71	47.14	70.74	70.74
G.18.126	80.00	25.60	6.40	4.75	9.58	48.08	29.49	22.00	1.00	15.25	0.29	0.19	0.09	23.39	12.42	12.42
G.18.127	79.06	32.20	8.00	6.20	9.06	3.43	37.77	62.00	12.00	16.52	1.04	0.09	0.00	9.48	35.62	35.62
G.18.128	76.47	30.60	7.70	13.04	10.34	14.32	46.74	121.00	3.00	17.79	0.30	0.19	0.54	8.86	59.02	59.02
G.18.129	78.47	32.00	8.00	3.67	5.93	19.40	37.17	1442.00	32.00	12.71	1.00	0.12	0.00	10.11	691.18	691.18
G.18.130	113.88	32.80	8.20	5.53	4.48	9.87	35.26	135.00	2.00	16.52	0.80	0.34	4.04	35.77	66.55	66.55
G.18.131	76.71	52.00	10.80	5.70	8.48	12.37	41.37	120.00	4.00	17.79	2.72	0.26	4.00	30.12	60.02	60.02
G.18.132	77.88	51.00	10.80	3.42	5.32	10.09	35.60	8057.00	90.00	20.33	2.62	0.21	4.31	27.95	3816.57	3816.57
G.18.133	78.94	79.40	19.90	95.00	119.71	41.27	54.31	1196.00	340.00	34.31	5.30	0.22	4.32	22.98	721.34	721.34
G.18.134	77.76	79.00	19.80	9.46	10.66	35.68	61.29	49.00	84.00	35.58	5.33	0.52	14.86	136.87	69.34	69.34
G.18.135	74.12	24.60	6.20	4.79	42.37	4.19	31.37	41.00	8.00	12.71	0.74	0.85	16.40	121.63	29.34	29.34
G.18.136	74.47	23.40	5.80	5.38	9.61	4.48	28.94	114.00	6.00	13.98	0.50	0.44	13.73	161.15	64.29	64.29
G.18.139	80.12	31.80	8.00	4.74	9.54	14.61	35.37	85.00	9.00	19.06	0.57	0.69	19.61	225.39	55.20	55.20
G.18.41	82.71	39.00	9.90	7.42	6.68	11.64	38.03	290.00	103.00	22.88	0.31	0.09	2.28	34.91	186.21	186.21
G.18.42	81.18	58.20	14.10	9.25	5.81	24.47	44.43	36.00	225.00	30.50	0.68	0.14	1.28	30.50	124.20	124.20
G.18.43	83.65	60.80	15.30	10.52	4.16	35.01	58.83	179.00	190.00	82.60	0.34	0.15	1.21	25.16	174.56	174.56
G.18.44	90.59	68.00	15.70	9.19	10.13	36.95	59.63	187.00	128.00	34.31	0.45	0.21	2.17	24.99	149.33	149.33
G.18.45	84.12	65.40	16.40	9.98	10.24	30.96	50.11	75.00	317.00	36.85	0.59	0.35	1.10	22.50	185.21	185.21
G.18.46	78.12	53.40	13.30	9.35	6.13	38.61	49.97	11.00	166.00	22.88	2.24	0.24	3.12	27.95	84.76	84.76
G.18.47	77.18	85.40	21.40	17.36	76.45	26.83	44.57	1173.00	2509.00	27.96	5.32	2.26	0.00	16.26	1725.62	1725.62
G.18.49	82.59	58.40	14.60	10.66	9.81	22.71	48.97	1832.00	132.00	158.85	0.62	0.17	1.97	24.22	921.35	921.35
G.18.50	82.82	48.40	12.10	8.62	9.03	17.36	44.03	648.00	456.00	24.15	0.86	0.27	2.00	25.08	518.69	518.69
G.18.51	80.94	46.00	11.50	6.89	4.72	19.64	41.63	30.00	41.00	25.42	0.69	0.20	2.18	18.99	34.68	34.68
G.18.52	81.88	50.40	12.60	8.25	4.98	22.07	47.89	52.00	203.00	27.96	1.05	0.32	2.23	32.57	121.49	121.49
G.18.53	82.35	49.20	12.30	9.70	4.51	18.49	38.57	369.00	42.00	31.77	0.40	0.21	3.31	41.77	194.96	194.96

ID	Quality Rating (qn)														Σ (qn*Wn)	WQI
	pH	EC	TDS	Na	K	Ca	Mg	Fe	Mn	HCO_3	Cl	SO_4	NO_3	F		
G.18.54	81.41	56.40	14.00	9.57	8.46	29.19	57.31	128.00	34.00	31.77	0.80	0.27	3.58	21.79	77.48	77.48
G.18.55	71.65	23.80	6.00	3.28	9.50	7.96	32.06	764.00	50.00	12.71	0.60	0.22	1.15	12.01	382.20	382.20
G.18.56	77.65	39.60	9.90	17.82	13.58	21.96	57.31	200.00	26.00	22.88	1.04	0.40	3.70	28.83	107.77	107.77
G.18.110	88.59	140.40	35.20	41.98	5.61	16.76	80.03	8.00	610.00	44.48	17.13	1.46	0.00	39.84	291.89	291.89
G.18.111	86.24	63.60	15.90	11.08	3.59	23.71	37.63	48.00	621.00	35.58	0.73	0.20	0.00	42.22	315.79	315.79
G.18.112	84.71	58.40	14.60	11.32	3.88	18.05	34.80	197.00	90.00	27.96	2.22	0.20	0.00	36.06	136.62	136.62
G.18.113	84.12	50.80	12.70	15.16	9.10	7.47	27.26	732.00	110.00	30.50	0.31	0.06	2.99	29.12	396.18	396.18
G.18.114	87.88	244.80	61.20	121.51	5.74	7.33	29.57	187.00	115.00	63.54	43.81	4.07	0.00	60.28	144.84	144.84
G.18.115	87.29	77.80	19.40	12.88	7.68	29.75	37.03	765.00	46.00	36.85	3.33	0.12	0.00	41.42	382.27	382.27
G.18.116	87.41	82.00	20.50	12.65	11.62	34.88	37.17	1225.00	63.00	35.58	0.99	0.05	0.00	34.47	605.32	605.32
G.18.117	88.24	76.80	19.20	15.73	9.64	112.84	67.57	585.00	6.00	43.21	0.54	0.18	1.42	11.28	277.96	277.96
G.18.118	89.29	86.60	21.60	18.09	8.83	26.85	72.43	3427.00	28.00	50.83	0.71	0.15	0.00	8.23	1618.80	1618.80
G.18.119	90.12	72.00	18.00	12.20	6.67	30.23	59.26	235.00	22.00	45.75	0.24	0.20	2.65	49.35	123.29	123.29
G.18.81	87.29	64.00	15.90	10.22	6.13	28.45	41.86	216.00	29.00	35.58	0.58	0.16	0.00	50.90	117.69	117.69
G.18.82	88.82	47.20	11.80	9.80	5.72	18.17	36.66	148.00	55.00	24.15	0.26	0.43	3.00	39.68	97.51	97.51
G.18.84	87.29	54.20	13.50	5.23	6.83	19.21	37.60	12.00	12.00	27.96	0.95	0.29	3.16	38.37	13.63	13.63
G.18.86	76.47	29.40	7.40	5.89	5.03	4.55	26.26	186.00	5.00	15.25	0.47	0.90	0.00	7.04	90.25	90.25
G.18.91	92.94	59.00	14.80	8.70	5.93	24.96	43.17	47.00	195.00	30.50	0.60	0.89	0.00	32.21	115.44	115.44
G.18.92	81.18	318.00	79.20	76.31	104.74	77.99	99.09	484.00	394.00	35.58	0.48	17.78	0.00	11.59	412.75	412.75
G.18.93	82.59	56.40	14.10	10.89	7.46	19.13	43.69	76.00	25.00	27.96	0.30	0.19	2.56	29.17	49.23	49.23
G.18.94	80.00	51.40	12.90	10.17	6.75	16.67	34.66	416.00	209.00	31.77	0.18	0.28	2.60	23.48	294.29	294.29
G.18.95	83.88	52.60	13.20	9.00	4.84	20.60	50.69	1.00	36.00	29.23	0.29	0.07	2.68	28.88	19.26	19.26
G.18.96	71.18	18.40	4.60	2.54	6.85	0.09	23.74	38.00	0.00	7.63	1.07	0.05	0.00	6.83	18.57	18.57
G.18.97	78.94	18.20	4.50	1.49	6.19	1.07	24.11	43.00	3.00	10.17	0.40	0.05	2.95	7.11	22.38	22.38
G.18.98	78.94	51.20	12.90	3.89	10.23	20.71	38.14	2786.00	28.00	19.06	2.07	1.92	0.00	13.13	1318.78	1318.78

ID	Quality Rating (qn)														Σ (qn*Wn)	WQI
	pH	EC	TDS	Na	K	Ca	Mg	Fe	Mn	HCO_3	Cl	SO_4	NO_3	F		
G.18.99	73.88	46.20	11.60	4.41	15.81	18.83	35.43	38.00	44.00	11.44	3.06	1.77	0.00	12.43	39.51	39.51
G.18.100	82.94	63.40	15.90	3.70	15.46	25.27	61.37	1019.00	642.00	34.31	1.13	1.76	2.05	19.18	779.27	779.27
G.18.101	79.41	92.60	23.10	10.56	22.63	28.80	65.97	74.00	1154.00	19.57	9.41	3.85	0.00	6.44	575.94	575.94
G.18.102	78.35	61.40	15.00	3.83	6.80	34.28	44.31	407.00	0.00	24.91	2.41	1.21	0.00	29.98	192.52	192.52
G.18.103	73.65	35.20	8.80	6.60	6.05	10.63	30.00	50.00	15.00	19.06	0.23	0.23	0.27	13.13	31.53	31.53
G.18.104	79.41	48.60	12.30	8.89	5.35	18.65	39.74	1820.00	231.00	27.96	0.31	0.22	0.06	26.88	962.15	962.15
G.18.57	79.41	61.60	15.40	9.12	5.66	28.29	48.54	708.00	180.00	27.96	0.96	0.26	2.28	26.39	417.59	417.59
G.18.58	75.29	40.00	10.00	5.10	4.92	16.80	40.97	1759.00	170.00	16.52	2.69	0.37	0.00	8.89	904.15	904.15
G.18.59	73.29	39.40	9.90	6.28	9.12	14.97	35.74	32.00	33.00	21.60	0.73	0.18	2.62	23.85	32.07	32.07
G.18.60	78.35	38.40	9.60	7.27	5.87	14.84	39.89	76.00	37.00	19.06	0.60	0.68	2.05	2.03	53.54	53.54
G.18.61	80.00	25.40	6.30	4.41	6.82	66.25	39.14	11.00	33.00	10.17	1.08	0.07	2.08	16.33	21.94	21.94
G.18.65	77.06	33.20	8.30	3.29	11.93	16.13	36.03	50.00	26.00	12.71	1.87	0.08	0.00	8.04	36.50	36.50
G.18.66	76.71	25.60	6.40	4.51	10.62	20.64	38.40	21.00	32.00	8.90	1.22	0.09	0.00	14.31	26.02	26.02
G.18.67	74.82	27.80	6.90	4.35	5.34	9.31	33.26	33.00	26.00	12.71	0.45	0.07	2.66	12.47	28.71	28.71
G.18.68	78.82	44.00	11.00	8.44	5.39	12.99	43.11	8.00	249.00	24.15	0.28	0.05	2.60	9.62	121.33	121.33
G.18.69	77.88	54.00	10.80	8.69	5.76	73.37	58.80	38.00	290.00	25.42	0.30	0.08	2.66	11.31	154.71	154.71
G.18.70	78.82	66.40	16.60	12.86	6.03	25.79	50.43	150.00	71.00	27.96	1.84	0.34	2.71	20.99	105.03	105.03
G.18.71	79.88	41.60	10.30	9.42	6.16	11.92	29.49	1009.00	368.00	21.60	0.39	0.25	0.44	30.23	646.70	646.70
G.18.72	77.18	42.60	10.60	9.21	6.86	15.96	28.66	1156.00	403.00	22.88	0.42	0.11	1.56	21.07	731.48	731.48
G.18.73	75.76	49.00	12.30	3.13	7.22	16.17	24.63	3549.00	40.00	10.17	6.91	0.28	0.00	10.64	1681.50	1681.50
G.18.74	79.65	41.20	10.30	8.84	6.48	11.99	29.97	96.00	372.00	21.60	0.58	0.24	1.77	32.74	221.20	221.20
G.18.75	71.65	30.40	7.60	4.22	1.11	8.53	22.74	11.00	5.00	10.17	2.60	0.88	3.03	6.58	8.25	8.25
G.18.76	70.00	23.80	5.90	2.94	6.77	3.96	18.40	199.00	20.00	6.35	1.33	0.14	0.00	16.92	103.78	103.78
G.18.77	80.24	50.80	12.70	8.65	6.10	20.13	37.34	549.00	123.00	27.96	0.40	0.28	3.23	30.50	316.64	316.64
G.18.78	84.35	85.40	21.30	12.32	6.63	42.33	50.06	84.00	70.00	38.13	4.10	2.48	0.00	38.90	74.53	74.53

ID	Quality Rating (qn)														Σ (qn*Wn)	WQI
	pH	EC	TDS	Na	K	Ca	Mg	Fe	Mn	HCO_3	Cl	SO_4	NO_3	F		
G.18.79	80.82	50.40	12.60	6.73	4.02	25.47	34.23	606.00	92.00	25.42	0.86	0.15	0.00	41.30	329.29	329.29
G.18.80	81.29	35.60	8.90	6.02	6.35	12.31	30.14	7.00	8.00	19.06	0.28	0.12	0.04	31.86	9.04	9.04
G.18.83	89.06	65.00	16.20	10.61	6.25	34.03	39.77	191.00	9.00	35.58	0.45	0.21	1.99	52.29	96.71	96.71
G.18.85	80.35	32.00	8.00	5.23	3.28	9.37	27.37	1122.00	31.00	16.52	0.19	0.34	0.07	17.88	541.22	541.22
G.18.87	74.71	68.40	17.10	6.99	5.75	31.76	43.94	379.00	233.00	15.25	8.02	0.28	0.00	9.01	287.51	287.51
G.18.88	84.71	50.00	12.50	9.09	5.36	20.87	38.49	27.00	11.00	27.96	0.41	0.08	0.00	13.07	18.97	18.97
G.18.120	83.53	93.80	23.40	13.44	9.42	30.72	66.94	1237.00	218.00	29.23	4.31	1.72	0.00	16.01	682.66	682.66
G.18.137	115.06	25.60	6.30	4.95	5.98	4.63	33.74	69.00	9.00	12.71	1.10	0.49	15.74	176.61	45.58	45.58
G.18.138	74.12	28.80	7.20	4.92	9.29	7.75	31.31	9.00	1.00	12.71	1.42	0.60	19.81	217.57	15.46	15.46